A NEUROHISTOLOGICAL STUDY OF THE SENSORI-MOTOR CORTEX

by J. J. SLOPER,

Being a thesis submitted in fulfilment of the requirements for the degree of Doctor of Philosophy in the University of Oxford

VOLUME II Illustrations

May 1977

St Peter's College
Oxford

TABLE OF CONTENTS

LIST OF ABBREVIATIONS

a	axon
b	collateral branch of axon
c	cell soma
d	dendrite
f	fibrils
g	Golgi apparatus
m	mitochondrion
n	nucleus
r	ribosomes
s	spine apparatus
t	axon terminal
u	unmyelinated axon
ad	apical dendrite
ci	cilium
co	cisternal organ
da	degenerating axon
dt	degenerating axon terminal
er	endoplasmic reticulum
gj	gap junction
gl	glial cell process
is	axon initial segment
nt	neurotubules
pg	pars granulosa of nucleolus
sc	subsurface cistern
sp	spine

psd presynaptic dendrite

B Betz cell soma

G glial cell soma

M motor cortex

N neuron

P pyramidal cell

S area 3b of the somatic sensory cortex

LS large stellate neuron

SS small stellate neuron

One small arrowhead indicates an asymmetric synapse from the postsynaptic side

Two small arrowheads indicate a symmetrical synapse from the postsynaptic side

Roman numerals are used to indicate the cortical layers

Illustrations to Chapter 3

ULTRASTRUCTURAL FEATURES OF THE SENSORI-MOTOR CORTEX

Fig. 3-1 Electron micrograph showing the superficial part of layer I of the motor cortex with the pial surface at the top. Note the myelinated axons which form part of the plexus of myelinated axons in this layer. There are also many small unmyelinated axons.
X 20,000

Fig. 3-2 Light micrograph showing the superficial parts of both somatic sensory cortex (Area 3b)(S) and motor cortex (M) in the walls of the central sulcus, stained by Weil's method to show myelinated axons. Note the marked difference in density of staining of the fibre plexuses in the two cortical areas which were immediately adjacent on the same section as shown. X 150

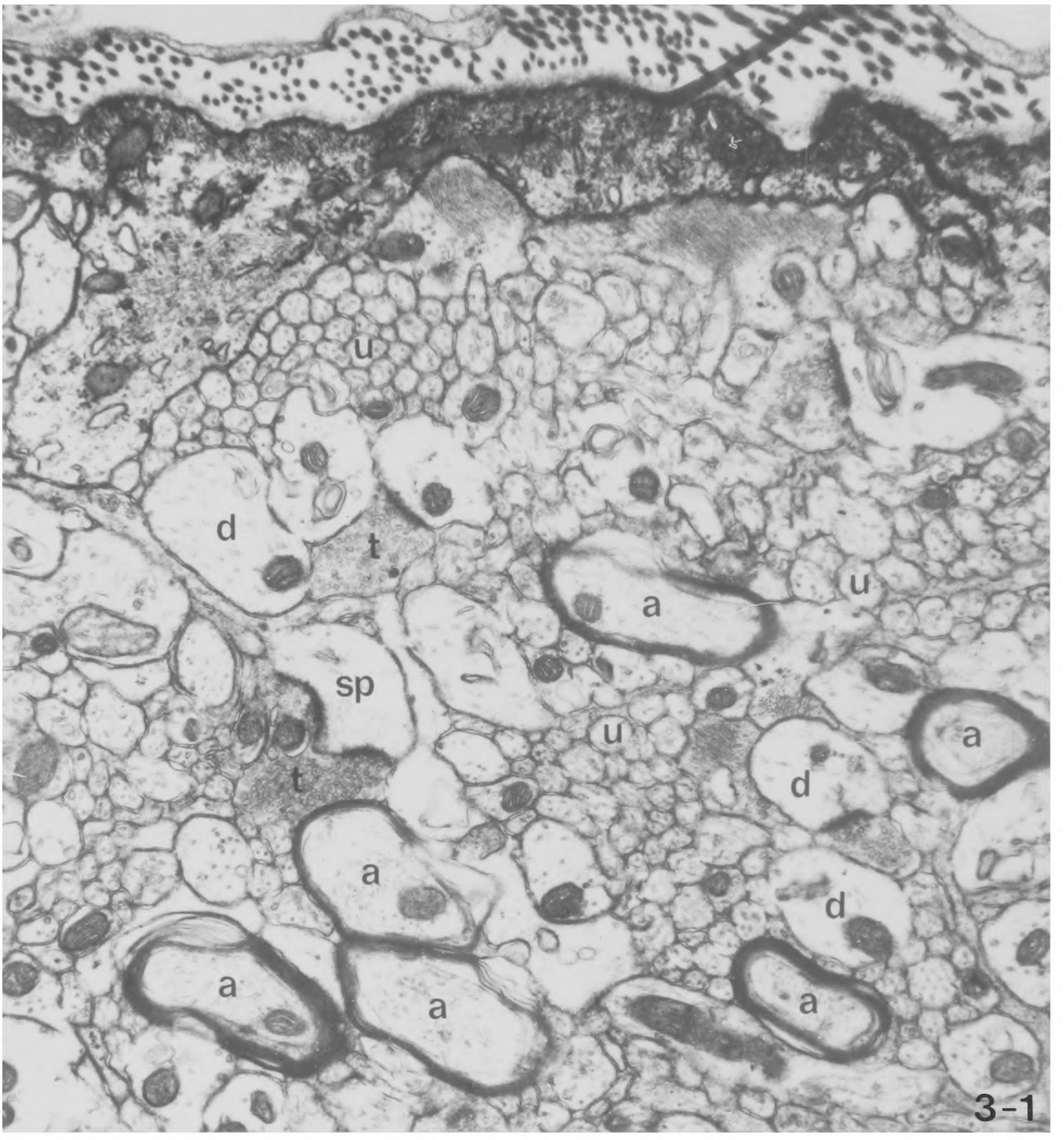

3-1

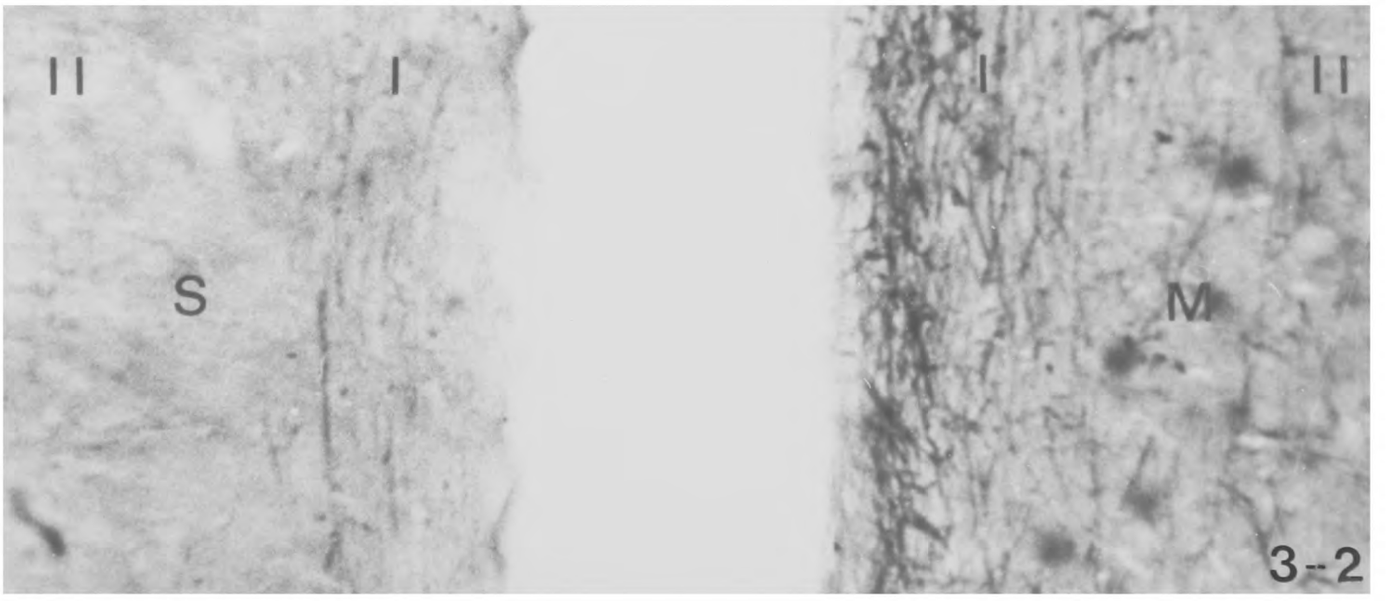

3-2

Fig. 3-3 Graph showing results of individual counts of the density of myelinated axons against depth in the motor and somatic sensory cortices. These show that the plexus is much more apparent on some sections than others.

LAYER I FIBRE COMPARISON - COUNTS OF INDIVIDUAL SECTIONS

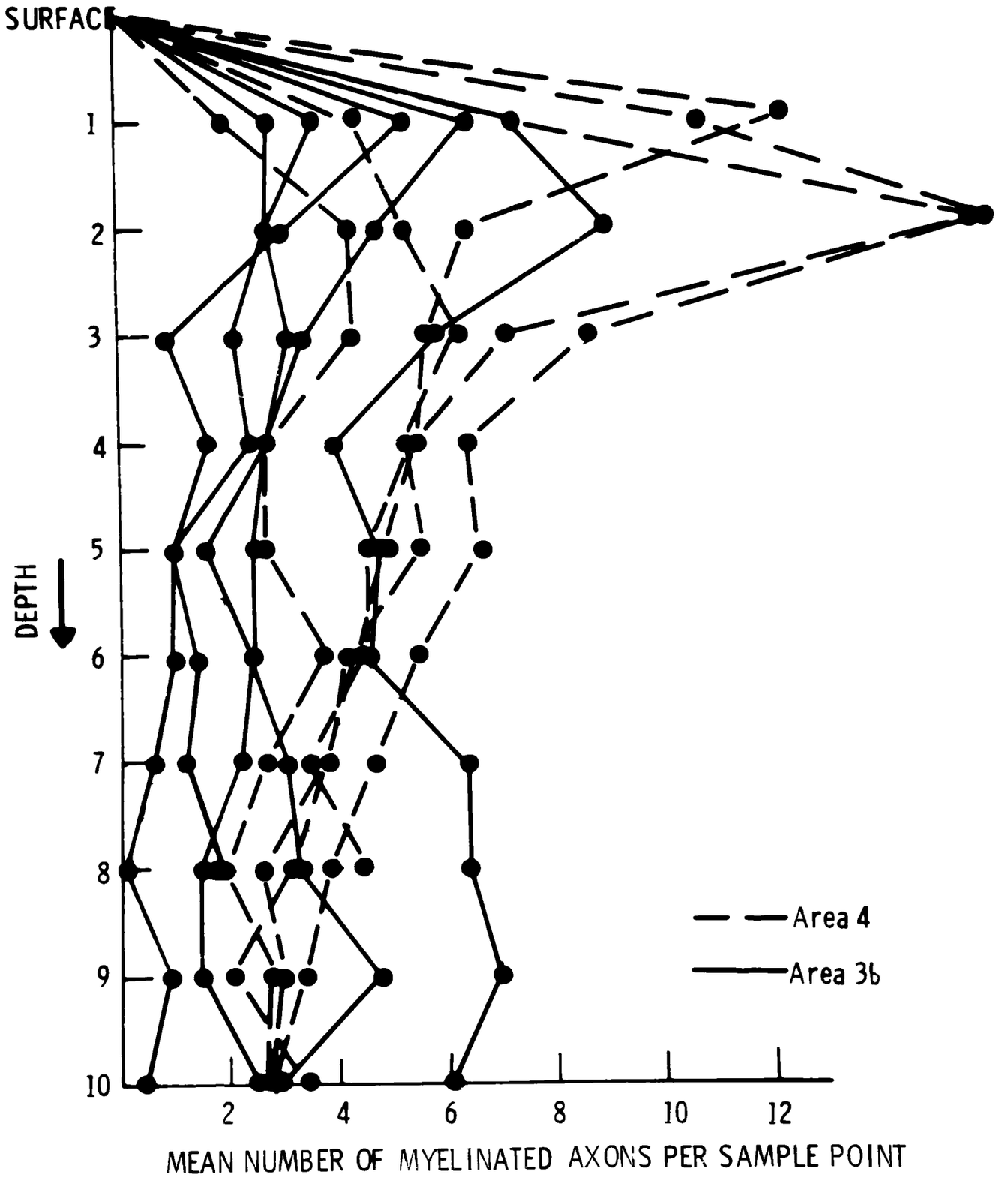

Fig. 3-4 Graph showing the pooled results of the layer I fibre counts and showing the overall greater density of the fibre plexus in the motor cortex.

LAYER I FIBRE COMPARISON-OVERALL RESULTS

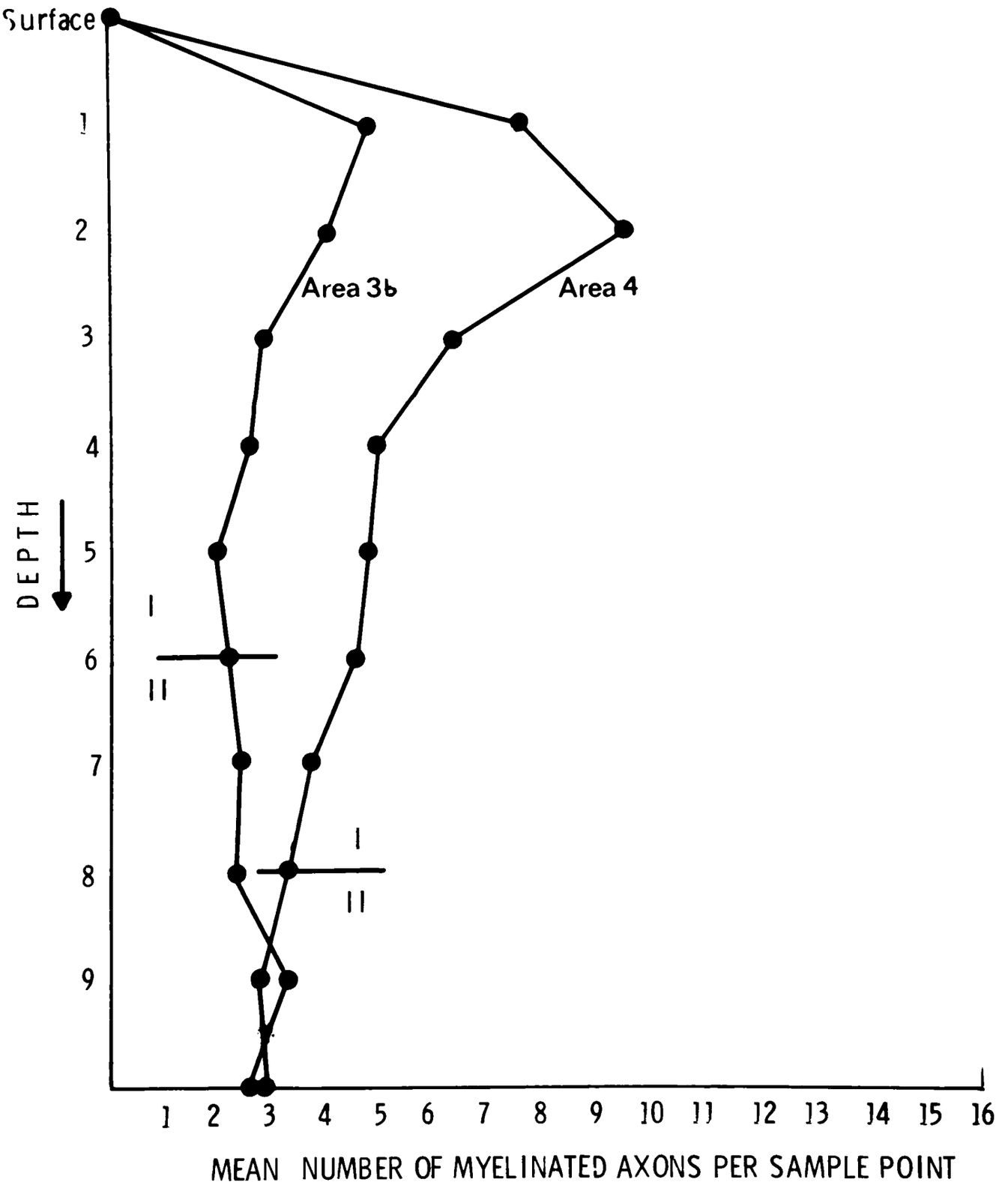

Fig. 3-5 Histograms comparing the size distribution of the myelinated axons in layer I of motor and somatic sensory cortices.

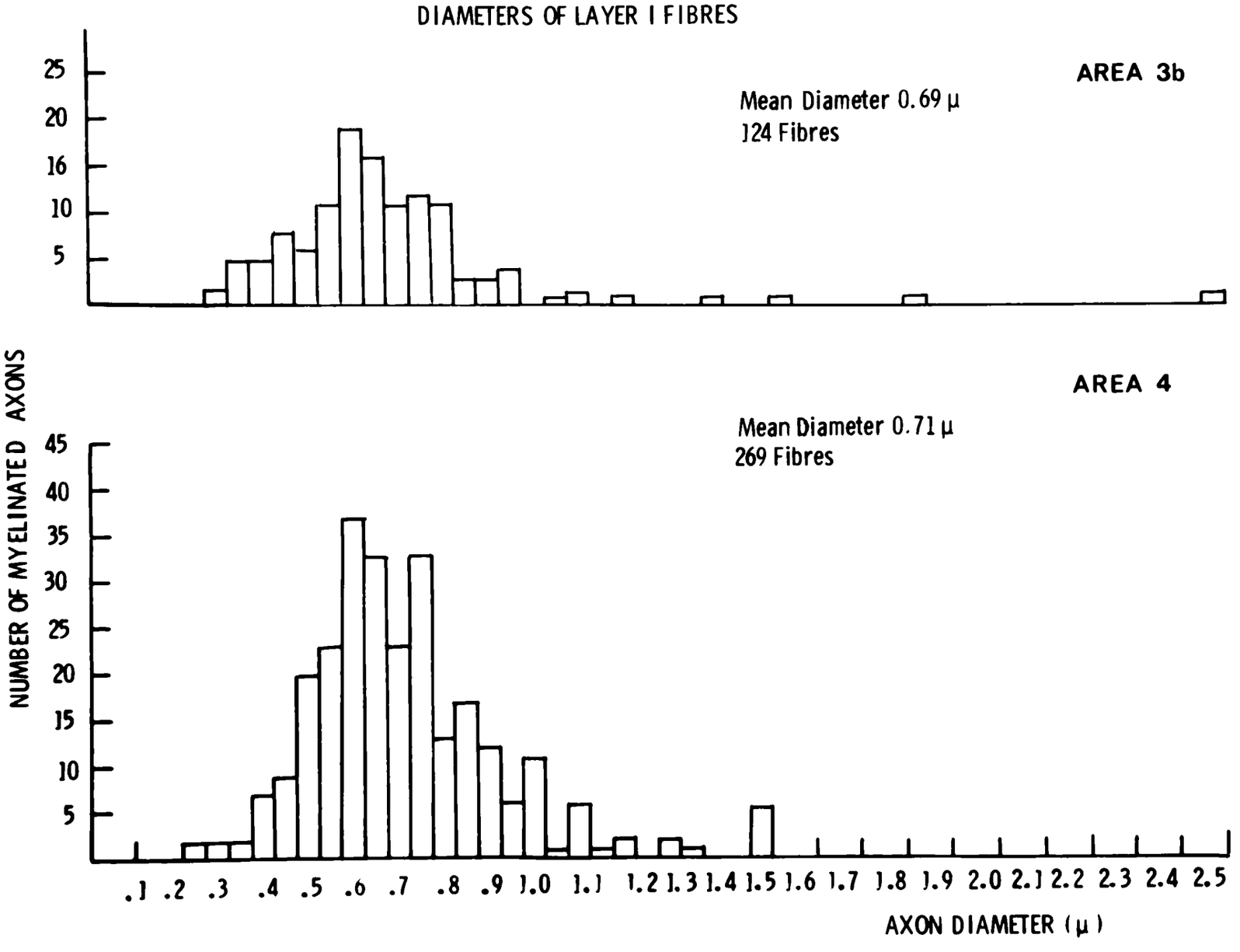
DIAMETERS OF LAYER I FIBRES
AREA 3b
Mean Diameter 0.69 μ
124 Fibres
AREA 4
Mean Diameter 0.71 μ
269 Fibres
NUMBER OF MYELINATED AXONS
25
20
16
10
5
45
40
35
30
25
20
15
10
5
.1 .2 .3 .4 .5 .6 .7 .8 .9 1.0 1.1 1.2 1.3 1.4 1.5 1.6 1.7 1.8 1.9 2.0 2.1 2.2 2.3 2.4 2.5
AXON DIAMETER (μ)

Fig. 3-6 Medium-sized pyramidal cell from layer III of motor cortex with a long length of its apical dendrite cut in continuity with the cell soma. An empty myelin sheath has become wrapped round the apical dendrite (arrowheads) giving the appearance of myelination.
X 3,900

Fig. 3-7 Higher power of this dendrite wrapped in myelin, from a serial section; unlike a true myelin sheath this myelin doubles back on itself at its limits (arrowheads). Note the synapse received by the dendrite (arrow).
X 15,000

Fig. 3-8 Varicose dendrite of the type receiving a high density of synapses from layer III of motor cortex.
X 29,000

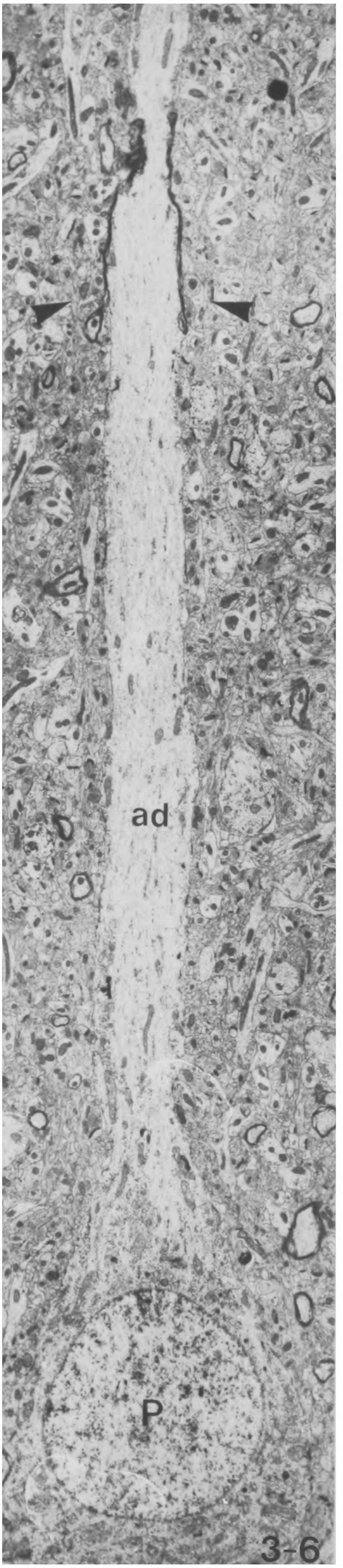

3-6

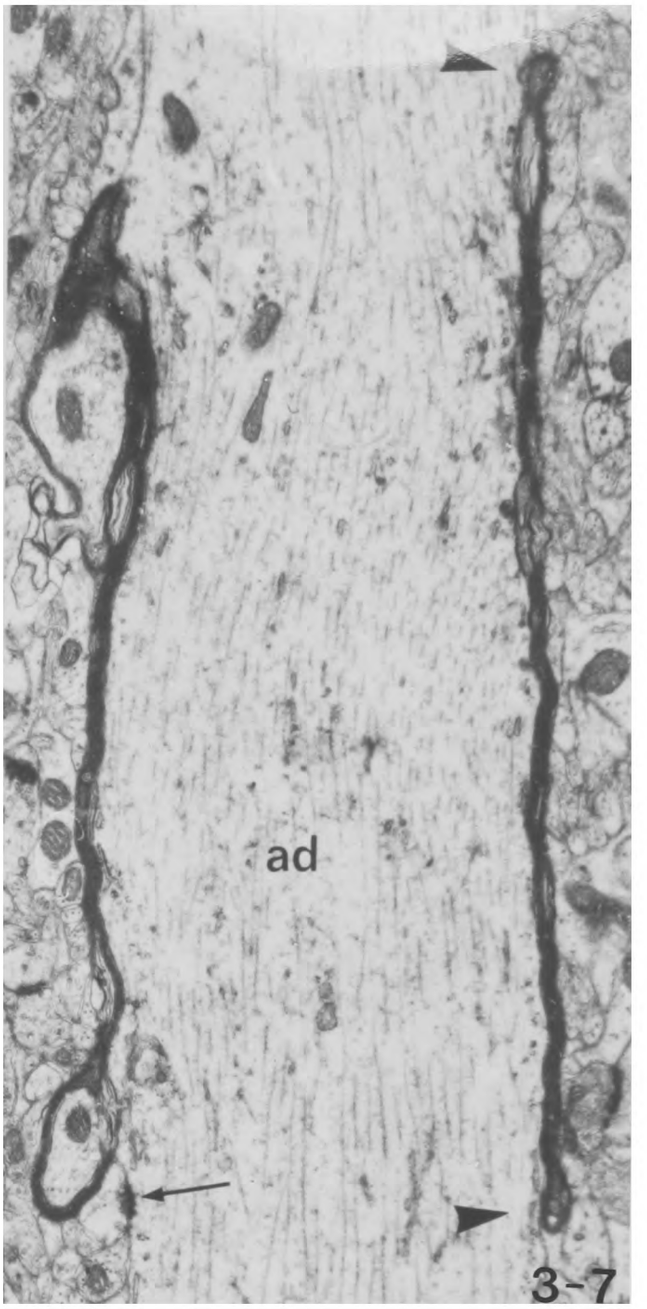

3-7

3-8

Fig. 3-9 Example of the type of varicose dendrite having a markedly varicose shape, clear cytoplasm and a moderate density of synapses. From layer I of motor cortex. X 32,000

Fig. 3-10 Example of the type of varicose dendrite having a less obviously varicose shape but containing a high density of organelles and receiving many synapses. From layer III of motor cortex. X 29,000

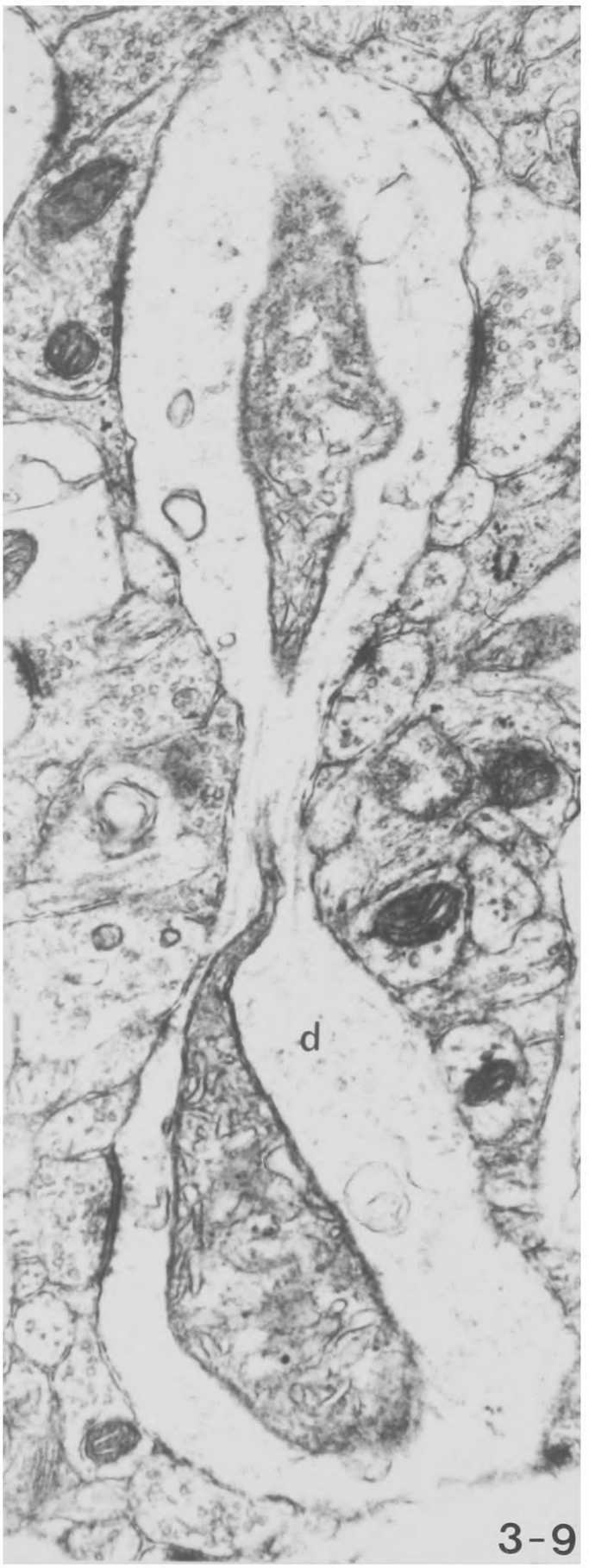

3-9

3-10

Fig. 3-11 Dendritic spine from layer II of motor cortex which contains a spine apparatus and receives an asymmetric synapse from a terminal (t_1), containing round vesicles and a symmetrical synapse from a terminal containing flattened synaptic vesicles (t_2). X 53,000

Fig. 3-12 and 3-13 Serial sections of a double-headed dendritic spine cut in continuity with its parent dendrite. It contains a spine apparatus and the upper head received synapses from 3 axon terminal profiles. That from t_1 is clearly of the asymmetric type and that from t_2 of the symmetrical type. X 29,000

Fig. 3-14 Axon terminal (t_1) which makes asymmetric synapses on to both a spine and the shaft of its parent dendrite. The spine also receives a synapse from a second axon terminal t_2. X 44,000

Fig. 3-15 Axon terminal t_2 which makes symmetrical synapses with a spine and the shaft of its parent dendrite. The spine also receives an asymmetric synapse from terminal t_1. X 44,000

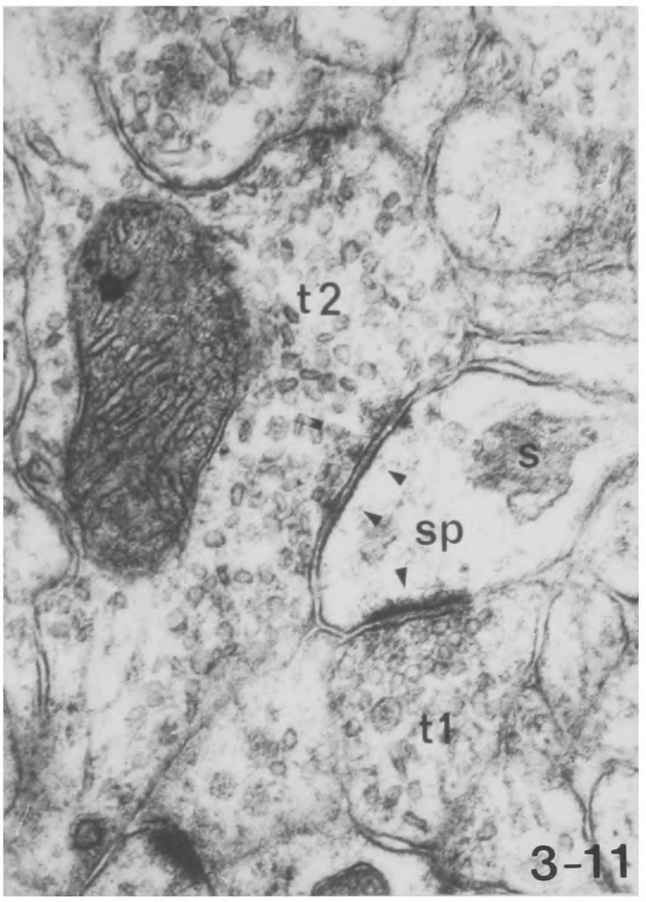

3-11

3-12

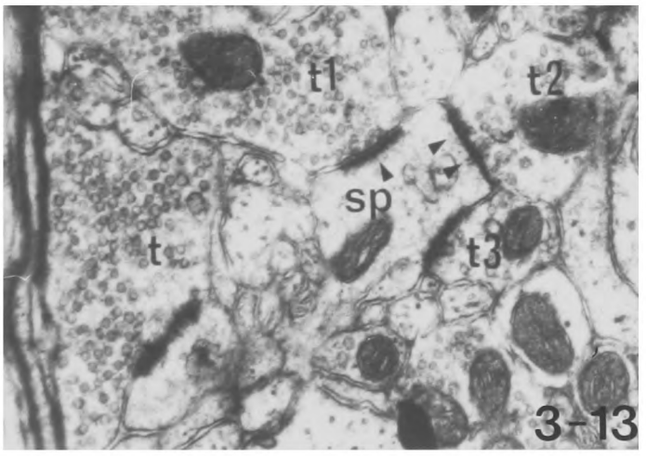

3-13

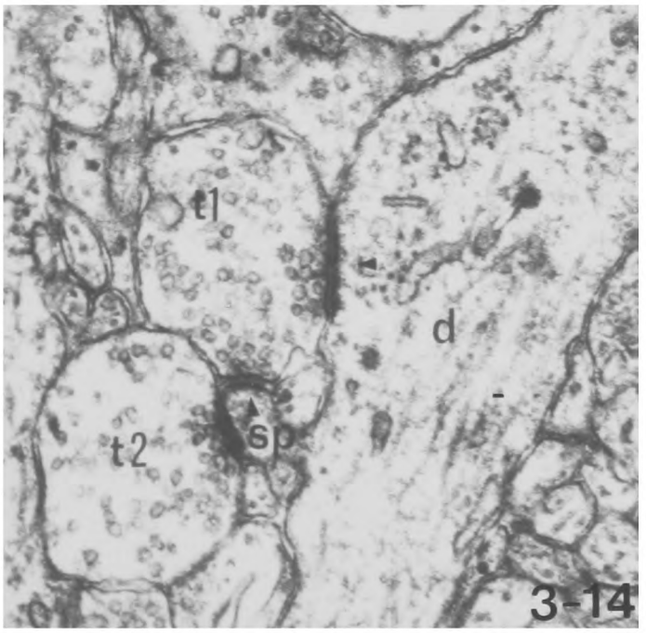

3-14

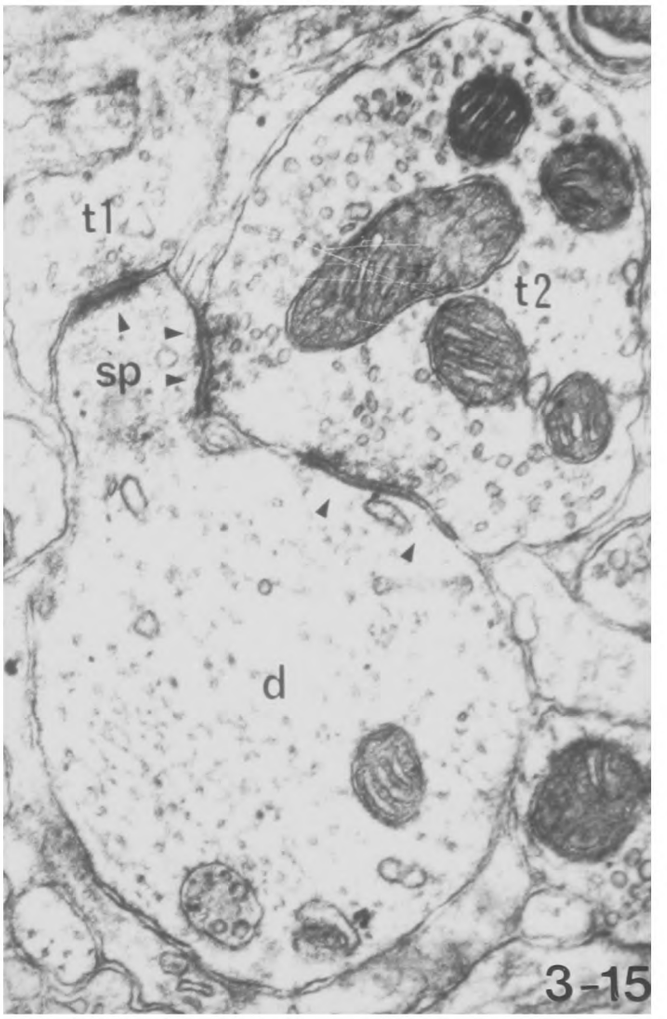

3-15

Fig. 3-16 Somatic spine (arrowhead) on the soma of a pyramidal cell, from layer III of motor cortex. X 9,000

Fig. 3-17 Detail of somatic spine of Fig. 3-16 which shows it to receive a symmetrical synapse. Note the darker flocculent cytoplasm in the spine. X 32,000

Figs. 3-18 and 3-19 Serial sections of a varicose axon containing large dense cored vesicles. Both X 18,000

Fig. 3-20 Example of a somatic spine. The axon terminal makes synapses both on to the spine and the cell soma, the latter of these synapses being clearly of the symmetrical type. X 29,000

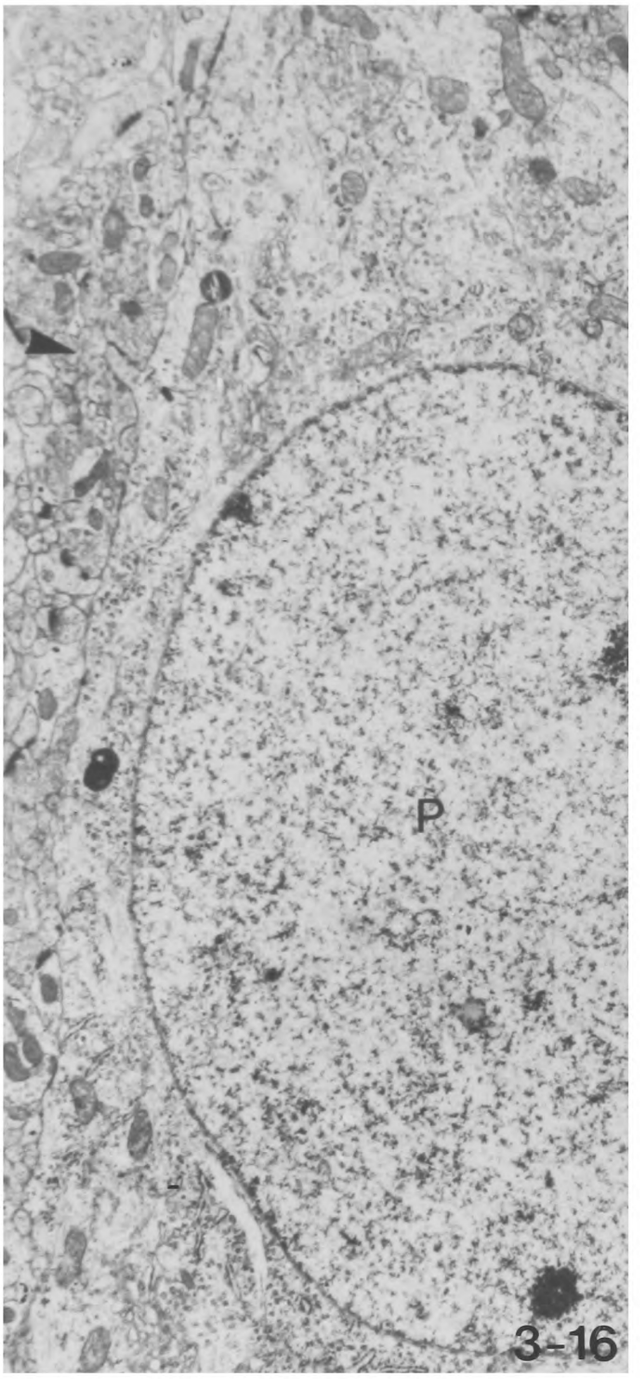
P
3-16


a
3-18

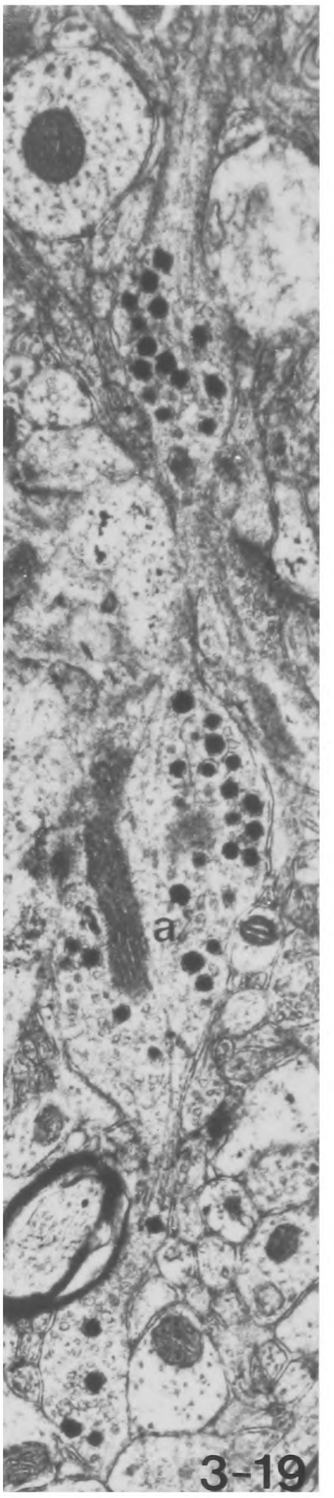
a
3-19

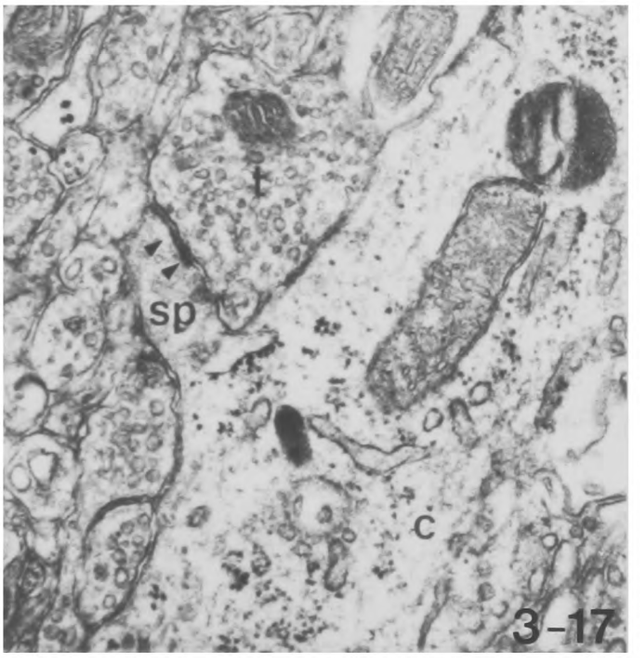
sp
c
3-17

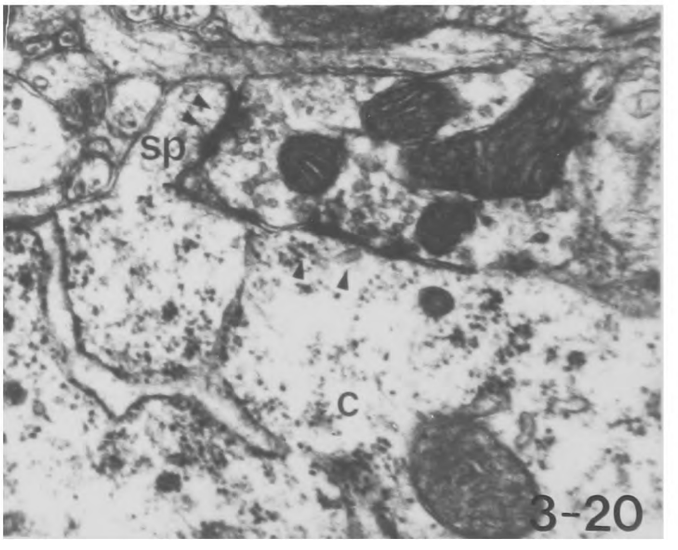
sp
c
3-20

Fig. 3-21 Horizontal myelinated axon in layer IV of motor cortex giving off a vertical branch at a Node of Ranvier. X 9,000

Fig. 3-22 Horizontal unmyelinated axon in layer IV of somatic sensory cortex which makes four "en passage" synapses, two of which are clearly of the symmetrical type. X 18,000

Fig. 3-23 Bundles of parallel fibrils (f) in a dendrite. X 29,000

Fig. 3-24 Similar bundle of fibrils in a dendrite cut in transverse section. X 29,000

Fig. 3-25 Higher magnification of fibrils of Fig. 3-24. X 90,000

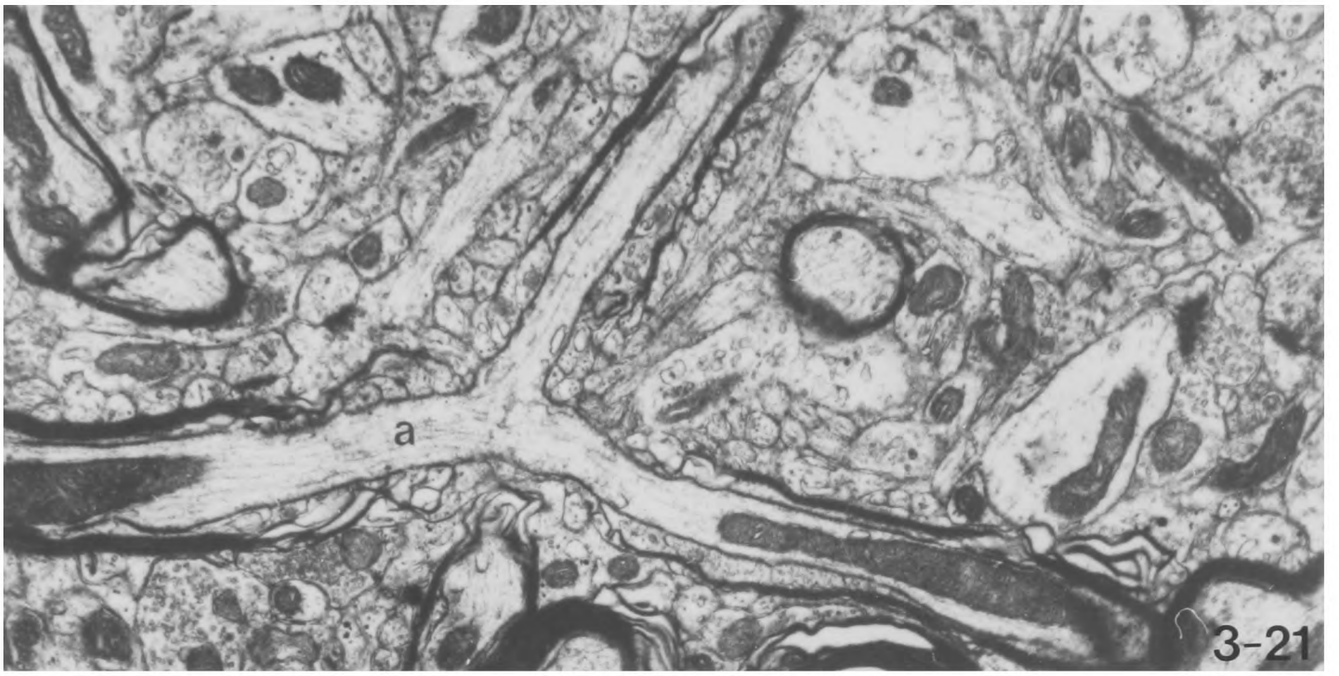
a
3-21

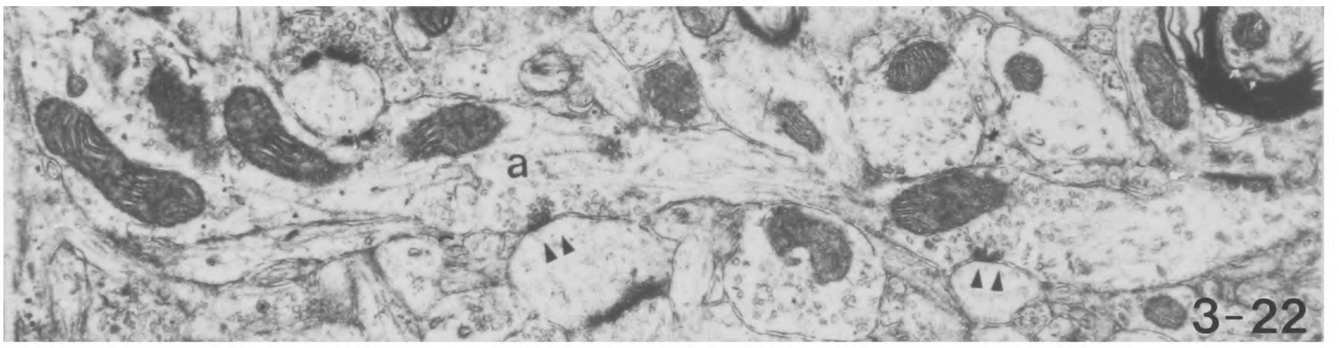
a
3-22

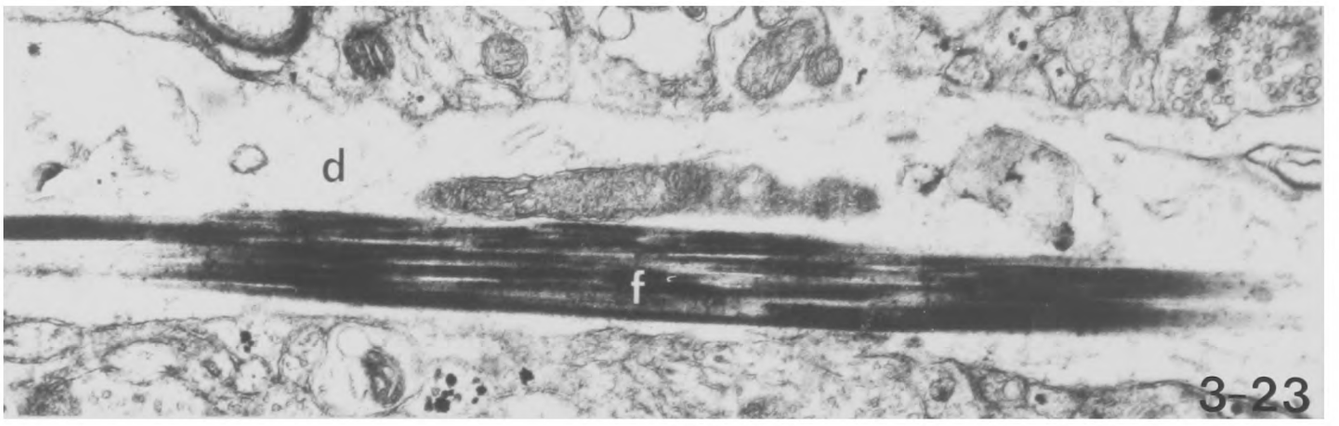
d
f
3-23

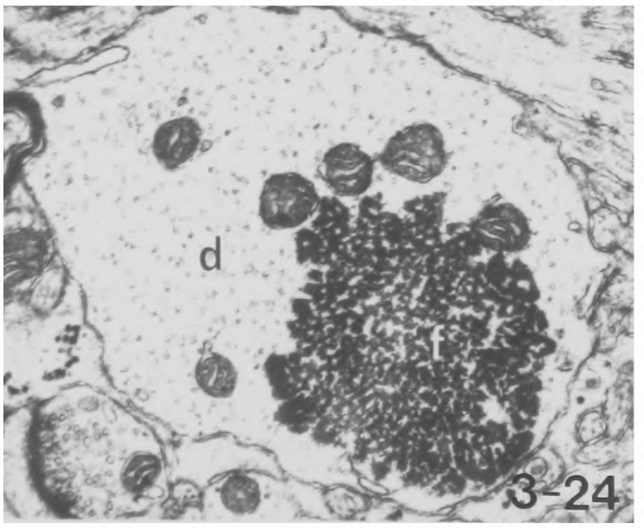
d
f
3-24

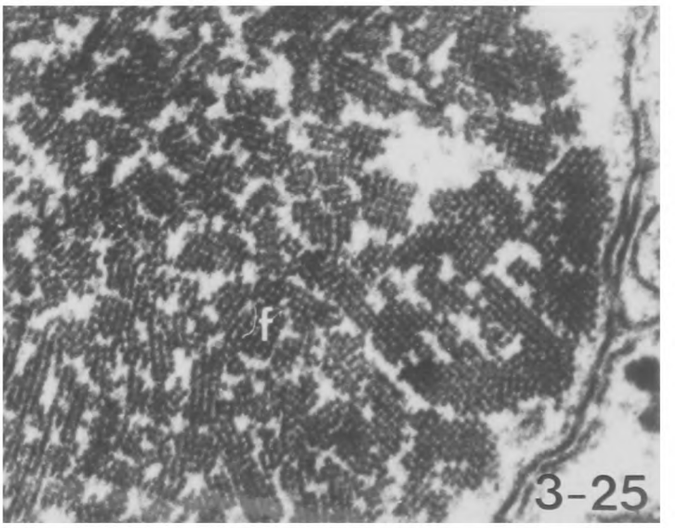
f
3-25

Figs. 3-26 and 3-27 Light micrographs of "thick" sections taken parallel to the pial surface in layers II and IV of motor cortex respectively. In layer II the apical dendrites, which are cut in transverse section and appear as small white circles (examples indicated by small arrowheads) are evenly distributed, whereas in layer IV they occur in groups (examples indicated by arrowheads). X 220

Fig. 3-28 Electron micrograph of a similar section through layer IV parallel to the pial surface showing a bundle of apical dendrites cut in transverse section (x) X 6,000

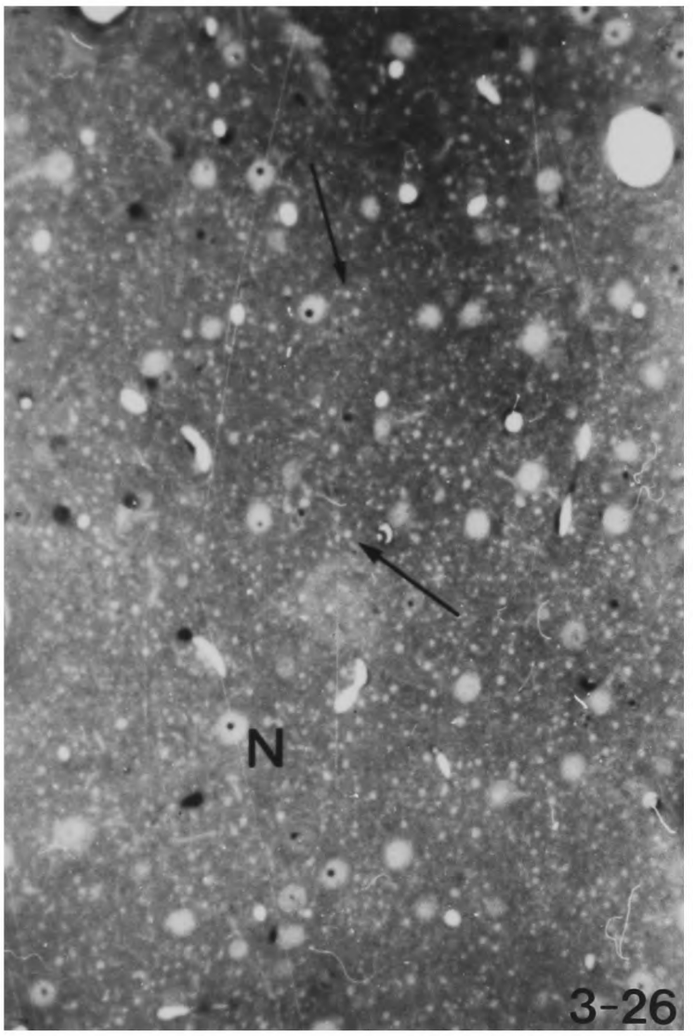

3-26

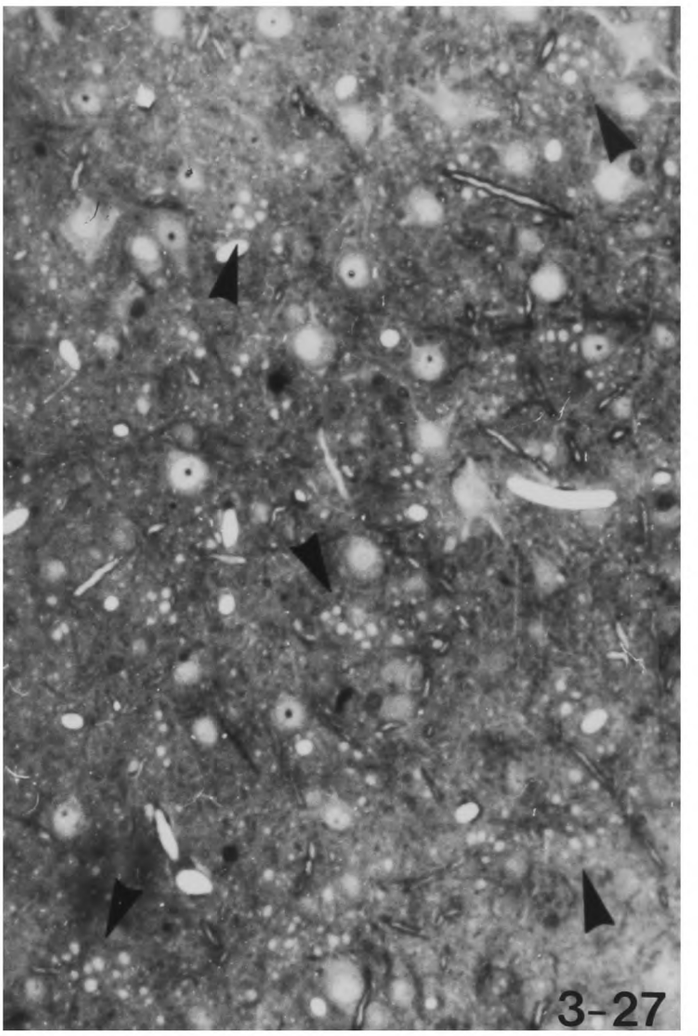

3-27

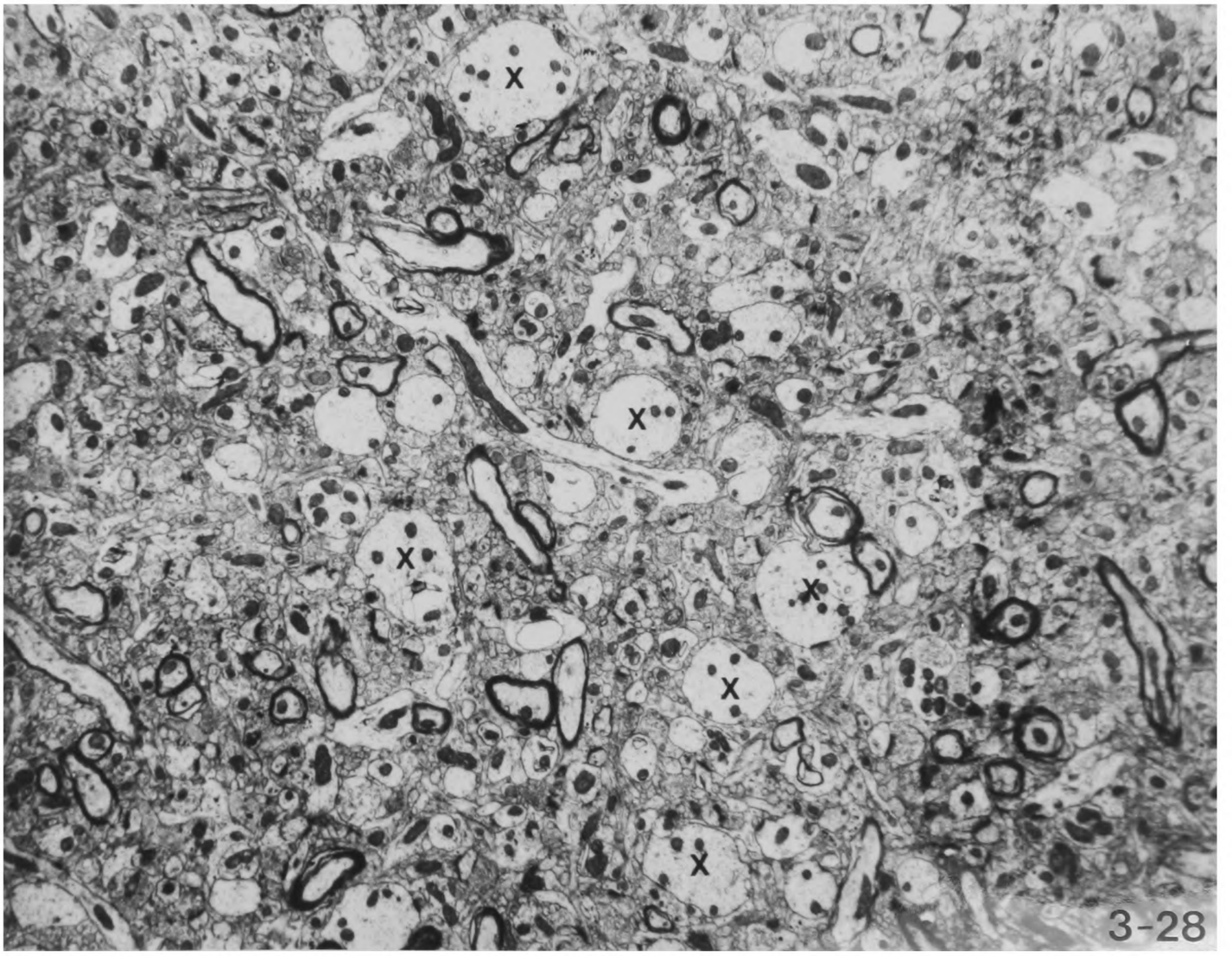

3-28

Fig. 3-29 Layer V of motor cortex showing a group of myelinated axons running vertically beside a pyramidal cell soma. The surface of the cortex is at the top of the figure. X 3,500

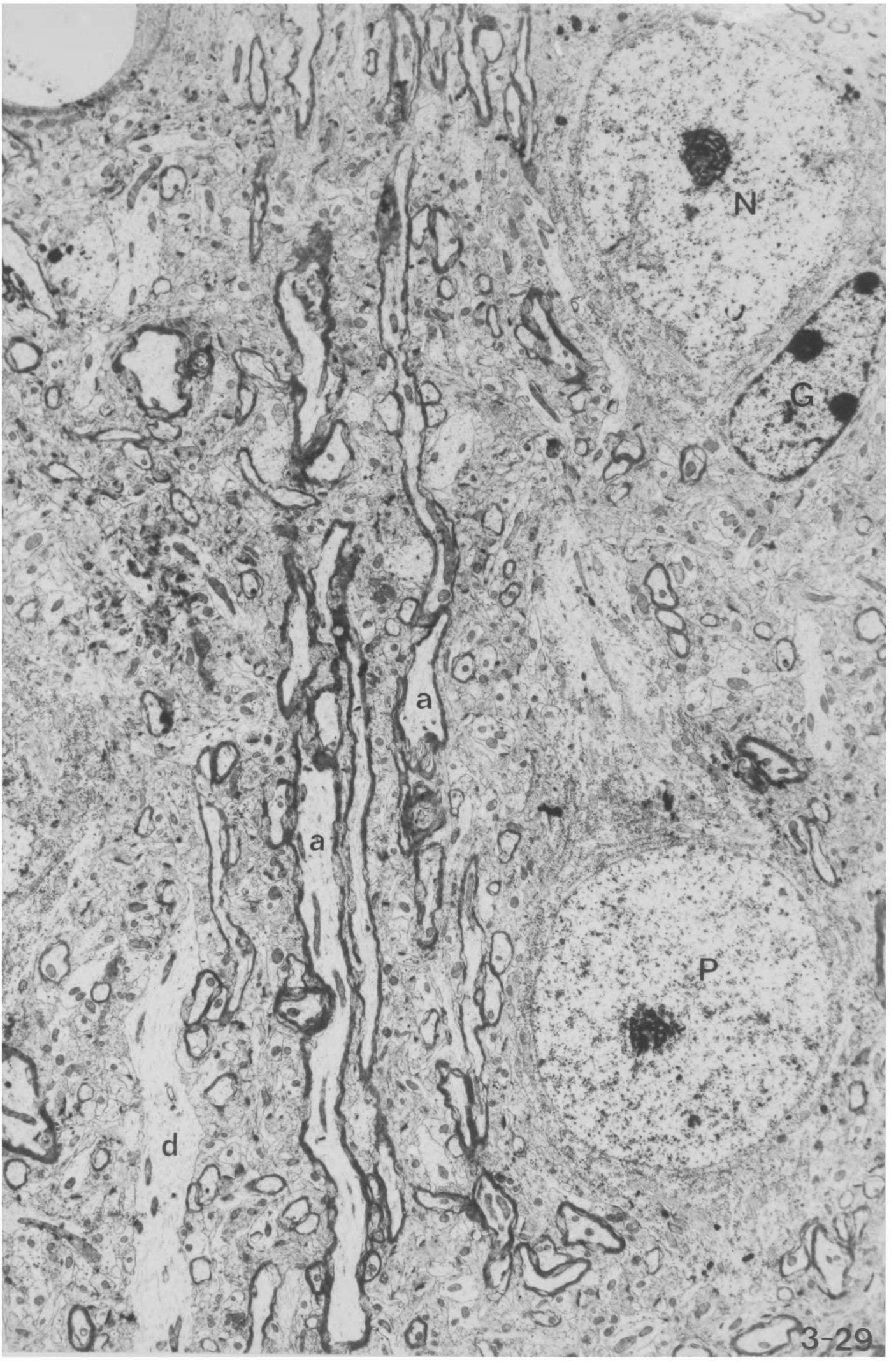

3-29

Fig. 3-30 Two subsurface cisternae in a large dendrite, both of which are closely related to the same mitochondrion. Note that both come into close contact with axonal profiles containing flattened vesicles. X 29,000

Fig. 3-31 Higher magnification of part of Fig. 3-30 showing the subsurface cistern coming into close relationship with the non-synaptic part of an axon terminal (large arrowhead) which is making a symmetrical synapse on to the dendrite. Note the way the cistern separates from the dendritic membrane opposite the synaptic membrane specialisation and the lack of synaptic vesicles in the axon terminal opposite the cistern. Note also the electron-dense material in the extracellular cleft between the axon terminal and dendritic plasma membrane opposite the cistern; there is no similar extracellular material where the cistern is opposite the adjacent profiles (arrows). X 67,000

Fig. 3-32 Subsurface cistern in a neuronal cell soma. The lower part of the cistern (arrow) shows the normal appearance of a cistern opposed to the non-synaptic part of a symmetrical type axon terminal, whereas the upper part of the cistern (large arrowhead) appears to be partially attached to a synaptic membrane complex, a rare finding. X 53,000

Fig. 3-33 Higher magnification of the subsurface cistern in Fig. 3-32. Note the dense material both between the subsurface cistern and the neuronal plasma mambrane and in the extracellular cleft between the neuronal plasma membrane and that of the axon terminal. This figure also illustrates the close similarity between the membrane specialisations associated with these subsurface cisternae and those of a symmetrical synapse. X 92,000

Fig. 3-34 Subsurface cisternae in the soma of a small neuron stained with E-PTA. The position of the unstained plasma membrane is indicated by the large arrowhead. X 47,000

Fig. 3-35 Complex subsurface cistern in a neuronal cell soma. Note the difference in appearance of the stacks of cisternae to the left and right of the large arrowhead. X 29,000

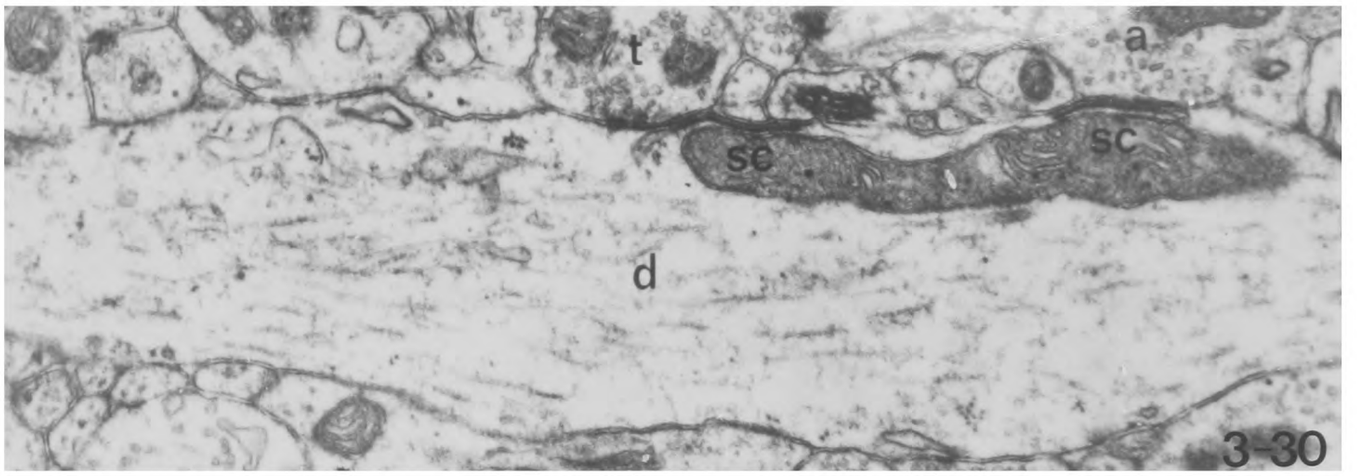

3-30

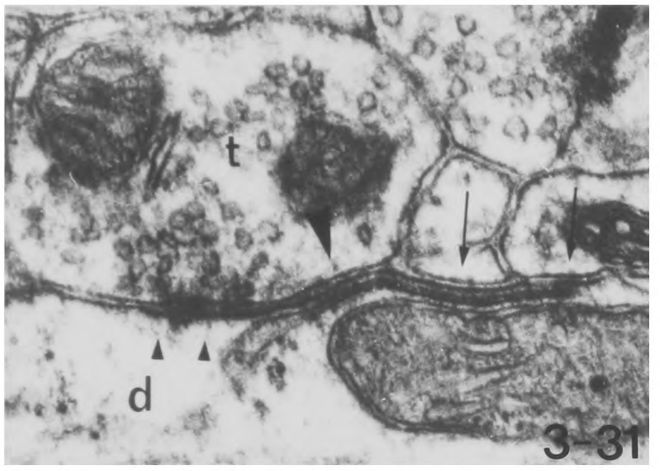

3-31

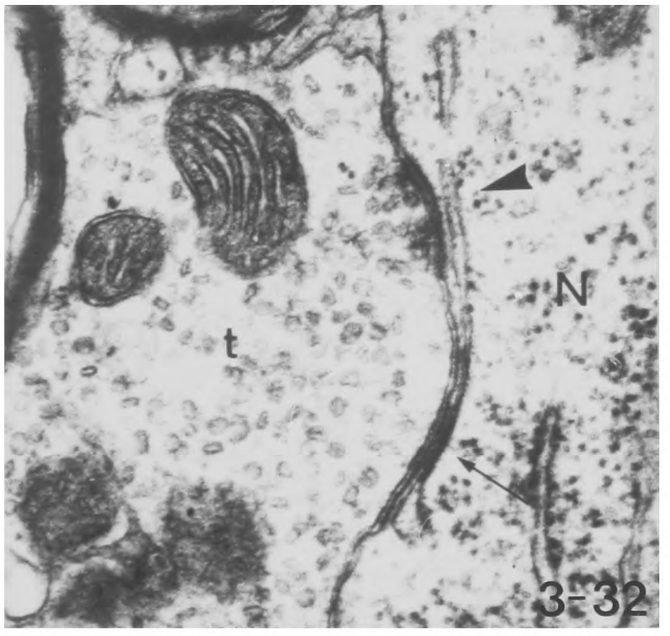

3-32

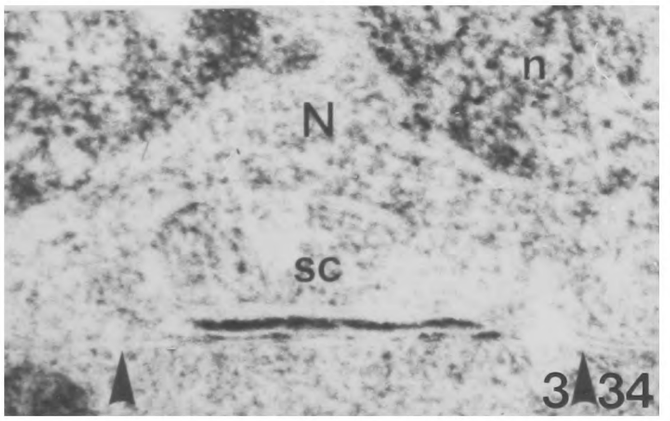

3-34

3-33

3-35

Fig. 3-36 Dendrite with a coated pit (arrowhead) apparently engulfing a portion of the adjacent axon terminal. X 29,000

Fig. 3-37 Higher power of Fig. 3-36 showing the cytoplasm of the axon terminal extending into the coated pit (arrowhead) and apparently being pinched off. X 67,000

Fig. 3-38 Coated pit (arrowhead) in continuity with the plasma membrane of a myelinated axon inside its myelin sheath and containing electron-dense material. X 45,000

Fig. 3-39 Synaptic membrane complex, spine apparatus and desmosome stained with E-PTA. Note the presynaptic dense projections (small arrow) of the presynaptic membrane complex, the unstained plasma membranes of both axon terminal and spine and the dense material both in the synaptic cleft and beneath the postsynaptic membrane. In contrast to the synaptic complex the desmosome (arrowhead) has no presynaptic projections. X 67,000

Fig. 3-40 Spine apparatus stained with E-PTA in a spine which is largely surrounded by a synaptic membrane complex. X 53,000

Fig. 3-41 Spine and spine apparatus stained with PTA <u>following</u> pre-osmification. Note that the plasma membranes are stained and that the dark staining of the dense plates of the spine apparatus and the synaptic membrane complex are inhibited. X 53,000

Fig. 3-42 Cilium in a neuron prepared conventionally. Note the undercoating beneath the cell membrane where it extends up the shaft of the cilium (arrowhead). X 29,000

Fig. 3-43 and 3-44 Nucleoli of a neuron stained with E-PTA and normal techniques respectively. Note that the paler staining of the pars granulosa (pg) in relation to the other parts of the nucleolus in the nucleolus stained with E-PTA (Fig. 3-43) compared with that stained normally. X 24,000 and 21,000

Fig. 3-45 Cilium stained with E-PTA. Note the dark staining of the membrane undercoating in the initial part of the cilium (arrowhead) (cf. Fig. 3-42) X 29,000


c
t
d
3-36

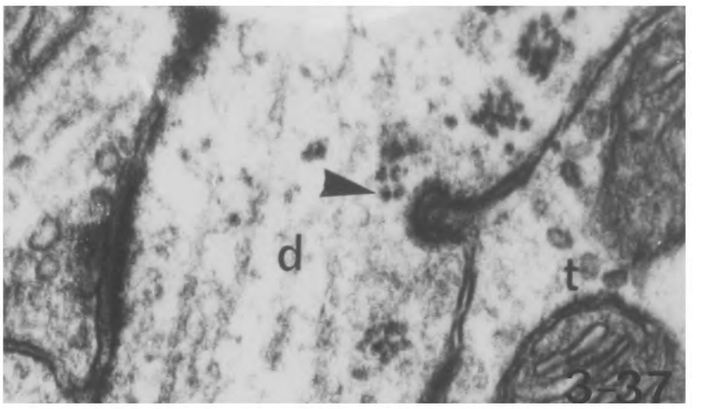
d
t
3-37

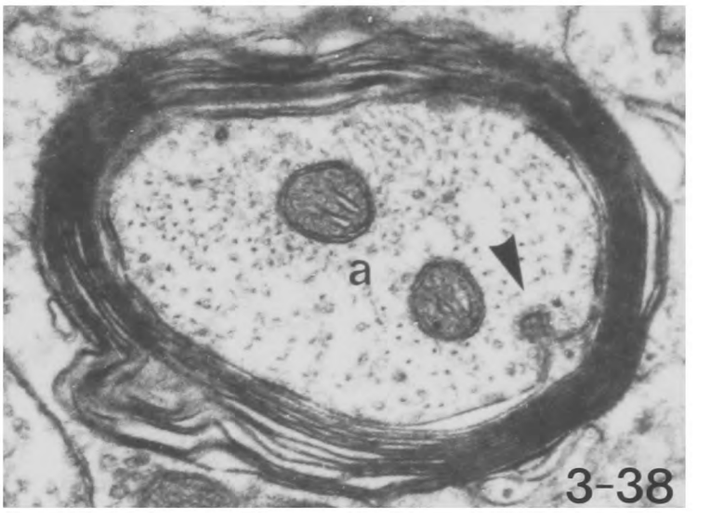
a
3-38


s
3-39

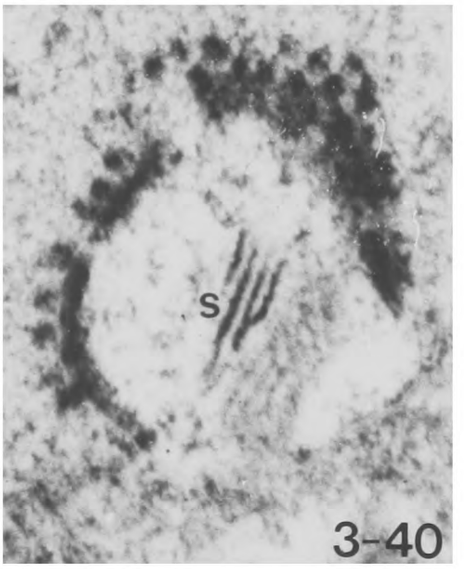
s
3-40

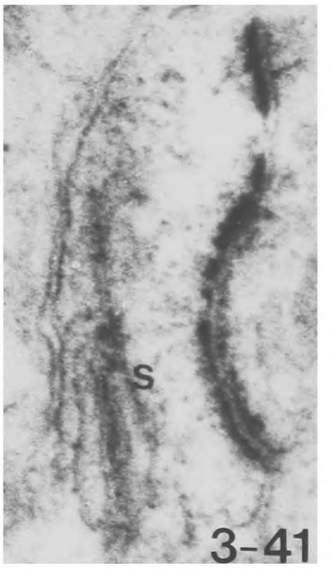
s
3-41


ci
c
3-42

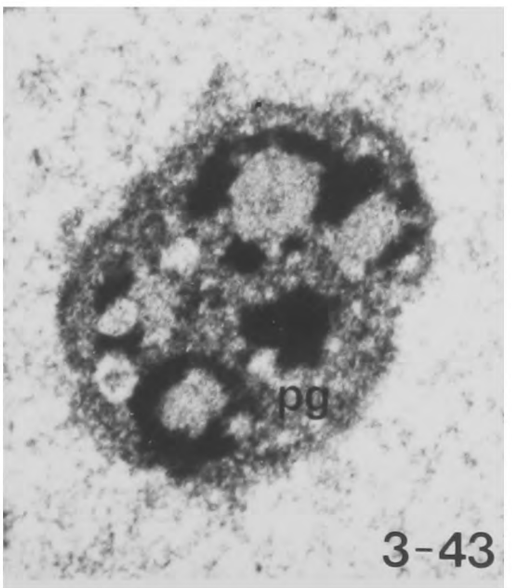
pg
3-43

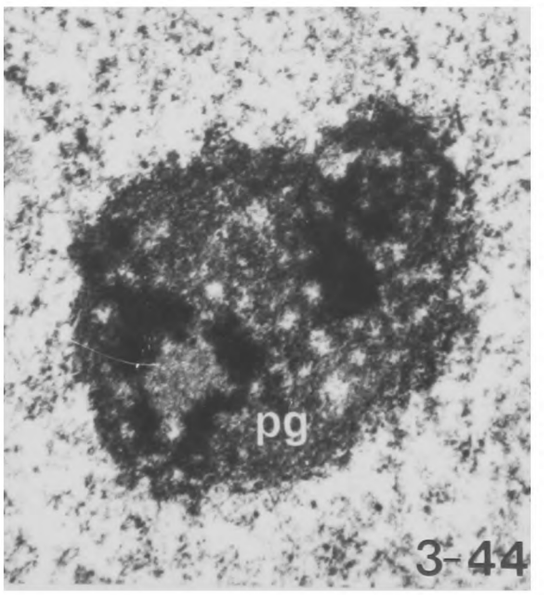
pg
3-44

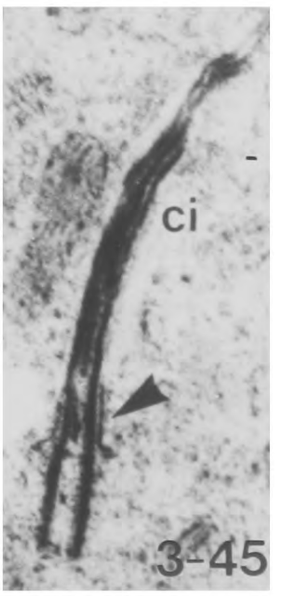
ci
3-45

Illustrations to Chapter 4

A QUALITATIVE AND QUANTITATIVE STUDY OF THE NEURONS OF THE MOTOR AND SOMATIC SENSORY CORTICES

Fig. 4-1 A pyramidal and two small stellate neurones from layer II of the motor cortex. Note the more darkly staining nuclei with clumped chromatin of the small stellate cells and their paler cytoplasm containing few organelles. X 4,500

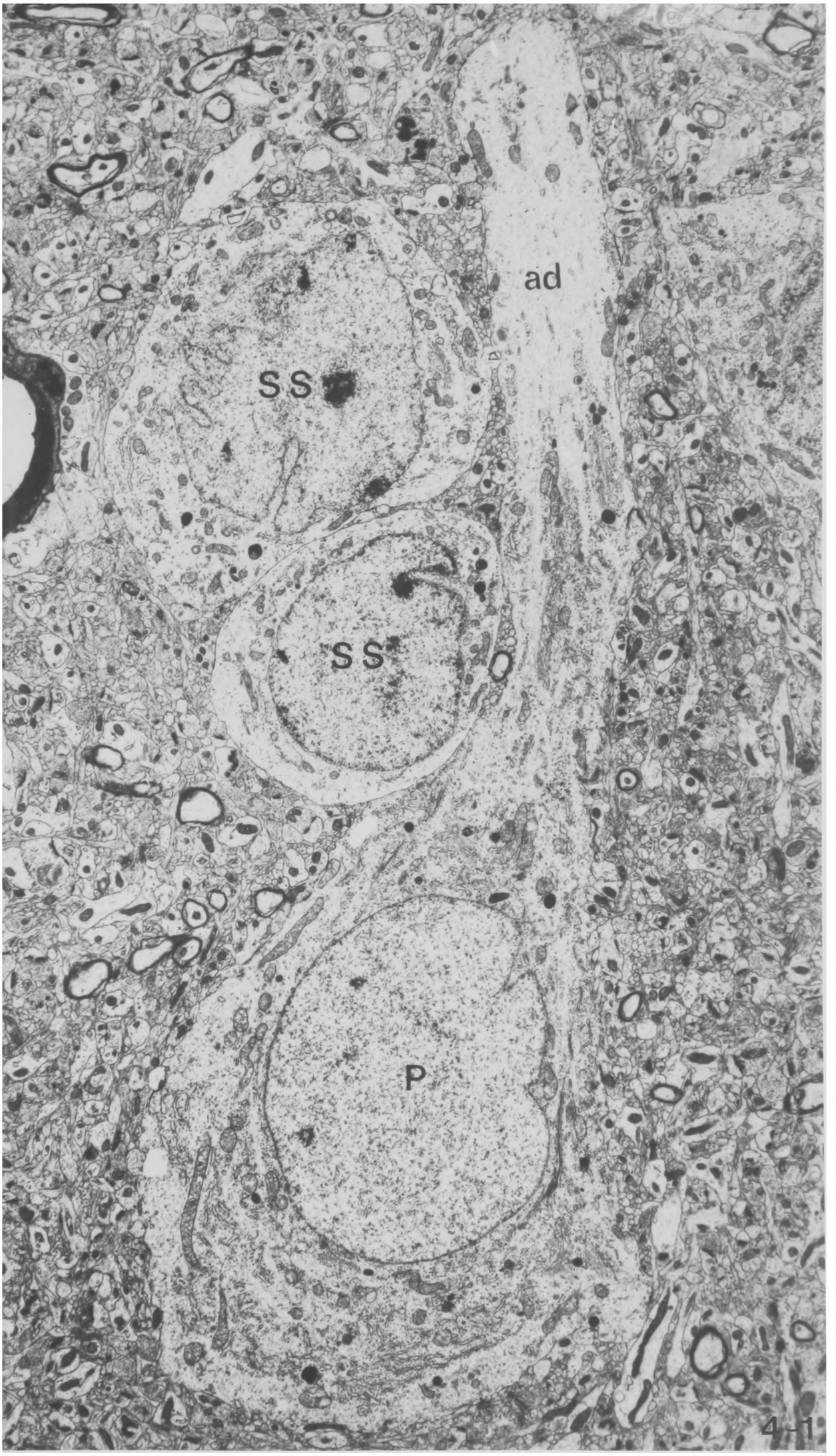

4-1

Fig. 4-2 A Betz cell from layer V of motor cortex. Note the pyramidal shape, the indented nucleus which is small in relation to the large amount of cytoplasm, and the clusters of endoplasmic reticulum. X 2,600

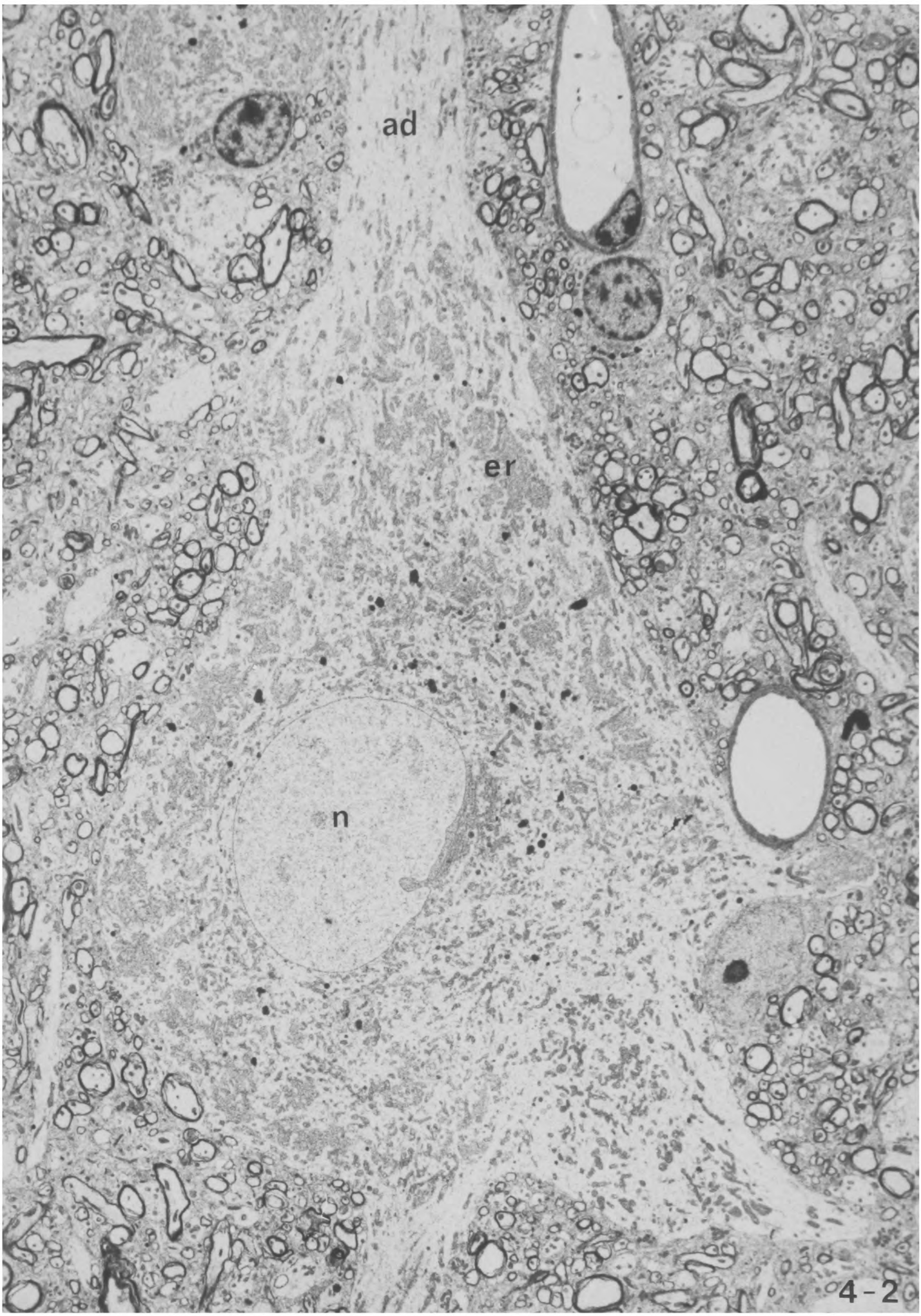

4-2

Fig. 4-3 The same Betz cell as in Fig. 4-2 in a serial "thick" section, stained with toluidine blue and seen under the light microscope. This Betz cell was initially found in the "thick" section and serial thin sections were then cut to study it in detail. X 850

Fig. 4-4 Detail of the nucleus of a Betz cell showing the characteristic complex nuclear indentations (arrowhead) and their associated cisternae of endoplasmic reticulum. The apical dendrite of the Betz cell is toward the top of the picture. X 3,900

Fig. 4-5 Part of the cytoplasm of a Betz cell showing the characteristic clumps of endoplasmic reticulum and also mitochondria and dense bodies. X 8,400

Fig. 4-6 Part of the soma of a Betz cell which receives two symmetrical axosomatic synapses from pale axon terminals containing flattened vesicles. Note also the clumps of rough endoplasmic reticulum. X 29,000

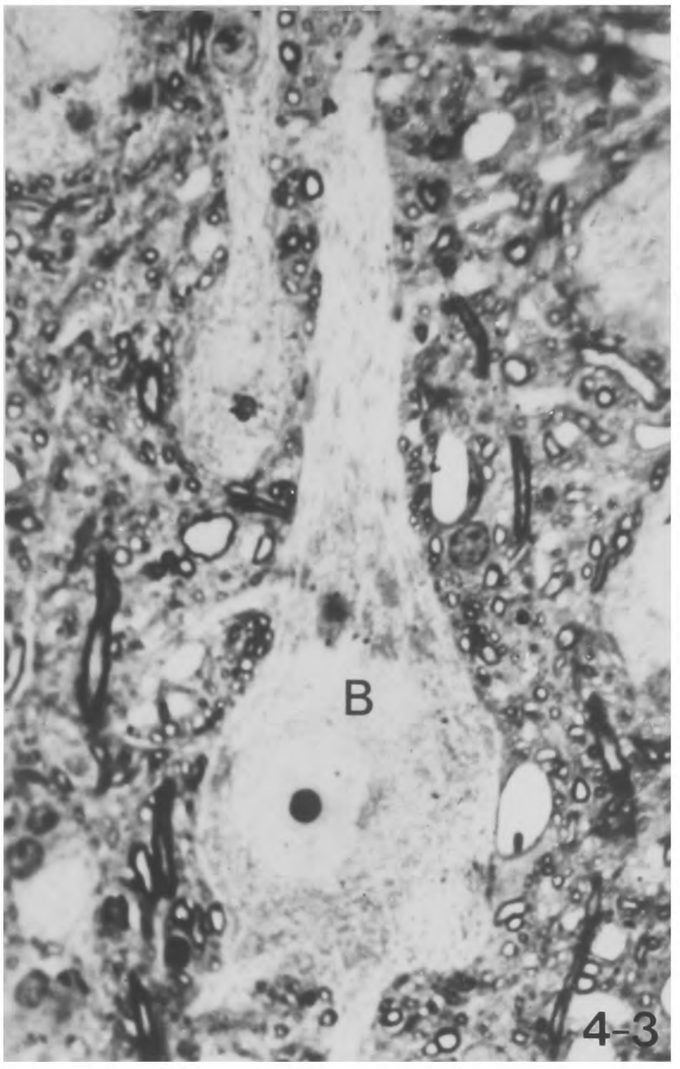

4-3

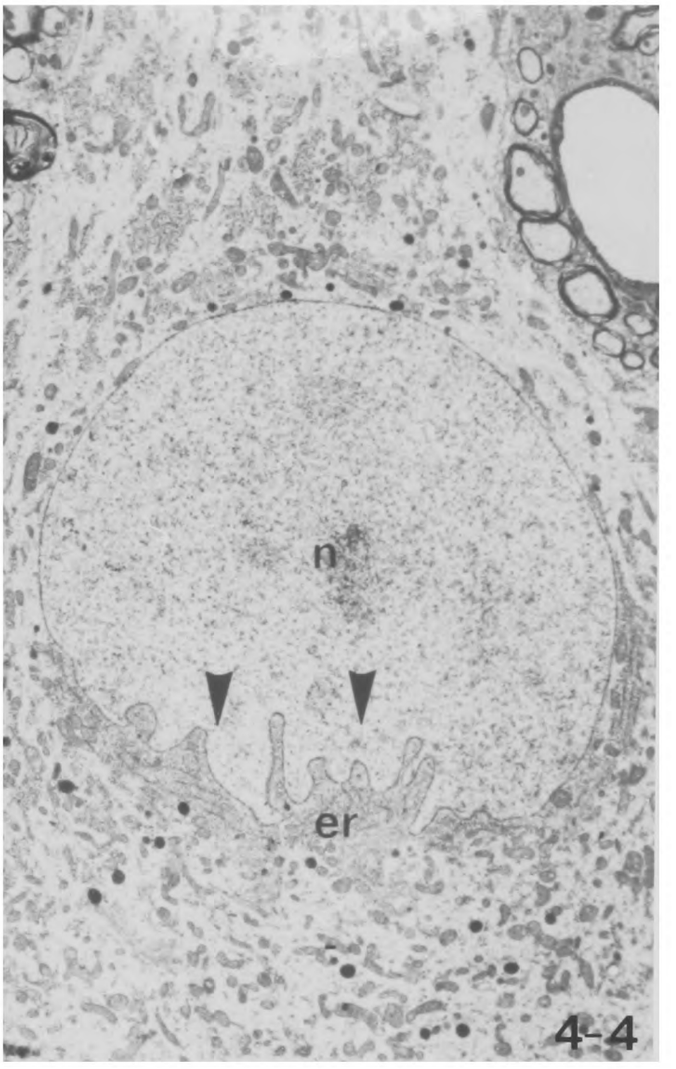

4-4

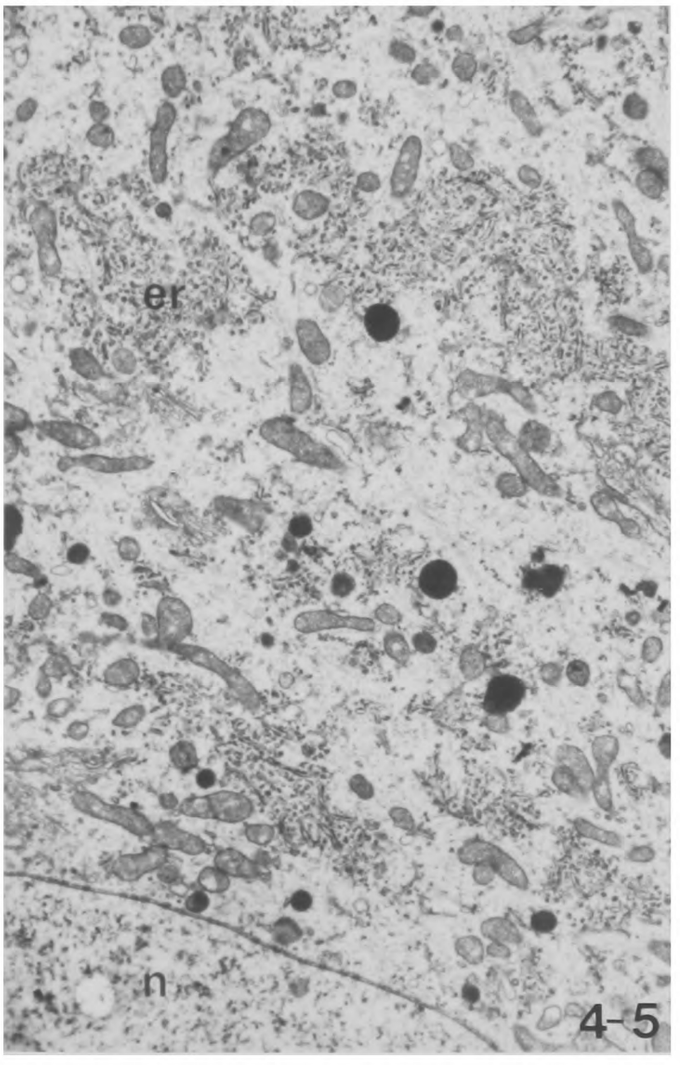

4-5

4-6

Fig. 4-7 Large stellate neuron from layer III of the motor cortex. Note the abundant cytoplasm full of organelles. The cell soma and dendrite receive a considerable number of synapses although not as many as in many examples. X 11,000

Fig. 4-8 The origin of the initial segment of the large stellate cell of fig. 4-7 from the continuation of its dendrite in a close serial section. The black bar occupies an equivalent position on the two illustrations. Note the curvature of the first part of the initial segment. X 11,000

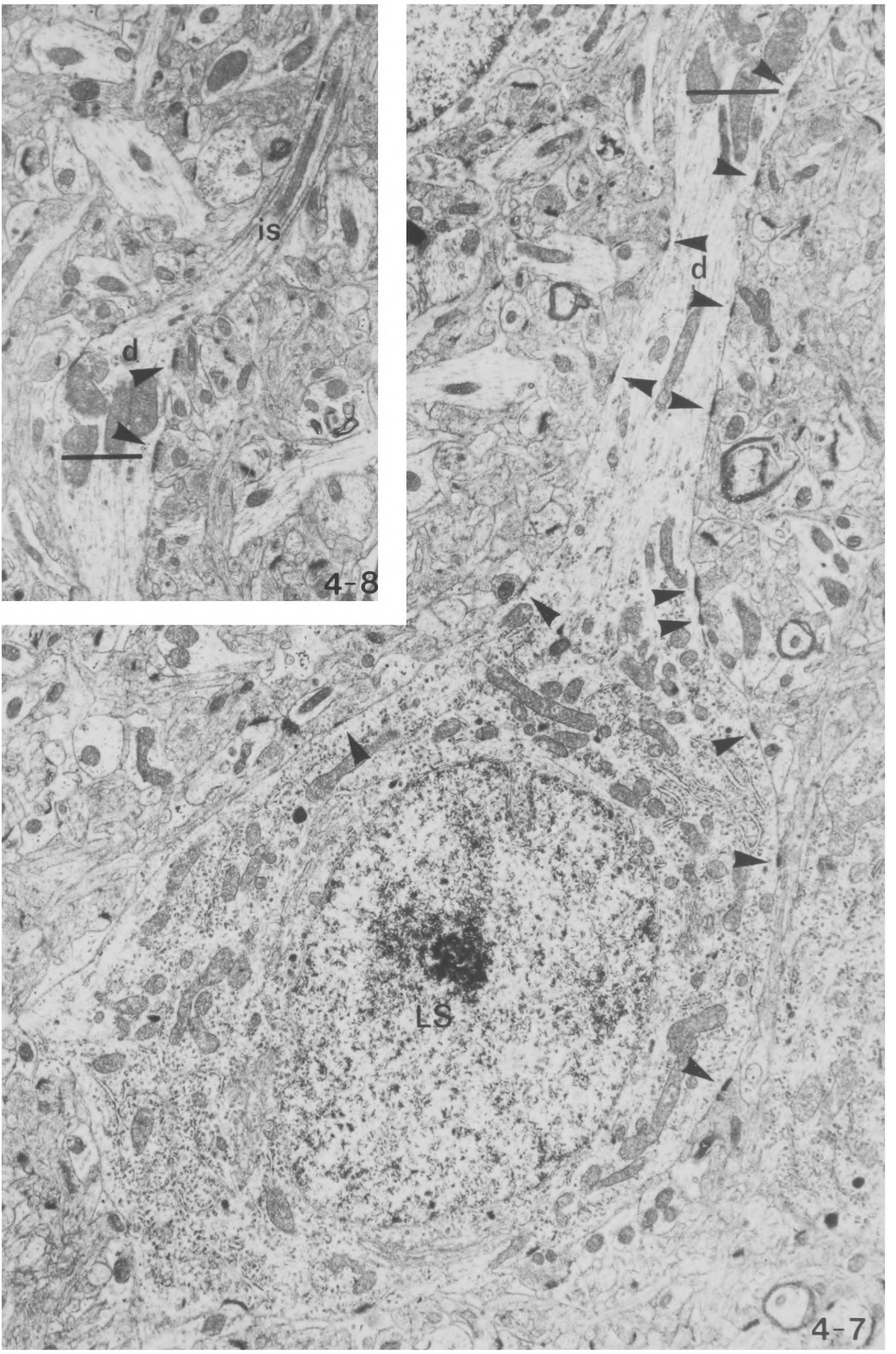
is
d
4-8
d
LS
4-7

Fig. 4-9 The dendrite of a large stellate cell from motor cortex which is unusual in having a spine. Note the large number of asymmetric synapses received by the shaft of the dendrite and the high concentration of organelles in its cytoplasm. X 14,000

Fig. 4-10 Transverse section of a large stellate dendrite from layer IV of somatic sensory cortex. Note the large number of synapses it receives, including a clearly asymmetric one, and the high density of mitochondria and ribosomes in its cytoplasm. X 29,000

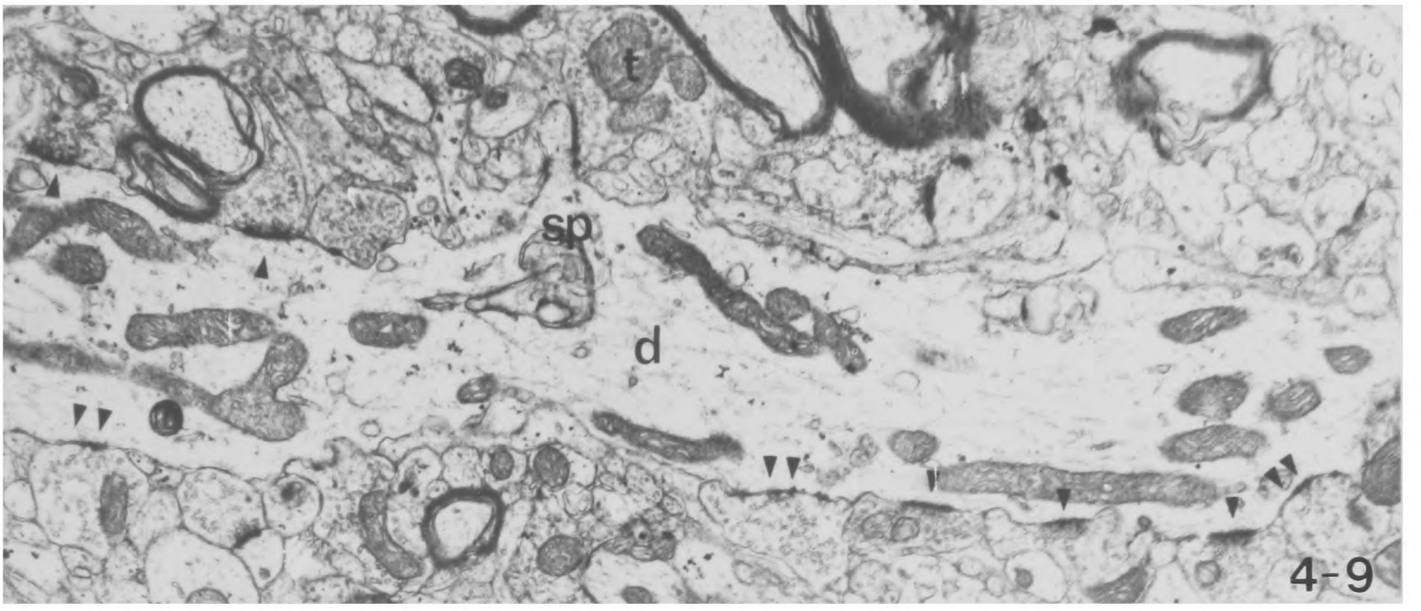

4-9

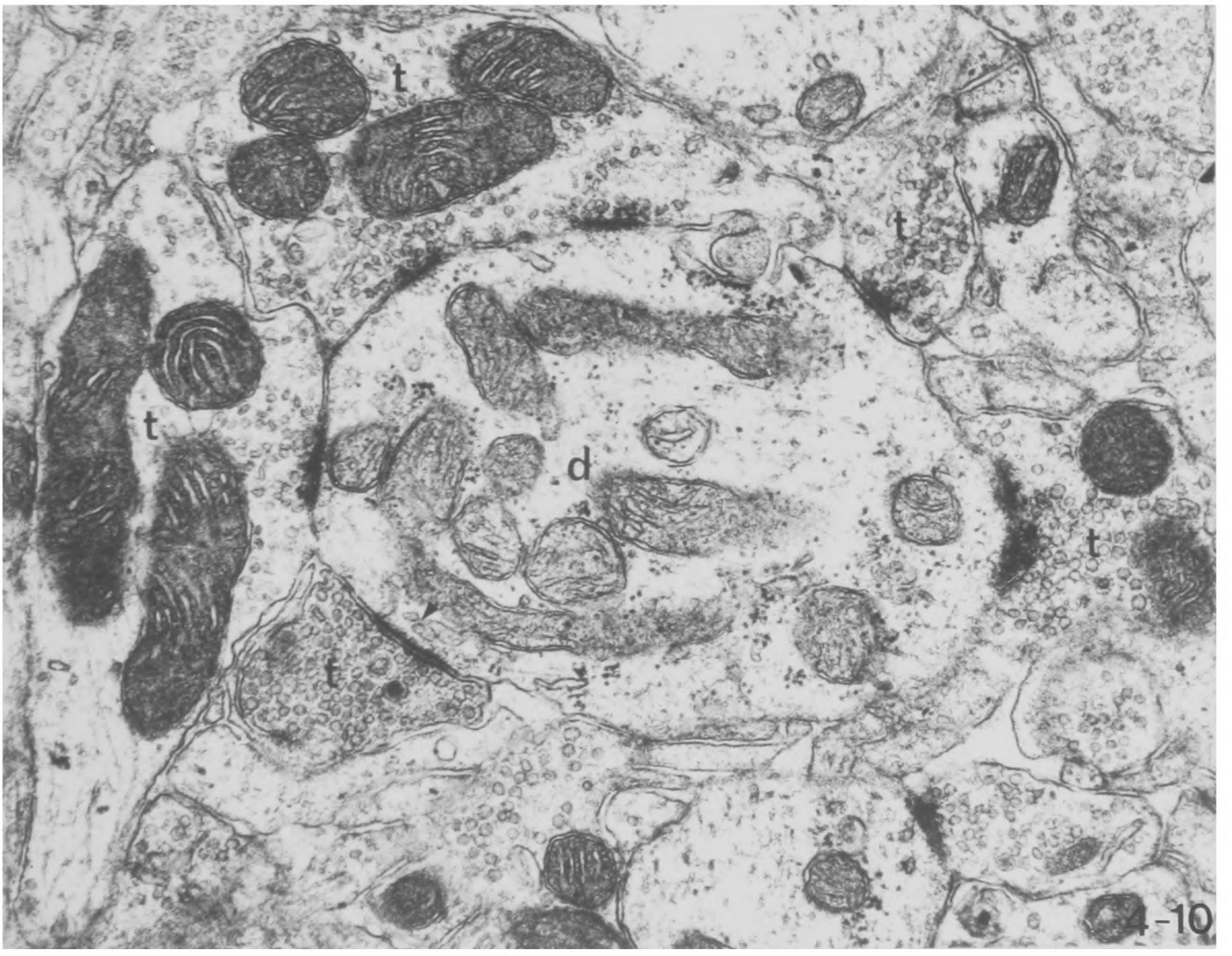

4-10

Figs. 4-11 and 4-12 Round small stellate cell from layer II of the motor cortex which receives an asymmetric synapse (arrowhead, lower left) which is shown at higher magnification in fig. 4-12. Note the indented nucleus with darkly staining clumped chromatin and the pale cytoplasm with few organelles.

X 8,400 and 29,000

Figs. 4-13 and 4-14 Round small stellate cell from layer II of the somatic sensory cortex (Area 3b)which receives an asymmetric synapse on its dendrite (arrowhead), shown at higher magnification in fig. 4-13 . Note the darkly staining clumps of chromatin in its indented nucleus and its pale cytoplasm.

X 29,000 and 8,400

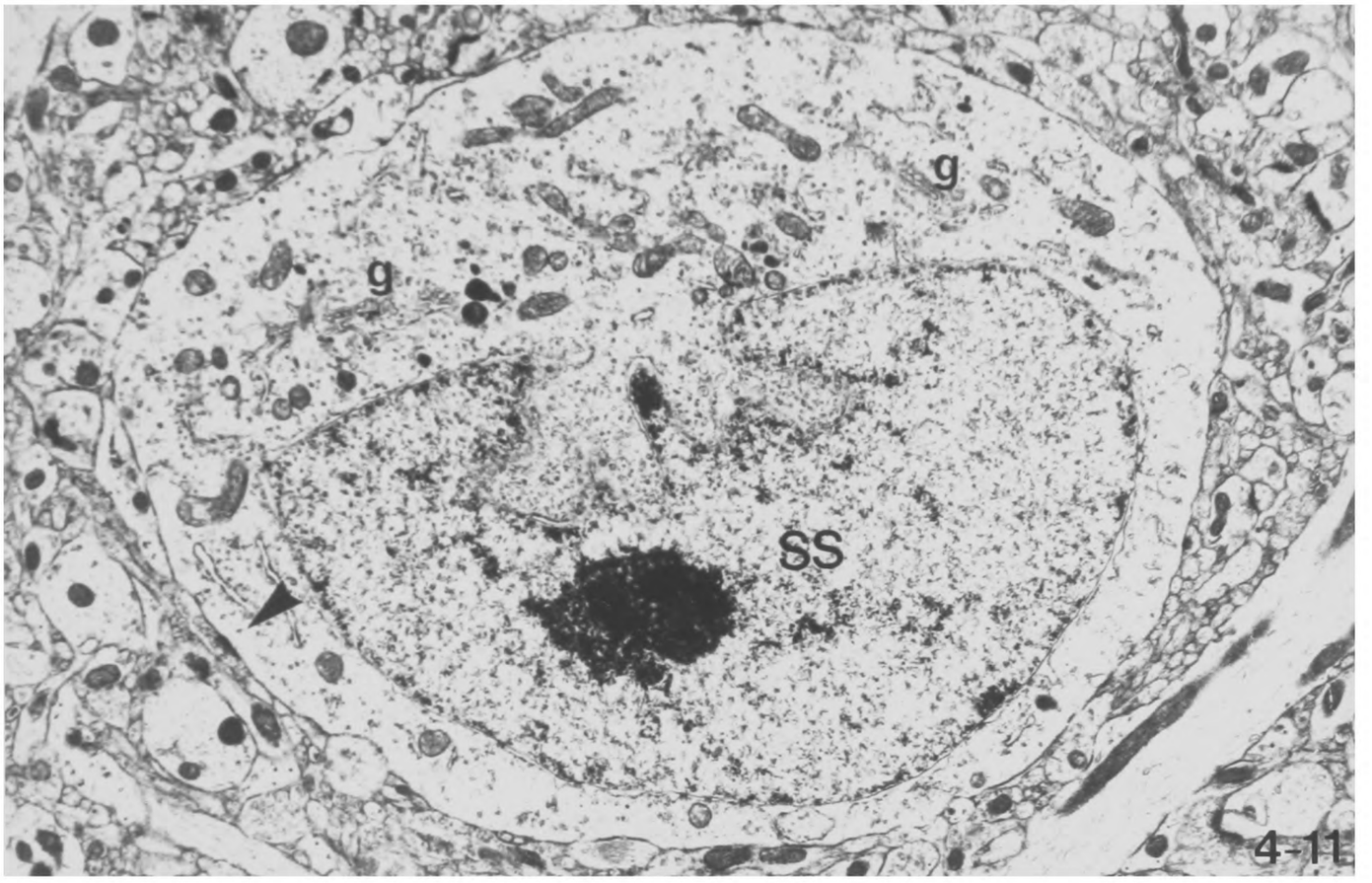

4-11

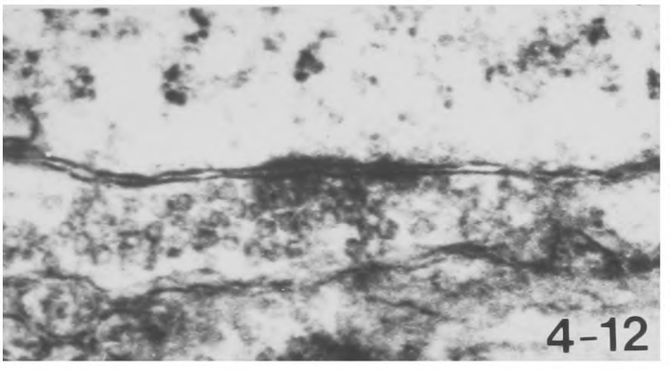

4-12

4-13

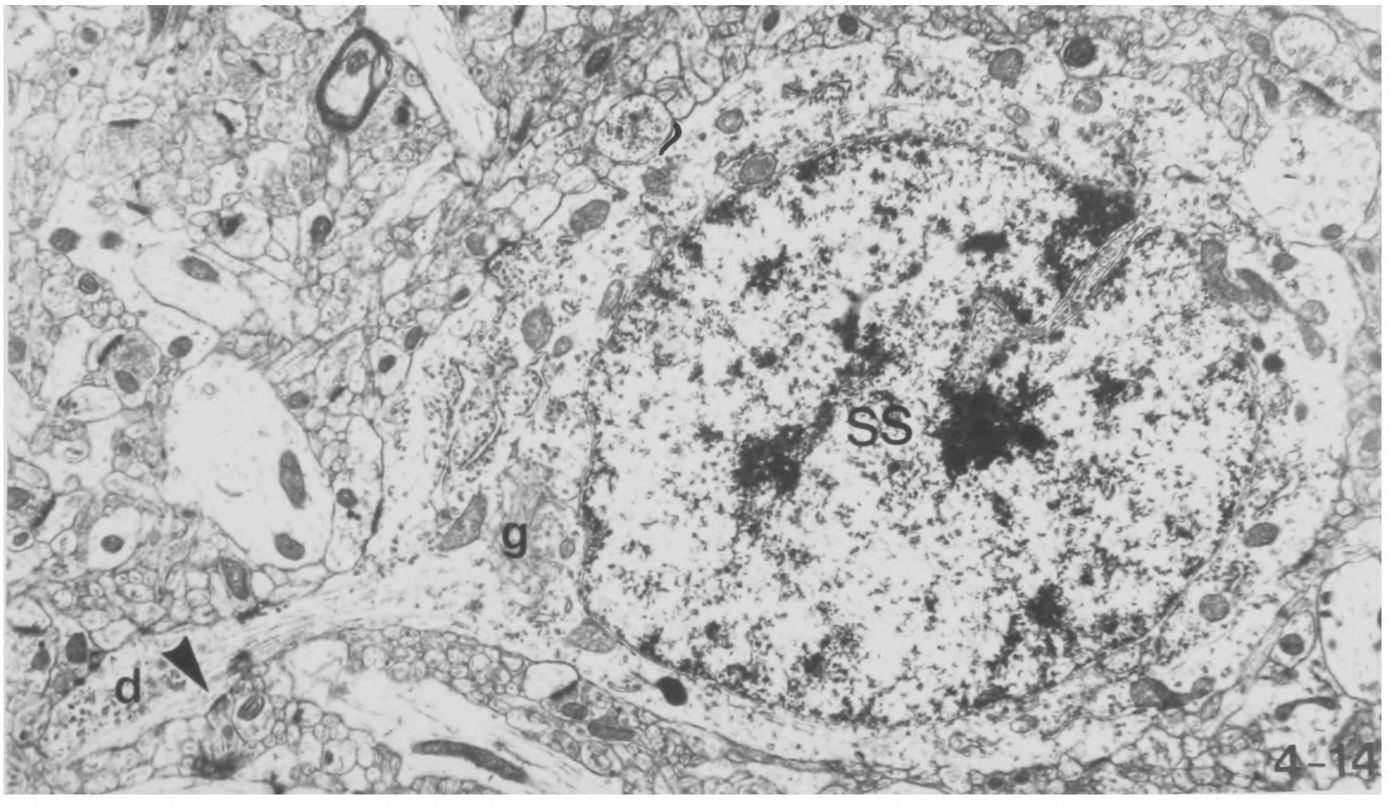

4-14

Fig. 4-15 Fusiform small stellate cell from layer V of motor cortex. Note the dark nucleus with clumped chromatin and the prominent Golgi apparatus. The cytoplasm is rather darker and has more organelles than a round small stellate, but the cell receives only one synapse in this section. X 9,000

Fig. 4-16 Detail of the symmetrical synapse received by the neuron of Fig. 4-15. X 40,000

Fig. 4-17 Detail from a serial section of the same fusiform small stellate cell as Fig. 4-15, showing it receiving an asymmetric axosomatic synapse. A symmetrical exposed membrane thickening (arrowhead) on the spine is apposed to the plasma membrane of the neurone where it is related to a subsurface cistern. X 40,000

Fig. 4-18 The same fusiform small stellate cell as Fig. 4-15 but 20 serial sections away and showing a dendrite arising from the opposite pole of the neurone. The neurone also receives a synapse in this section (arrowhead) but in many of the sections of this series no synapse was present on this neurone. X 9,000

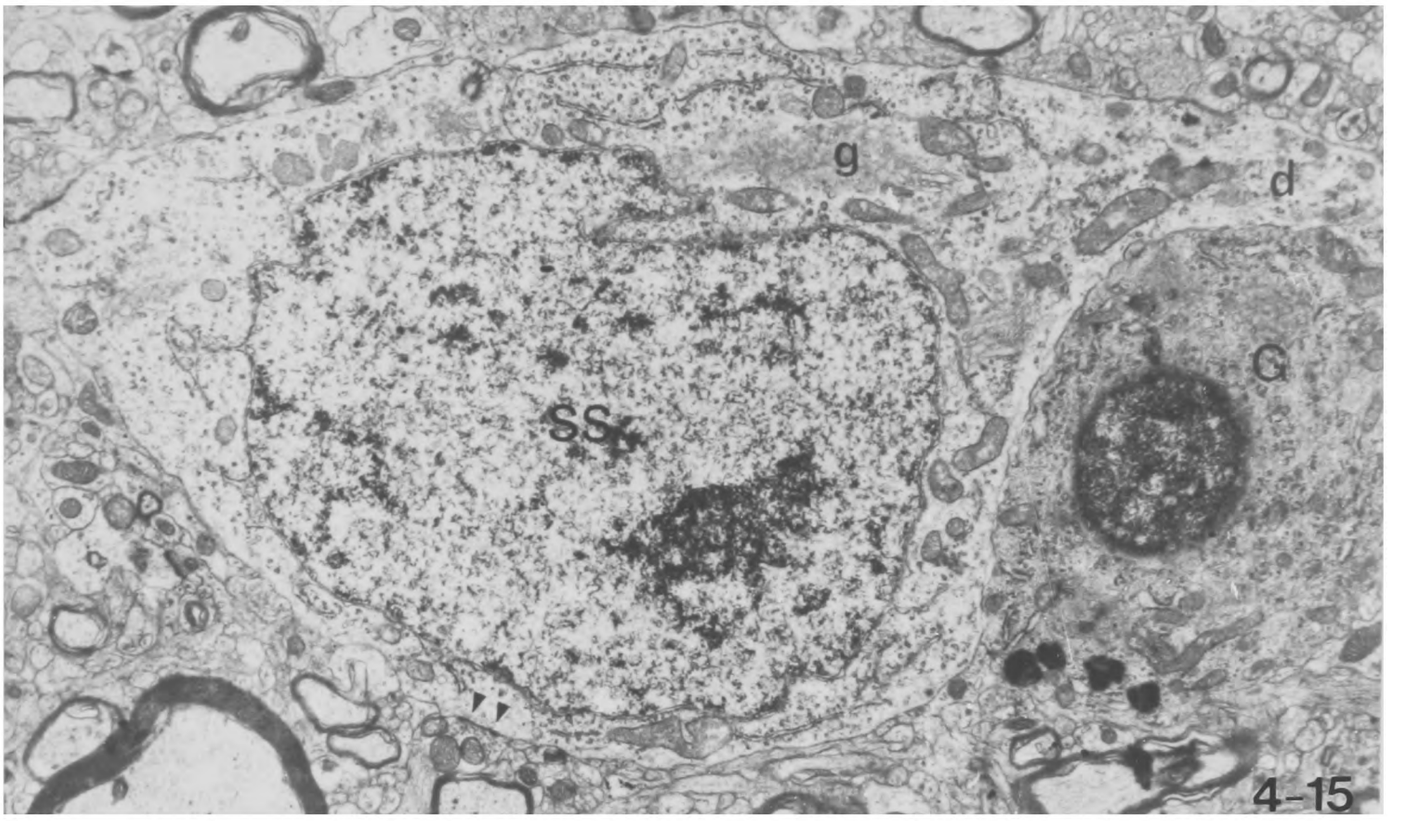

4-15

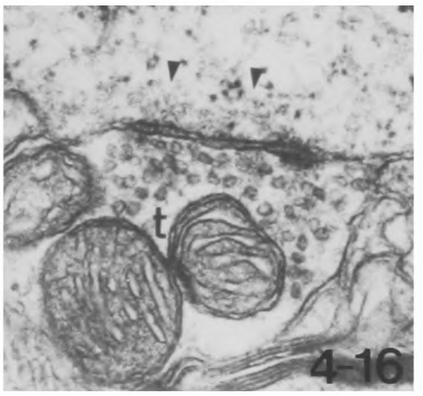

4-16

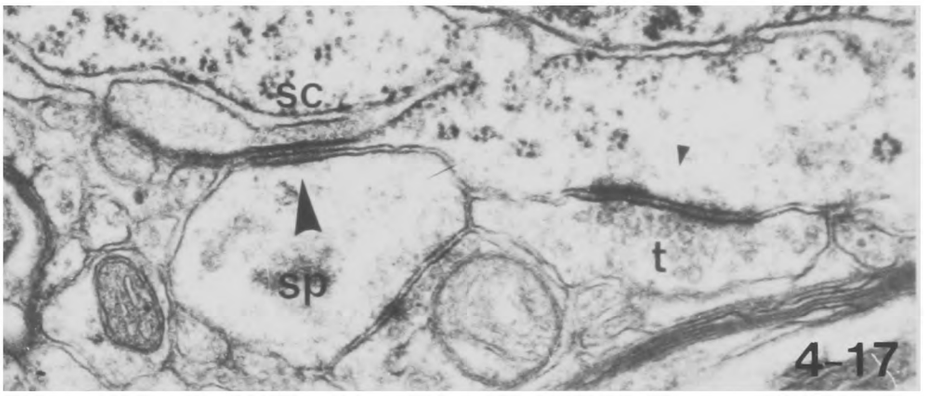

4-17

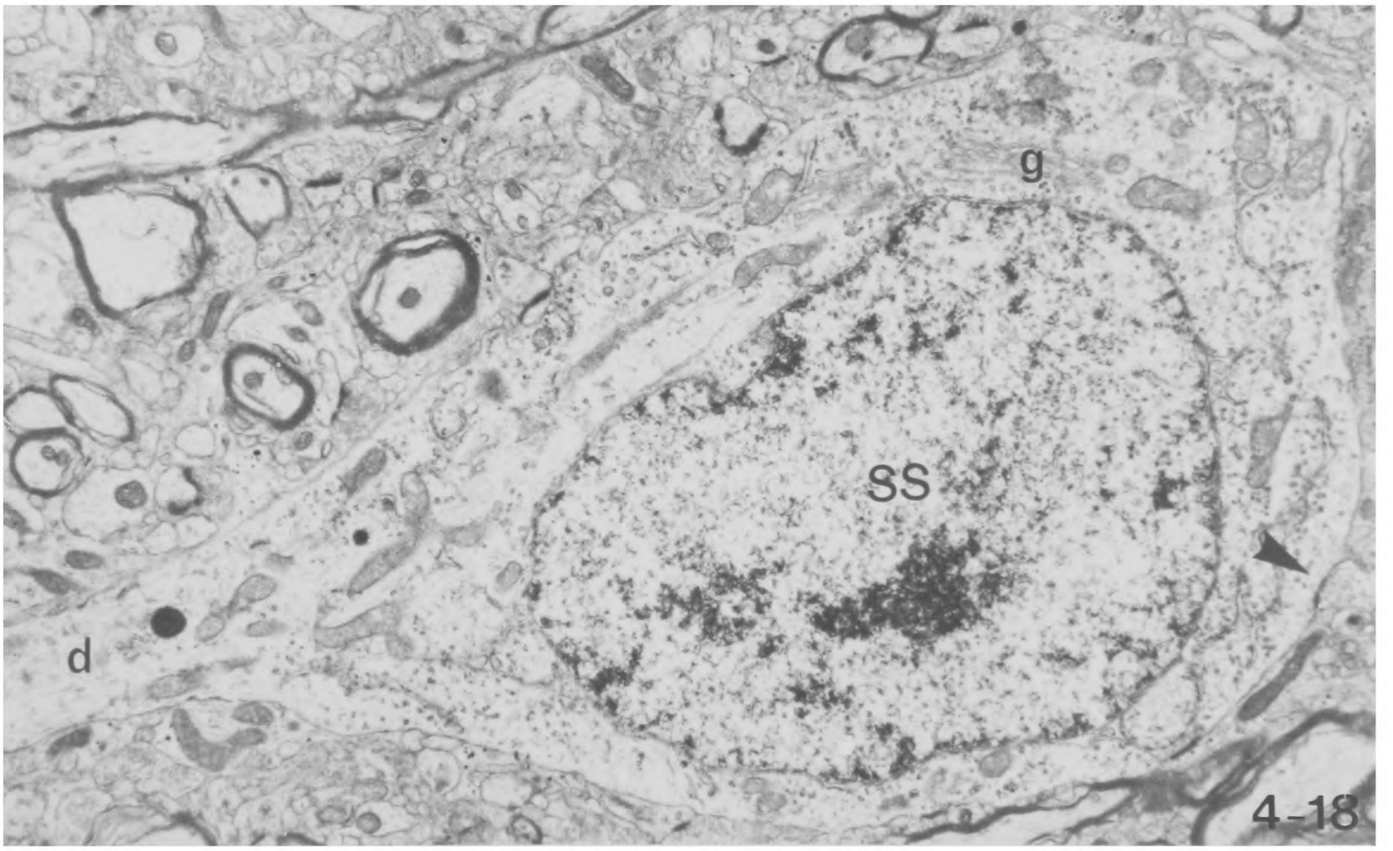

4-18

Fig. 4-19 Small stellate cell from layer V of motor cortex, showing the origin of its axon initial segment which is directed toward the surface of the cortex. X 9,000

Fig. 4-20 Higher magnification of the initial segment of the same cell as Fig. 4-19, 5 serial sections away. Note the typical bundle of neurotubules and membrane undercoating (arrowhead) in the initial segment and its small diameter. X 31,000

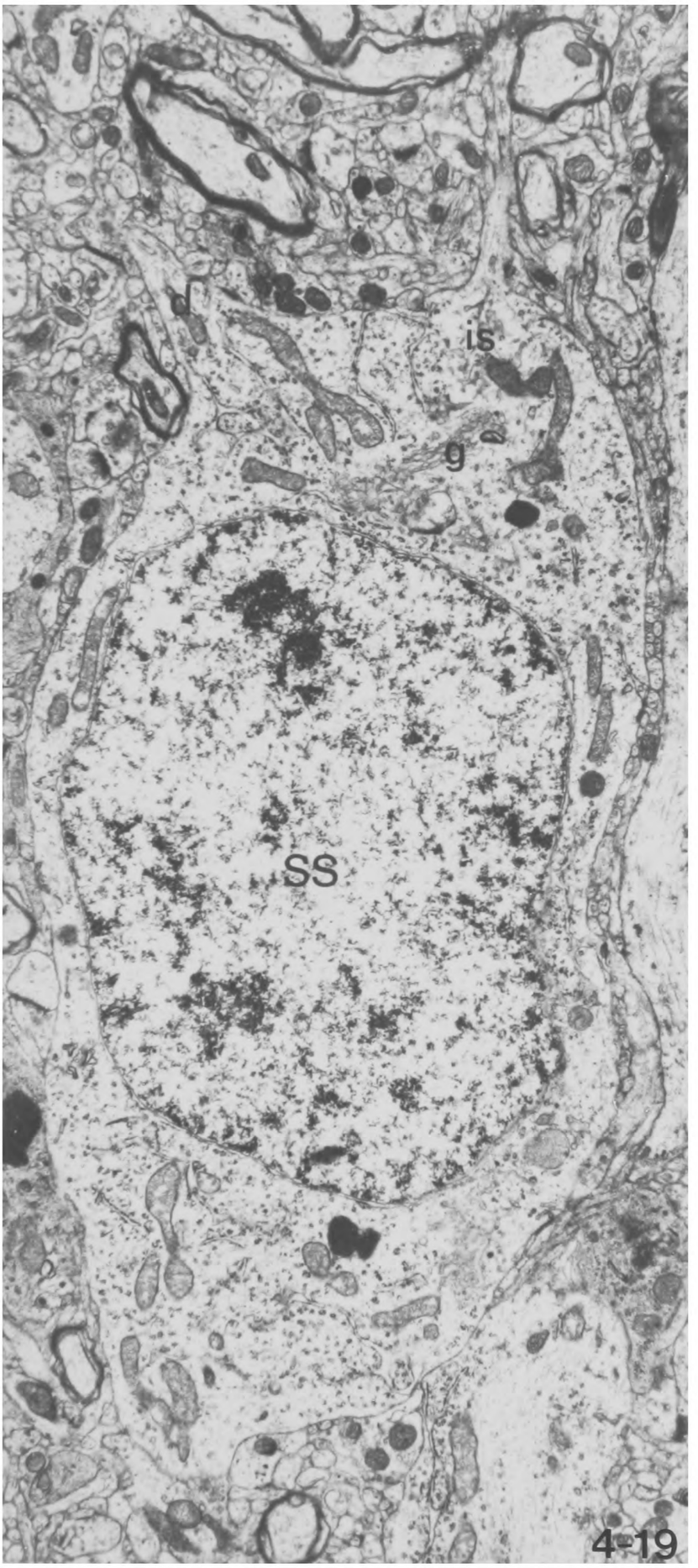

4-19

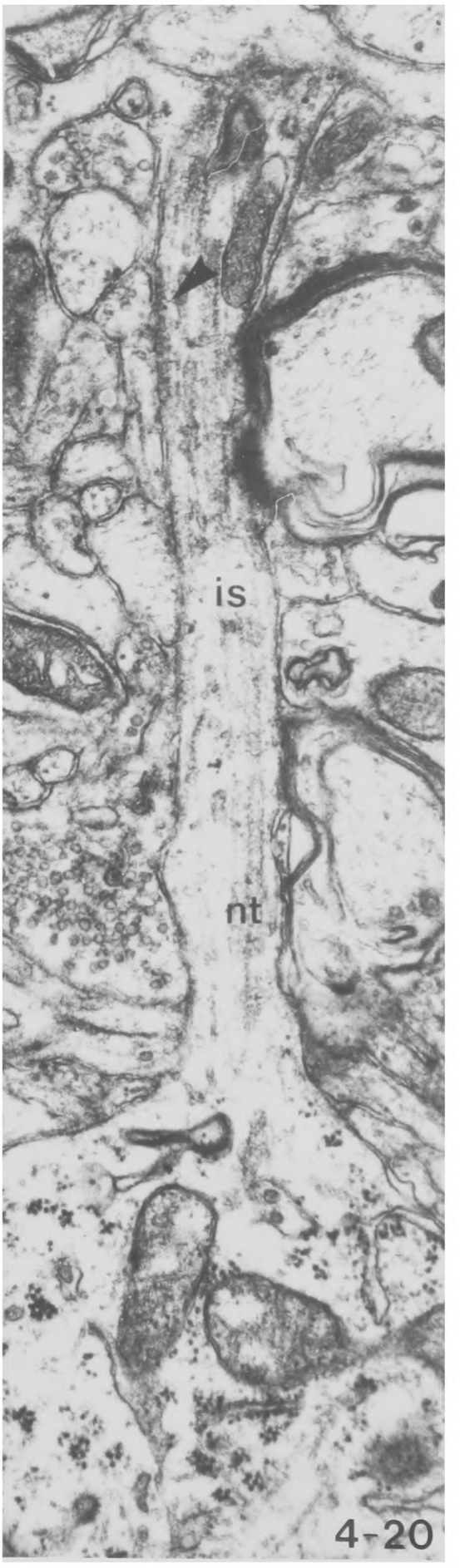

4-20

Fig. 4-21 Neuron from layer V of motor cortex. This is an example of an unusual type of neuron from layer V which is large, receives few synapses and has an axon initial segment directed towards the cortical surface, and is therefore probably a Martinotti cell. X 6,300

Fig. 4-22 Initial segment of neurone of Fig. 4-21 at higher magnification and in the next serial section. X 19,000


nt
is
4-22

d
is
4-21

Fig. 4-23 Histograms showing the distribution of mean cell diameters in motor and somatic sensory cortices.

HISTOGRAMS OF MEAN CELL DIAMETER IN MOTOR AND SOMATIC SENSORY CORTICES

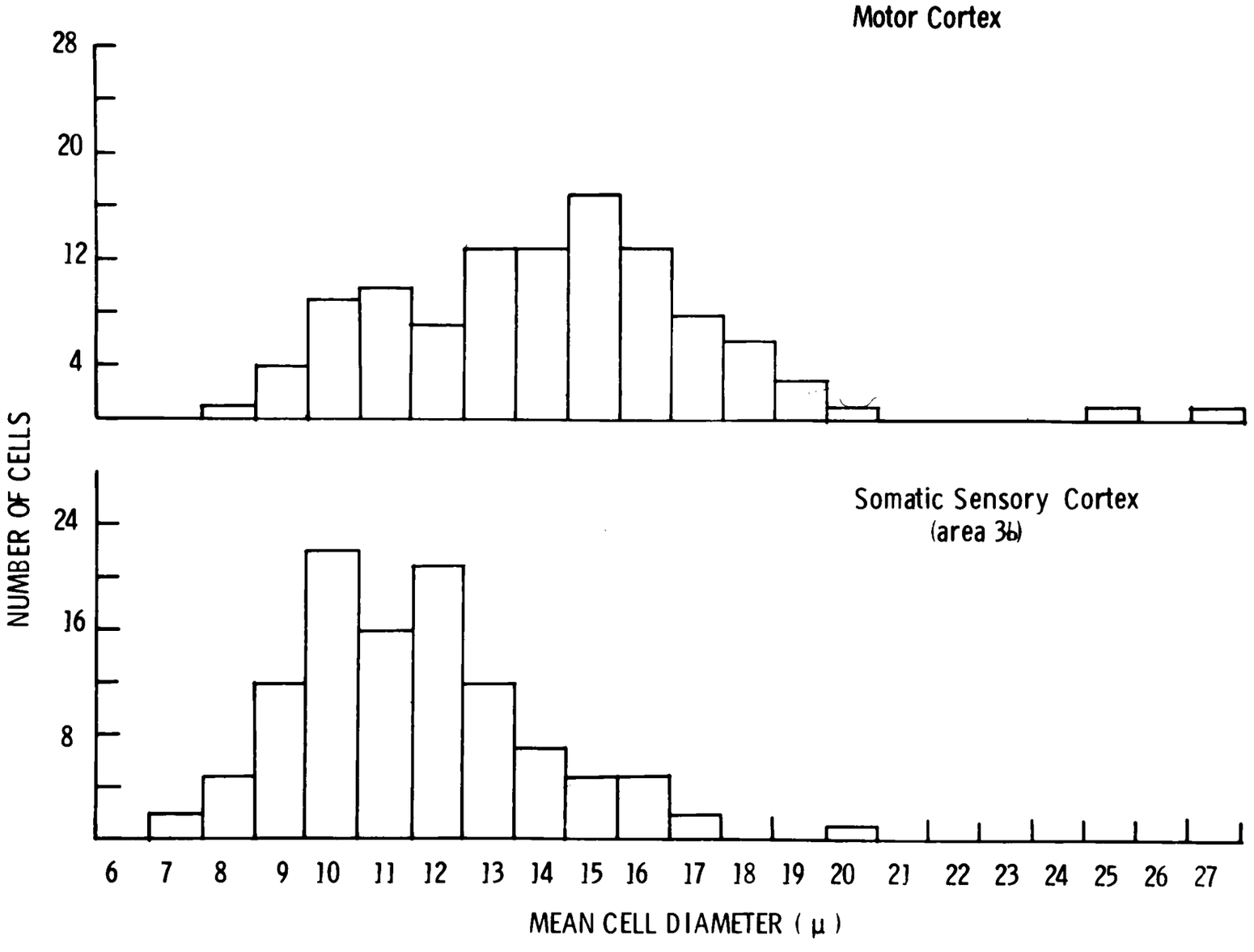

Fig. 4-24 Histogram of the size distributions of cells with and without apical dendrites in the motor cortex. Note the lack of small cells having apical dendrites.

THE FREQUENCY OF APICAL DENDRITES AT DIFFERENT CELL DIAMETERS

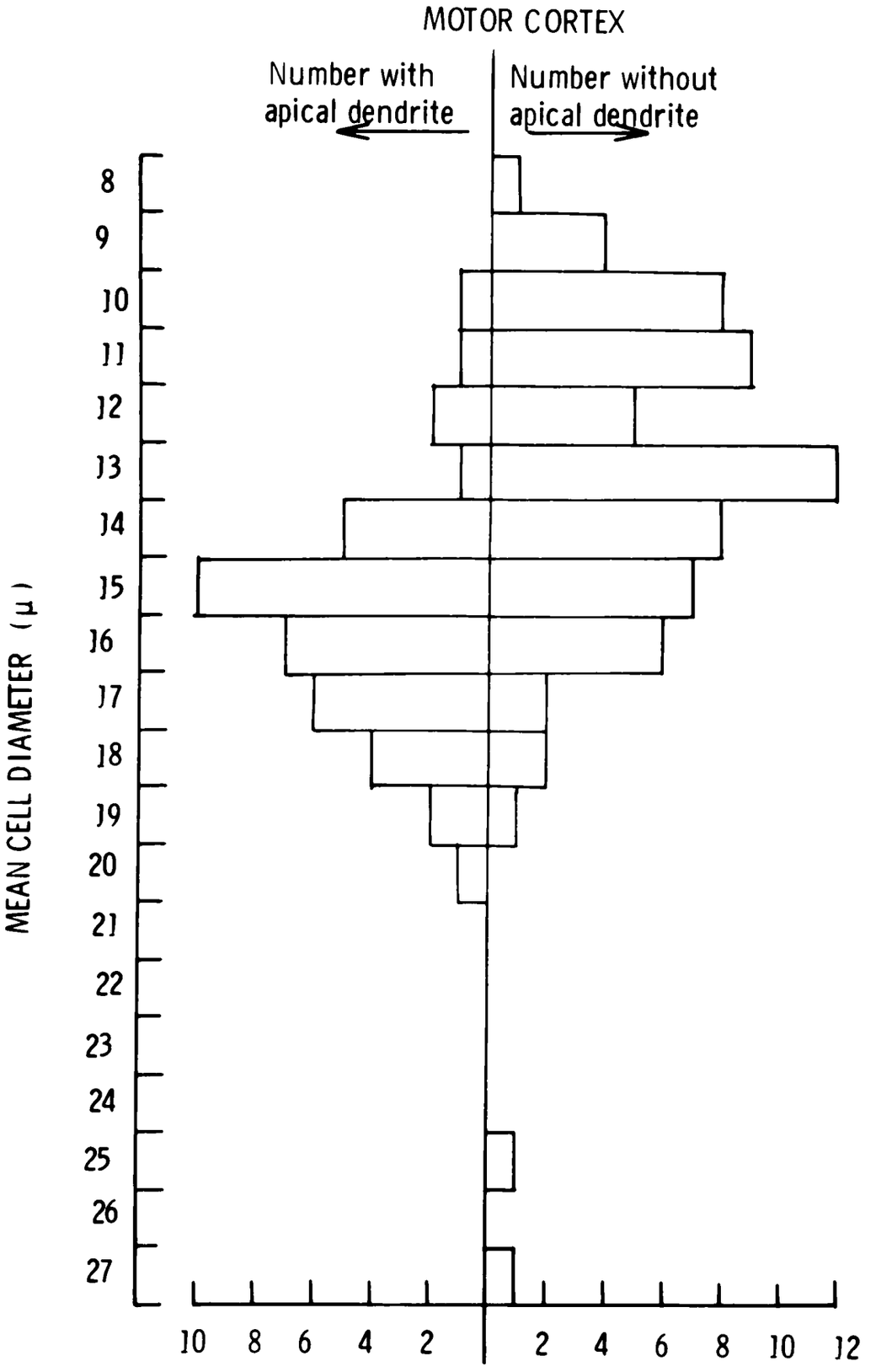

Fig. 4-25 Histogram of the size distribution of cells with and without apical dendrites in the somatic sensory cortex. Note that a smaller proportion of small neurons have apical dendrites compared to the larger neurons.

THE FREQUENCY OF APICAL DENDRITES AT DIFFERENT CELL DIAMETERS

Somatic Sensory Cortex (area 3b)

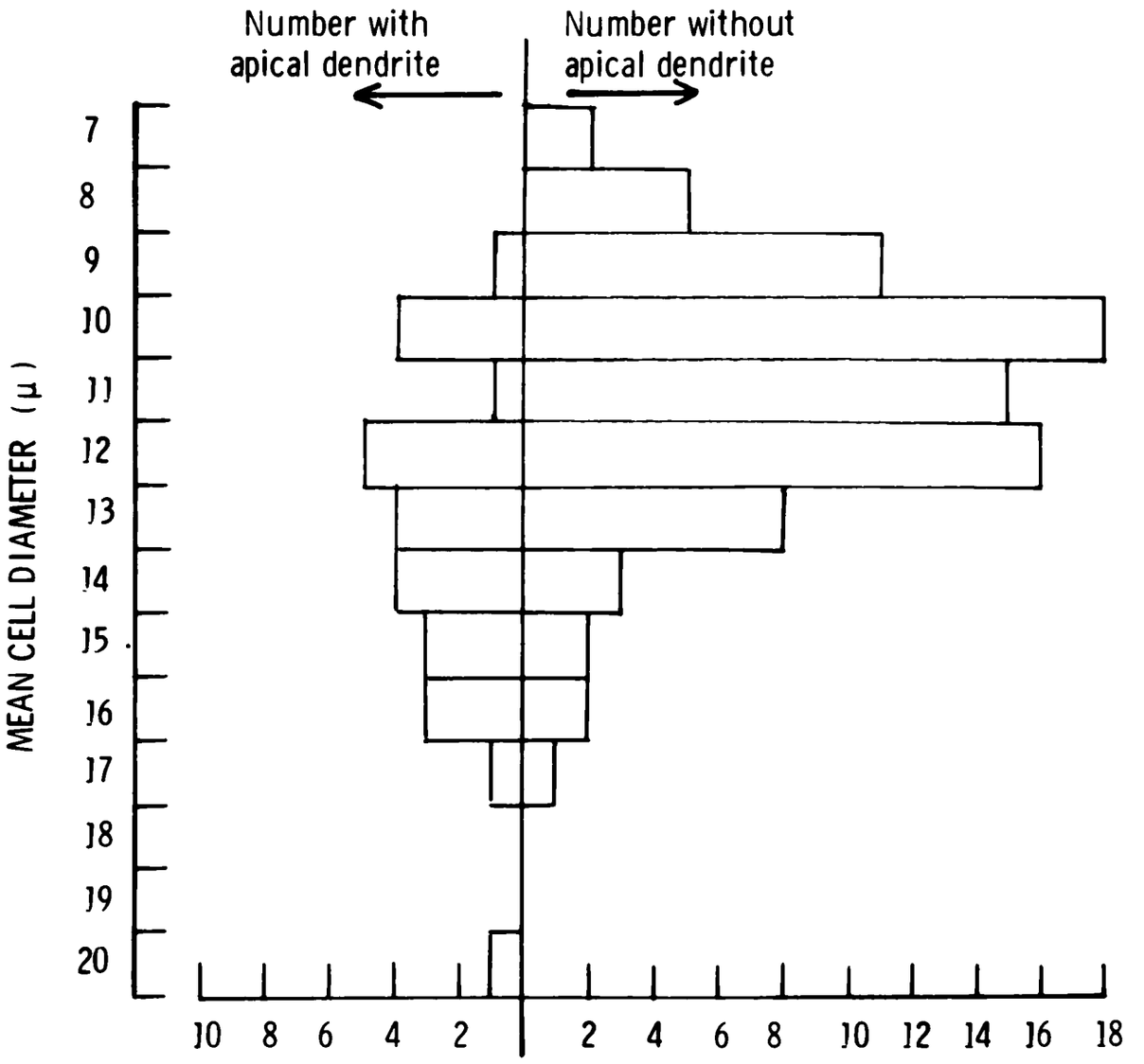

Fig. 4-26 Histograms showing the distribution of the numbers of synapses found per cell profile in a single section in motor and somatic sensory cortex. Note that only a small proportion of cells receive a large number of synapses.

NUMBERS OF SYNAPSES PER CELL PROFILE

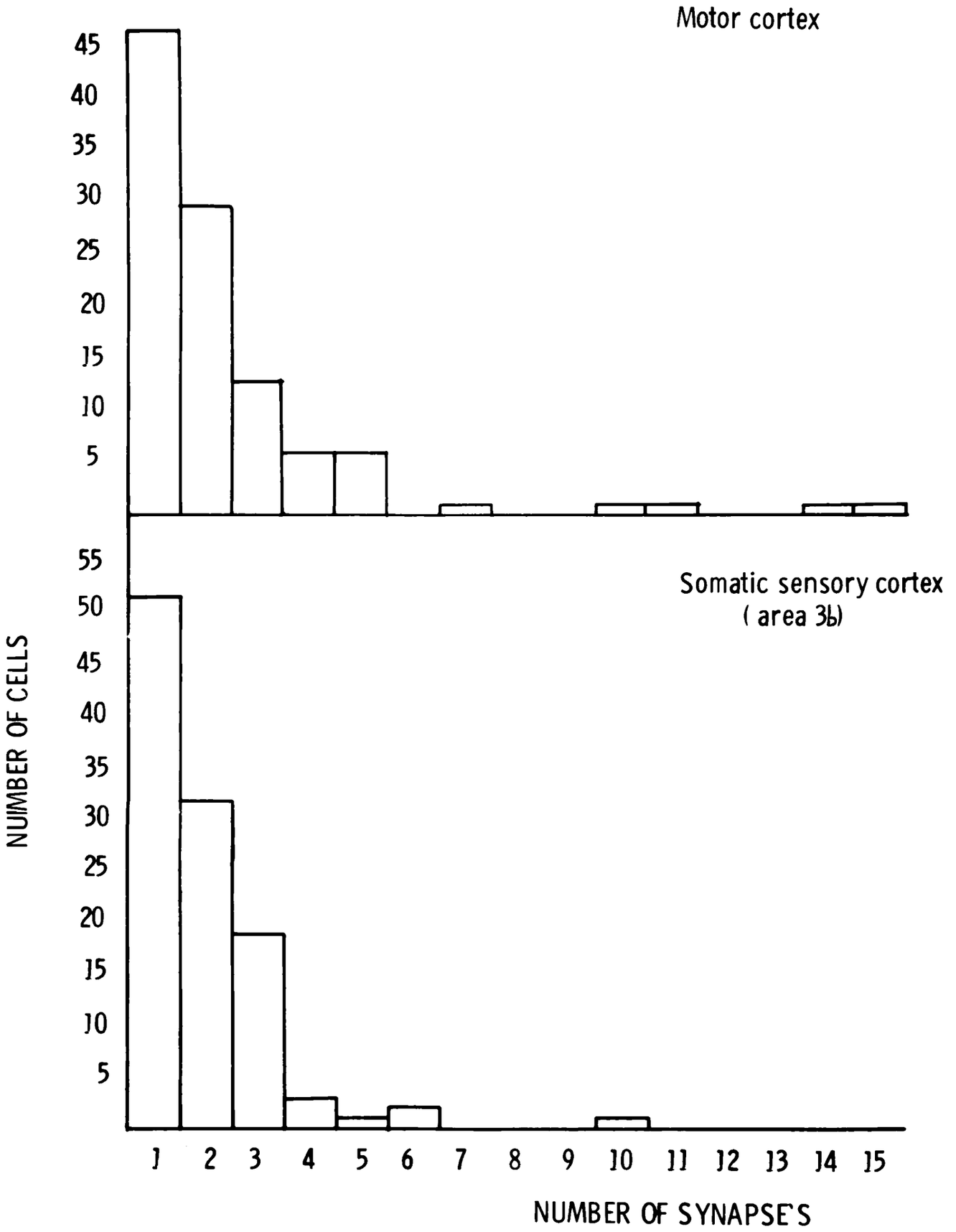

Fig. 4-27 The number of synapses received by a neurone in the motor cortex plotted against its mean diameter. Each number on the graph indicates the number of neurones having that combination of mean diameter and number of synapses. Note the neurones receiving the largest numbers of synapses do not in general have a particularly large mean diameter and that most of the largest diameter cells do not receive many more synapses than the small neurones.

NUMBER OF SYNAPSES PER CELL PROFILE AGAINST MEAN CELL DIAMETER - MOTOR CORTEX

Number of Synapses \ Mean Cell Diameter (μ)	7	8	9	10	11	12	13	14	15	16	17	18	19	20	21	22	23	24	25	26	27	28
17																						
16																						
15											1											
14																					1	
13																						
12																						
11										1												
10									1													
9																						
8																						
7								1														
6																						
5			1	1	1		1			1		1										
4							1		1	1		1		1					1			
3			1	1	2		1		2	2		2	2									
2			1	3	2	2	5	4	8	2	3											
1		1	1	4	5	5	5	8	5	6	4	2	1									

Fig. 4-27

Fig. 4-28 The number of synapses received by a neurone in the somatic sensory cortex plotted against its mean diameter. The numbers on the graph represent the numbers of neurones having that combination of mean diameter and number of synapses.

NUMBER OF SYNAPSES PER CELL PROFILE AGAINST MEAN CELL DIAMETER - SOMATIC SENSORY CORTEX (AREA 3b

Number of Synapses \ Mean Cell Diameter (μ)	6	7	8	9	10	11	12	13	14	15	16	17	18	19	20	21	22	23	24	25
16																				
15																				
14																				
13																				
12																				
11																				
10							1													
9																				
8																				
7																				
6				1		1														
5					1															
4						1	1					1								
3			1	1	2	2	7	3	1	1					1					
2			3	4	4	4	6	5	2		13	1								
1		2	1	6	15	8	6	4	4	4	2									

Fig. 4-28

Fig. 4-29 A correlation matrix of the parameters determined for each cell in the motor cortex. A '+' indicates a statistically significant positive correlation between the two features in this population of neurones, a '-' indicates a significant negative correlation and a 'o' indicates no statistically significant correlation.

CORRELATION MATRIX OF CELL SOMATA FROM MOTOR CORTEX

	Depth from pia	Mean diameter	Area: total	Area: nucleus	Area: cytoplasm	Cyt/nucleus	Apical dendrite	No.of dendrites	No.of synapses	Asymmetrics	Nuclear indents	Dark nucleus	Endoplasmic retic.	Merging cytoplasm
Depth from pia		O	O	O	O	O	O	O	O	O	+	-	+	-
Mean diameter	O		+	+	+	+	+	+	+	O	O	-	+	O
Area: total	O	+		+	+	+	+	+	+	O	O	-	+	O
Area: nucleus	O	+	+		+	O	+	+	O	-	O	-	+	O
Area: cytoplasm	O	+	+	+		+	+	+	+	+	O	-	+	O
Cytoplasm/nucleus	O	+	+	O	+		O	O	+	+	O	O	+	O
Apical dendrite	O	+	+	+	+	O		+	-	-	O	O	O	O
No. of dendrites	O	+	+	+	+	O	+		O	O	O	-	O	O
No. of synapses	O	+	+	O	+	+	-	O		+	O	O	+	O
Asymmetrics	O	O	O	-	+	+	-	O	+		O	O	+	O
Nuclear indents	+	O	O	O	O	O	O	O	O	O		+	O	O
Dark nucleus	-	-	-	-	-	O	O	-	O	O	+		-	O
Endoplasmic reticulum	+	+	+	+	+	+	O	O	+	+	O	-		O
Merging cytoplasm	-	O	O	O	O	O	O	O	O	O	O	O	O	

Fig. 4-29

Fig. 4-30 Maps of the strips of motor cortex and somatic sensory cortex studied showing the position and type of each cell.

MAPS OF NEURONAL SOMATA

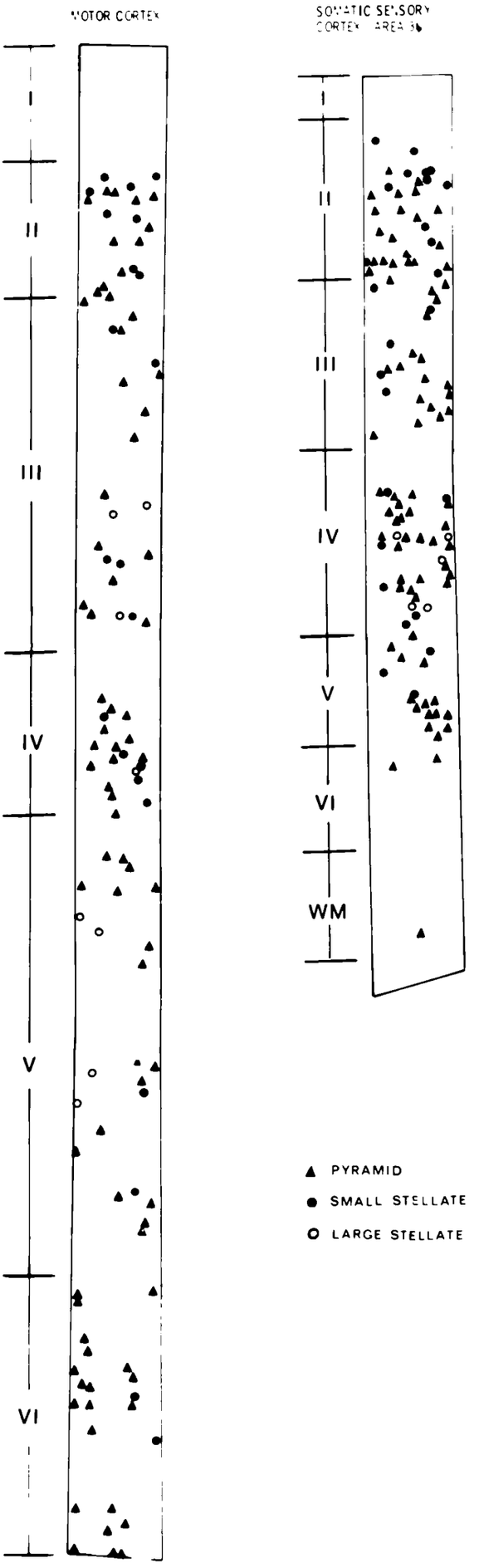

Fig. 4-31 Histogram showing the distribution of numbers of cells against depth from the surface in the motor cortex.

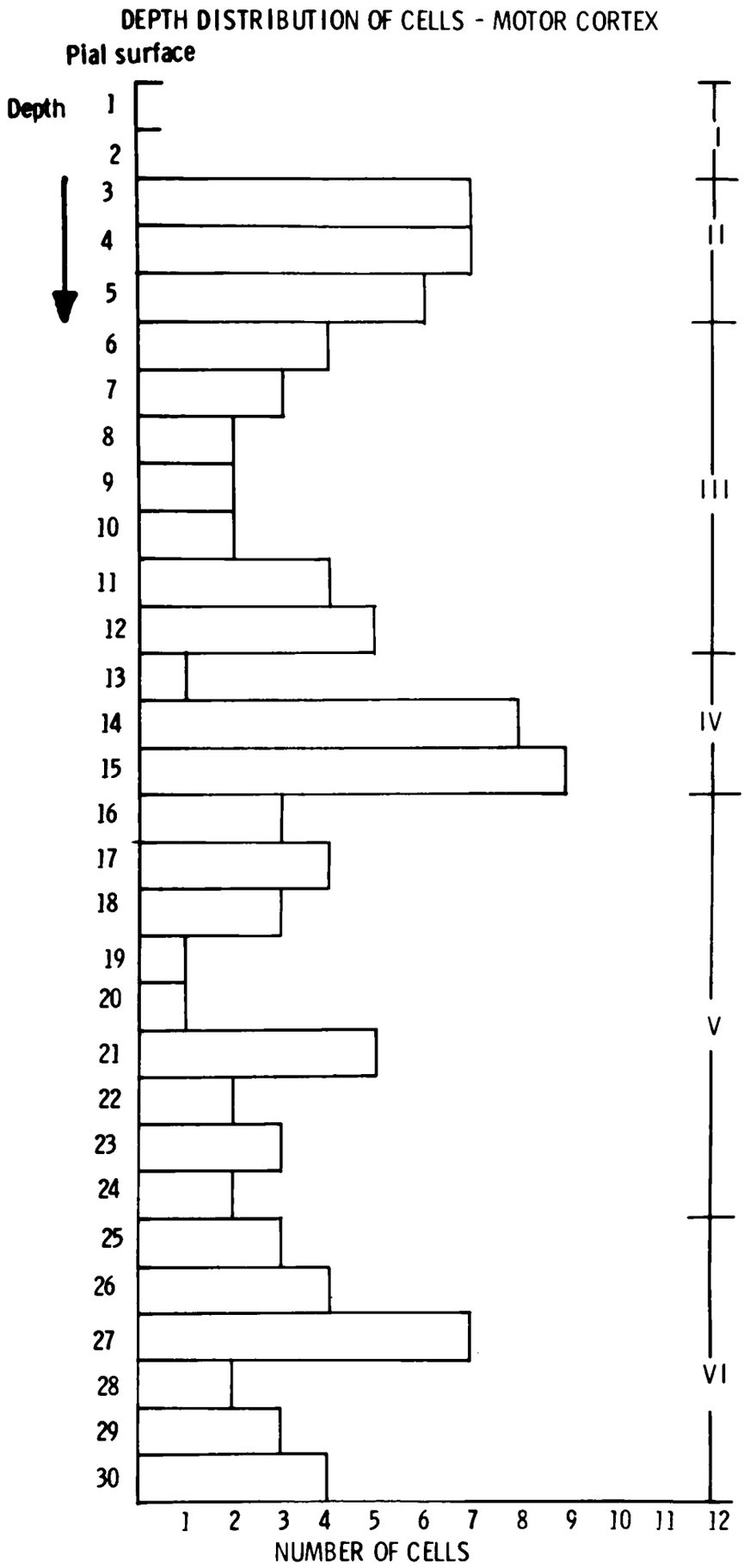
DEPTH DISTRIBUTION OF CELLS - MOTOR CORTEX
Pial surface
Depth
1
2
3
4
5
6
7
8
9
10
11
12
13
14
15
16
17
18
19
20
21
22
23
24
25
26
27
28
29
30
I
II
III
IV
V
VI
1 2 3 4 5 6 7 8 9 10 11 12
NUMBER OF CELLS

Fig. 4-32 Histogram showing the distribution of numbers of cells against depth from the surface in the somatic sensory cortex.

DEPTH DISTRIBUTION OF CELLS-SOMATIC SENSORY CORTEX (Area 3b)

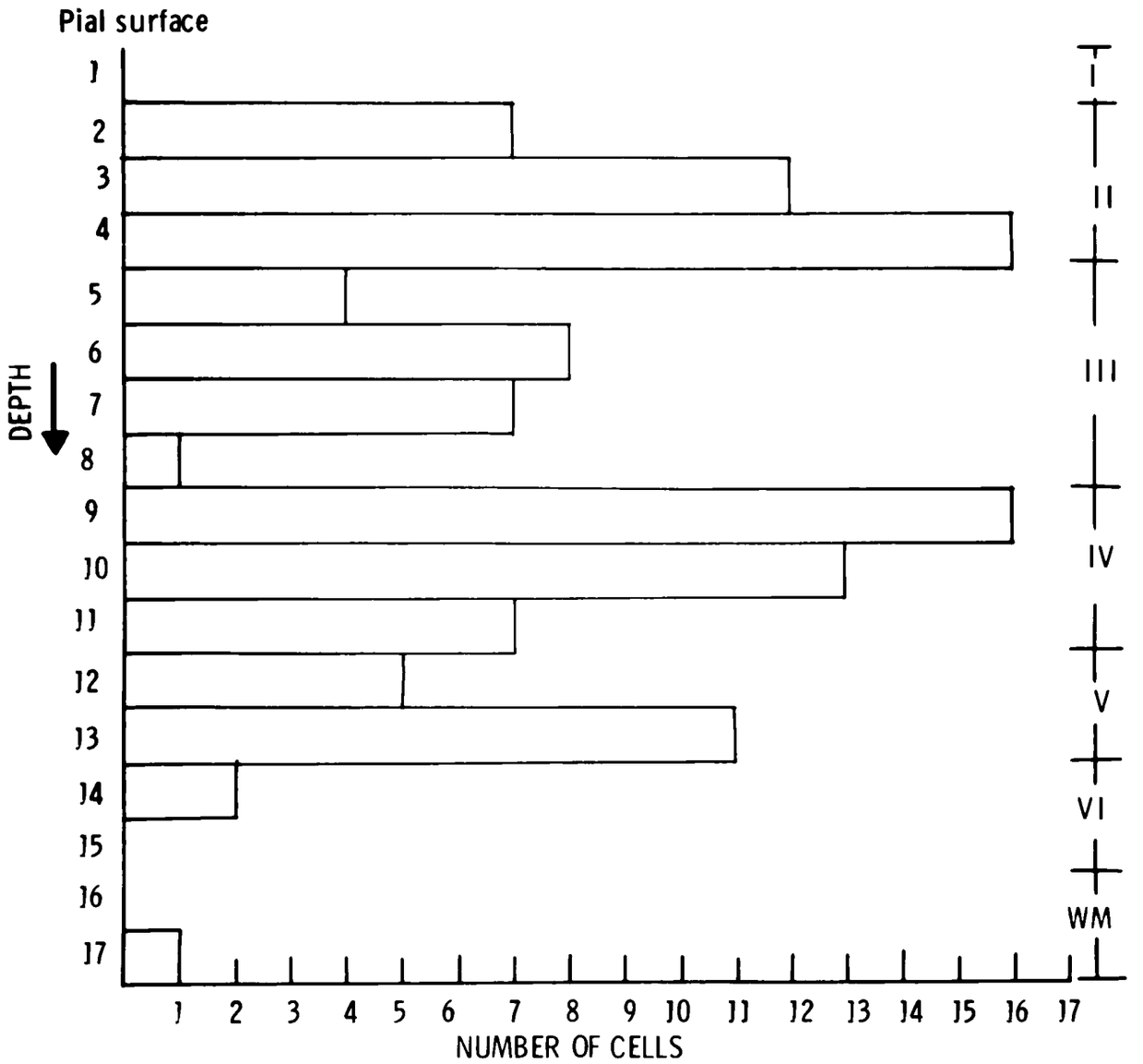

Fig. 4-33 Histogram showing the distribution with depth of the three types of neuron in the motor cortex.

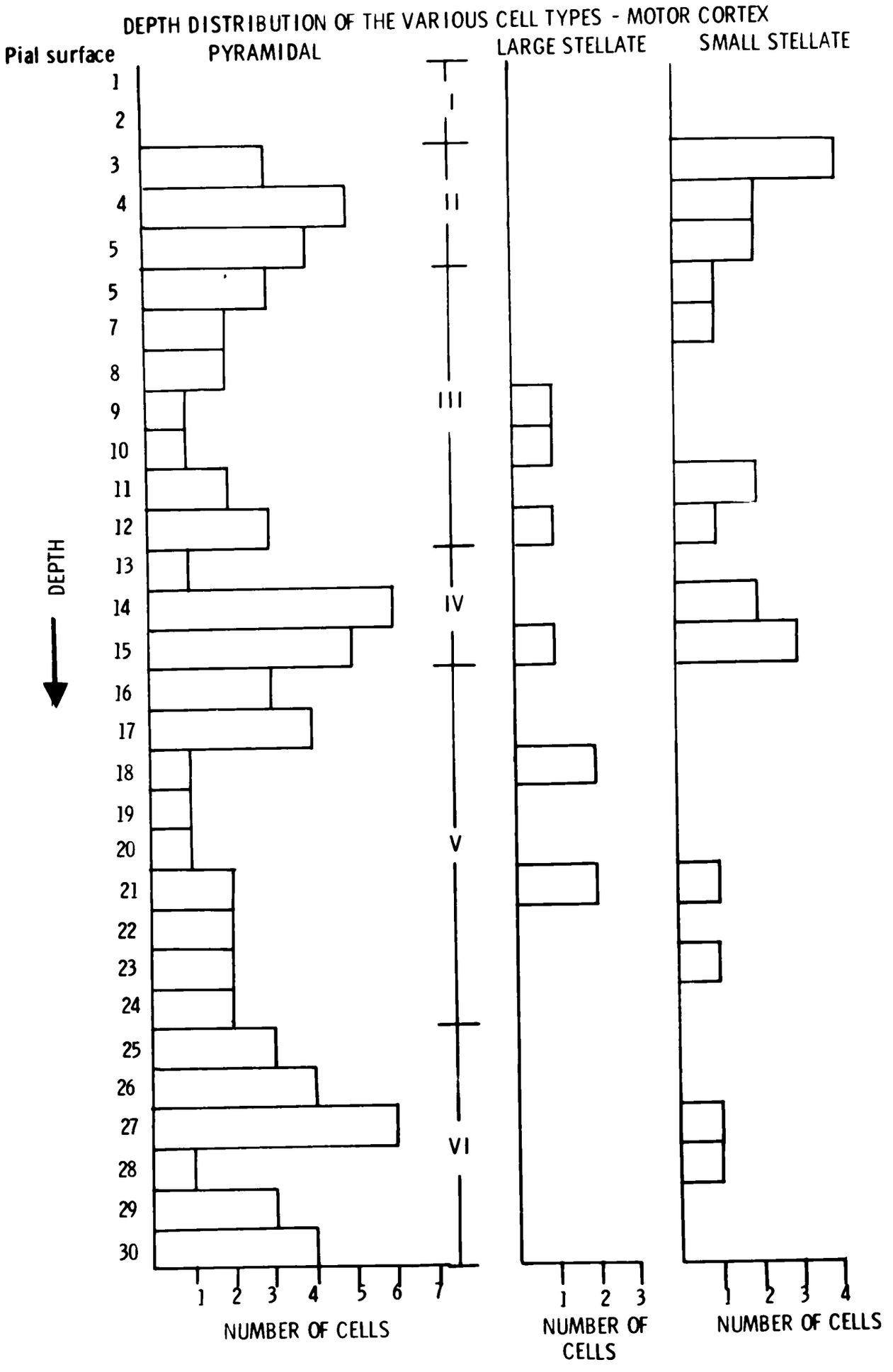
DEPTH DISTRIBUTION OF THE VARIOUS CELL TYPES - MOTOR CORTEX
Pial surface
PYRAMIDAL
LARGE STELLATE
SMALL STELLATE
DEPTH
1
2
3
4
5
5
7
8
9
10
11
12
13
14
15
16
17
18
19
20
21
22
23
24
25
26
27
28
29
30
I
II
III
IV
V
VI
1 2 3 4 5 6 7
NUMBER OF CELLS
1 2 3
NUMBER OF CELLS
1 2 3 4
NUMBER OF CELLS

Fig. 4-34 Histogram showing the distribution with depth of the three types of neuron in area 3b of the somatic sensory cortex.

DEPTH DISTRIBUTION OF THE DIFFERENT CELL TYPES . SOMATIC SENSORY CORTEX (area 3b)

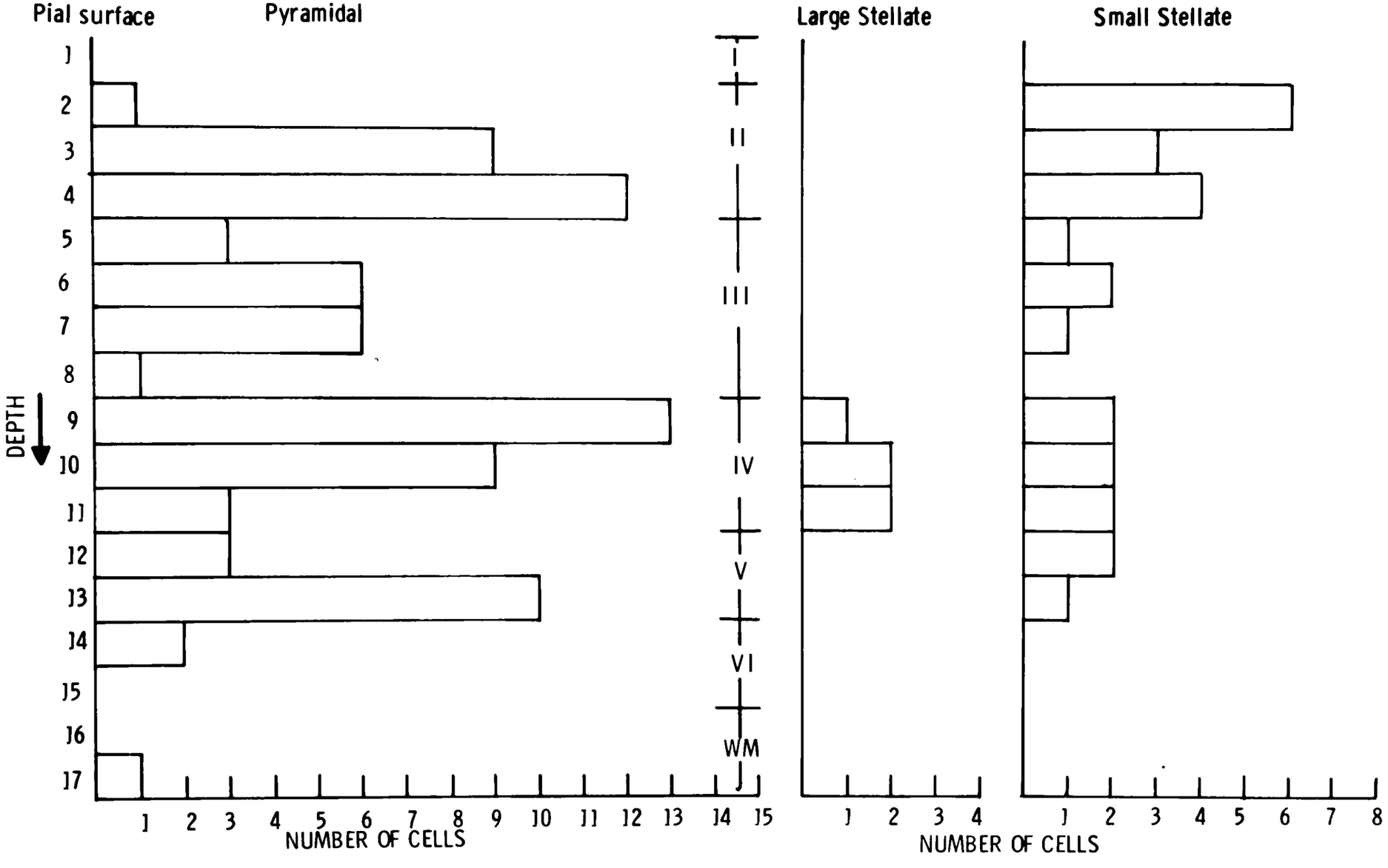

Fig. 4-35 Histograms showing the distributions of the mean diameters of pyramid cells in the somatic sensory and motor cortices.

HISTOGRAM OF MEAN CELL DIAMETER OF PYRAMIDAL CELLS IN MOTOR AND SOMATIC SENSORY CORTICES.

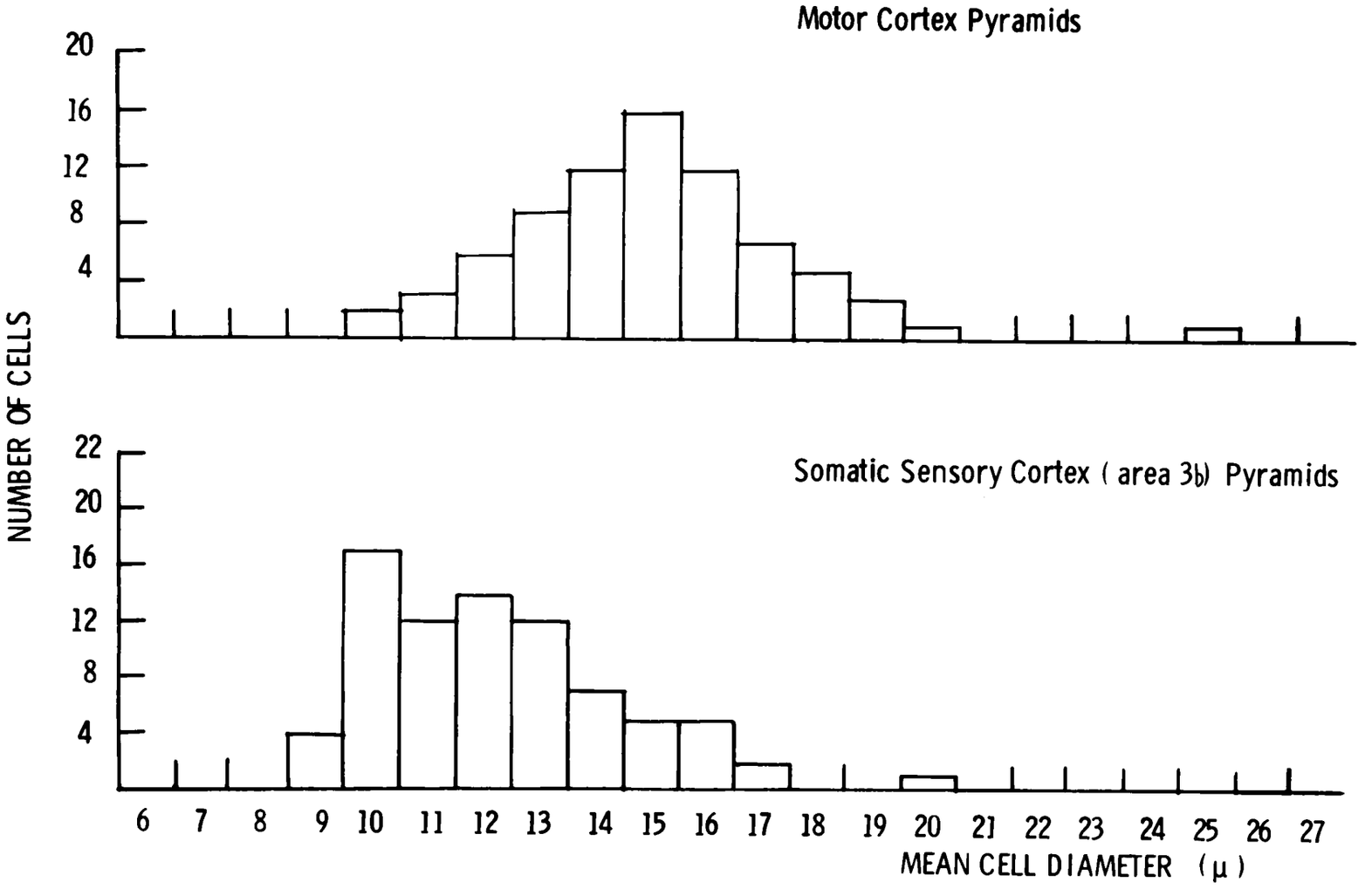

Fig. 4-36 Histograms showing the size distribution of small and large stellate cells in the motor and somatic sensory cortices.

HISTOGRAMS OF MEAN CELL DIAMETER OF LARGE AND SMALL STELLATE CELLS IN MOTOR AND SOMATIC SENSORY CORTICES (area 3b)

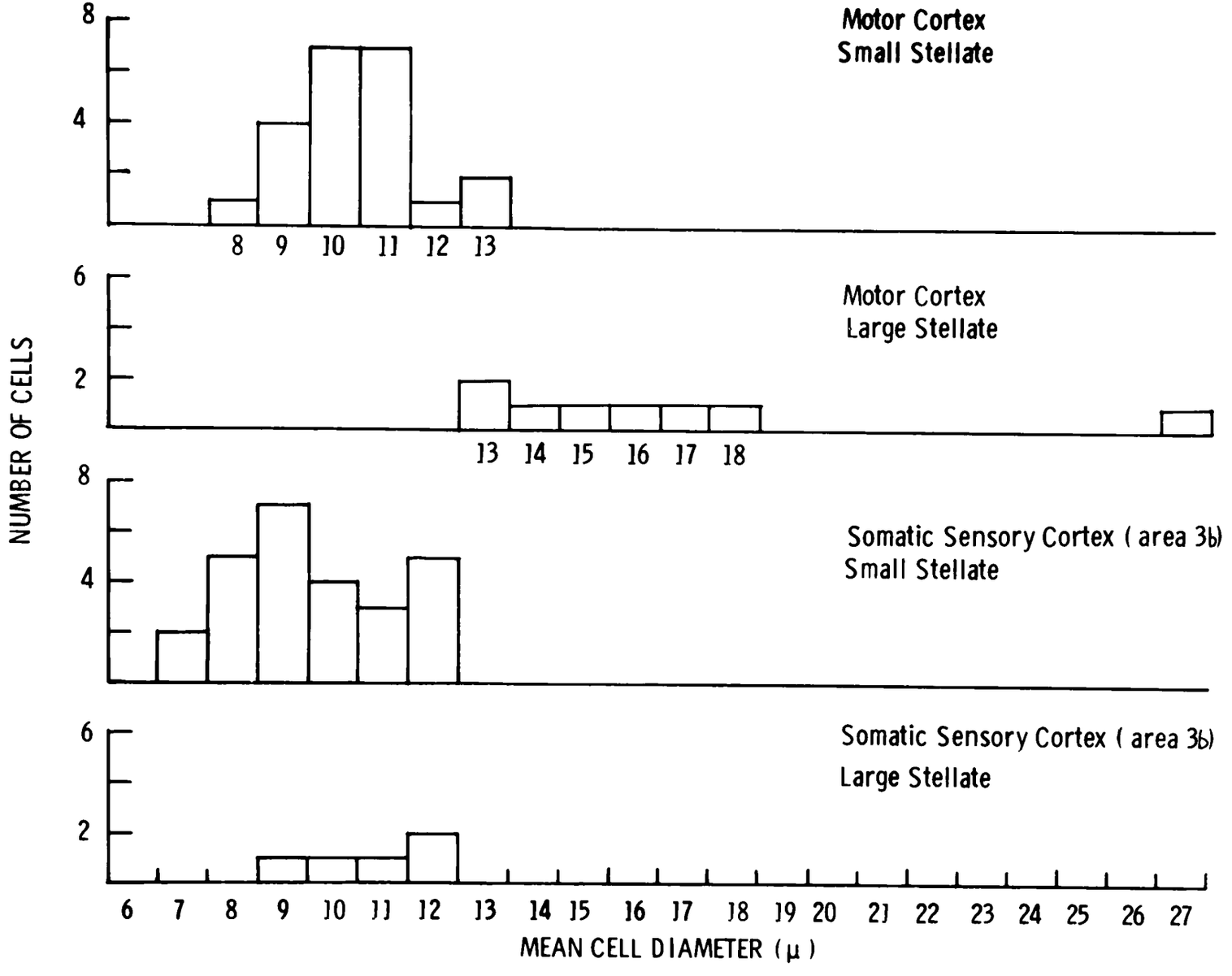

Fig. 4-37 Graph showing the relationship of mean cell diameter to depth from the pial surface in the motor cortex. Each number on the graph indicates the number of cells having that mean diameter at that depth from the surface.

RELATION OF MEAN CELL DIAMETER TO DEPTH OF PIA - MOTOR CORTEX

Depth	Mean cell dia. (μ) 8	9	10	11	12	13	14	15	16	17	18	19	20	21	22	23	24	25	26	27
1																				
2																				
3			2	3		1			1											
4			1		1	1		2	2											
5		1		1		2		1	1											
6			1						2	1										
7				1					1		1									
8											1	1								
9							1		1											
10										1	1									
11		1		2									1							
12	1					1	1			1	1									
13					1															
14			1		1	3		1	1	1										
15		2	1			1	1	1		1	1	1								
16					1			1	1											
17								2	1			1								
18						1												1		1
19										1										
20							1													
21				1	1			2	1											
22							1	1												
23				1			1				1									
24								2												
25					1		1	1												
26					1	2		1												
27		1				1	3	2												
28		1								1										
29			1				1		1											
30		1					2			1										

Fig. 4-37

Fig. 4-38 Graph showing the relationship of mean cell diameter to depth in the somatic sensory cortex. Each number on the graph indicates the number of cells having that mean diameter at that depth from the pial surface.

RELATION OF MEAN CELL DIAMETER TO DEPTH FROM PIA - SOMATIC SENSORY CORTEX (AREA 3b)

Depth	Mean Cell Diameter (μ) 7	8	9	10	11	12	13	14	15	16	17	18	19	20
1														
2	1	1	2	2		1								
3		1	1	2	2	2	4							
4		1		4	2	4	2	1		1	1			
5			1	2	1									
6				2		3	1	1		1				
7		1		1	1			2	2					
8					1									
9			2	1	5	3	1	2		1	1			
10	1		4	3	1	2	1			1				
11		1	1	4		1								1
12				1	2	1								
13			1		1	3	2	1	2	1				
14						1	1							
15														
16									1					
17									1					

Fig. 4-38

Fig. 4-39 Histograms showing the distributions of the numbers of synapses received by pyramidal cell profiles in the section studied in motor and somatic sensory cortices.

NUMBERS OF SYNAPSES PER PYRAMIDAL CELL PROFILE

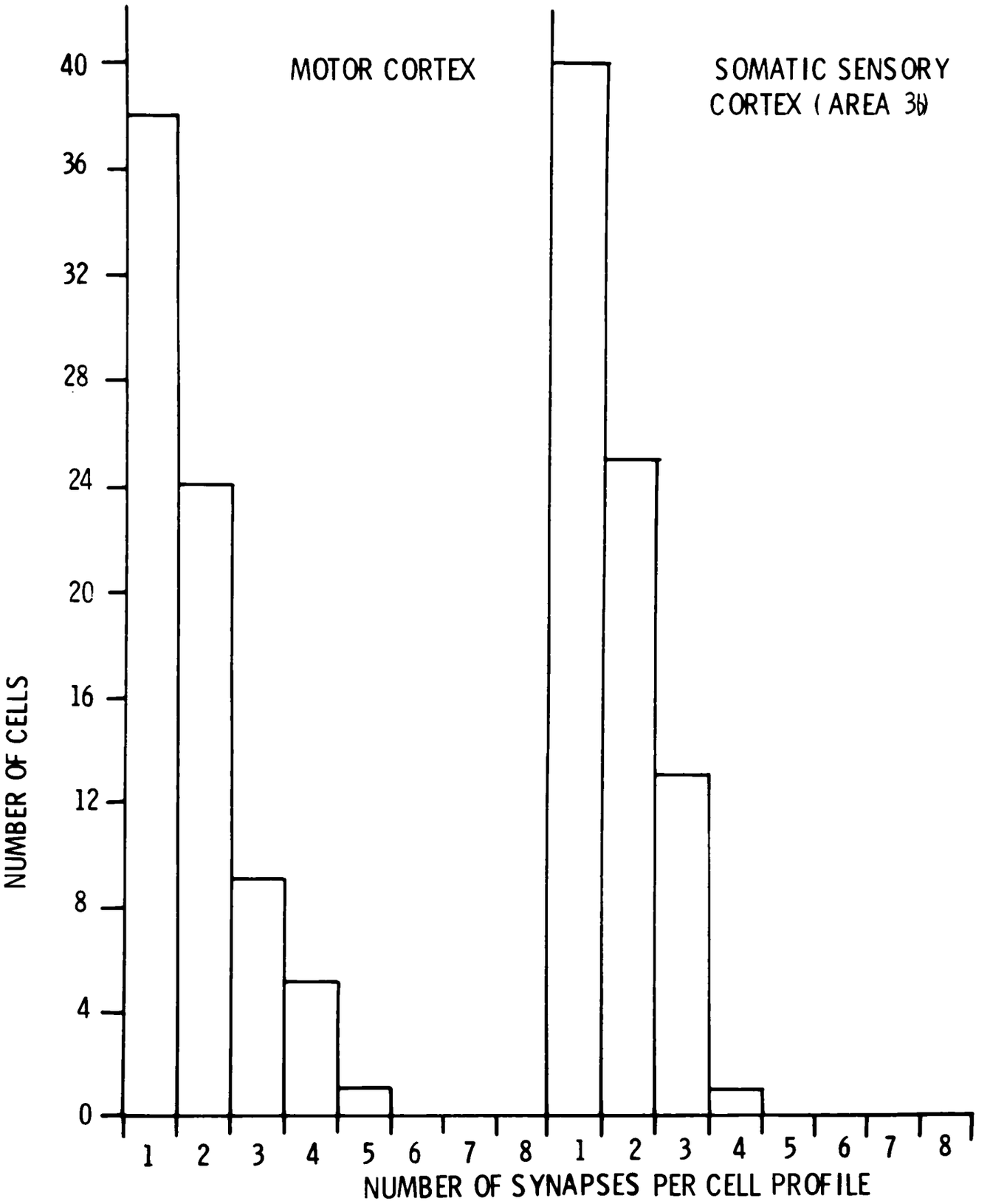

Fig. 4-40 The histograms of the numbers of synapses per pyramidal cell profile of fig. 4-39 are compared with Poisson distributions having the same mean. Note the close correspondence between observed and predicted distributions in both motor and somatic sensory cortices.

PREDICTED AND OBSERVED NUMBERS OF SYNAPSES PER PYRAMIDAL CELL PROFILE

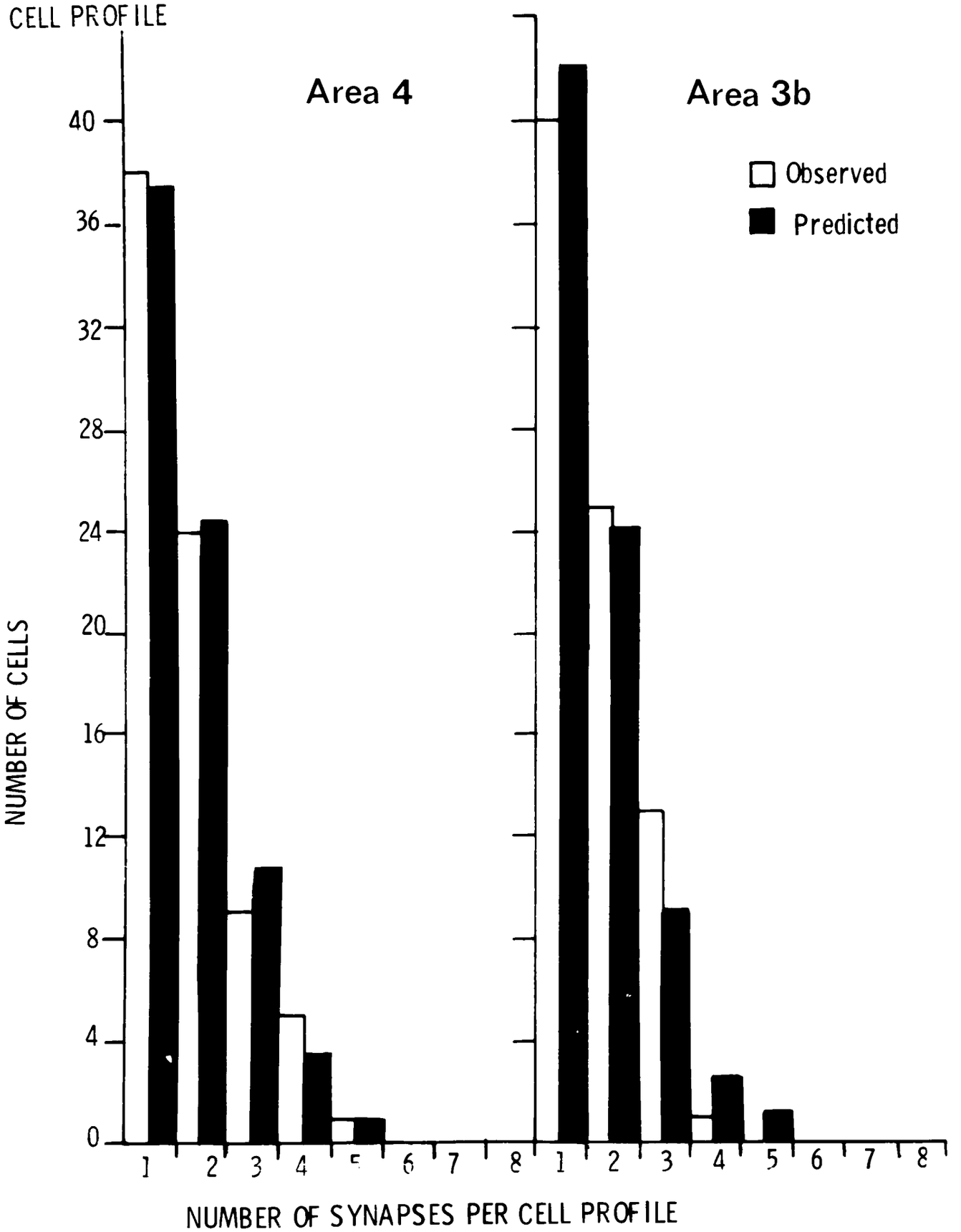

Fig. 4-41 Histograms showing the distributions of the numbers of synapses received by stellate cell somata in motor and somatic sensory cortices, all stellate cells being considered as a single population.

NUMBERS OF SYNAPSES PER CELL PROFILE FOR ALL STELLATE CELLS

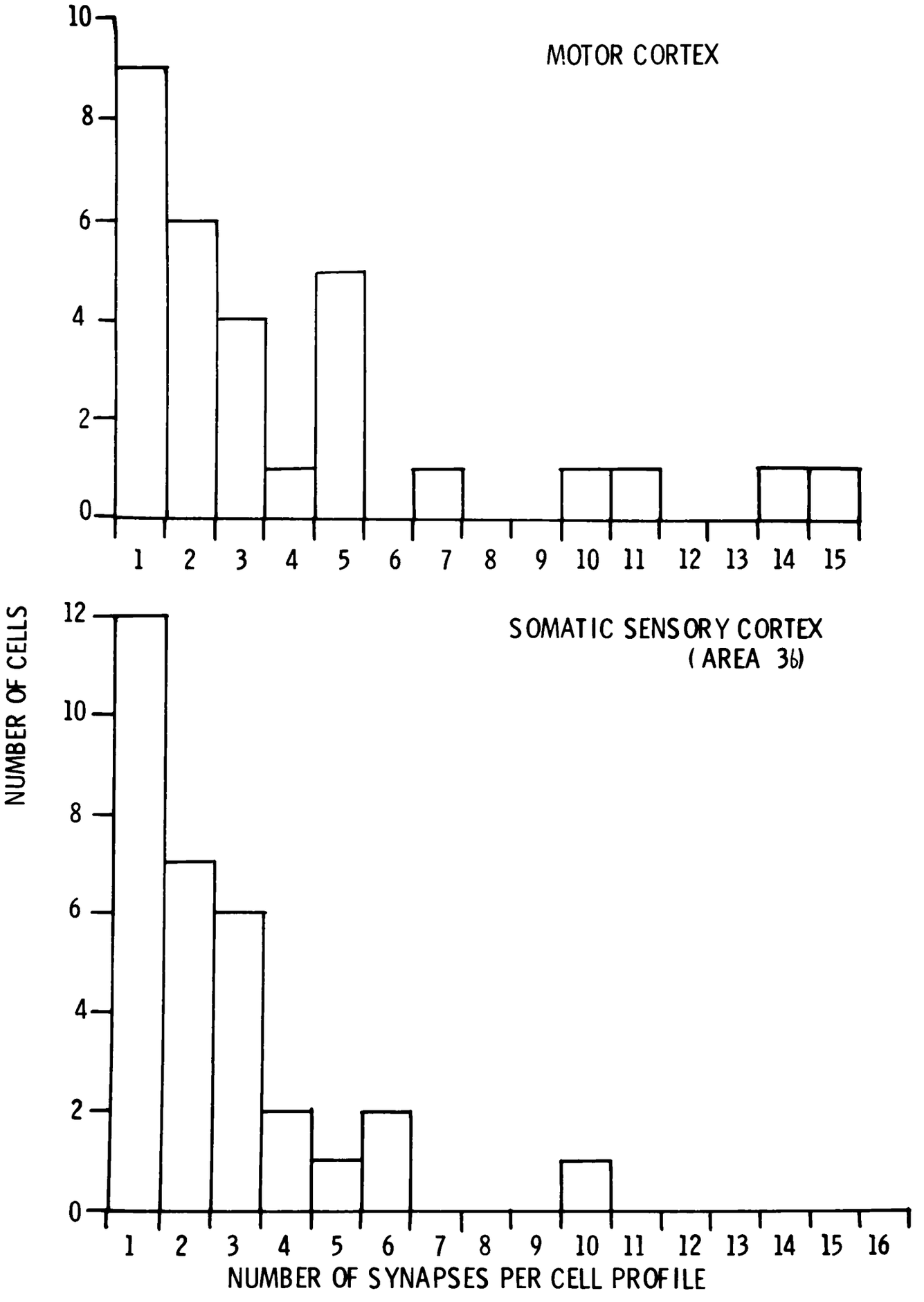

Fig. 4-42 The histograms of the numbers of synapse per cell profile of fig. 4-41 for all stellate cells are compared with Poisson distributions having the same mean. Note the marked excess of cells observed with very large and small numbers of synapses compared to the predicted distribution in the motor cortex, with a relative deficiency around the mean value. Similar discrepancies are apparent in the somatic sensory cortex but are less marked.

PREDICTED AND OBSERVED NUMBERS OF SYNAPSES PER CELL PROFILE FOR ALL STELLATE CELLS.

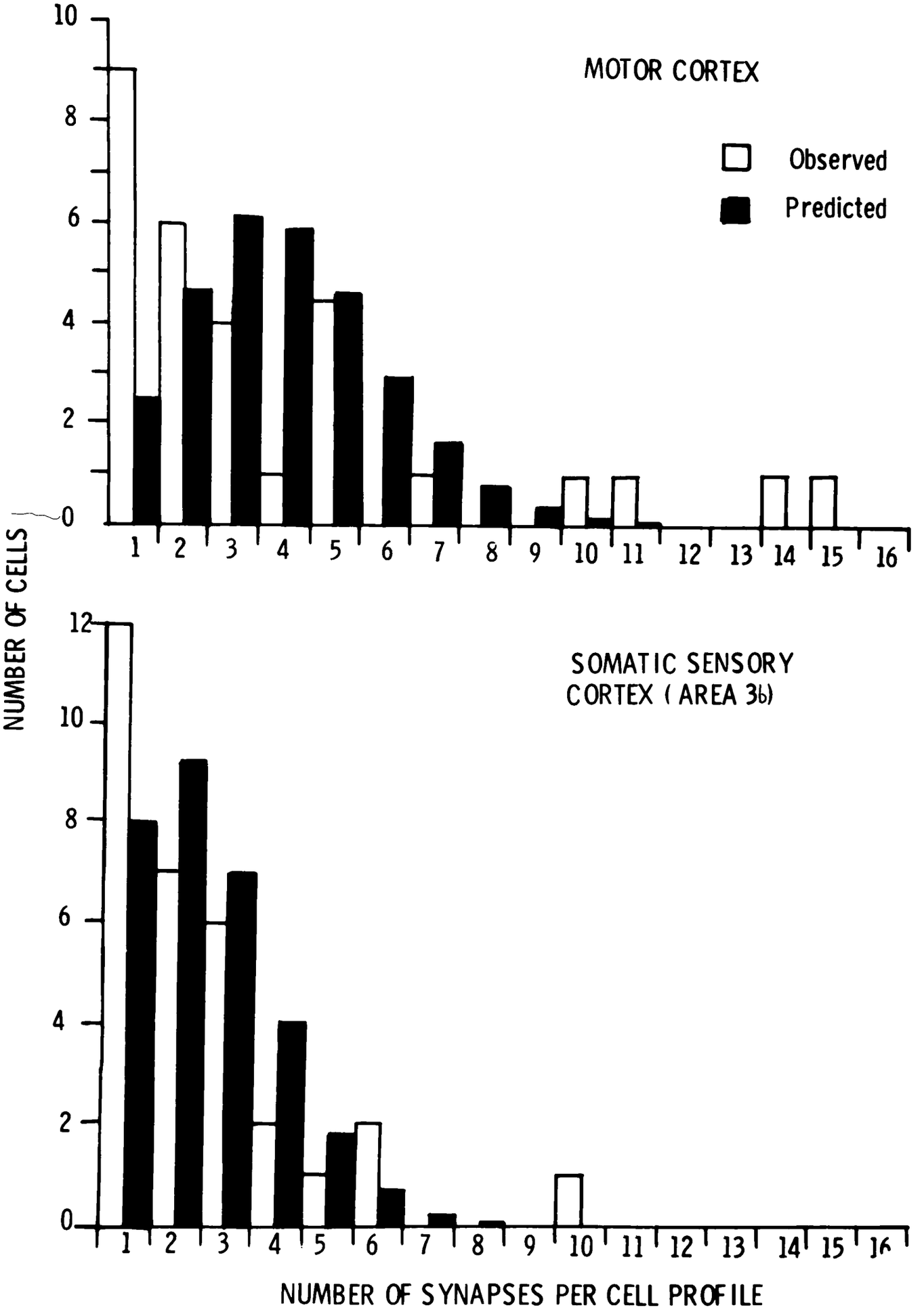

Fig. 4-43 Histograms showing the numbers of synapses received by large and small stellate cell somata in the motor cortex.

NUMBERS OF SYNAPSES PER CELL PROFILE FOR LARGE AND SMALL STELLATE CELLS IN THE MOTOR CORTEX.

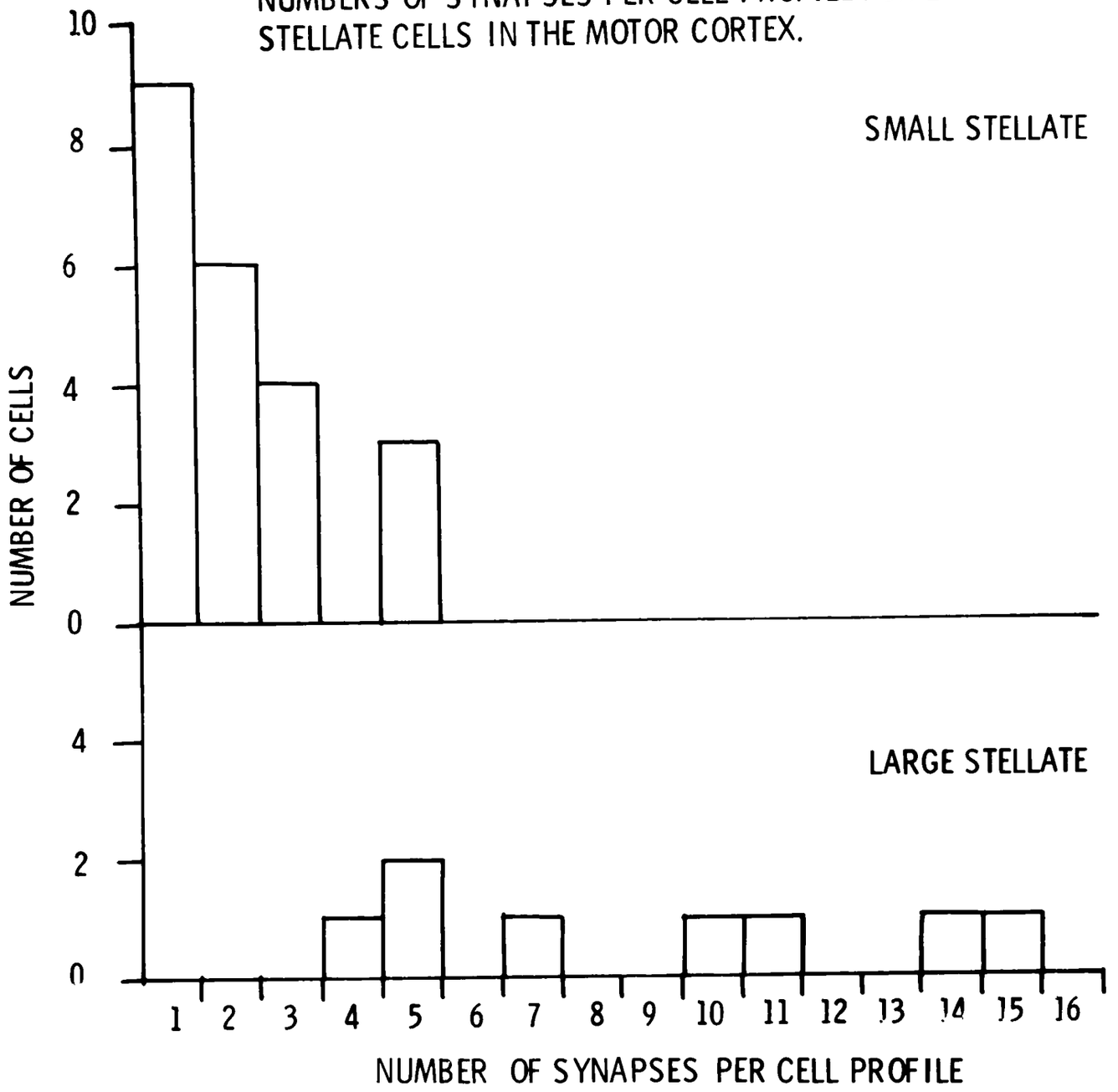

Fig. 4-44 Histograms showing the numbers of synapses received by large and small stellate cell somata in the somatic sensory cortex.

NUMBERS OF SYNAPSES PER CELL PROFILE FOR LARGE AND SMALL STELLATE CELLS IN THE SOMATIC SENSORY CORTEX.

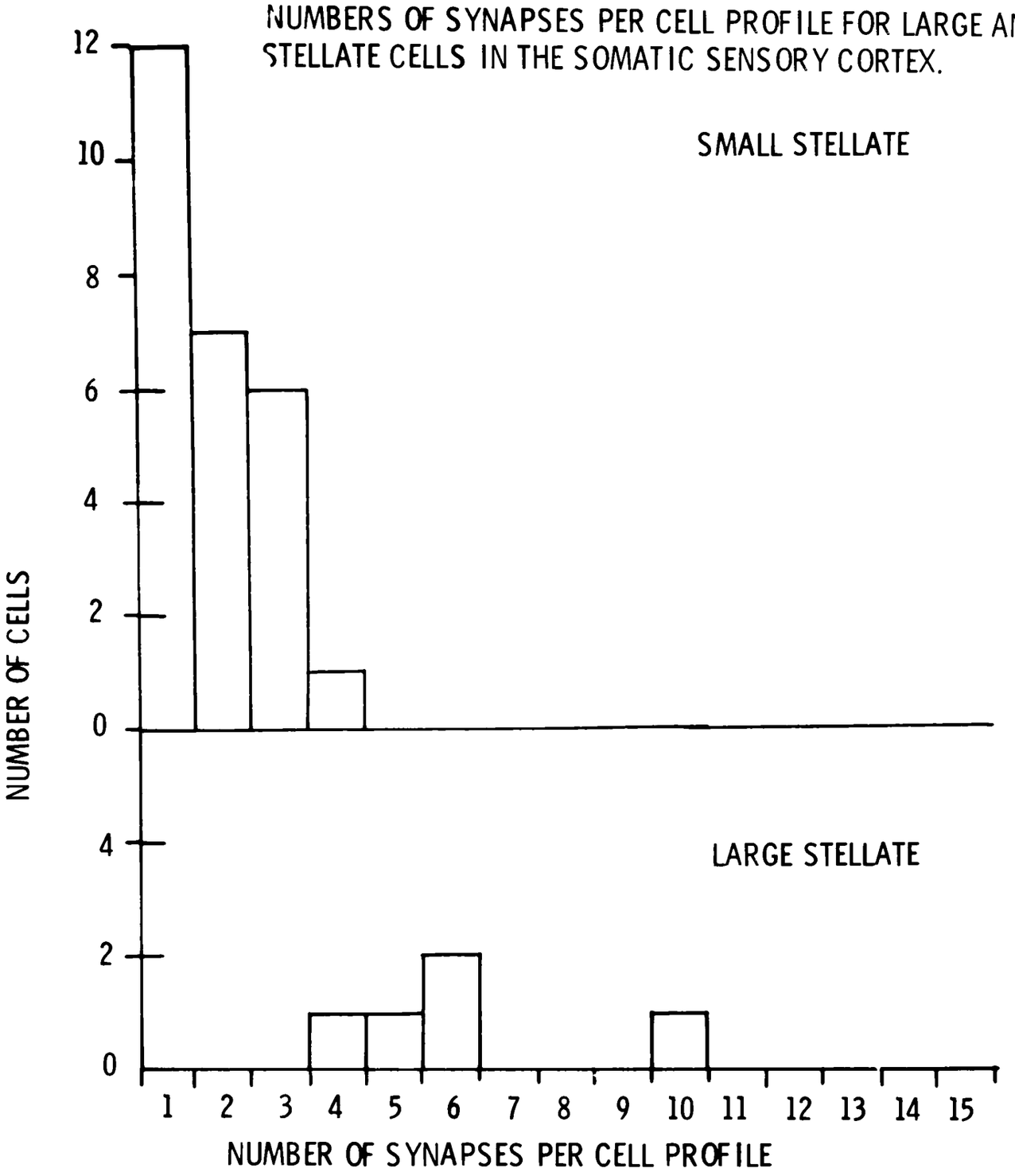

Fig. 4-45 The histograms of the number of synapses per cell profile for large and small stellate cells in the motor cortex (fig. 4-43) are compared to predicted Poisson distributions. That for small stellate cells is a reasonable fit statistically; the number of large stellate cells observed is too small for statistical comparison or to give an accurate estimate of the population distribution although the fit appears reasonable visually.

OBSERVED AND PREDICTED NUMBERS OF SYNAPSES PER CELL PROFILE FOR LARGE AND SMALL STELLATE CELLS IN THE MOTOR CORTEX

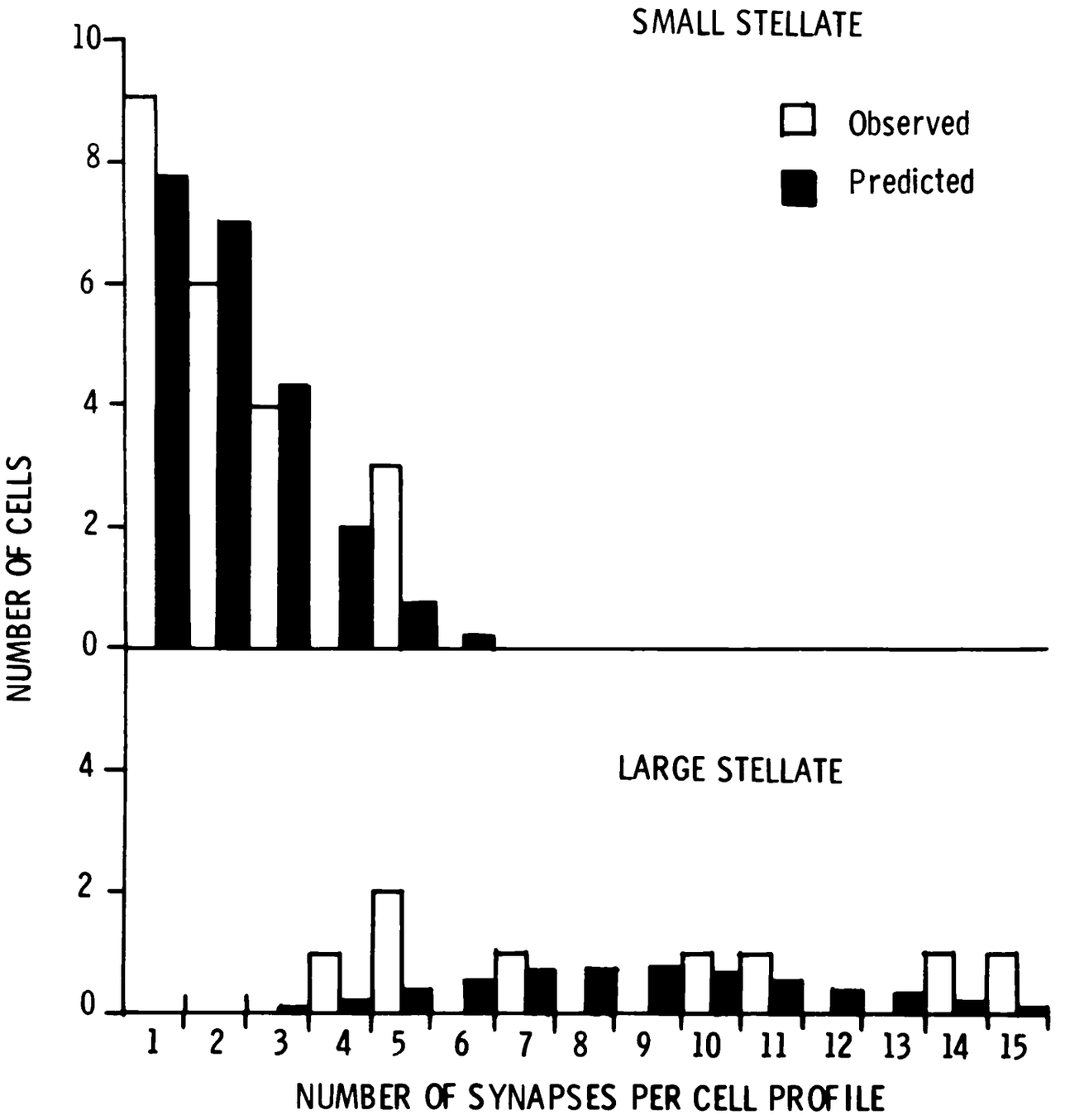

Fig. 4-46 The histograms of the numbers of synapses per cell profile for large and small stellate cells in the somatic sensory cortex (fig. 4-44) are compared to predicted Poisson distributions. That for small stellate cells is a reasonable fit statistically and that for large stellate cells is a reasonable visual fit although too few large stellate cells were observed for statistical comparison.

OBSERVED AND PREDICTED NUMBERS OF SYNAPSES PER CELL PROFILE FOR LARGE AND SMALL STELLATE CELLS IN THE SOMATIC SENSORY CORTEX

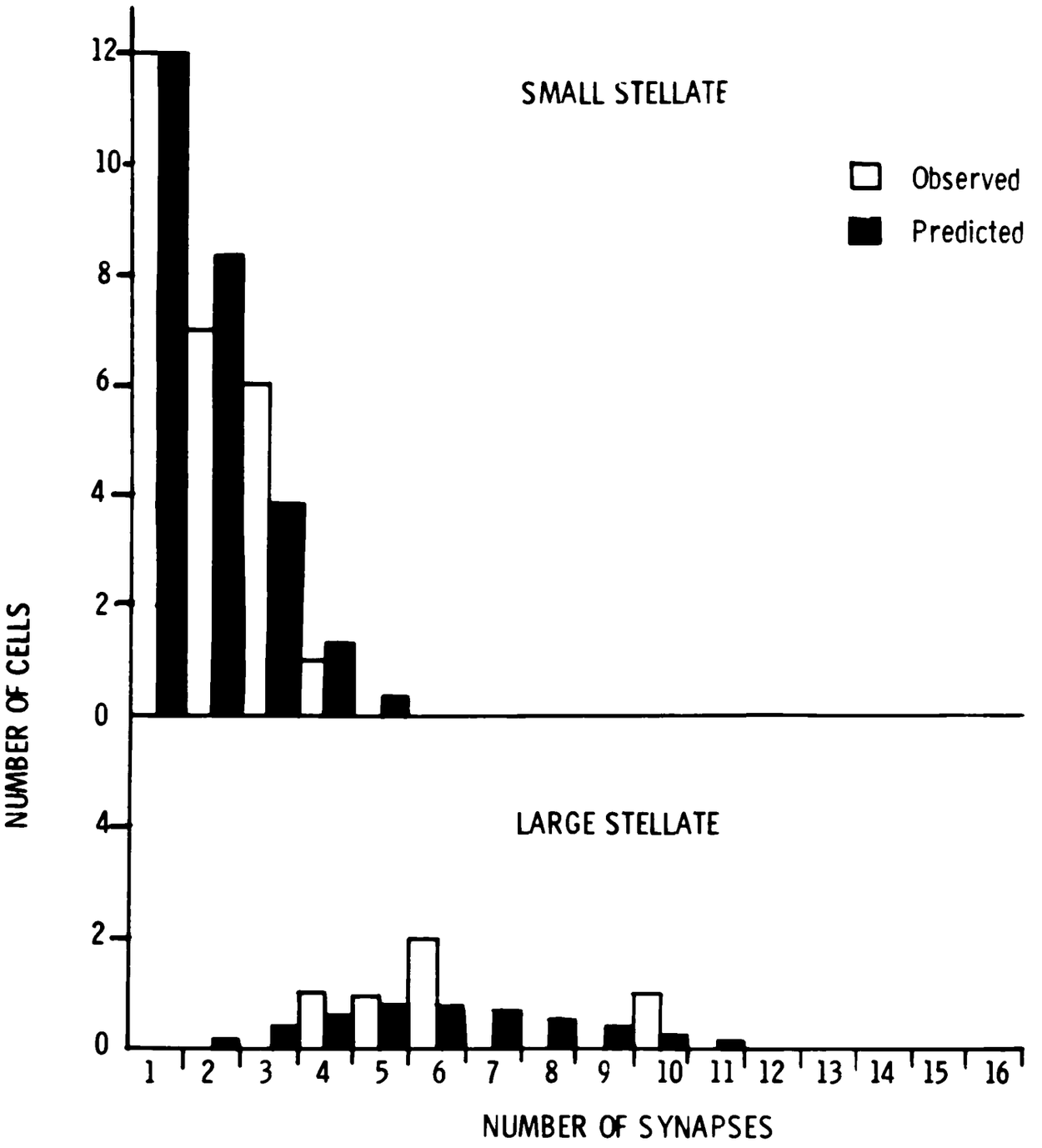

Fig. 4-47 Graphs showing the combined distributions of mean cell diameter and the number of synapses received for pyramidal cells in motor and somatic sensory cortices. Each number on the graph indicates the number of pyramids having that combination of mean diameter and number of synapses (cf. the distributions for all cells in figs. 4-27 and 4-28).

NUMBER OF SYNAPSES PER CELL PROFILE AGAINST MEAN CELL DIAMETER - PYRAMIDS

MOTOR CORTEX

Number of synapses per cell profile	Mean Cell Diameter (μ) 7	8	9	10	11	12	13	14	15	16	17	18	19	20	21	22	23	24	25	26
7																				
6																				
5										1										
4									1	1		1		1					1	
3							1		2	2		2	2							
2				1	1	2	3	4	8	2	3									
1				1	2	4	5	8	5	6	4	2	1							

SOMATIC SENSORY CORTEX (AREA 3)

Number of synapses per cell profile	Mean Cell Diameter (μ) 7	8	9	10	11	12	13	14	15	16	17	18	19	20	21	22	23	24	25	26
7																				
6																				
5																				
4											1									
3					2	5	3	1	1					1						
2			2	3	4	5	5	2		3	1									
1			2	14	6	4	4	4	4	2										

Fig. 4-17

Fig. 4-48 Graph showing the combined distributions of mean cell diameter and number of synapses received for large stellate cells in the motor cortex. Note the much steeper rise in the number of synapses received with increasing cell diameter in comparison with pyramidal cells (fig. 4-47).

NUMBER OF SYNAPSES PER CELL PROFILE AGAINST MEAN CELL DIAMETER - LARGE STELLATE CELLS

MOTOR CORTEX

Number of Synapses per Cell Profile	Mean Cell Diameter (μ) 12	13	14	15	16	17	18	19	20	21	22	23	24	25	26	27	28
16																	
15						1											
14																1	
13																	
12																	
11					1												
10				1													
9																	
8																	
7			1														
6																	
5		1					1										
4		1															
3																	
2																	
1																	

Fig. 4-48.

Fig. 4-49 Graph showing the combined distributions of mean cell diameter and number of synapses received for large stellate cells in the somatic sensory cortex.

NUMBER OF SYNAPSES PER CELL PROFILE AGAINST MEAN CELL DIAMETER - LARGE STELLATE CELLS

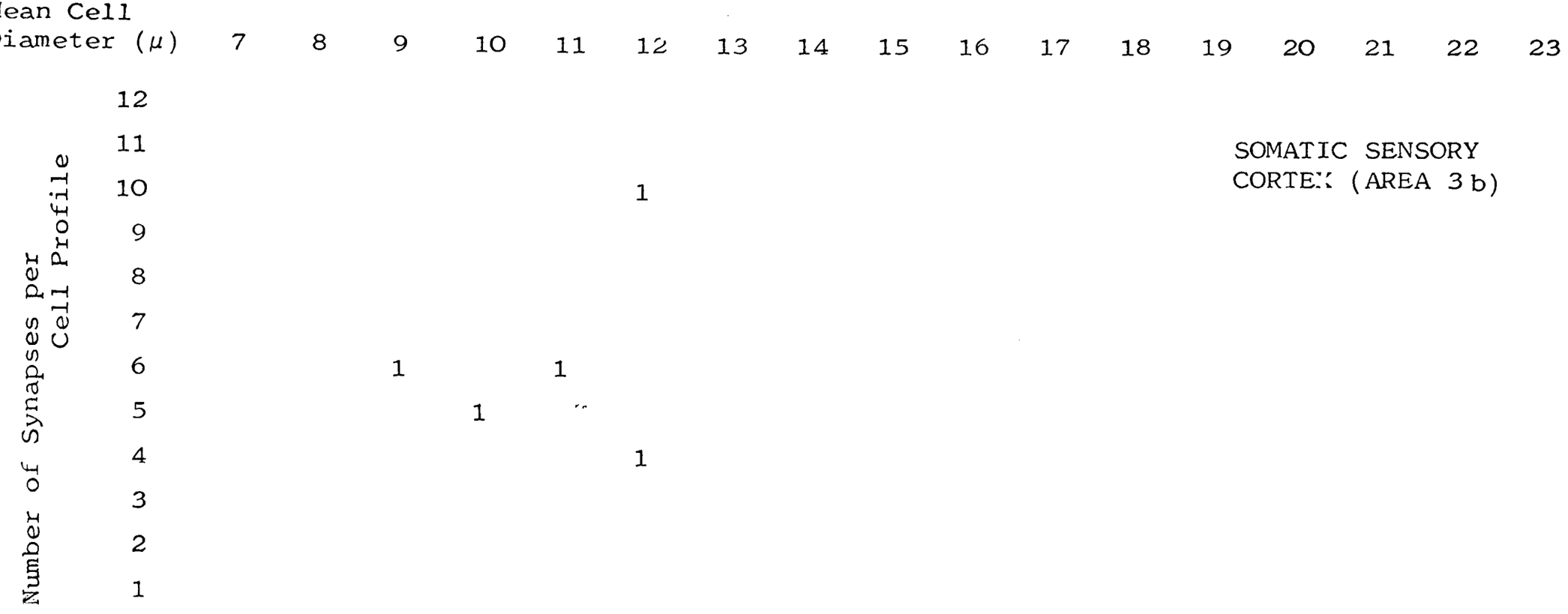

Fig. 4-49

Fig. 4-50 Graph showing the combined distributions of mean cell diameter and number of synapses received for small stellate cells in motor and somatic sensory cortices.

NUMBER OF SYNAPSES PER CELL PROFILE AGAINST MEAN CELL DIAMETER - SMALL STELLATES

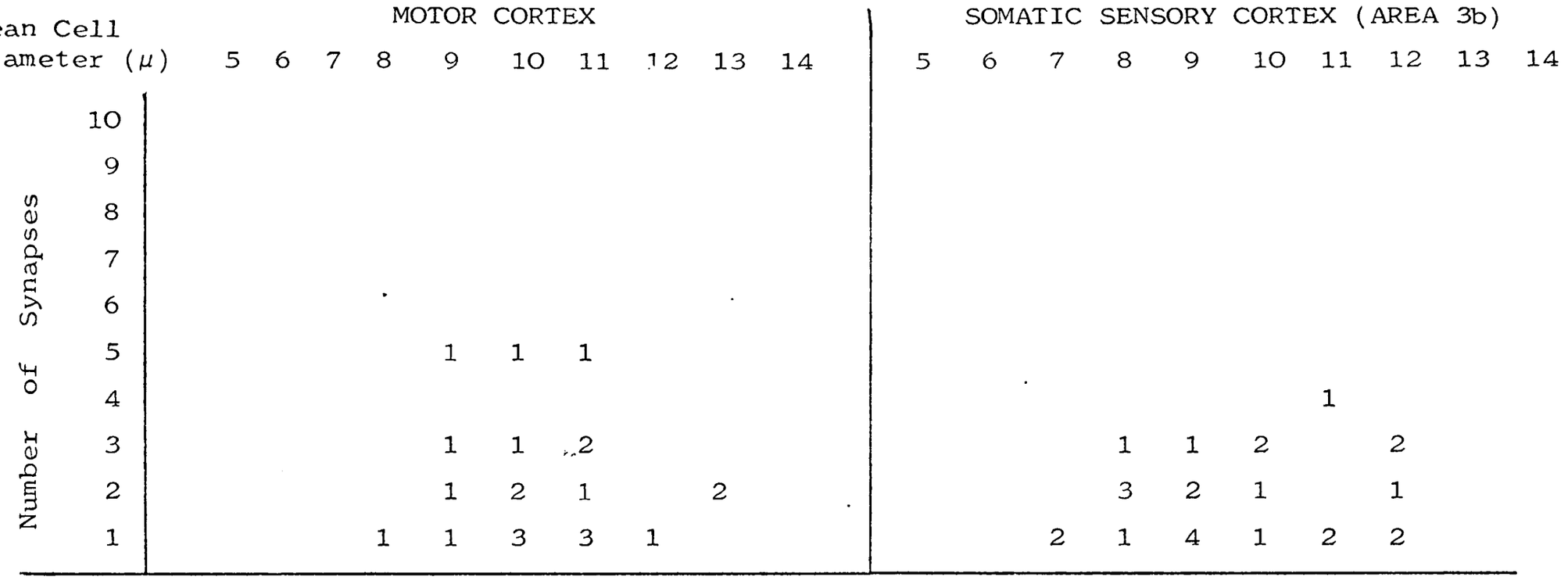

Fig. 4-50

Fig. 4-51 Graph showing the combined distributions of mean cell diameter and number of synapses received for all stellate cells in the motor cortex. A straight line may be drawn on the graph as shown to separate the large and small stellate populations (cf. figs. 4-48 and 4-50).

NUMBER OF SYNAPSES PER CELL PROFILE AGAINST MEAN CELL DIAMETER - MOTOR CORTEX

ALL STELLATE CELLS

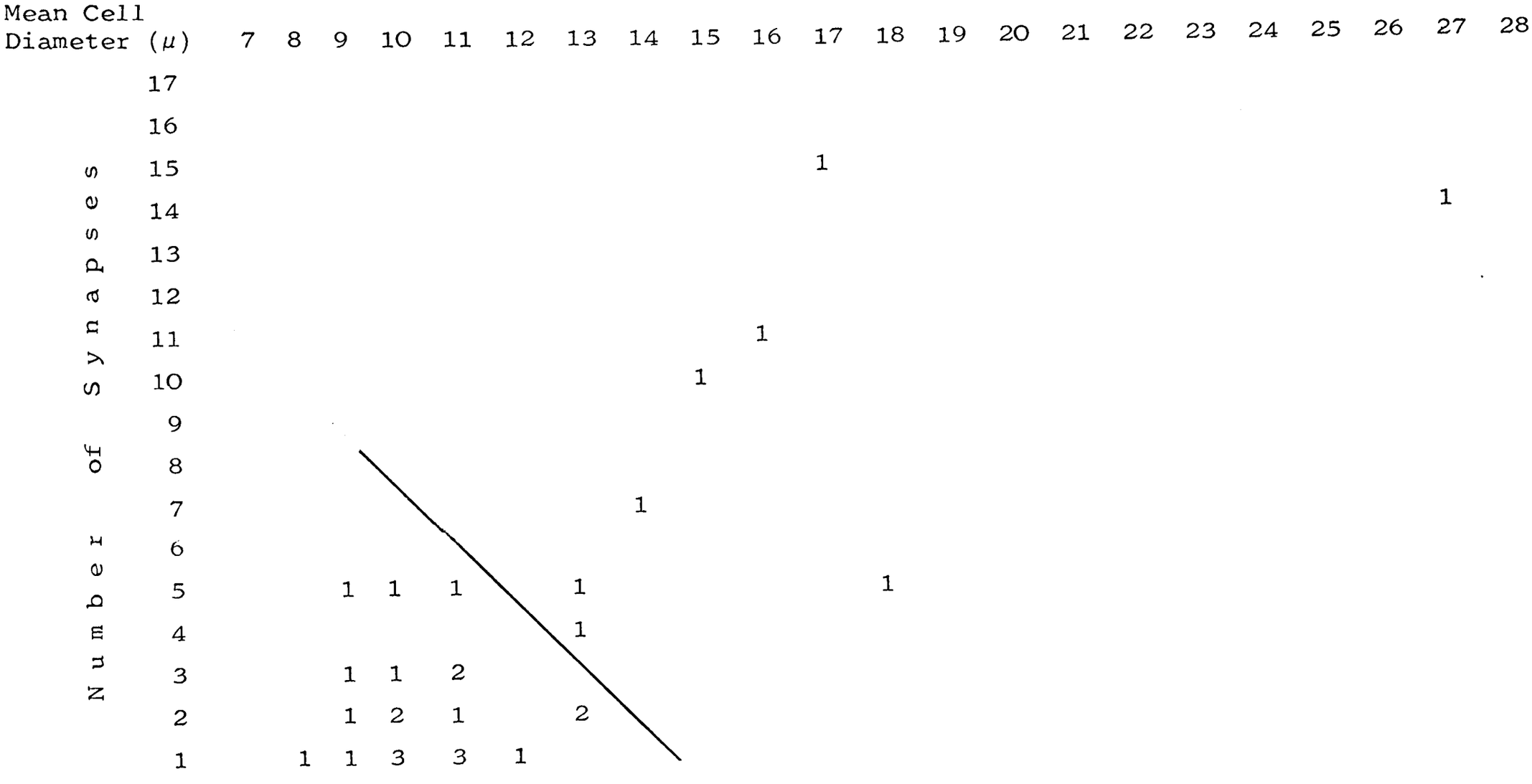

Fig. 4-52 Graph showing the combined distributions of mean cell diameter and number of synapses received for all stellate cells in the somatic sensory cortex. A straight line may be drawn on the graph as shown to separate the large and small stellate populations.

NUMBER OF SYNAPSES PER CELL PROFILE AGAINST MEAN CELL DIAMETER - SOMATIC SENSORY CORTEX

ALL STELLATE CELLS

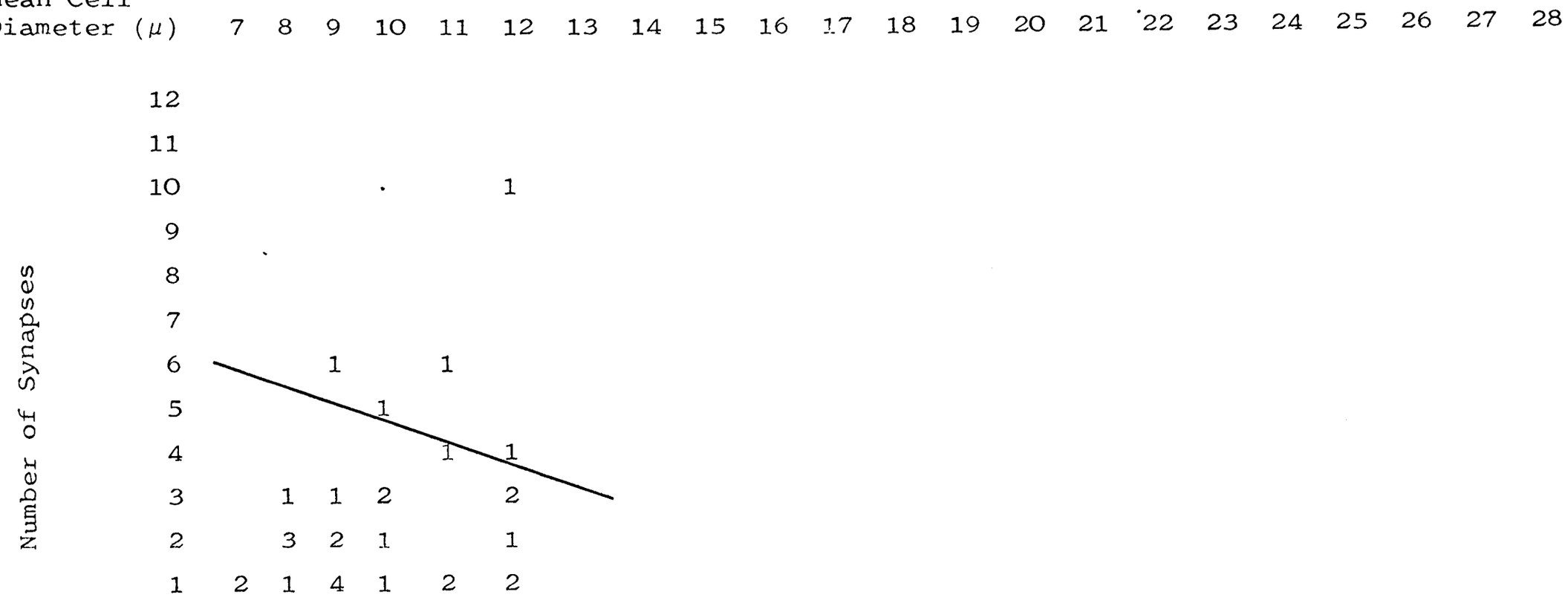

Fig. 4-52

Fig. 4-53 Histograms showing the numbers of dendrites arising from the cell soma in the sections studied for the three cell types in both motor and somatic sensory cortices.

NUMBERS OF DENDRITES ARISING FROM THE CELL PROFILE

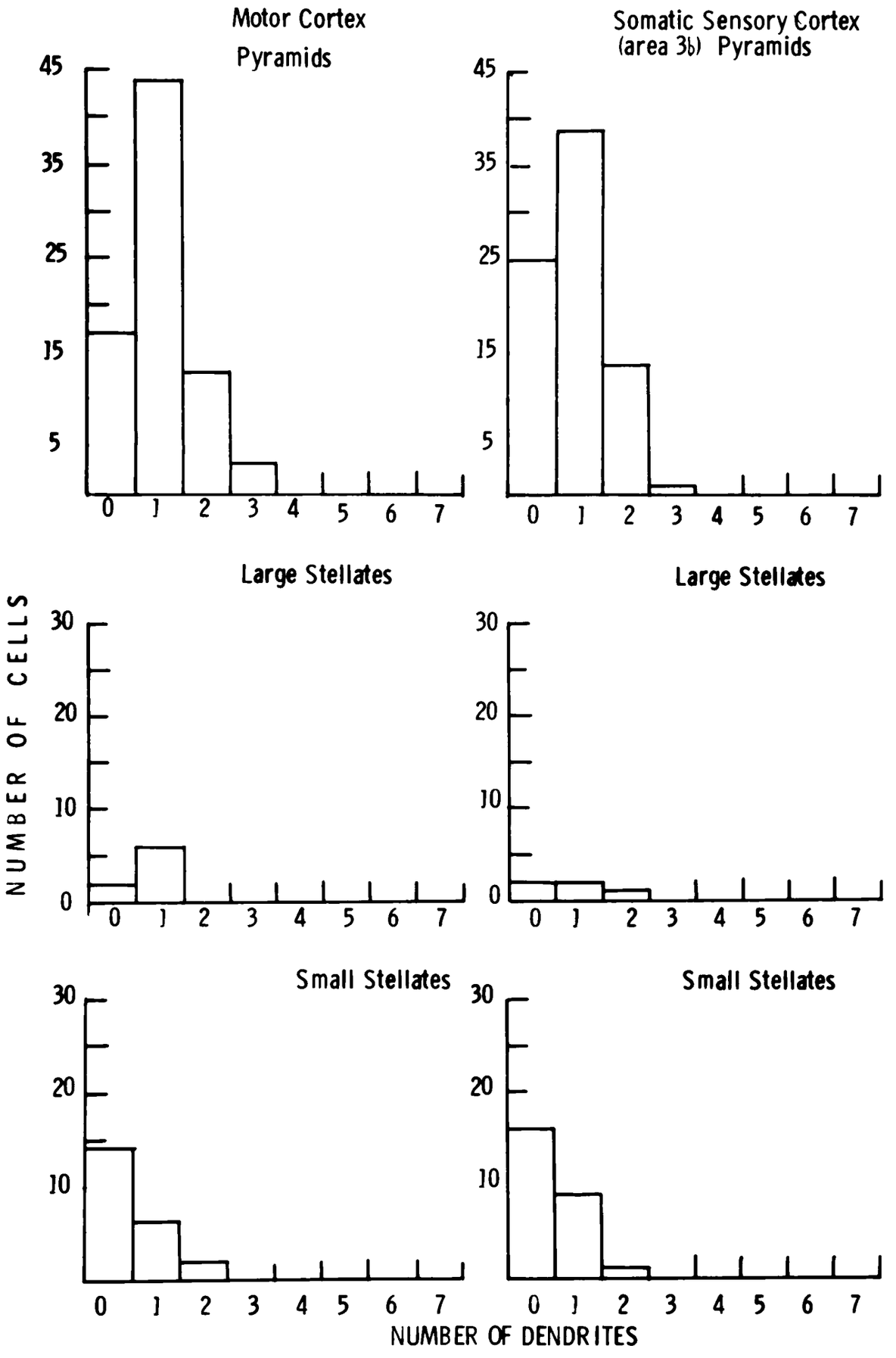

Fig. 4-54 Histograms of the mean diameters and numbers of synapses received by those stellate cell somata found to receive axo-somatic synapses from degenerating thalamo-cortical axon terminals in the experimental study of the motor cortex. Reproduced from Chapter 9.

MEAN DIAMETERS AND NUMBERS OF SYNAPSES RECEIVED BY CELL SOMATA RECEIVING DEGENERATING THALAMO-CORTICAL TERMINALS. IN THE MOTOR CORTEX

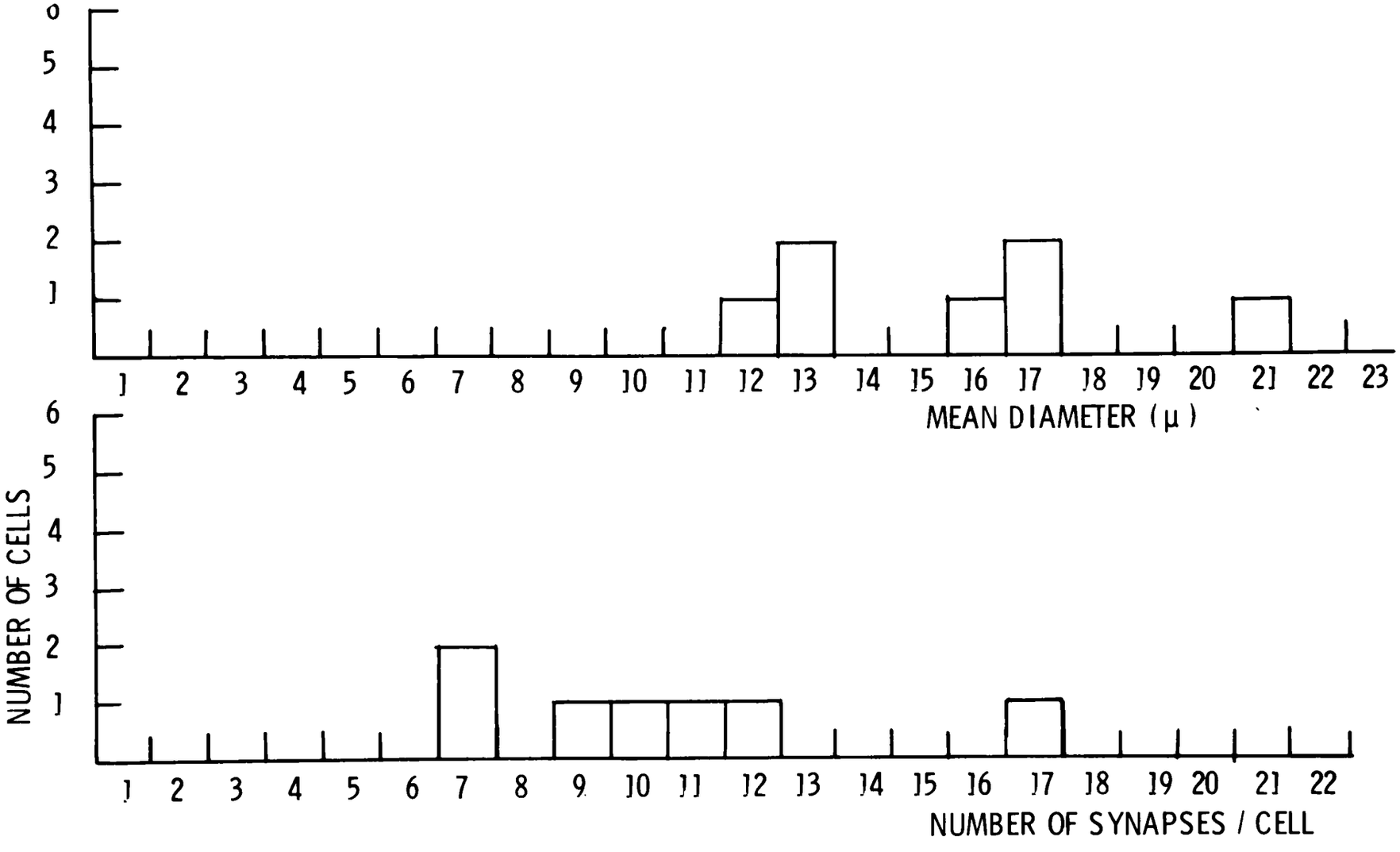

Illustrations to Chapter 5

A STUDY OF THE AXON INITIAL SEGMENT AND PROXIMAL AXON OF NEURONS IN THE MOTOR AND SOMATIC SENSORY CORTICES

Figs. 5-1 to 5-13 Pyramidal axon initial segment which was traced in continuity from the cell soma to the first Node of Ranvier of its myelinated axon.

Fig. 5-1 Pyramidal cell soma in layer III of motor cortex with the first part of its axon initial segment which is directed towards the white matter.

Section No. 45 X 4,600

Fig. 5-2 Serial section to fig. 5-1 showing the continuation of the axon initial segment. The same dendrite (d) is marked on both sections and this and other landmarks could be followed through the intervening sections.

Section No. 36 X 8,400

Fig. 5-3 Axon initial segment of figs. 5-1 and 5-2 traced to the beginning of its myelin sheath (large arrowheads) in a serial section. The same axon 'a' is marked in both figs. 5-2 and 5-3 and this and other landmarks were traced through the intervening sections. Note the large number of synapses received by the initial segment right up to the beginning of the myelin sheath.

Section No. 26 X 8,400

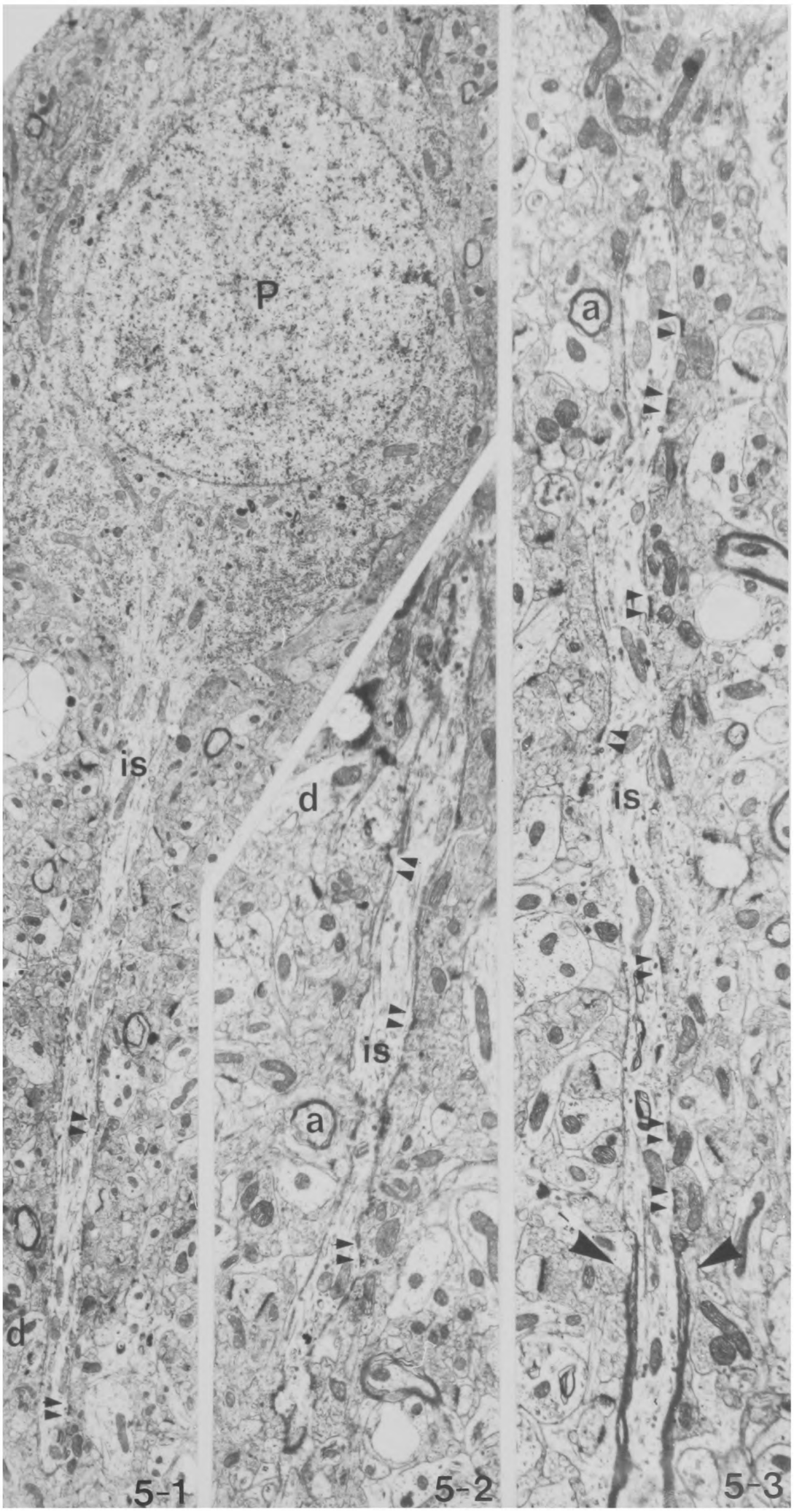
P
is
d
is
a
d
a
is
5-1
5-2
5-3

Figs. 5-4 to 5-13 The myelinated axon of the cell of figs. 5-1 to 5-3 was traced in continuity to its first Node of Ranvier where it gave rise to two collaterals, the second of which was myelinated. In all the figures the proximal end of the axon is to the left.

Fig. 5-4 The axon emerging from the myelin sheath of its first internode. The unmyelinated continuation of the axon (u) was traced in continuity with the proximal (left) end of the axon in fig. 5-9 where the next myelin sheath started. Note that the unmyelinated continuation of the main axon is well past dendrite (d).
Section No. 44 X 29,000

Figs. 5-5 to 5-8 Serial sections 34, 33, 31 and 29 respectively of the same axon as fig. 5-4. Note how in progressing to the lower numbered sections the collateral (b) becomes separated from the parent axon. The continuation of the parent axon (u) was followed in serial section of increasing number. All X 22,000

Fig. 5-9 Section 65. This shows the continuation of the parent axon (u) which was traced in continuity through the sections between 44 (fig. 5-4) and 65. The parent axon has now become myelinated again (a'). Note the cisternal organ-like structure (Arrowhead) in the expansion from which the second collateral b' arises. X 29,000

Figs. 5-10 to 5-13 Sections 69, 73, 74 and 81 respectively. These sections show the second axon collateral b' becoming separated off from the continuation of the parent axon a'. The collateral can be seen to become myelinated as it is traced through these serial sections. All X 22,000

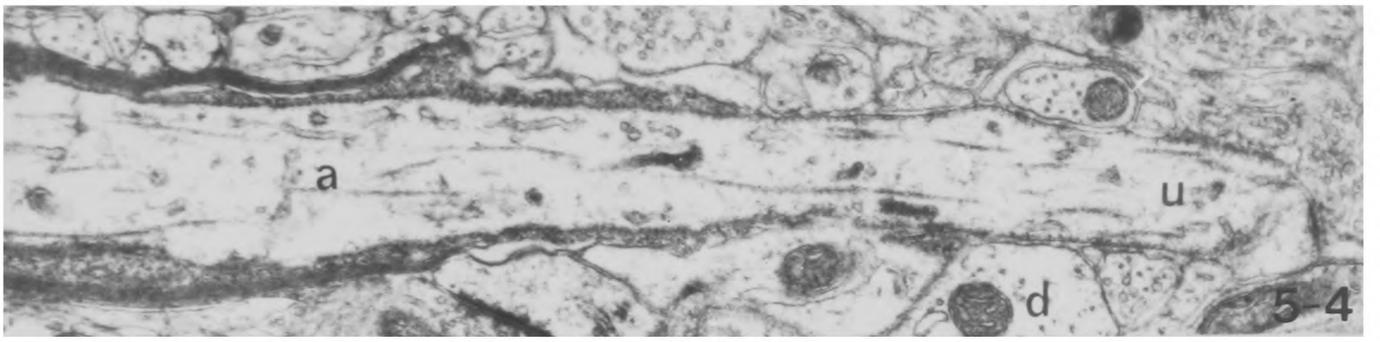
a
u
d
5-4

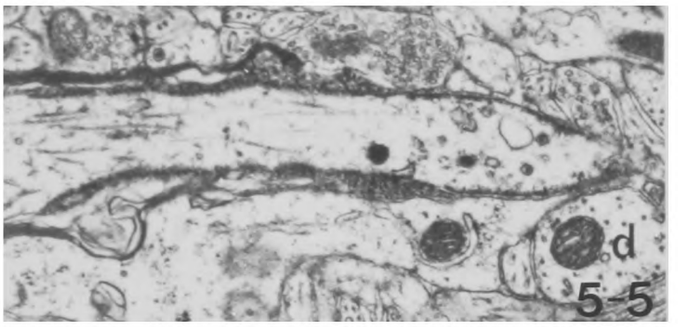
d
5-5

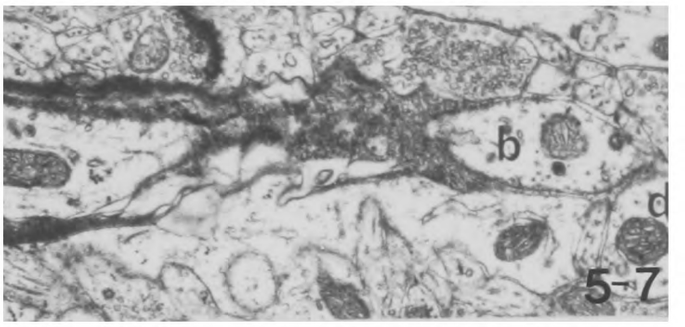
b
d
5-7

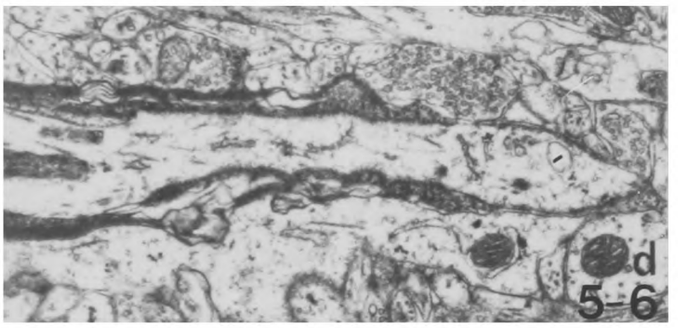
d
5-6

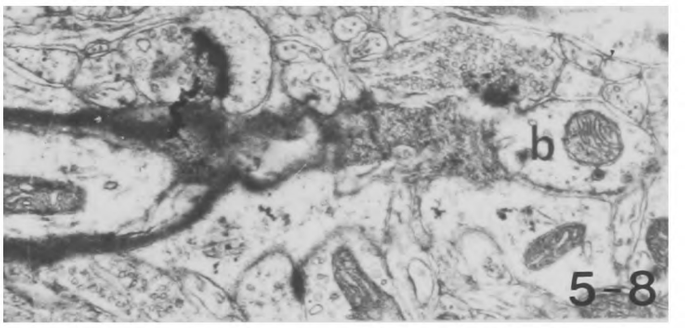
b
5-8

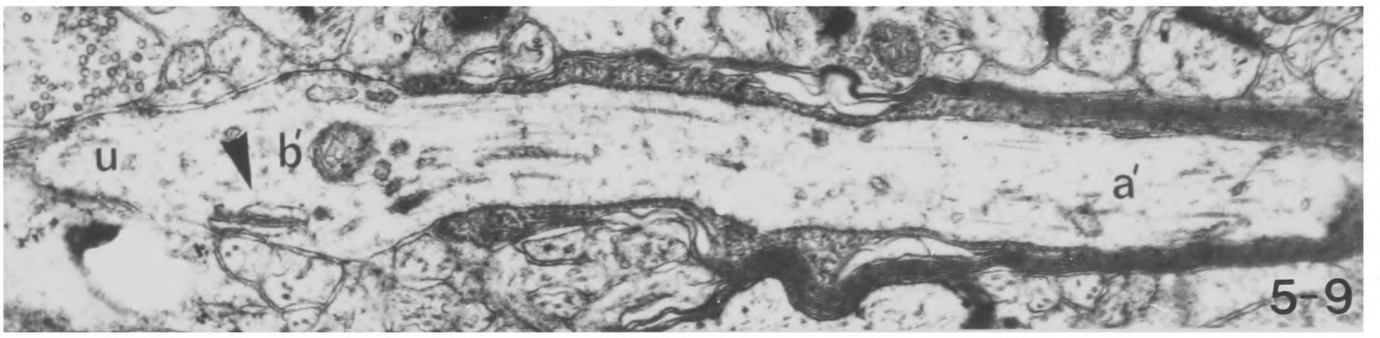
u
b′
a′
5-9

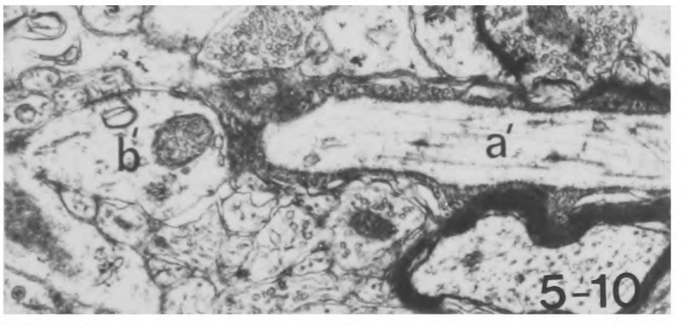
b′
a′
5-10

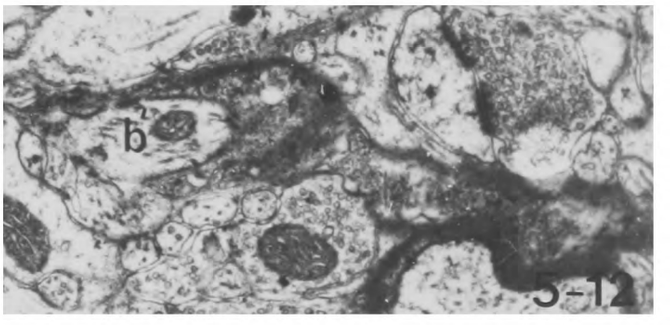
b
5-12

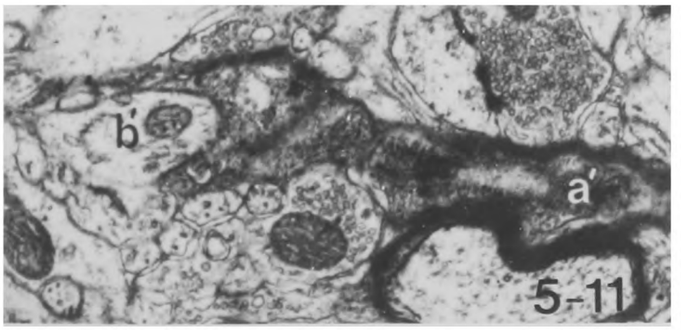
b′
a′
5-11

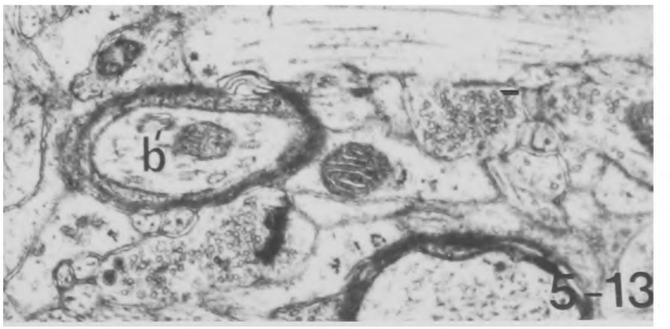
b′
5-13

Large stellate cell initial segment.

Fig. 5-14 Large stellate cell from layer IV of motor cortex with an axon initial segment directed toward the pial surface. Note the large size of the cell soma, its abundant cytoplasm full of organelles and the large number of synapses it receives (arrows). The large arrowhead indicates the first part of the myelinated axon of this cell as shown by serial sections.

Section No. 1 X 4,000

Fig. 5-15 Serial section showing the first part of the initial segment of the large stellate cell in fig. 5-14. Note the lack of synapses on the initial segment although synapses are present on the immediately adjacent cell soma.

Section No. 7 X 9,000

Fig. 5-16 The initial segment of the large stellate cell of fig. 5-14 showing it entering its myelin sheath.

Section No. 8. X 9,000

The relative positions of figs. 5-14 to 5-16 are given by the axons a and x marked in all three serial sections.

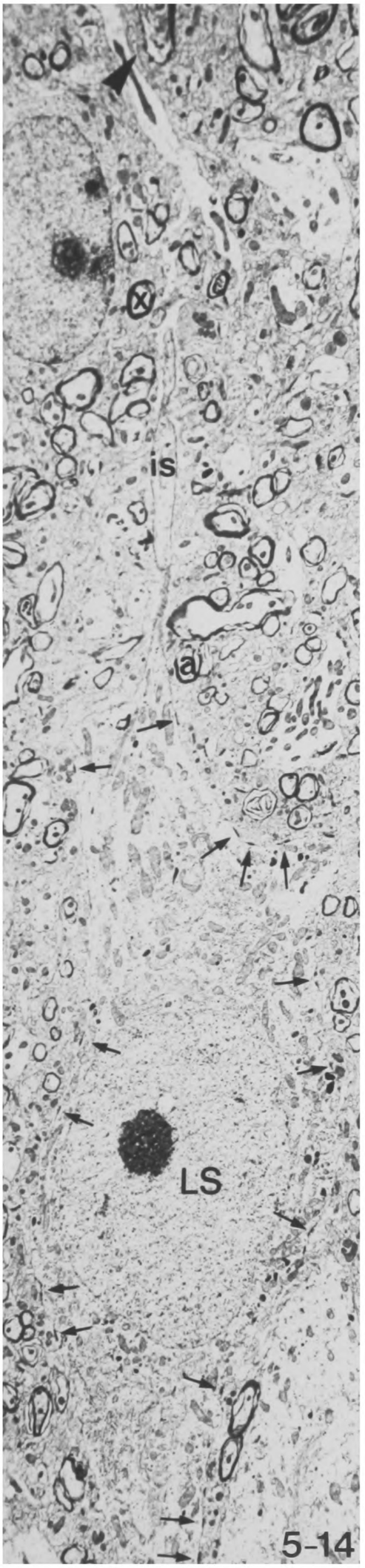

5-14

5-15

5-16

Fig. 5-17 Graph showing the relationship between the mean diameter of a cell soma and the diameter of its axon. There is approximately linear relationship with large cells giving rise to proportionately wider axons.

AXON DIAMETER AGAINST MEAN CELL DIAMETER FOR FULL LENGTH INITIAL SEGMENTS

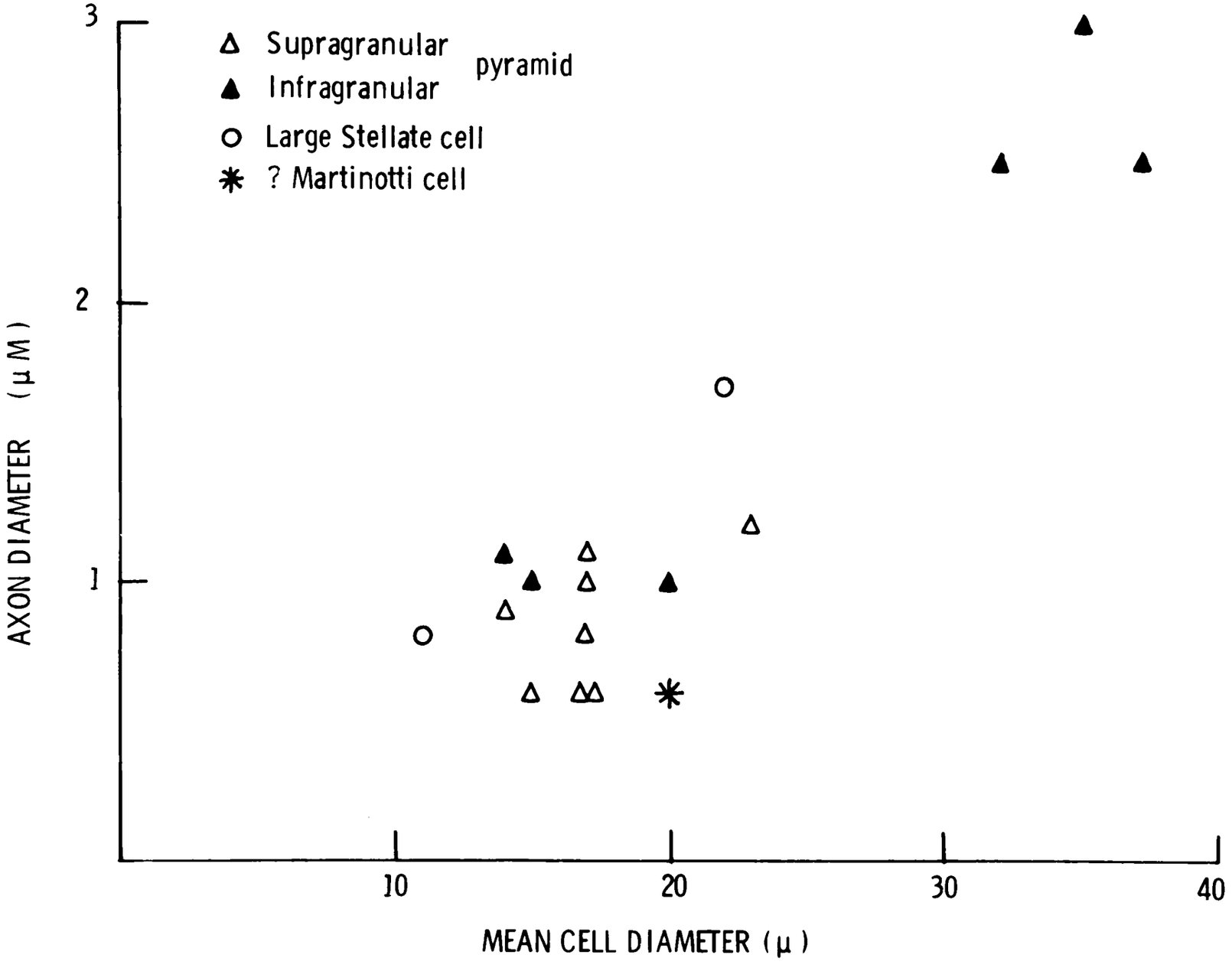

Fig. 5-18 Graph showing the relationship between the mean diameter of a cell soma and the length of its axon initial segment. Note that although the two large stellate initial segments are shorter than those of the pyramidal cells there is no tendency for larger cells to have larger initial segments within one cell type comparable to the increase in initial segment diameter (fig. 5-17).

LENGTH OF AXON INITIAL SEGMENT AGAINST MEAN CELL DIAMETER

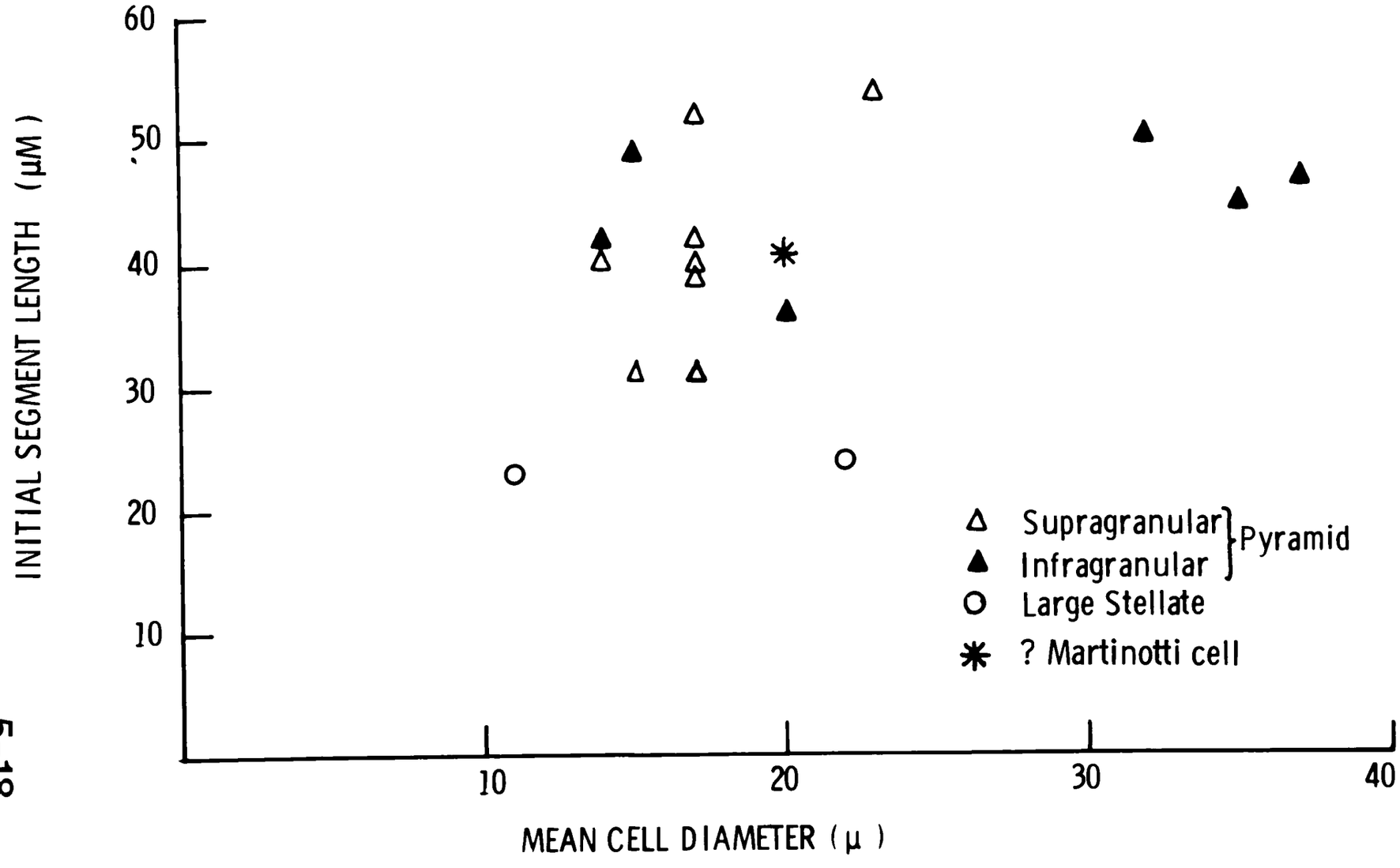

Fig. 5-19 Graph showing the relationship between the length of the axon initial segment and the diameter of the axon which it gives rise to. As with mean cell diameter (fig. 5-18) larger diameter axons do not arise from proportionately longer axon initial segments.

LENGTH OF AXON INITIAL SEGMENT AGAINST AXON DIAMETER

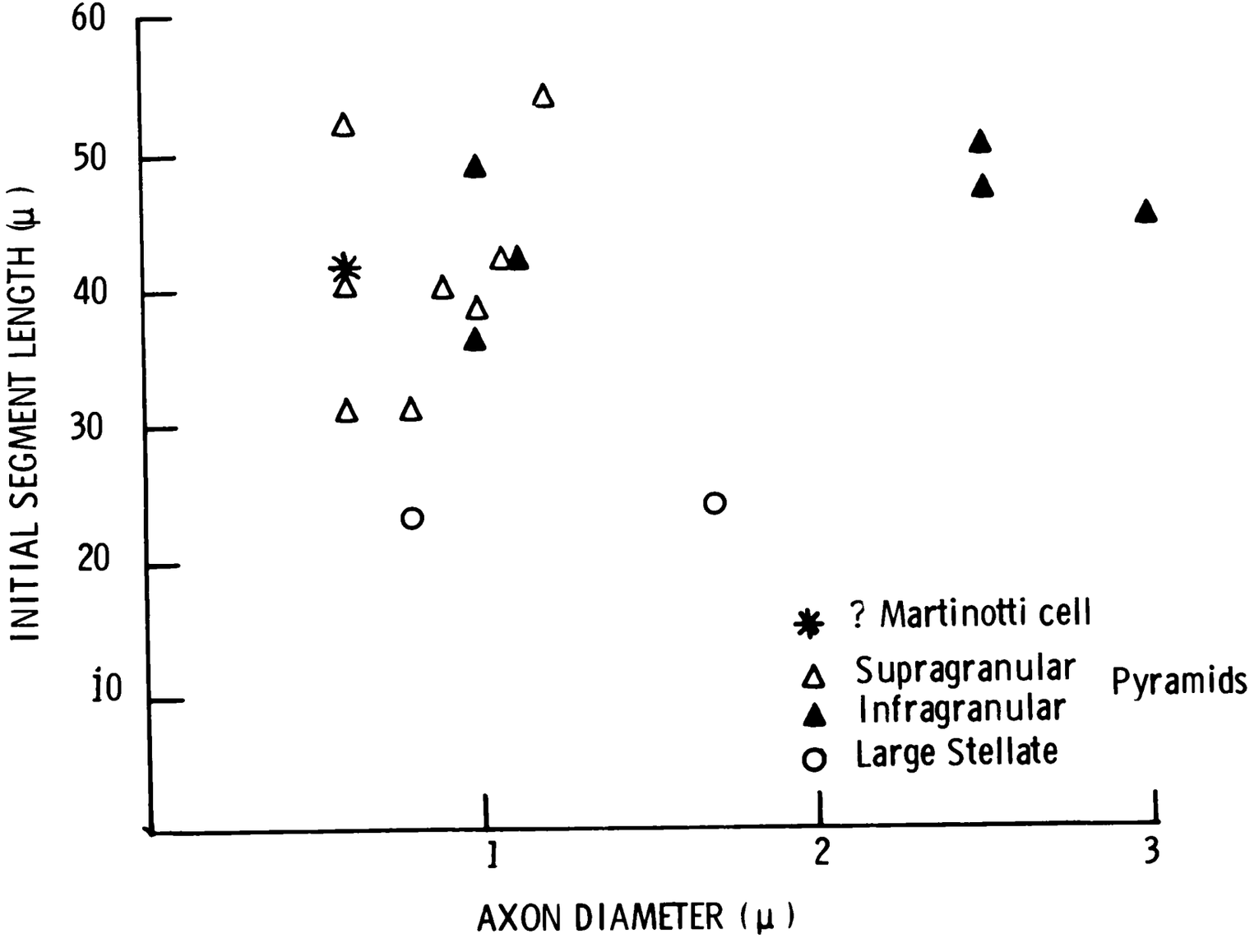

Fig. 5-20 Histogram showing the distribution of synapses along the length of the complete pyramidal axon initial segments, each initial segment being divided into 5 μ segments.

PYRAMIDAL INITIAL SEGMENTS. NUMBERS OF SYNAPSES AGAINST ABSOLUTE DISTANCE FROM CELL SOMA.

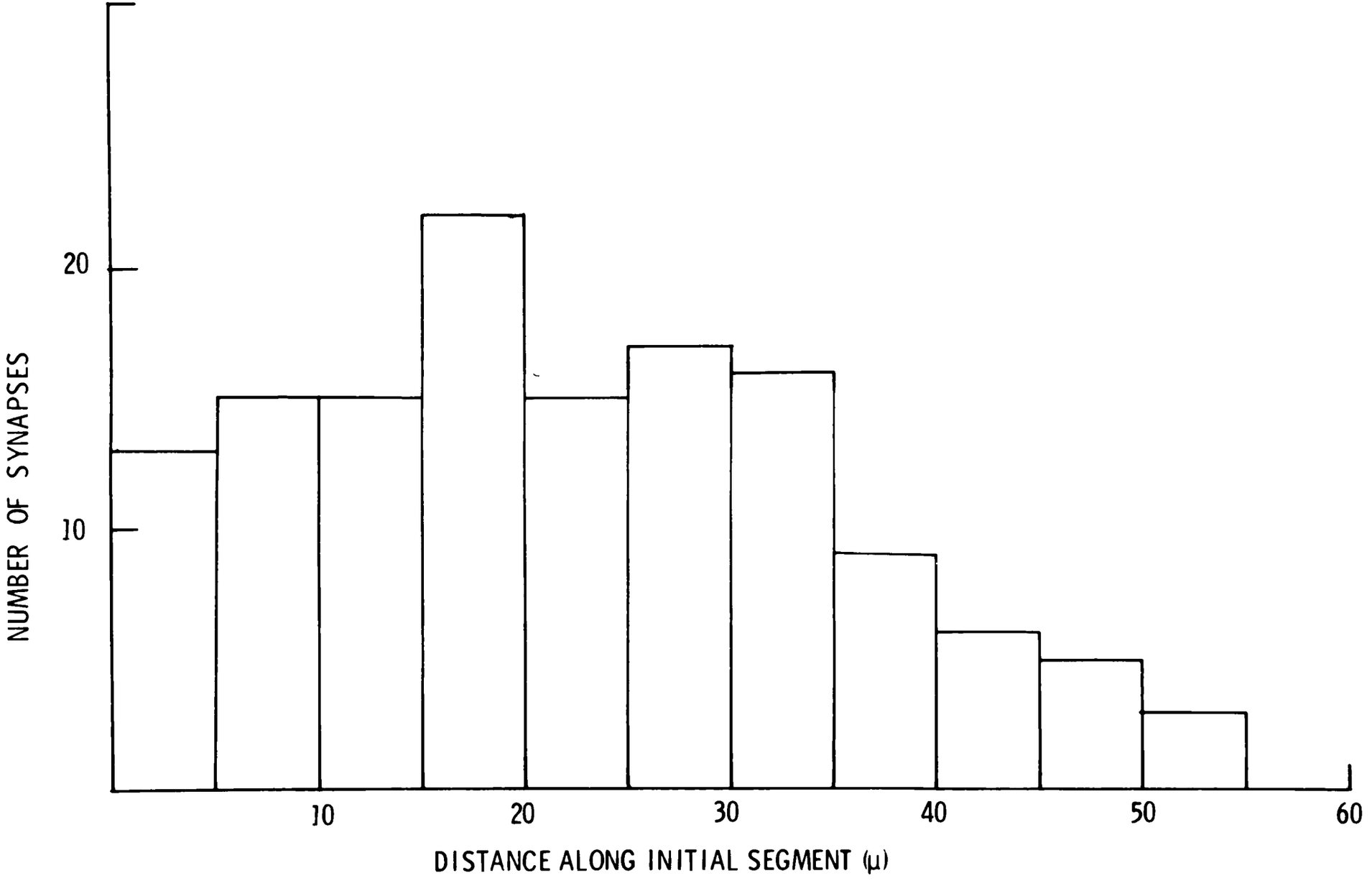

Fig. 5-21 Histogram showing the distribution of synapses along the length of the complete pyramidal initial segment, each initial segment being divided into ten equal parts.

PYRAMIDAL INITIAL SEGMENTS . NUMBERS OF SYNAPSES IN EACH TENTH OF INITIAL SEGMENT LENGTH.

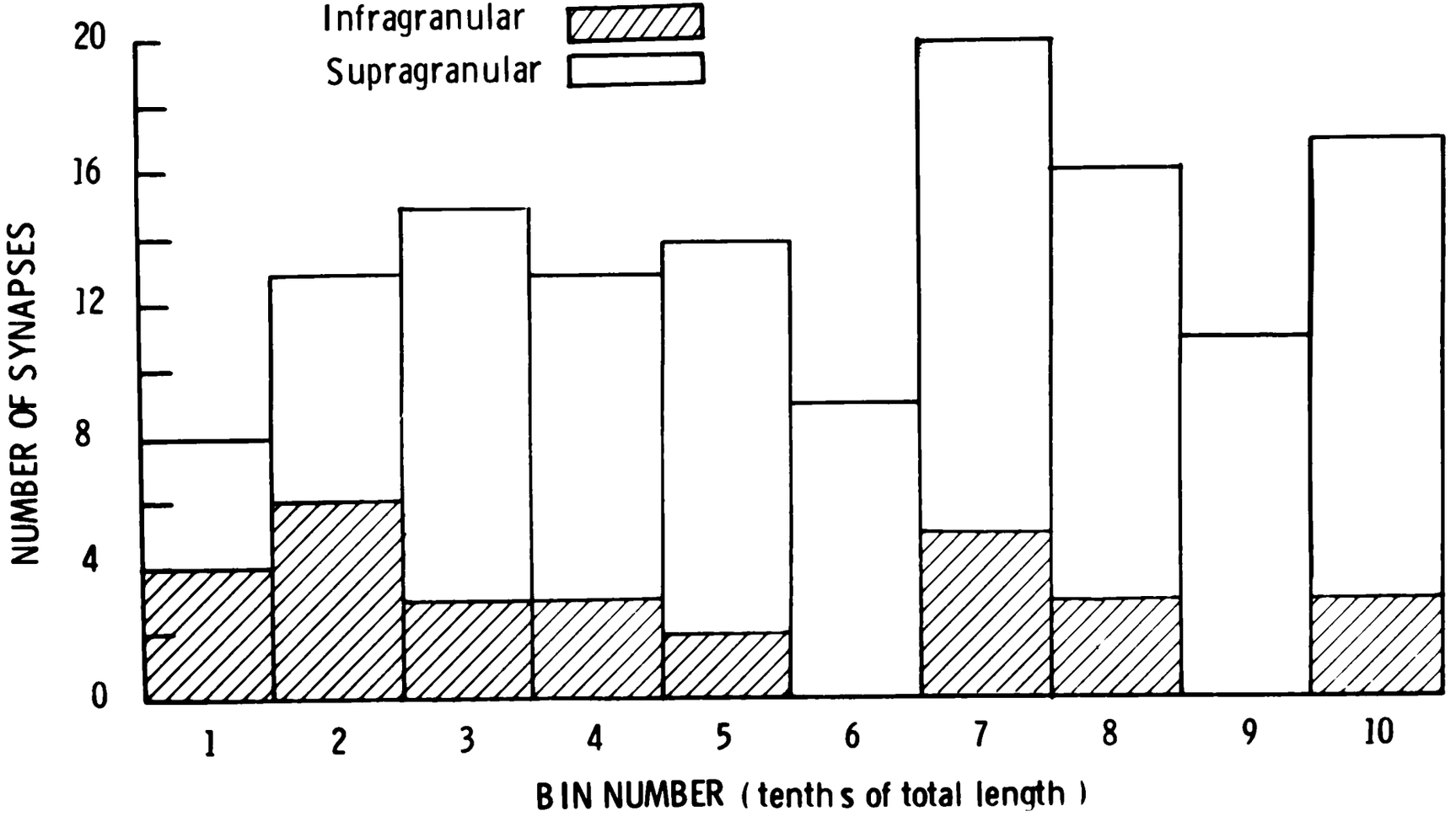

Fig. 5-22 Graph showing the number of synapses found on each complete pyramidal initial segment against the initial segment diameter. Initial segments of supragranular pyramids can be seen to receive consistently more synapses than those of infragranular pyramids and no more synapses were found on large diameter initial segments of infragranular pyramids than on small ones, thus indicating a similar synaptic density (see Appendix 2).

NUMBER OF SYNAPSES FOUND ON FULL LENGTH PYRAMIDAL INITIAL SEGMENTS AGAINST INITIAL SEGMENT DIAMETER

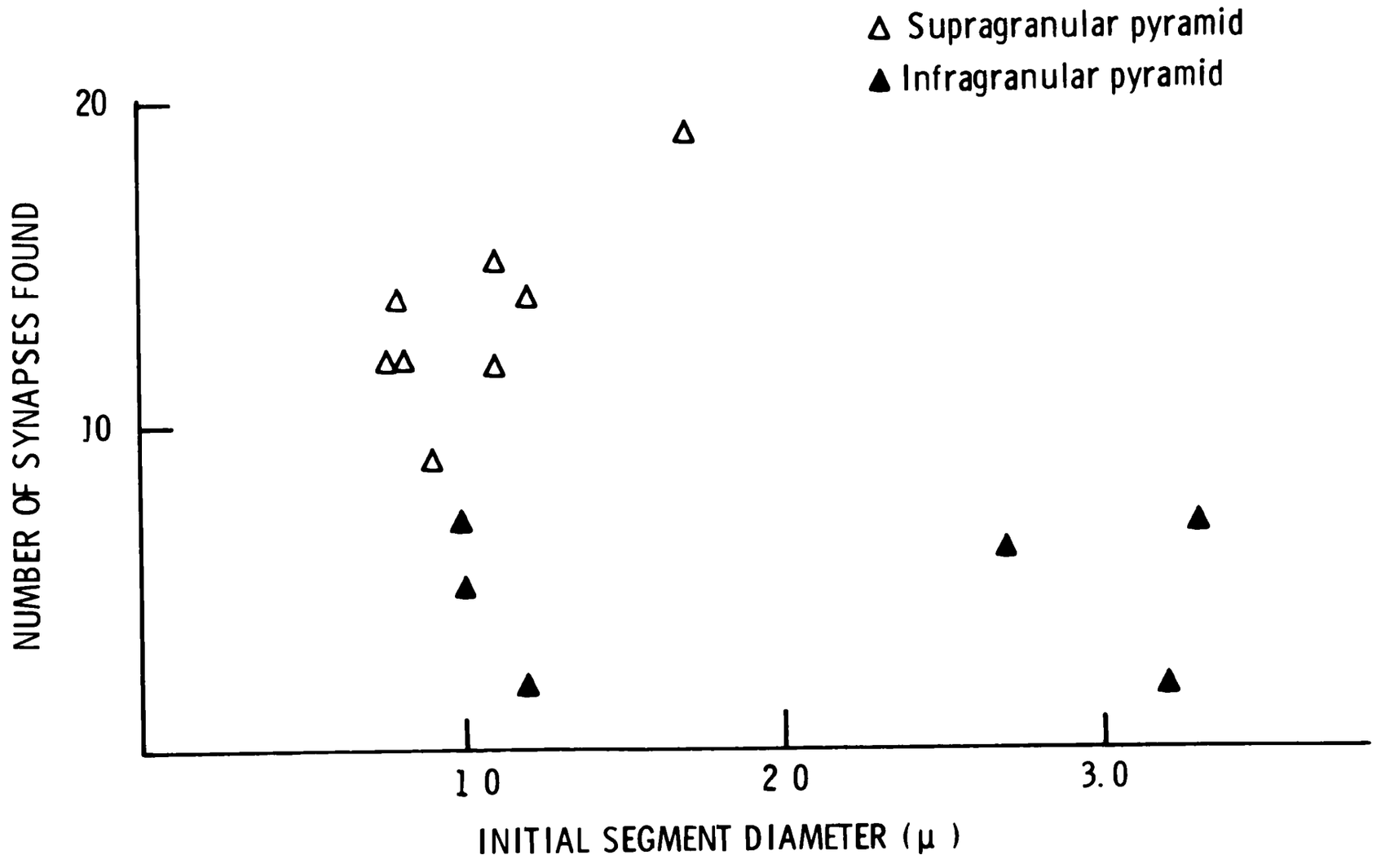

ig. 5-23 Graph showing the calculated total number of synapses received by each full-length pyramidal initial segment against its diameter. Note the separation of supragranular and infragranular pyramids.

TOTAL NUMBER OF INITIAL SEGMENT SYNAPSES AGAINST INITIAL SEGMENT DIAMETER

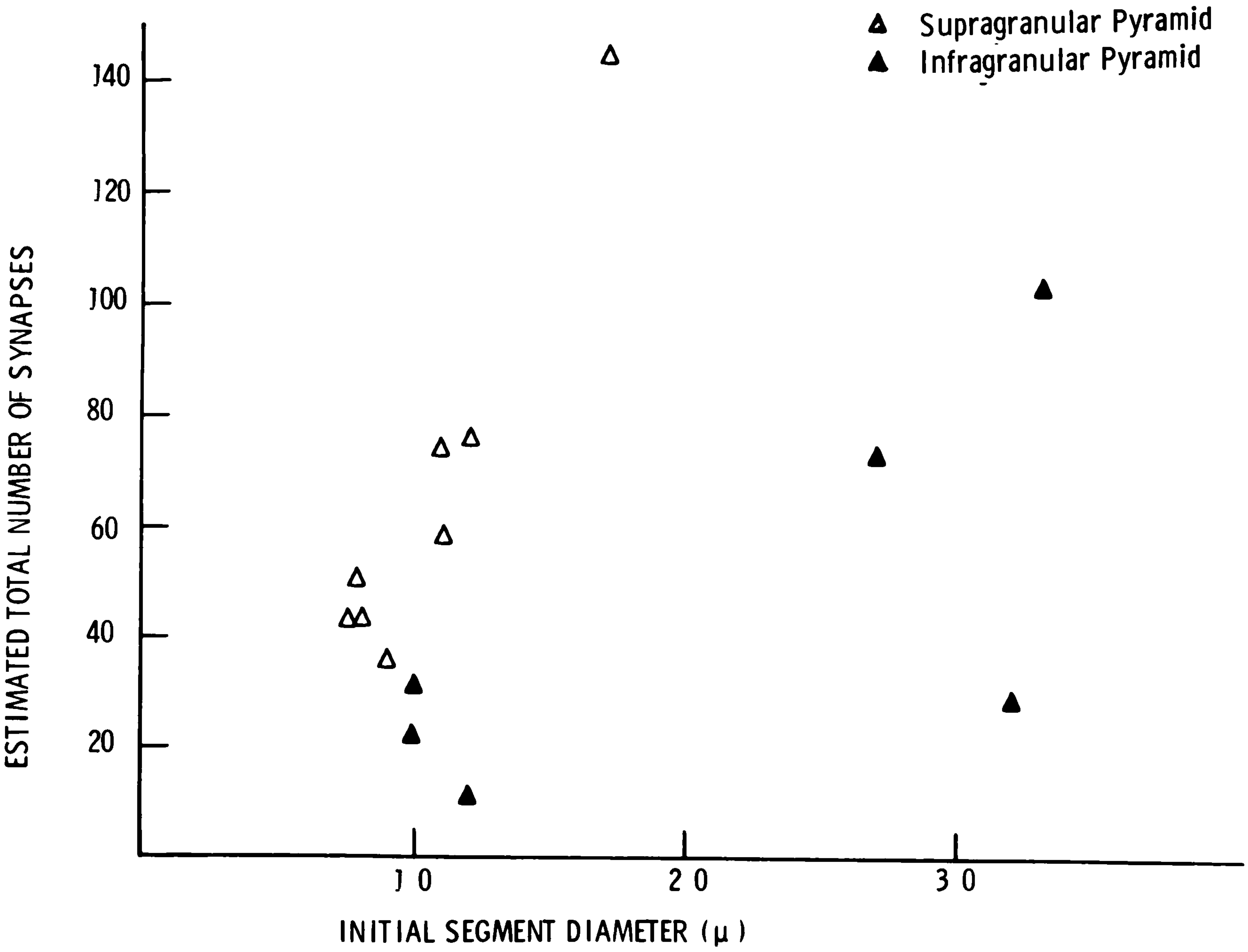

Fig. 5-24 Graph showing the calculated total number of synapses received by each full-length pyramidal initial segment against the mean diameter of its cell soma. Note the separation of supragranular and infragranular pyramids.

TOTAL NUMBER OF INITIAL SEGMENT SYNAPSES AGAINST MEAN CELL DIAMETER

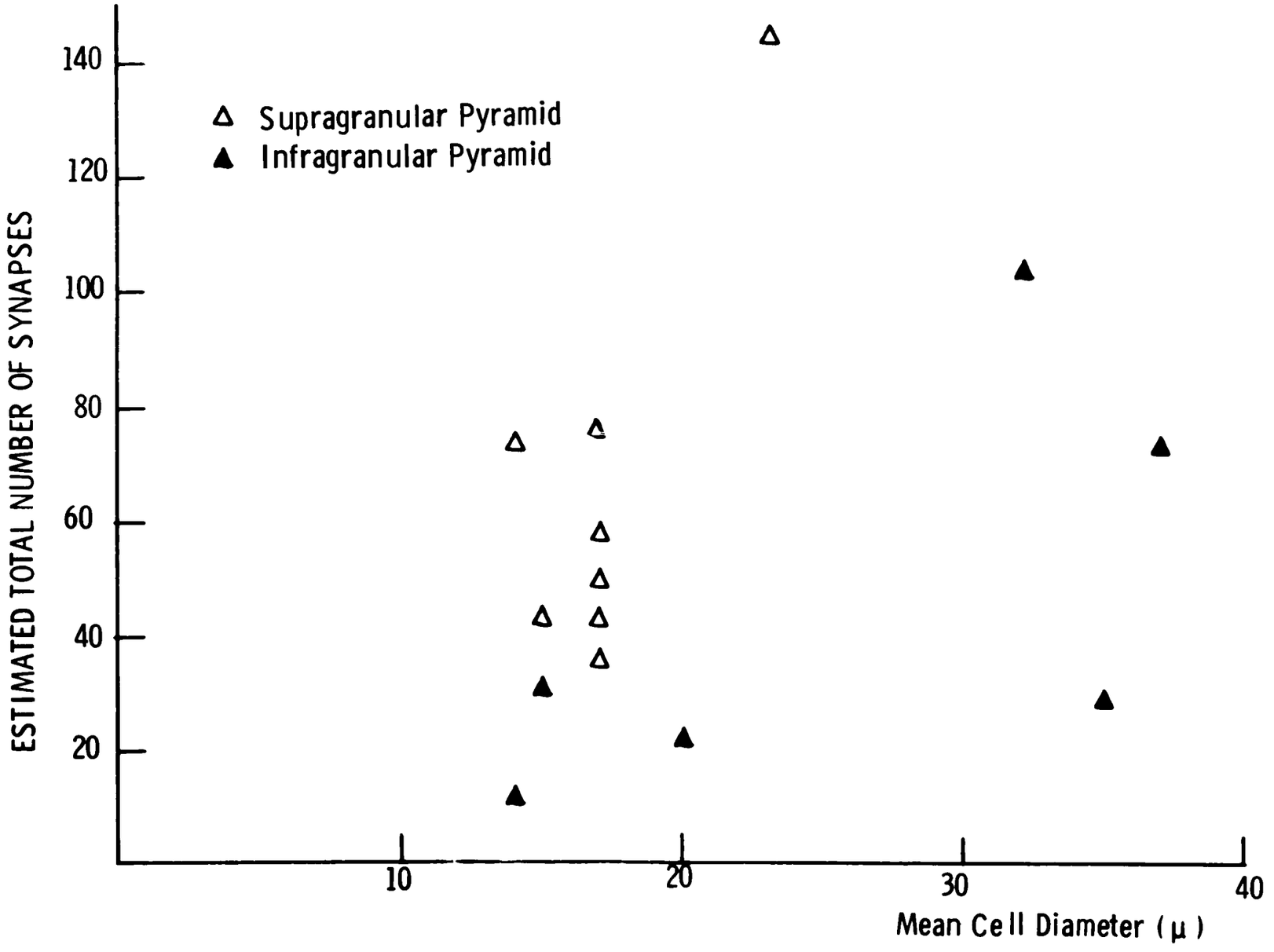

Fig. 5-25 Graph showing the relationship of the diameters of the cell soma and axon initial segment for the various cell types. In general larger diameter cells give rise to larger diameter axon initial segments with there being no marked difference between cells of similar size but different types.

RELATIONSHIP OF DIAMETER OF SOMA AND INITIAL SEGMENT

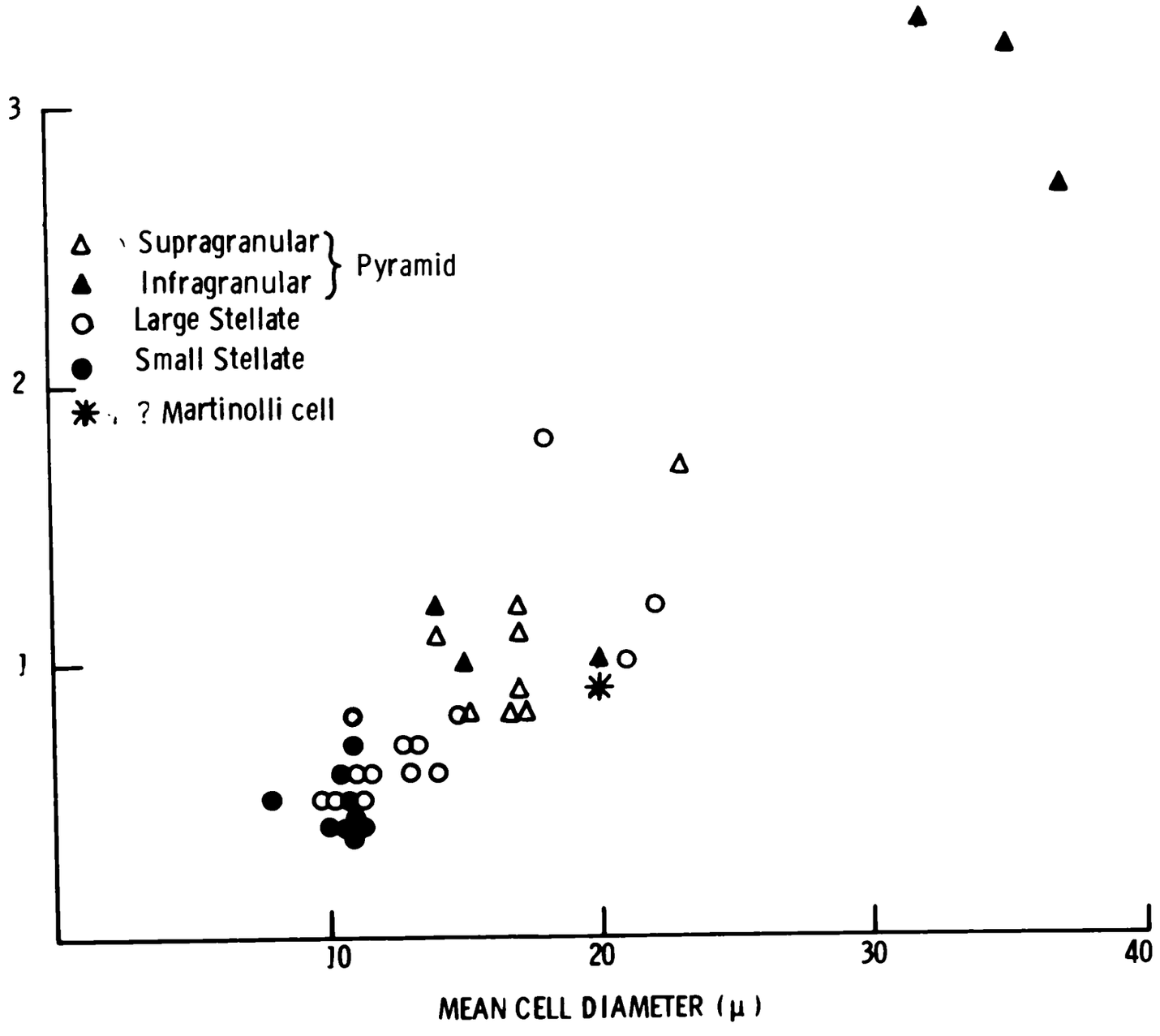

Fig. 5-26 A Betz cell in layer V of motor cortex which in serial sections was shown to give rise to the axon initial segment of figs. 5-27 to 5-31. X 1300

Fig. 5-27 Axon initial segment of the Betz cell of fig. 5-26 in a serial section. The nucleus of the cell is no longer in the plane of the section although a considerable amount of cytoplasm is still seen. Much of the apparent tapering of the initial segment is due to its not being parallel to the plane of the section. The continuity of the initial segment with the myelinated axon (a) was confirmed in serial sections (e.g., fig. 5-31). X 3000

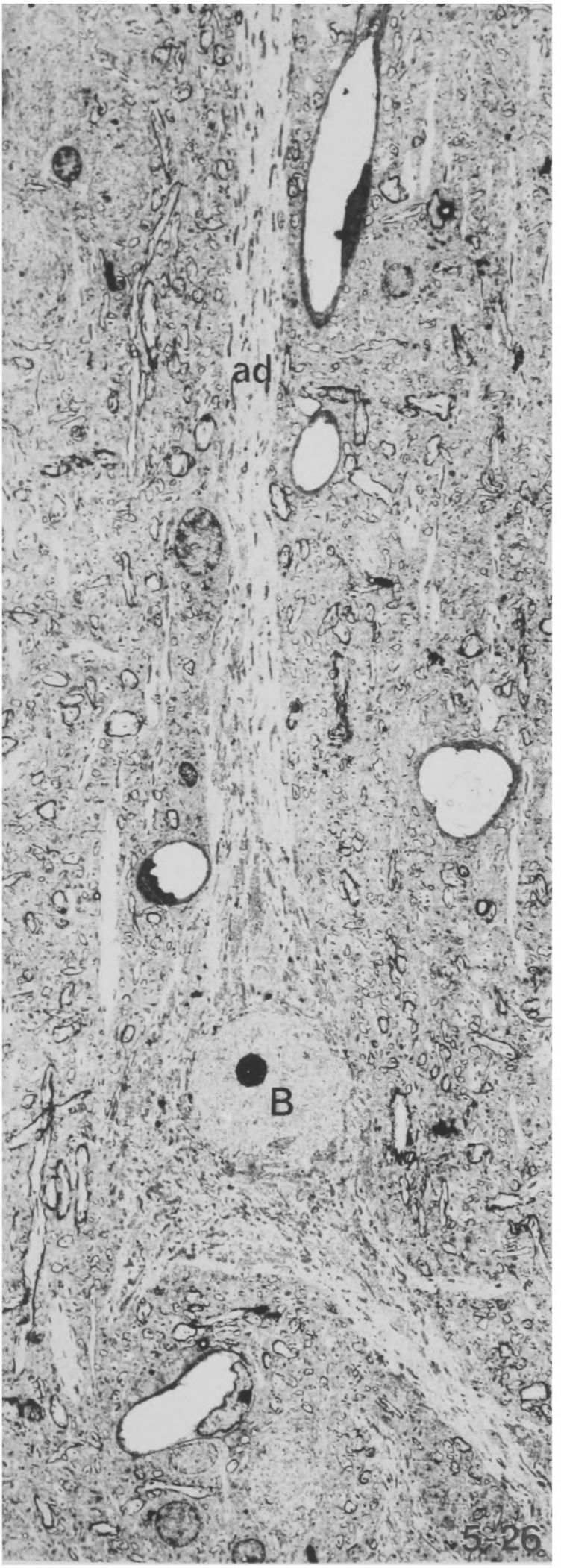

5-26

5-27

Fig. 5-28 Part of the axon hillock and the proximal part of the Betz cell axon initial segment of fig. 5-27. There is a spine on the initial segment which receives synapses from two axon terminals. X 9,000

Fig. 5-29 High power of the axonal spine of fig. 5-28. The lower synapse is clearly of the symmetrical type and in adjacent serial sections the other synapse was symmetrical, and both terminals also made synapses on to the shaft of the initial segment as well as on to the spine. No other synapses were present on the spine. X 32,000

Fig. 5-30 High power of part of the shaft of the Betz cell initial segment of fig. 5-27. Note the membrane undercoating (e.g. arrowhead) and bundle of neurotubules, both of these features being less striking than usual because of the large diameter of the initial segment. Note also the two synapses it receives. X 14,000

Fig. 5-31 High power of the last part of the Betz cell initial segment and the beginning of the myelin sheath in a serial section to fig. 5-27. X 24,000

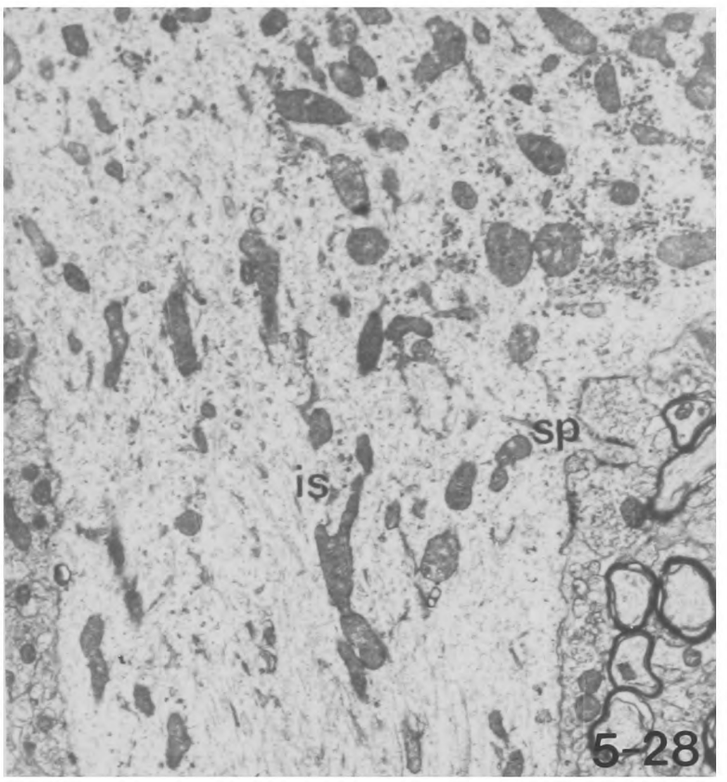

5-28

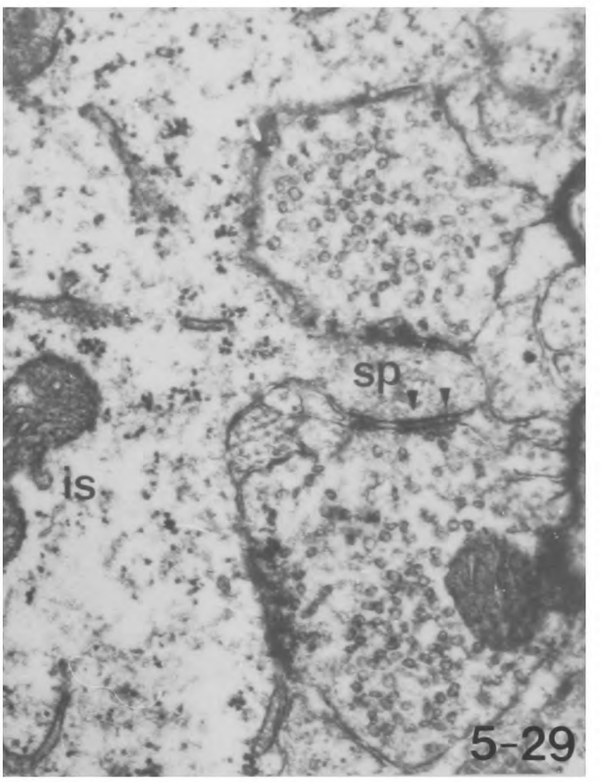

5-29

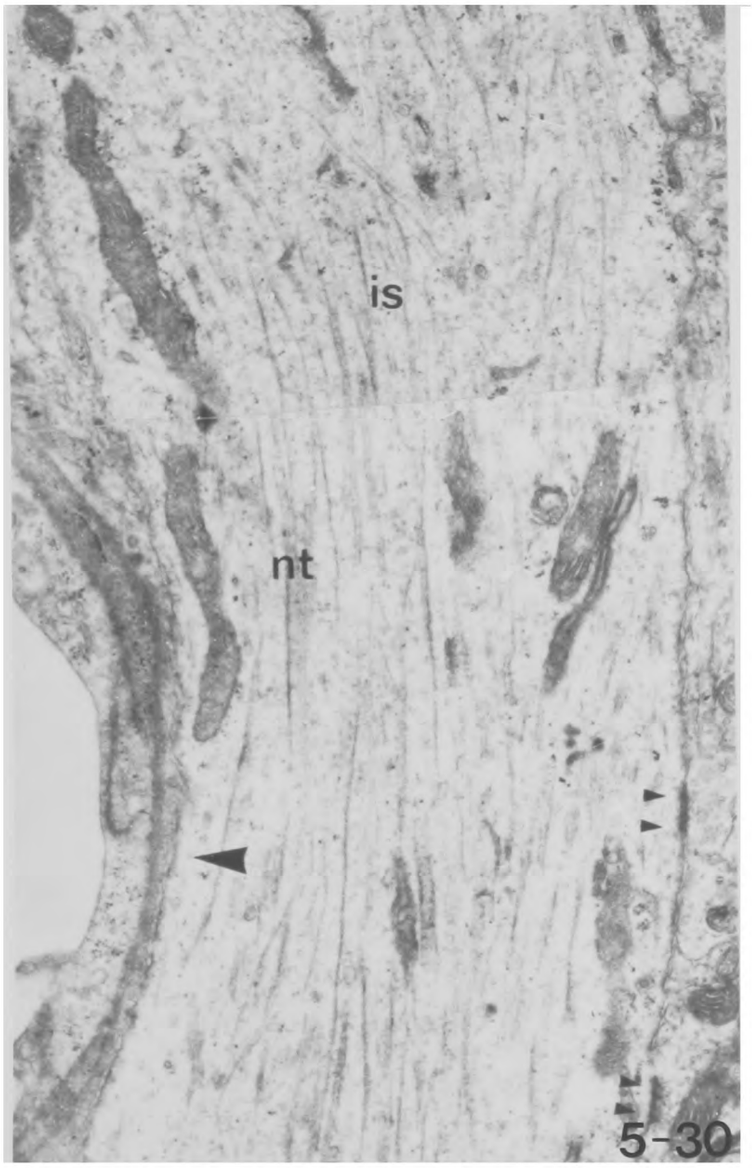

5-30

5-31

Cisternal organs and subsurface cisternae in initial segments.

Fig. 5-32 Cisternal organ in a pyramidal axon initial segment. Note how it becomes closely apposed to the plasma membrane of the initial segment opposite the non-synaptic regions of two axon terminals T_1 and T_2, but avoids the synaptic membrane complex. T_2 made a symmetrical synapse on to the initial segment in the region of the arrowhead in an adjacent section. Note also the associated mitochondrion. X 29,000

Figs. 5-33 to 5-36 Adjacent serial sections showing an axon initial segment and cisternal organ cut transversely in sections parallel to the pial surface. Note how the cisternal organ is closely applied to the initial segment membrane opposite the non-synaptic part of the axon terminal (t) (arrow) but consistently avoids the synaptic region itself, where the terminal makes a symmetrical synapse on to the initial segment. All X 48,000

Fig. 5-37 A cisternal organ showing its close apposition to the plasma membrane of the axon initial segment opposite the non-synaptic region (arrow) of the axon terminal (t) which makes a symmetrical synapse on to the initial segment. X 53,000

Fig. 5-38 An exposed membrane thickening on a small dendrite (d). This has become apposed to an axon initial segment in which there is an associated subsurface cistern. This association is the same as that seen when exposed membrane thickenings become apposed to dendrites on cell somata. Note the mitochondrion associated with the subsurface cistern and the membrane undercoating and neurotubules of the initial segment and the synapse it receives. X 29,000

Fig. 5-39 Higher magnification of the exposed membrane thickening and associated subsurface cistern of fig. 5-38. X 67,000

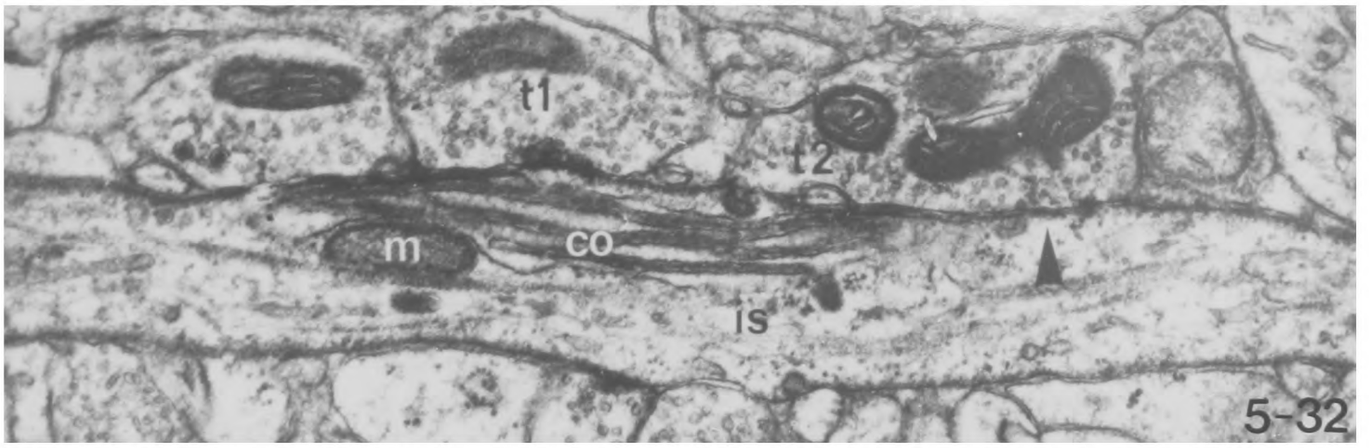
t1
t2
m
co
is
5-32

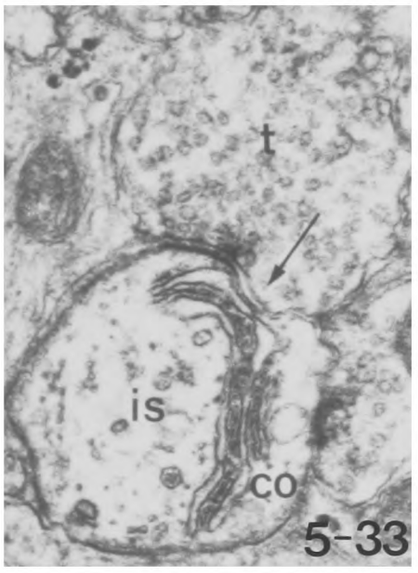
t
is
co
5-33

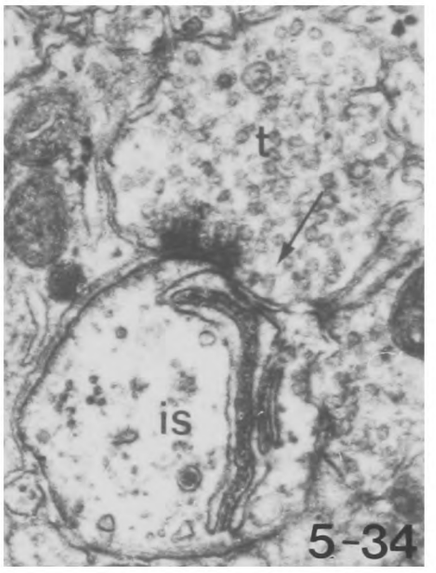
t
is
5-34

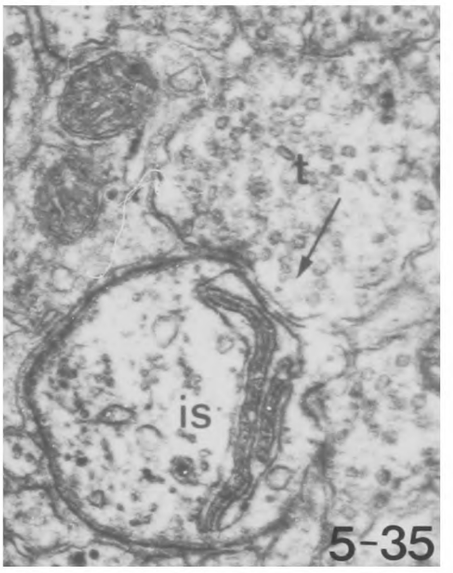
t
is
5-35


t
is
5-36

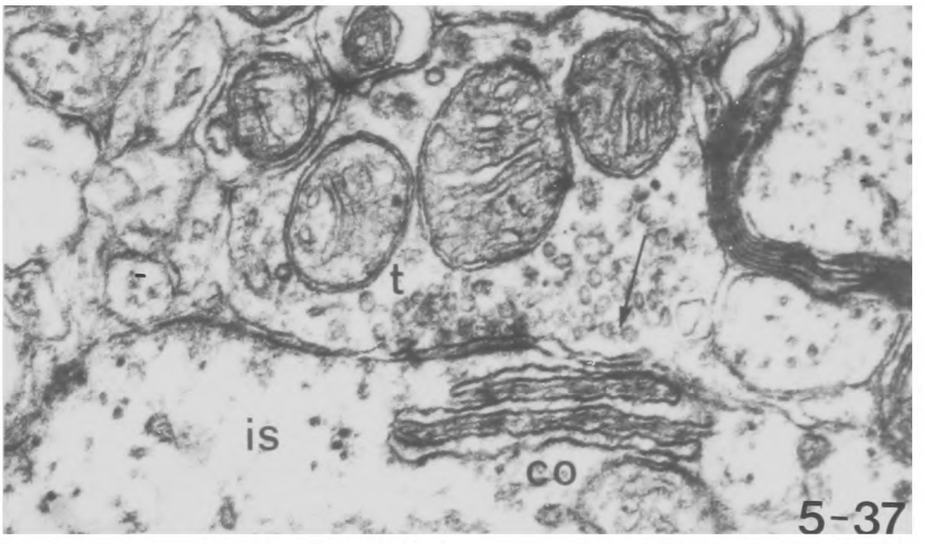
t
is
co
5-37

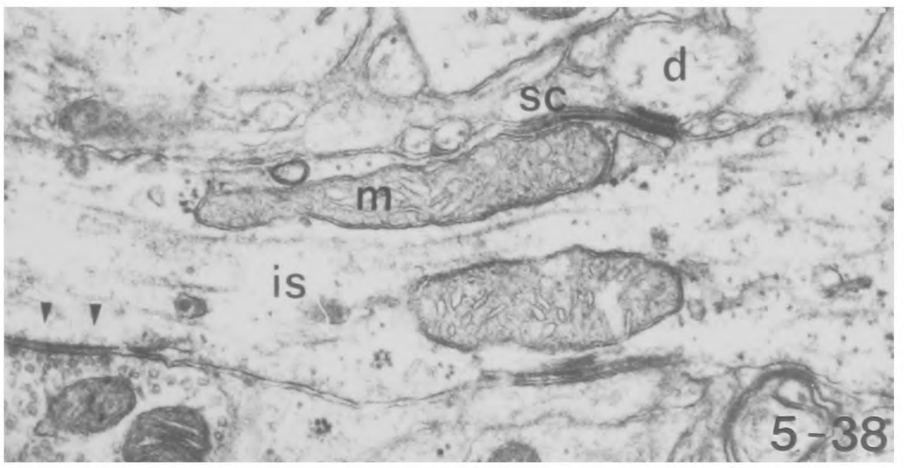
d
sc
m
is
5-38

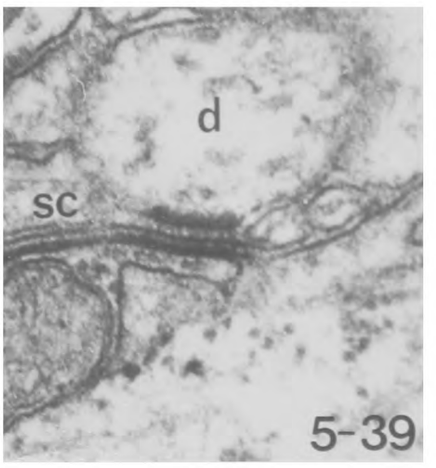
d
sc
5-39

Spines on axon initial segments.

Fig. 5-40 Part of an axon initial segment having a large sessile spine (sp.1) which receives a symmetrical synapse, and a second spine (sp.2) which does not receive a synapse in this particular section but does in an adjacent one. X 32,000

Fig. 5-41 A length of axon initial segment with a large and small sessile spine, both of which receive synapses. X 29,000

Fig. 5-42 Peg-like sessile spine on an axon initial segment. Note that it receives a synapse and contains a small cisternal organ which appears remarkably like a spine apparatus. X 29,000

Fig. 5-43 Example of an initial segment spine with a narrow stem and an expanded head which receives a symmetrical synapse. X 32,000

Fig. 5-44 A small sessile spine on an axon initial segment. Note the cisternal organ immediately adjacent to the spine which receives a symmetrical synapse. X 29,000

Fig. 5-45 A small initial segment spine with an expanded head receiving a symmetrical synapse. X 29,000

Fig. 5-46 An example of an axon initial segment which has two spines, both of which receive synapses from the same axon terminal (t). X 18,000

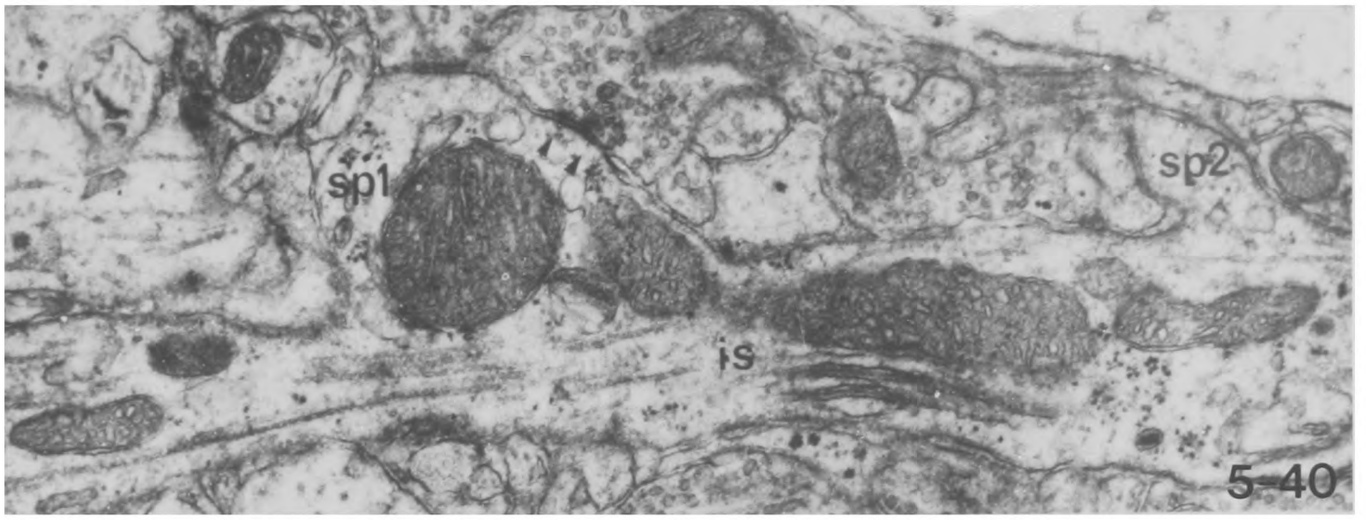
sp1
sp2
is
5-40

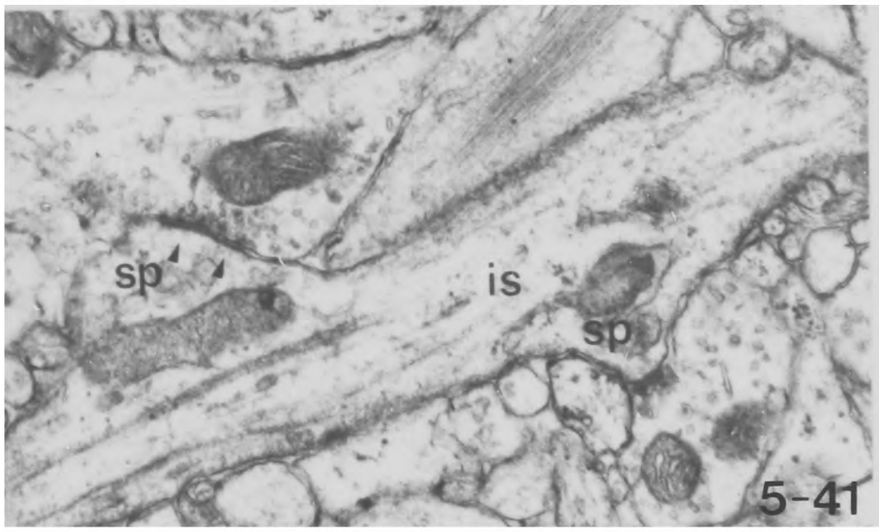
sp
is
sp
5-41

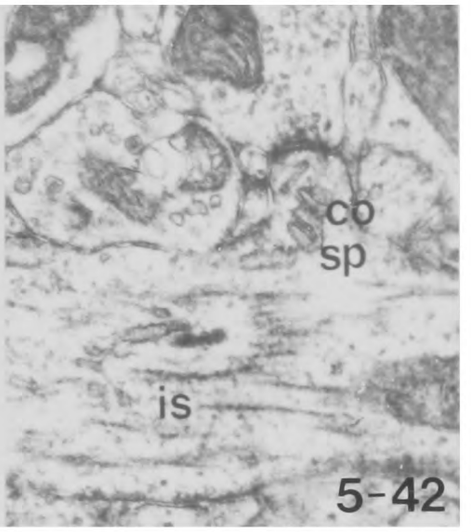
co
sp
is
5-42

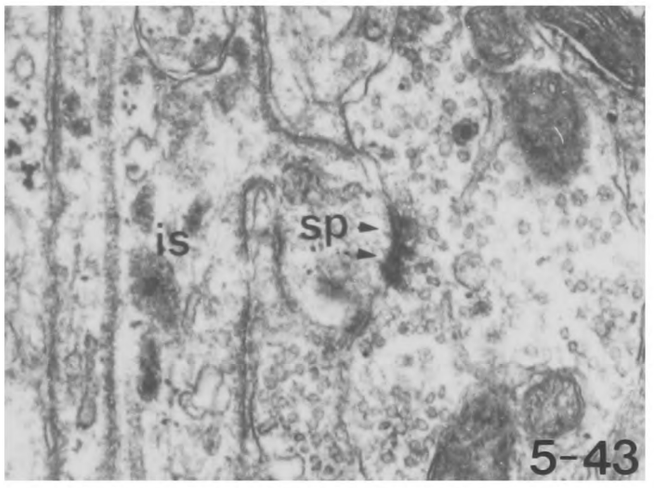
is
sp
5-43

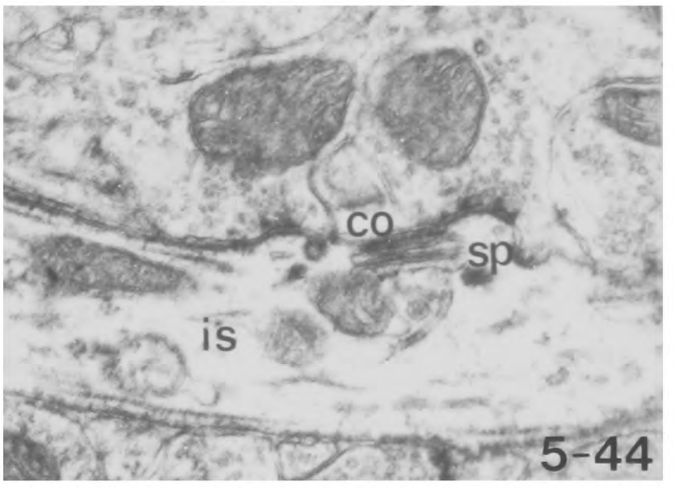
co
sp
is
5-44

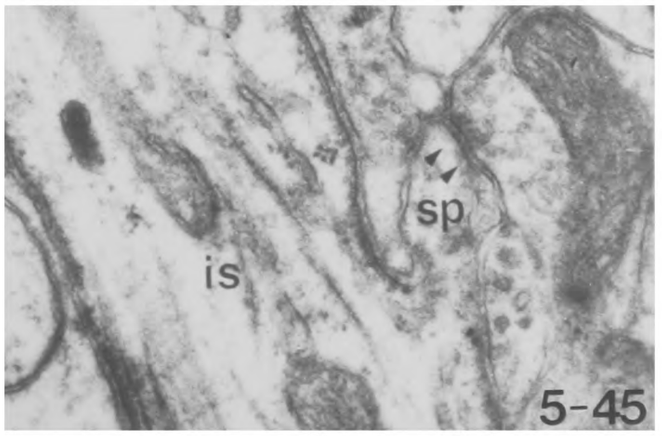
sp
is
5-45

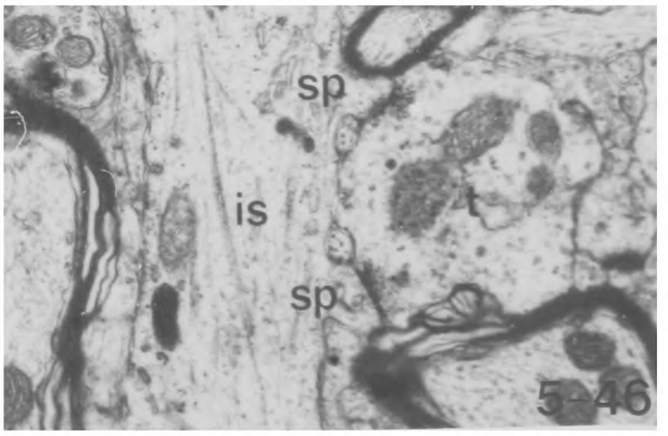
sp
is
t
sp
5-46

Figs. 5-47 to 5-59 The initial segment of a pyramidal cell which was shown in serial sections to give rise to an unmyelinated and then myelinated axon and to make an efferent synapse on to a dendrite.

Fig. 5-47 A pyramidal cell soma in layer II of motor cortex, giving rise to its initial segment.

Section No. 3 X 5,000

Fig. 5-48 Serial section to show the immediate continuation of the pyramidal cell initial segment from fig. 5-47. Note the part of the cell (P) still present at the top of the figure.

Section 14 X 8,400

Fig. 5-49 The continuation of the initial segment from figs. 5-47 and 5-48 in a further serial section. Note the same dendrite (d) present in all three sections. The proximal part of the initial segment is now to the left of the figure.

Section No. 22 X 9,000

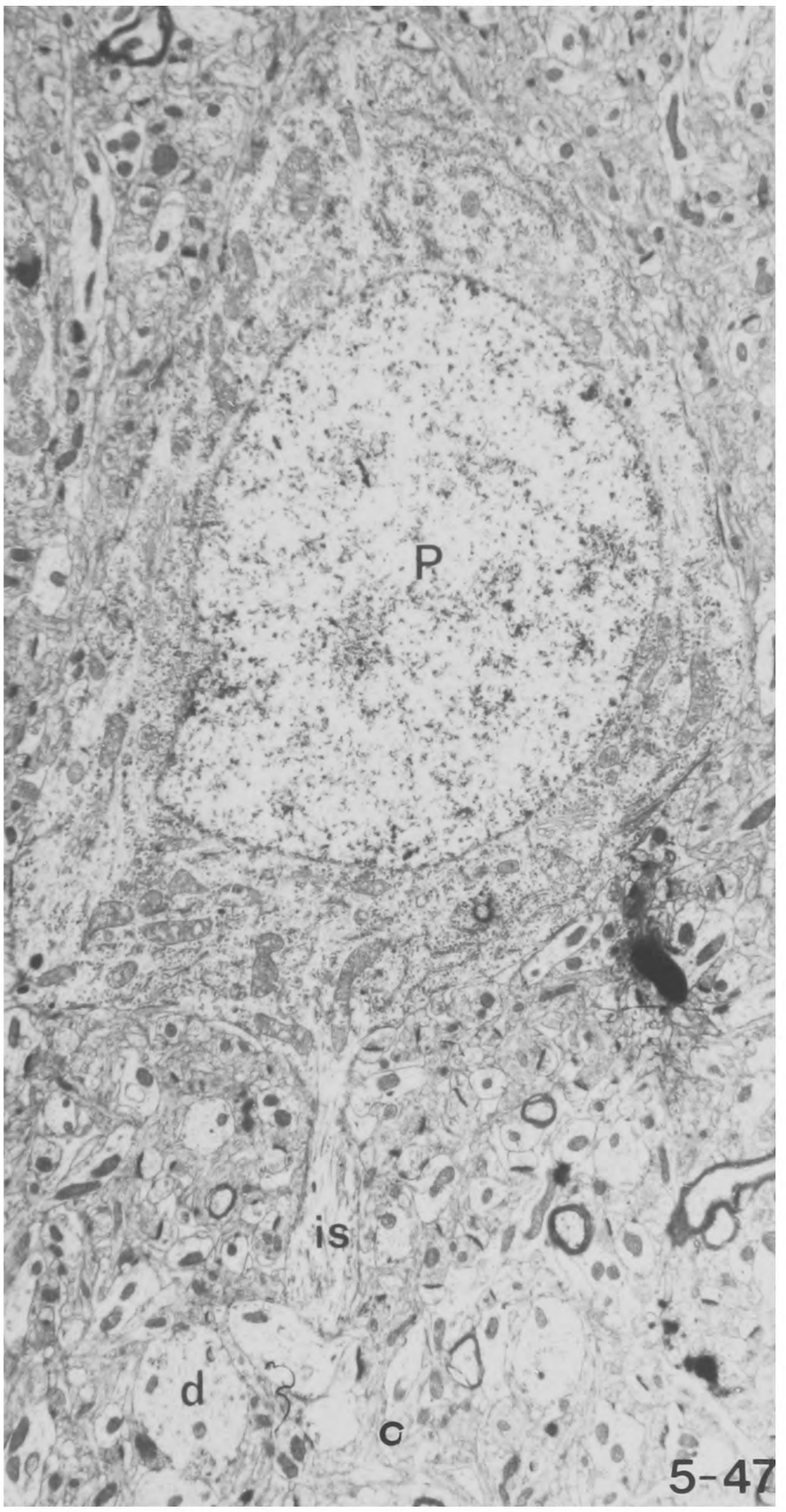

5-47

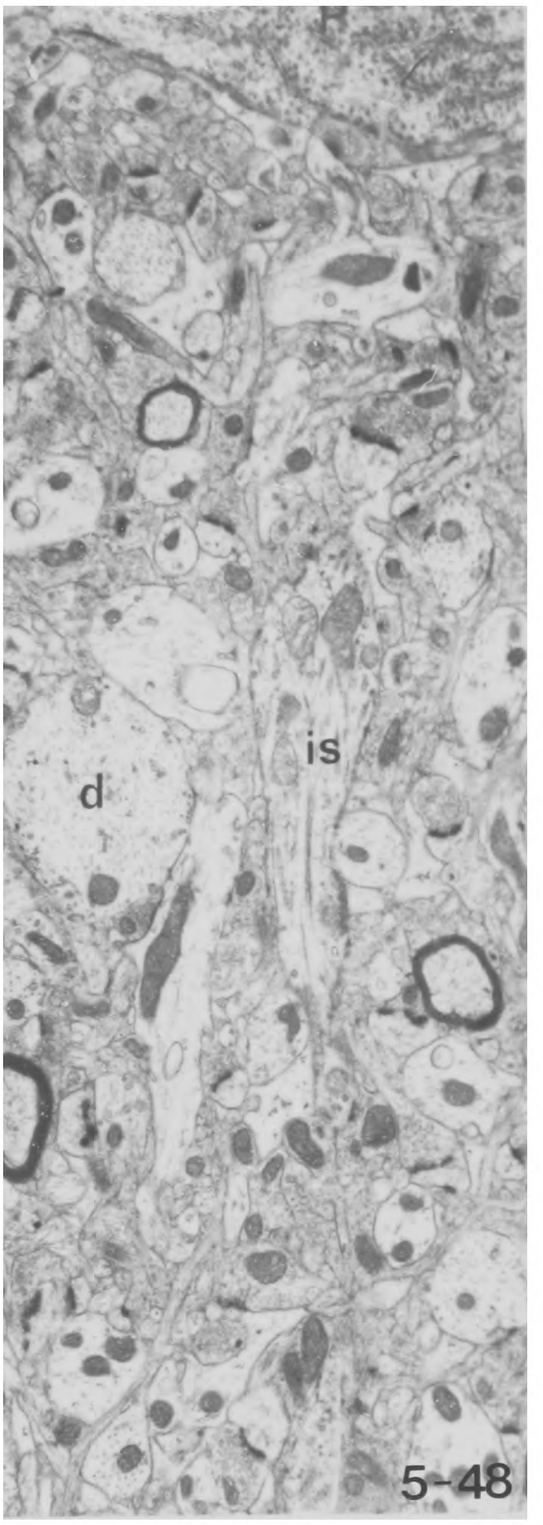

5-48

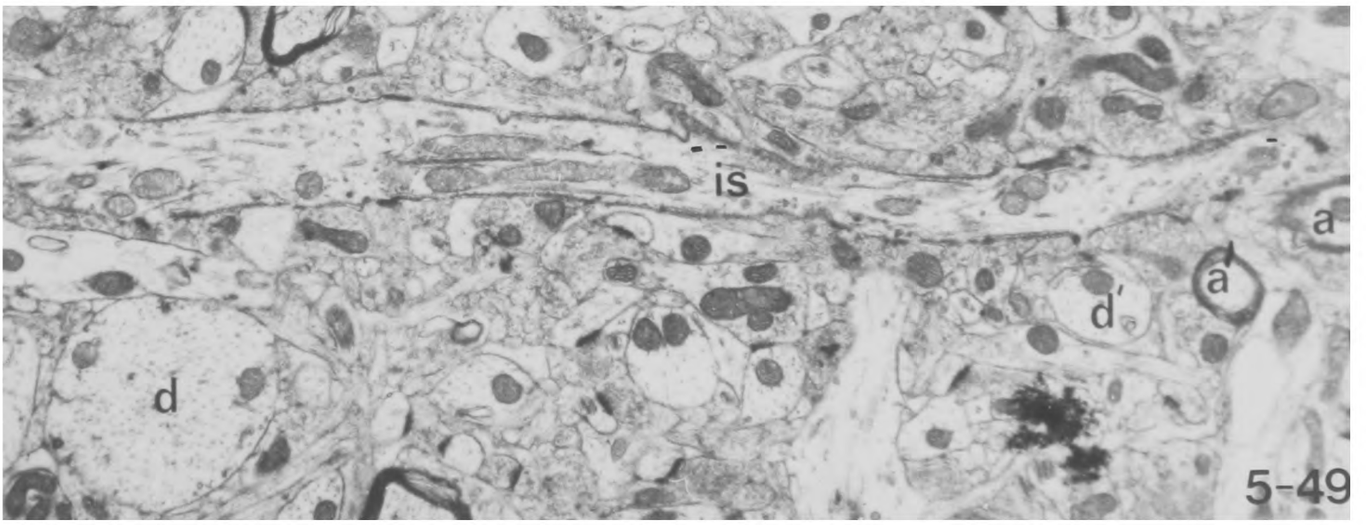

5-49

Figs. 5-50 and 5-51 The continuation in a further serial section of the axon initial segment of the pyramidal cell in Fig. 5-47. Note the axons a and a' and the dendrite d' present in both figures 5-49 and 5-50. Figs. 5-50 and 5-51 are continuous at the black bars, and the continuity of the two narrowed regions of this length of initial segment was unequivocally confirmed in serial sections, one of which is shown in fig. 5-54. In fig. 5-51 the initial segment loses its characteristic features and makes an efferent synapse on to a dendrite (arrowhead).
Section No. 17 X 9,000

Figs. 5-52 and 5-53 The distal (right hand) region of the initial segment of fig. 5-51 at higher magnification, and in the next serial section, figs. 5-52 and 5-53 being continuous at the black bar. In fig. 5-52 note the membrane undercoating (e.g. between the arrows) and the bundle of neurotubules, both characteristics of an axon initial segment. In fig. 5-53 both these features are lost and the unmyelinated axon makes an asymmetric synapse (arrowhead) on to the dendrite d. Note however the afferent symmetrical synapse on to the initial segment/unmyelinated axon immediately distal to the efferent synapse (arrow).
Section 18 X 29,000

Fig. 5-54 Serial section of the initial segment confirming its continuity at the proximal narrowed segment in fig. 5-50.
Section No. 14 X 8,400

Fig. 5-55 The efferent synapse of fig. 5-53 in a serial section confirming its clearly asymmetric character. Section No. 17 X 29,000

Fig. 5-56 A further serial section of the efferent synapse of figs. 5-53 and 5-55. Note how the synaptic vesicles are scattered in contrast to the close-packed vesicles of a dendro-dendritic synapse.
Section No. 20 X 29,000

Fig. 5-57 The post-synaptic dendrite in a further serial section. Note the number of synapses it receives, including one clearly asymmetrical one and its smaller diameter compared to figs. 5-55 and 5-56.
Section No. 5 X 29,000

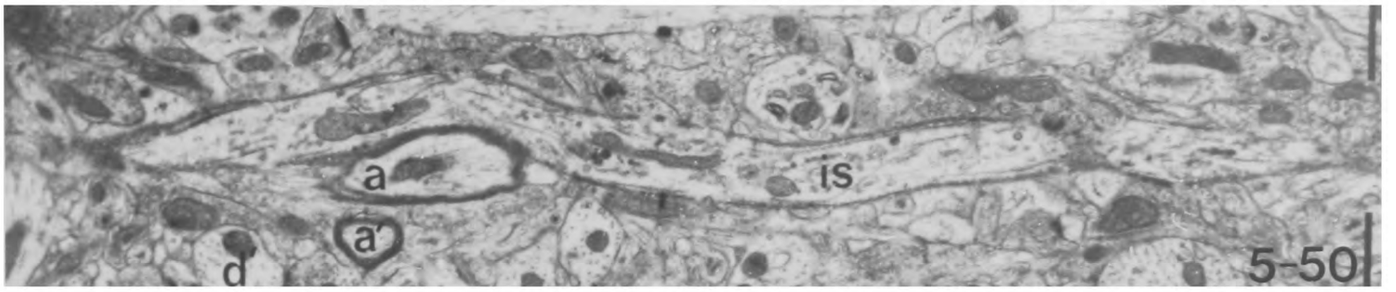

5-50

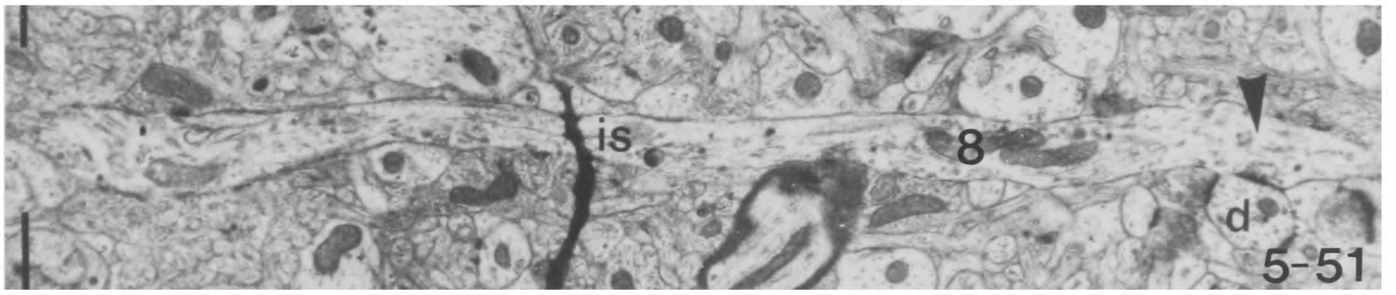

5-51

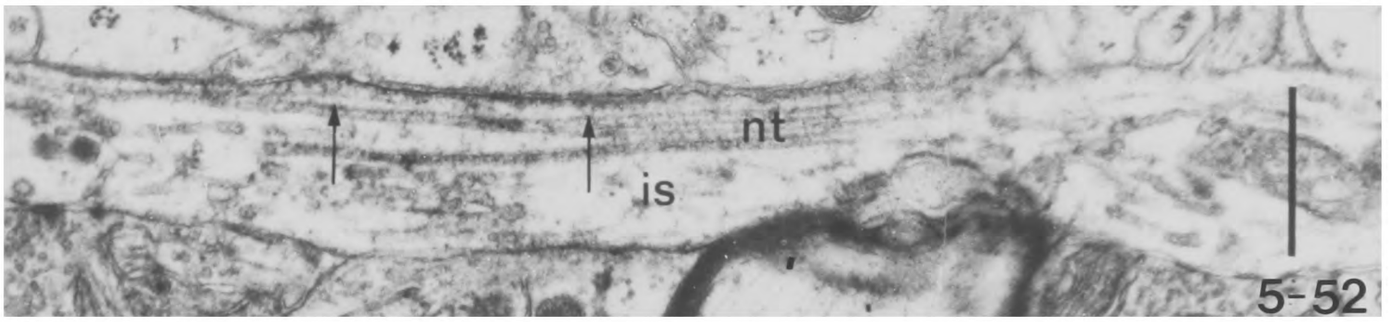

5-52

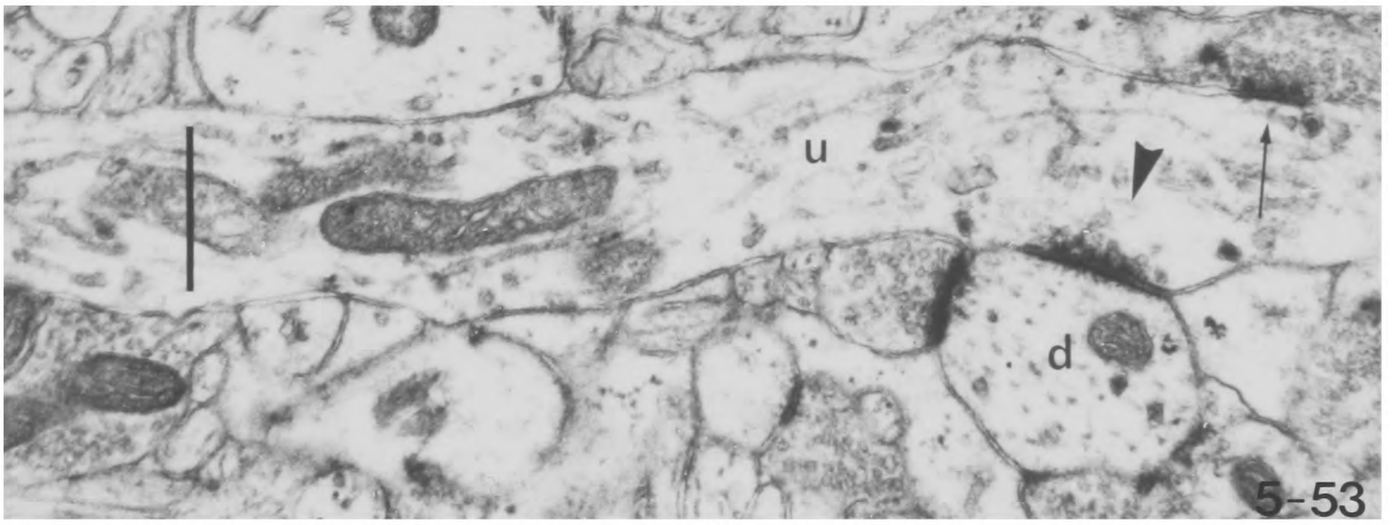

5-53

5-54

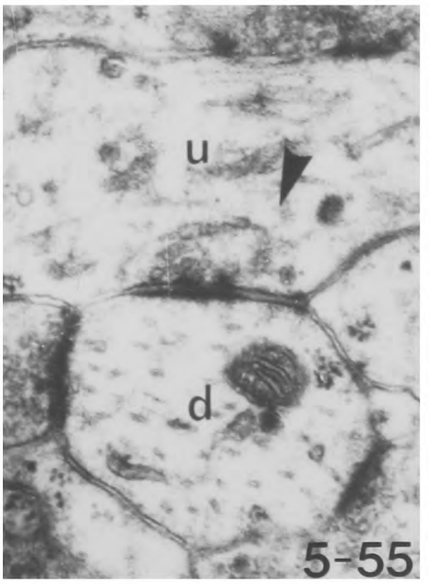

5-55

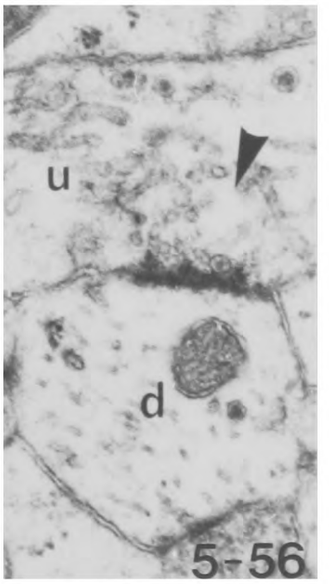

5-56

5-57

Fig. 5-58 Diagramatic representation of the pyramidal cell and axon initial segment of figs. 5-47 to 5-57 and 5-59. The initial segment has the typical features of membrane undercoating and bundles of neurotubules from its origin to approximately 50 μ from the cell soma. It then loses these and makes a synapse on to a dendrite (d) but receives a further afferent synapse immediately distal to this. The initial segment then continues as an unmyelinated axon (u). It contains a subsurface cistern opposite an exposed membrane thickening on a dendritic spine at 65 μ and gives off two collateral branches (b) at 75 μ and 95 μ before becoming myelinated at 103 μ from the cell soma (a).

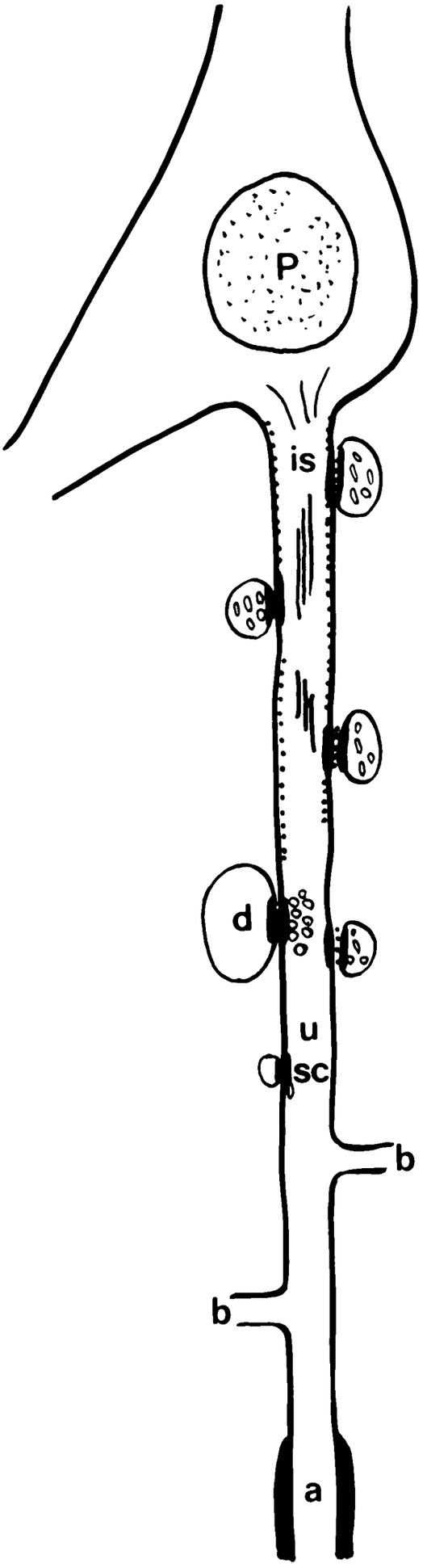

-0

-43 μ

-50 μ

-65 μ

- 75 μ

- 95 μ

-103 μ

Fig. 5-59 The continuation of the unmyelinated axon formed from the initial segment of figs. 5-47 to 5-56 showing it becoming a myelinated axon. The whole of this initial segment/axon is shown diagramatically in fig. 5-58.

Section No. 59 X 29,000

Fig. 5-60 A pyramidal cell with its axon initial segment in material block-stained with E-PTA. Note how the initial segment stands out from the neuropil because of the specific staining of its membrane undercoating. X 6,000

Fig. 5-61 Higher power of the initial segment of fig. 5-60 showing the staining of the membrane undercoating but not of the membrane itself. Note also the bundle of neurotubules and the cisternal organ.

X 29,000

Fig. 5-62 An initial segment arising from a dendrite in E-PTA-stained material. Note the staining of the membrane undercoating of the initial segment and the symmetrical synapse it receives. X18,000

Fig. 5-63 Part of the initial segment of fig. 5-62 at higher magnification. Note the staining of the membrane undercoating, the lack of staining of the plasma membrane itself, and the staining of a thin layer of extracellular material outside it. Note also the symmetrical synapse on to the initial segment.

X 39,000

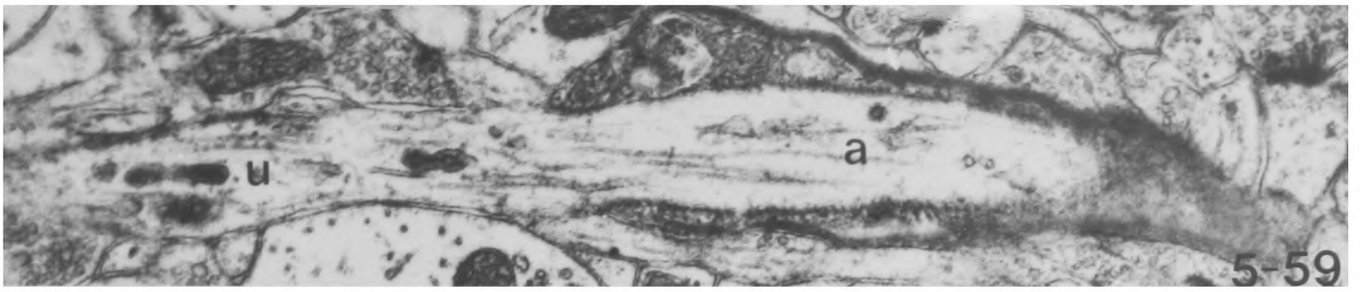
u
a
5-59

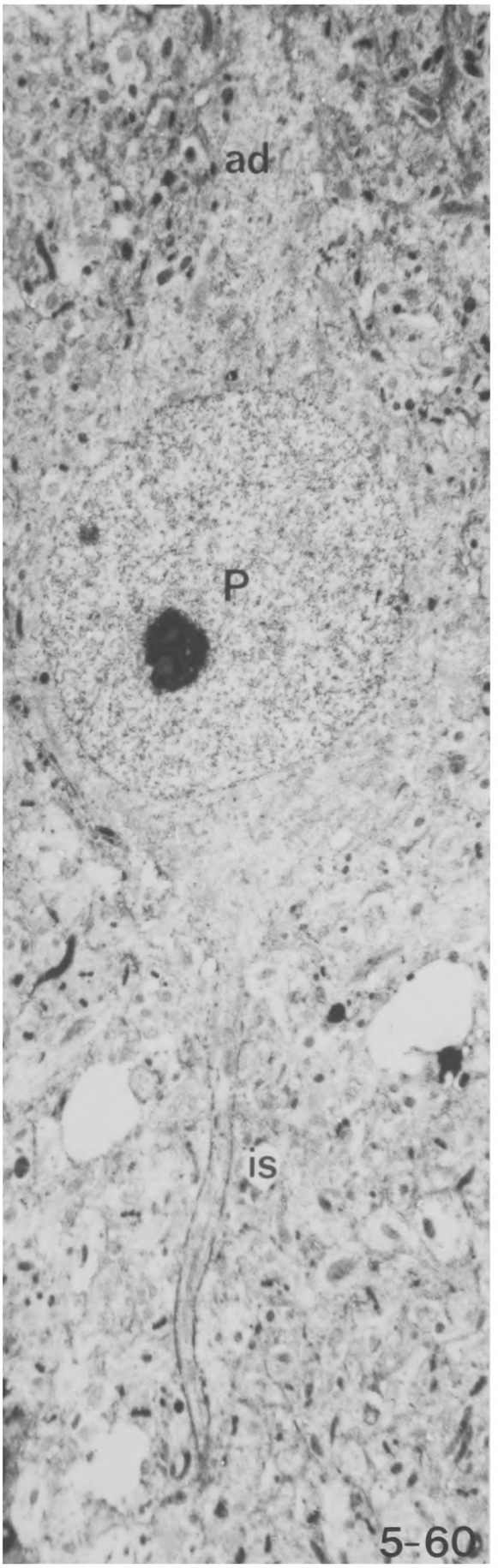
ad
P
is
5-60

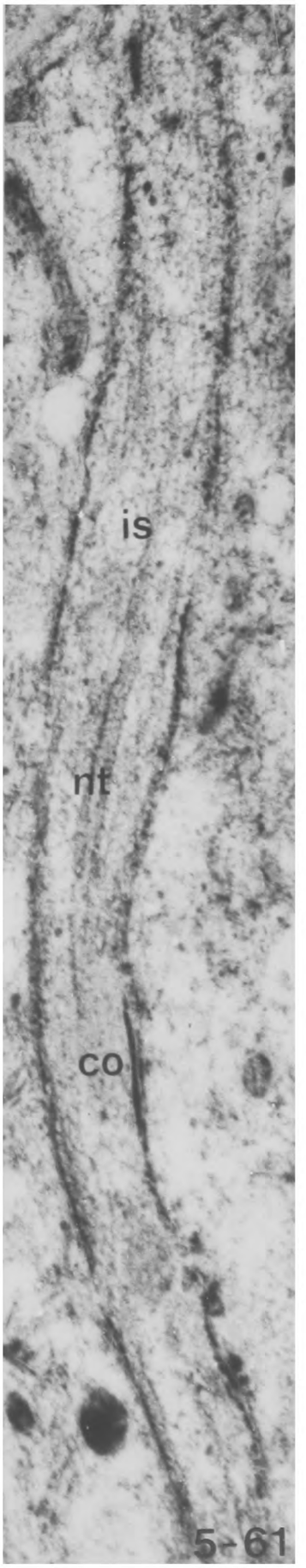
is
nf
co
5-61

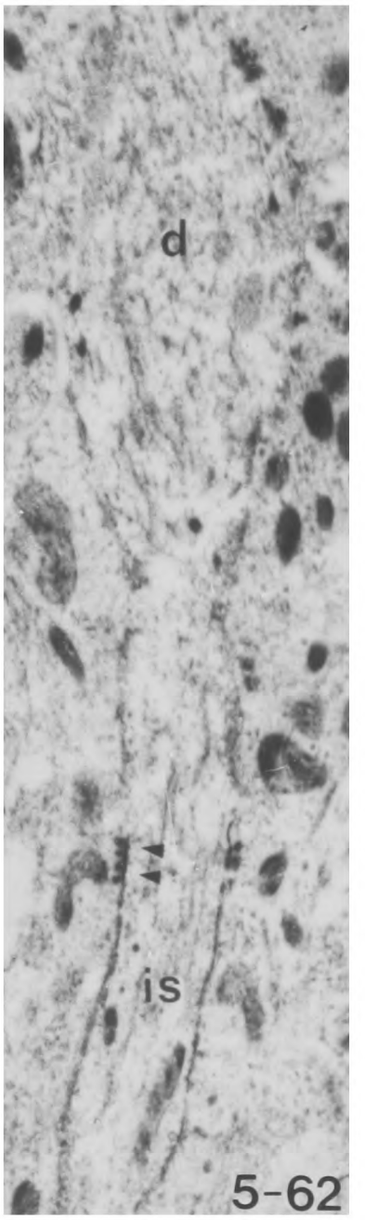
d
is
5-62

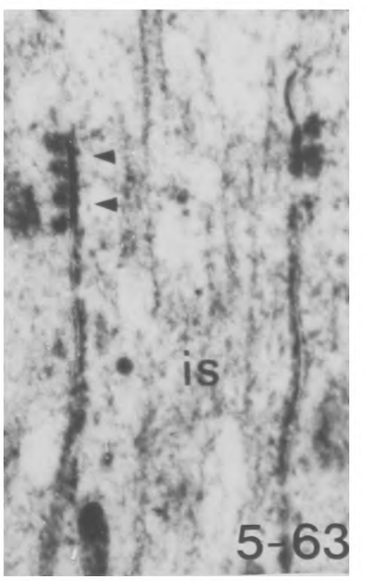
is
5-63

Fig. 5-64 An axon initial segment giving rise to a myelinated axon (a)in material block-stained with E-PTA. Note how the stained membrane undercoating stops at the beginning of the myelin sheath (arrowheads). Note also the granular appearance of the membrane undercoating where it is cut obliquely (arrow). X 18,000

Fig. 5-65 Initial segment in material block-stained with E-PTA to show the specific staining of the dense plates of the cisternal organ. Note also the synapse on to the initial segment. X 29,000

Fig. 5-66 Initial segment and cisternal organ in material stained with E-PTA <u>after</u> osmification. Note how the staining of the dense plates of the sub-surface cistern is inhibited. X 29,000

Fig. 5-67 Transverse section of an axon initial segment containing a cisternal organ in material block-stained with E-PTA. Note how the dense plate of the cisternal organ is closely applied to the surface of the initial segment adjacent to the synapse complex (arrow) but becomes separated opposite the synaptic complex itself (arrowhead). X 53,000

Fig. 5-68 Transverse section of an axon initial segment in material block-stained with E-PTA. The initial segment has a spine which receives a symmetrical synapse (arrowhead) and it contains a cisternal organ. X 53,000

Fig. 5-69 Part of an axon initial segment in material stained with E-PTA showing a vesicle arising from the membrane undercoating (arrowhead). X 48,000

Fig. 5-70 Synaptic membrane complex (arrow) and desmosome (arrowhead) stained with E-PTA. Note that the synaptic complex has discrete presynaptic projections whereas the dense material of the desmosome is continuous on both sides of the membranes. X 53,000

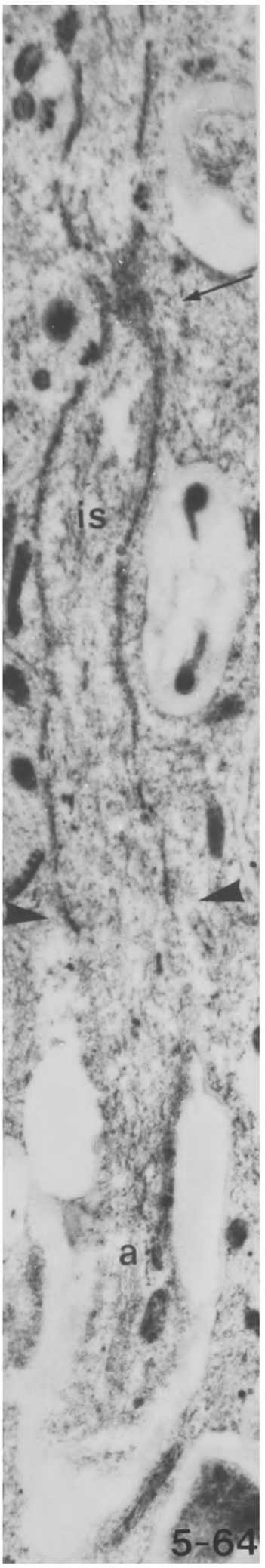
is
a
5-64

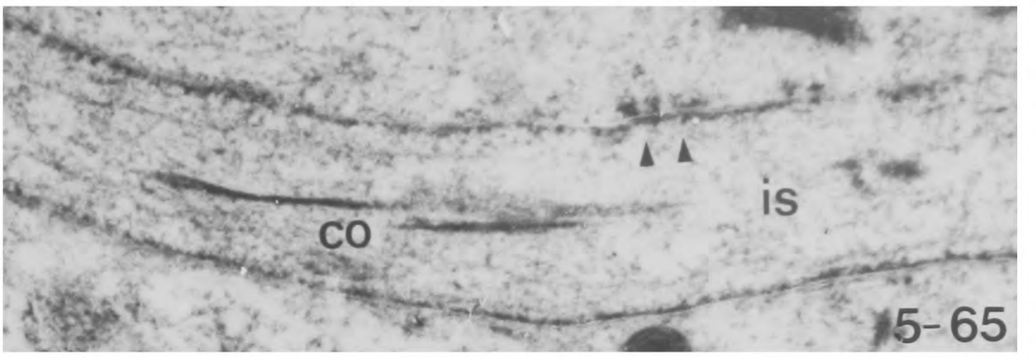
co
is
5-65

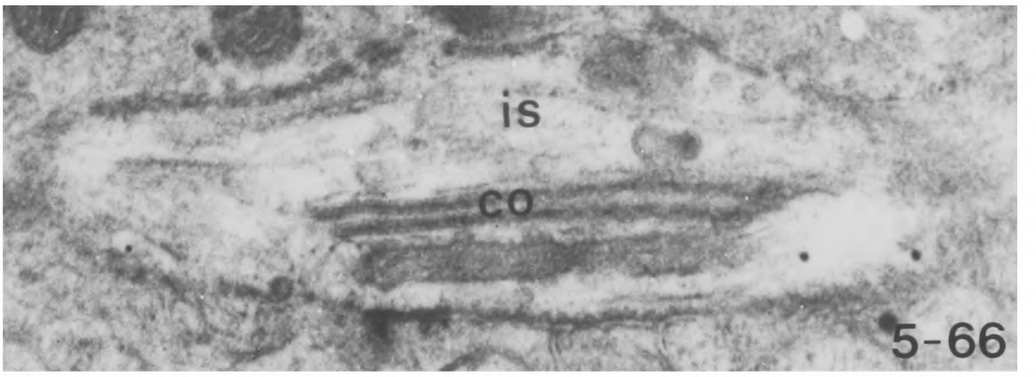
is
co
5-66

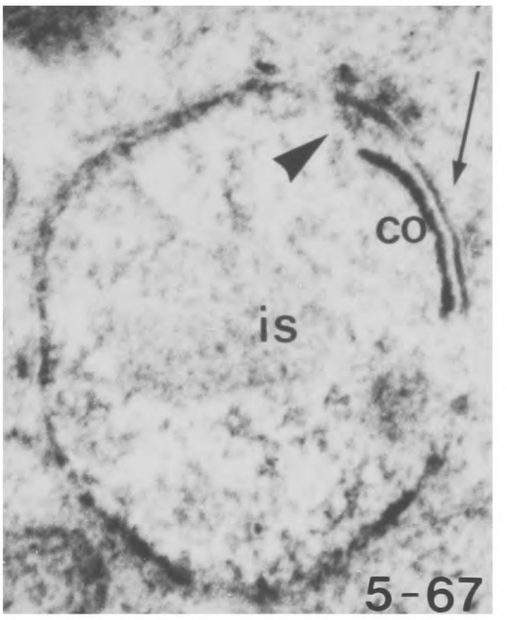
co
is
5-67

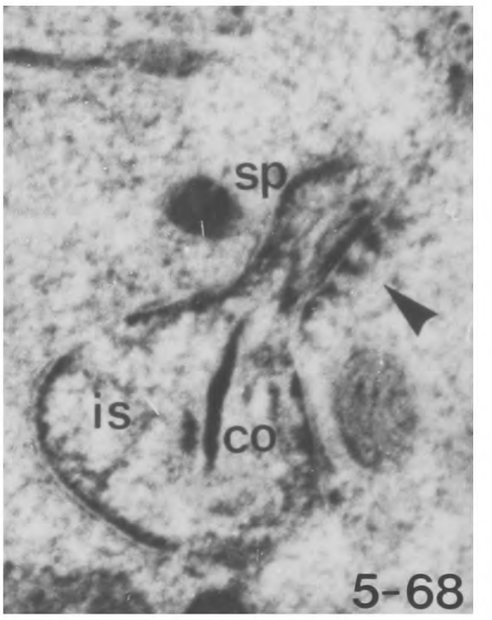
sp
is
co
5-68


is
5-69

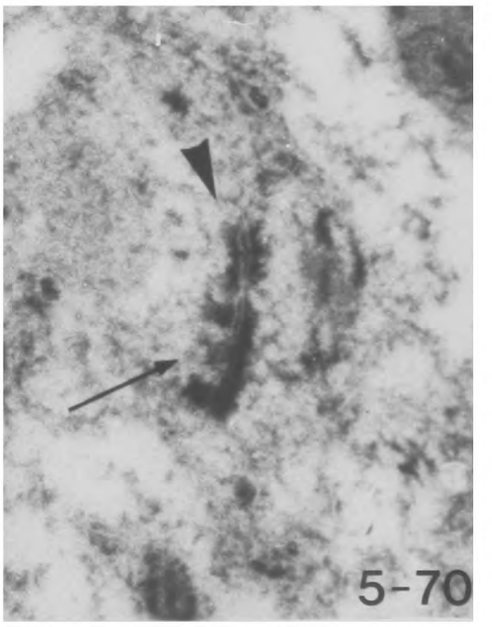
5-70

Fig. 5-71 Graph showing the relationship between the length and diameter of the complete axon initial segments studied here compared to those of spinal motor neurones studied by Conradi (1969b). Note that initial segments of larger diameter are no longer than those of small diameter.

LENGTH OF AXON INITIAL SEGMENTS AGAINST DIAMETER FOR PYRAMIDAL CELLS, STELLATE CELLS, AND SPINAL MOTOR NEURONES (CONRADI 1969)

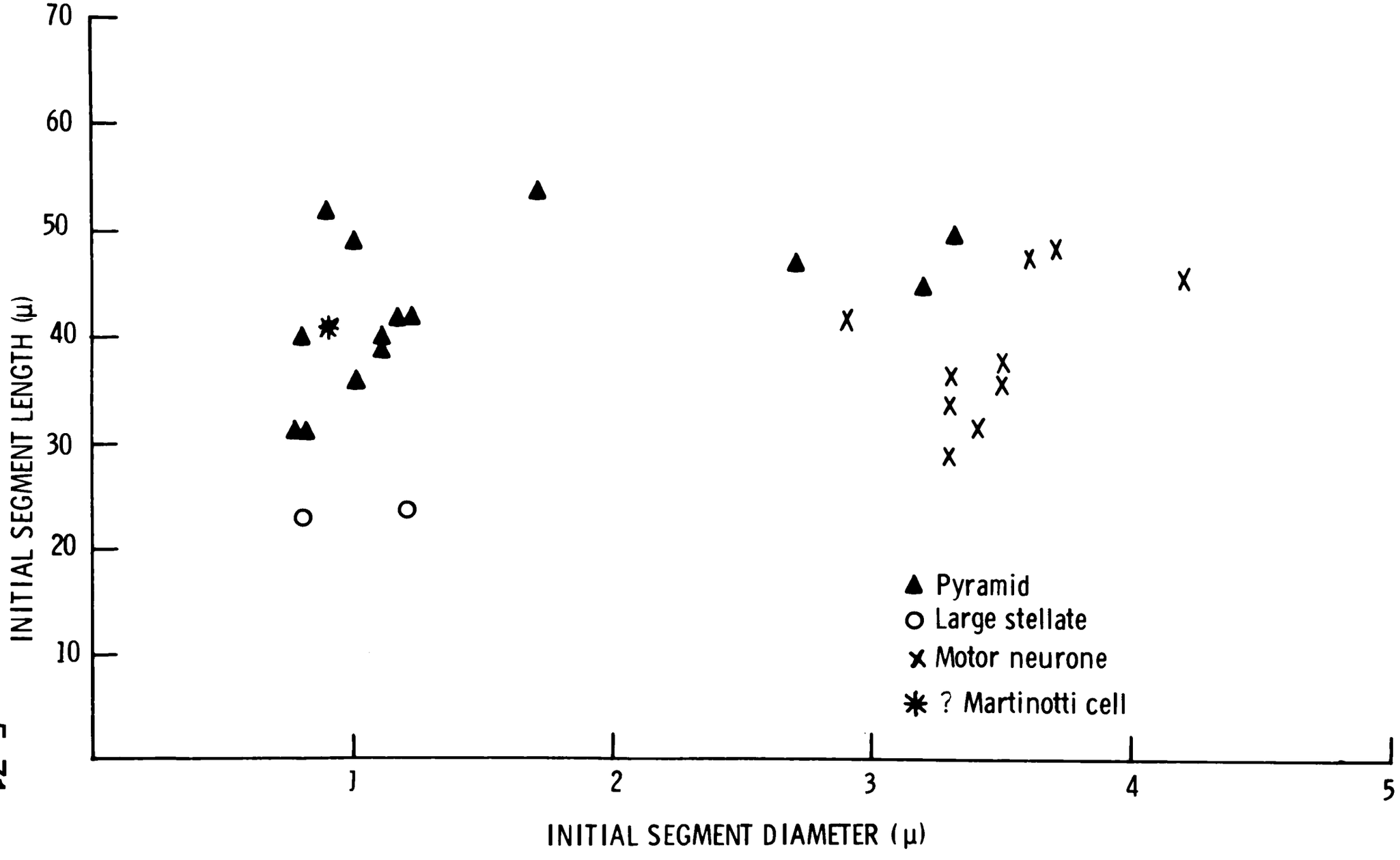

Fig. 5-72 Diagrams showing the variety of shapes and synaptic relationships of the spines found on axon initial segments.

A & B	Small sessile spines receiving a single synapse.
C & D	Large sessile spines of differing shapes, each receiving two synapses.
E	Oblique elongated peg-like spine.
F	Spine with a narrow neck and expanded spherical head receiving one synapse.
G	Spine with narrow neck and elongated head receiving one synapse.
H	Conical spine with narrow neck which receives two synapses.
I	Sessile spine receiving a synapse from an axon terminal which also makes a synapse on to the adjacent shaft of the initial segment.
J	A single axon terminal which makes synapses on to two adjacent sessile spines.
K	A spine with a conical head and narrow stalk which receives two synapses, each from a terminal which also makes a synapse directly on to the shaft of the initial segment.

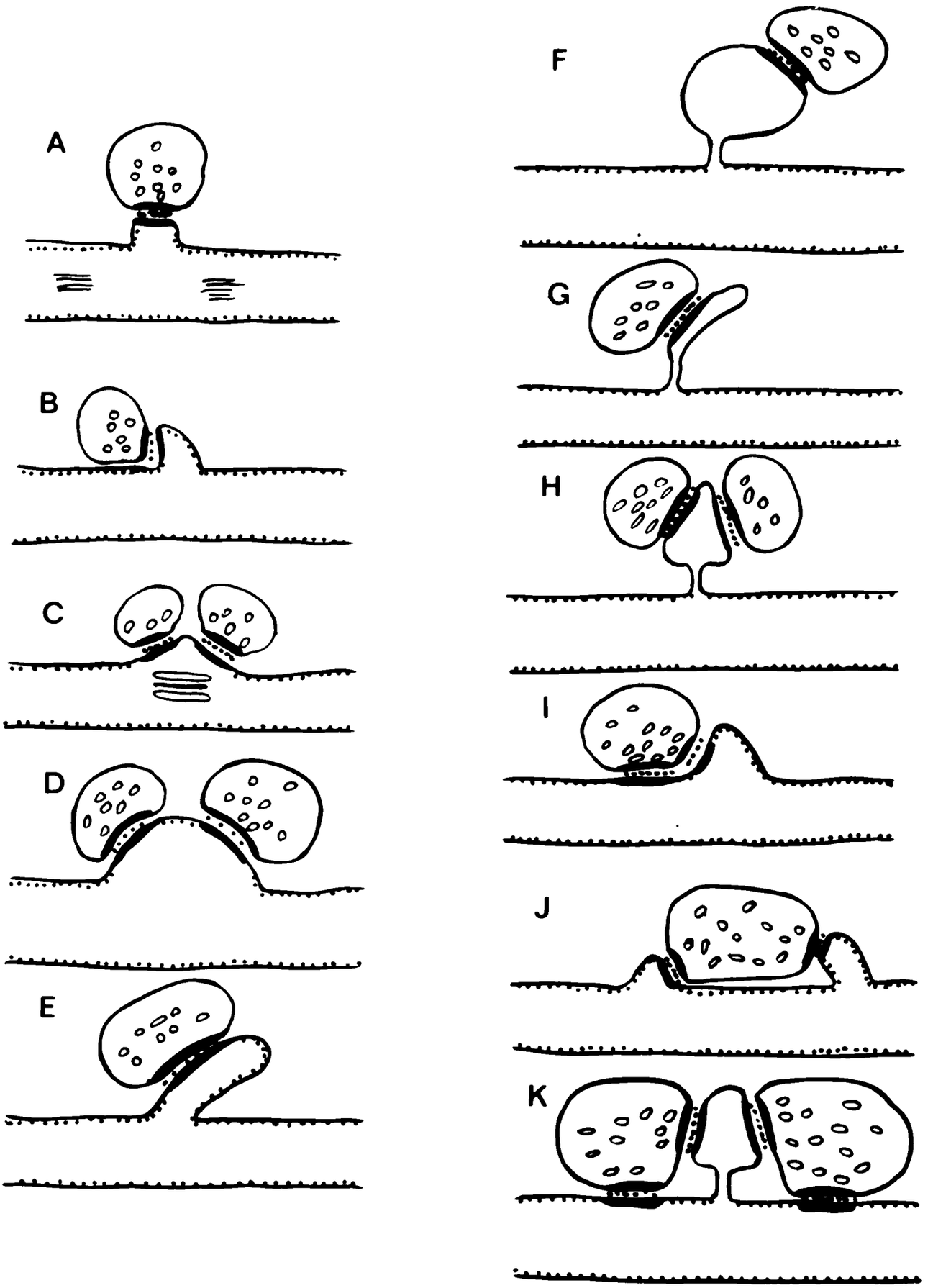
A
B
C
D
E
F
G
H
I
J
K

Illustrations to Chapter 6

DENDRO-DENDRITIC AND RECIPROCAL SYNAPSES IN THE MOTOR CORTEX

Fig. 6-1 A large presynaptic dendrite cut in longitudinal section makes a dendro-dendritic synapse (arrowhead) with a dendrite. Note the large number of synapses received by the presynaptic dendrite and the desmosome associated with the dendro-dendritic synapse (arrow).
Section No. 6 X 18,500

Fig. 6-2 Higher magnification of the dendro-dendritic synapse (arrowhead) and desmosome (arrow) of fig. 6-1. Note the cluster of ribosomes in the presynaptic dendrite. X 67,000

Fig. 6-3 Serial section of the region of the dendro-dendritic synapse and desmosome of figs. 6-1 and 6-2, showing a gap junction at the same interface as the dendro-dendritic synapse and desmosome.
X 115,000

Fig. 6-4 A large presynaptic dendrite making a dendro-dendritic synapse (arrowhead) on to a spine. Note the synapses on to the presynaptic dendrite and the large number of mitochondrial profiles in it. In serial sections the spine was traced to its parent dendrite. X 18,000

Fig. 6-5 Higher magnification of the dendro-dendritic synapse (arrowhead) of fig. 6-4. X 42,000

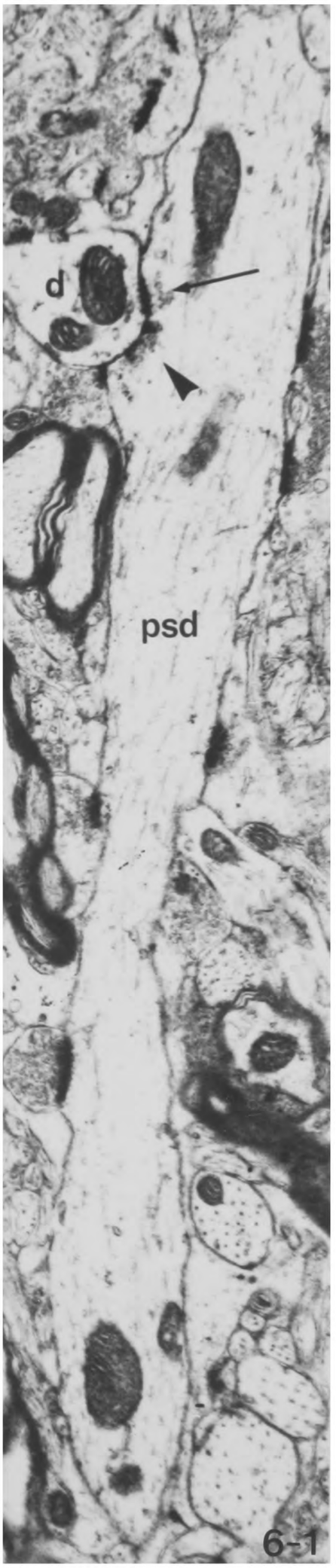
d
psd
6-1


d
r
psd
6-2

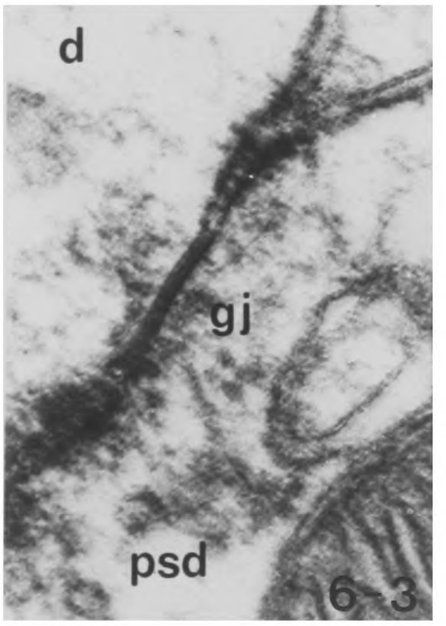
d
gj
psd
6-3

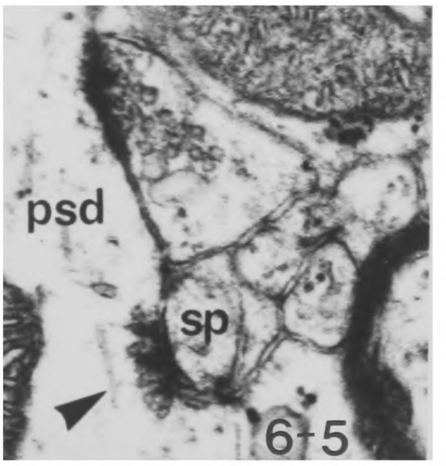
psd
sp
6-5

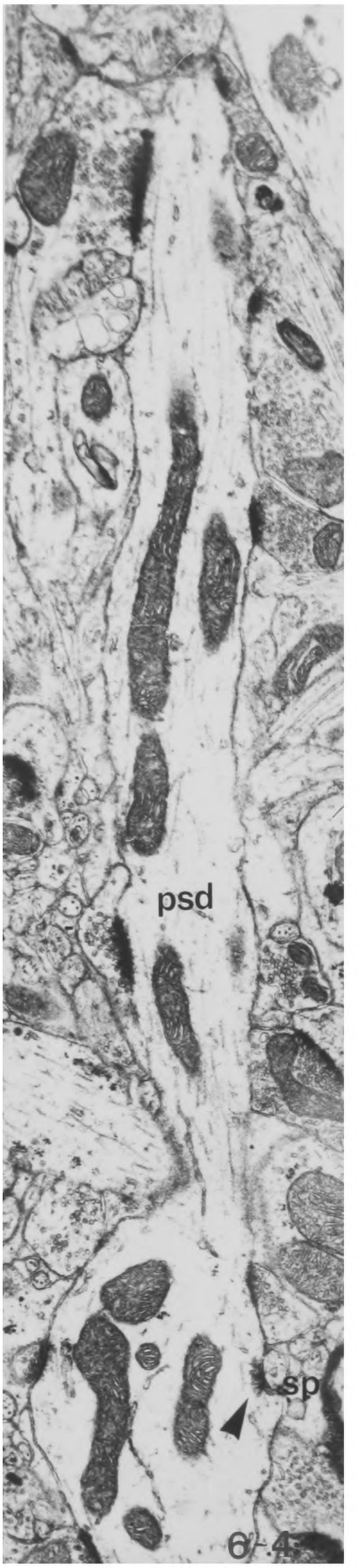
psd
sp
6-4

Fig. 6-6 Dendro-dendritic synapse (arrowhead) and desmosome (arrow) between a presynaptic dendrite and a spine. The spine also receives both an asymmetric and a symmetrical synapse from two axon terminals t1 and t2 respectively. Note the endoplasmic reticulum and clusters of ribosomes in the presynaptic dendrite which was also shown to receive a synapse in serial sections.

Section No. 14 X 32,000

Fig. 6-7 The spine which received a dendro-dendritic synapse in fig. 6-6 shown in continuity with its parent dendrite(d) in a serial section.

Section No. 16 X 32,000

Fig. 6-8 A presynaptic dendrite which receives a synapse from the axon terminal (t) and makes a dendro-dendritic synapse on to a spine (arrowhead). Note the way the presynaptic dendrite appears filled with mitochondrial profiles. X 42,000

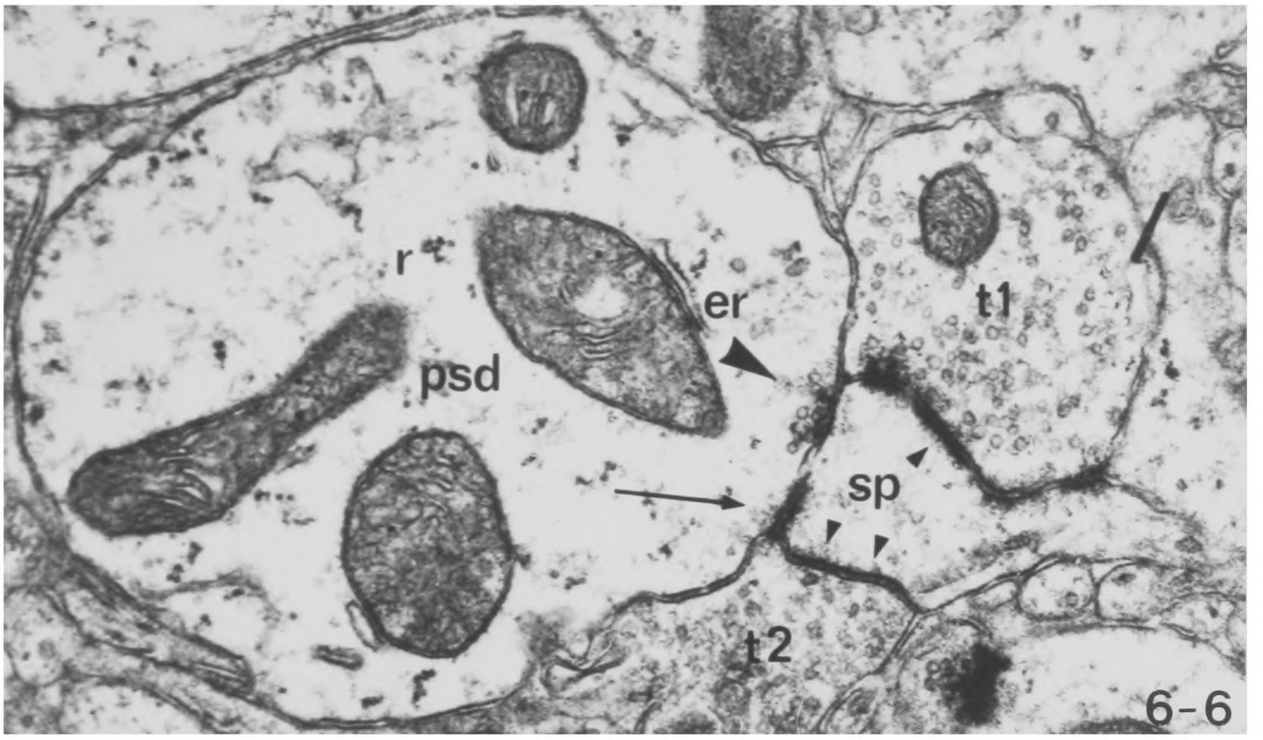
r
er
t1
psd
sp
t2
6-6

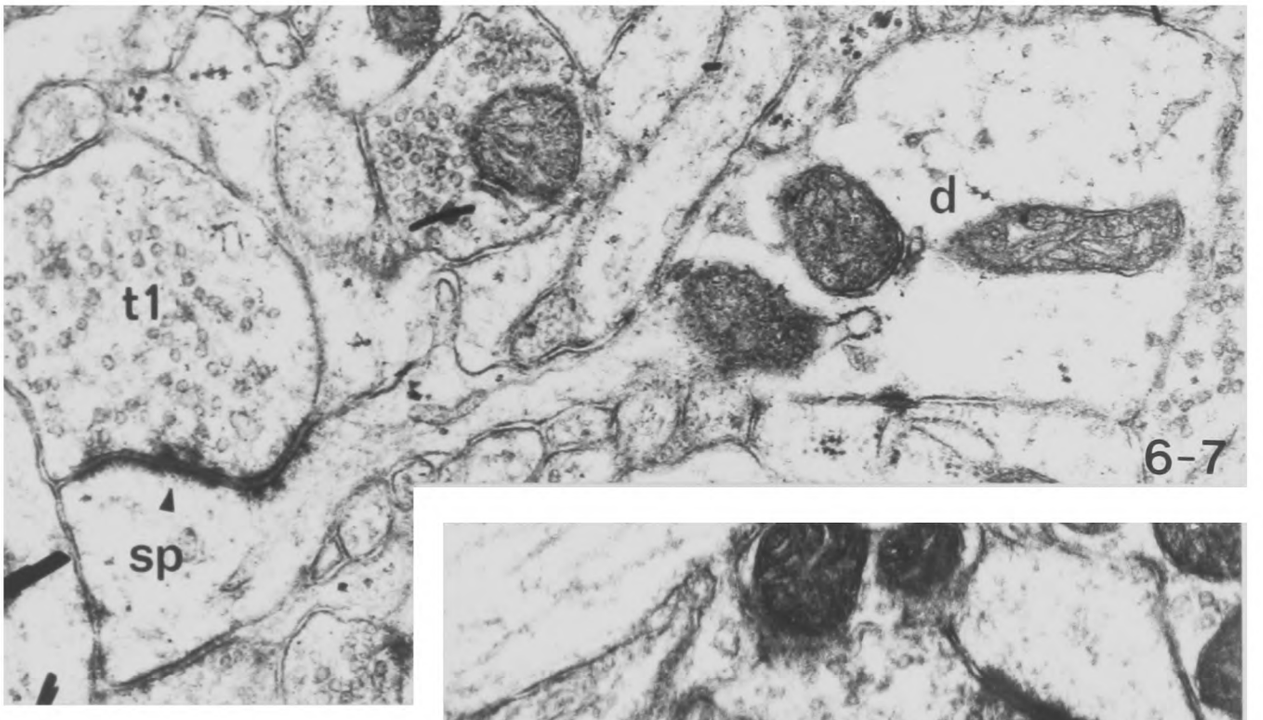
d
t1
6-7

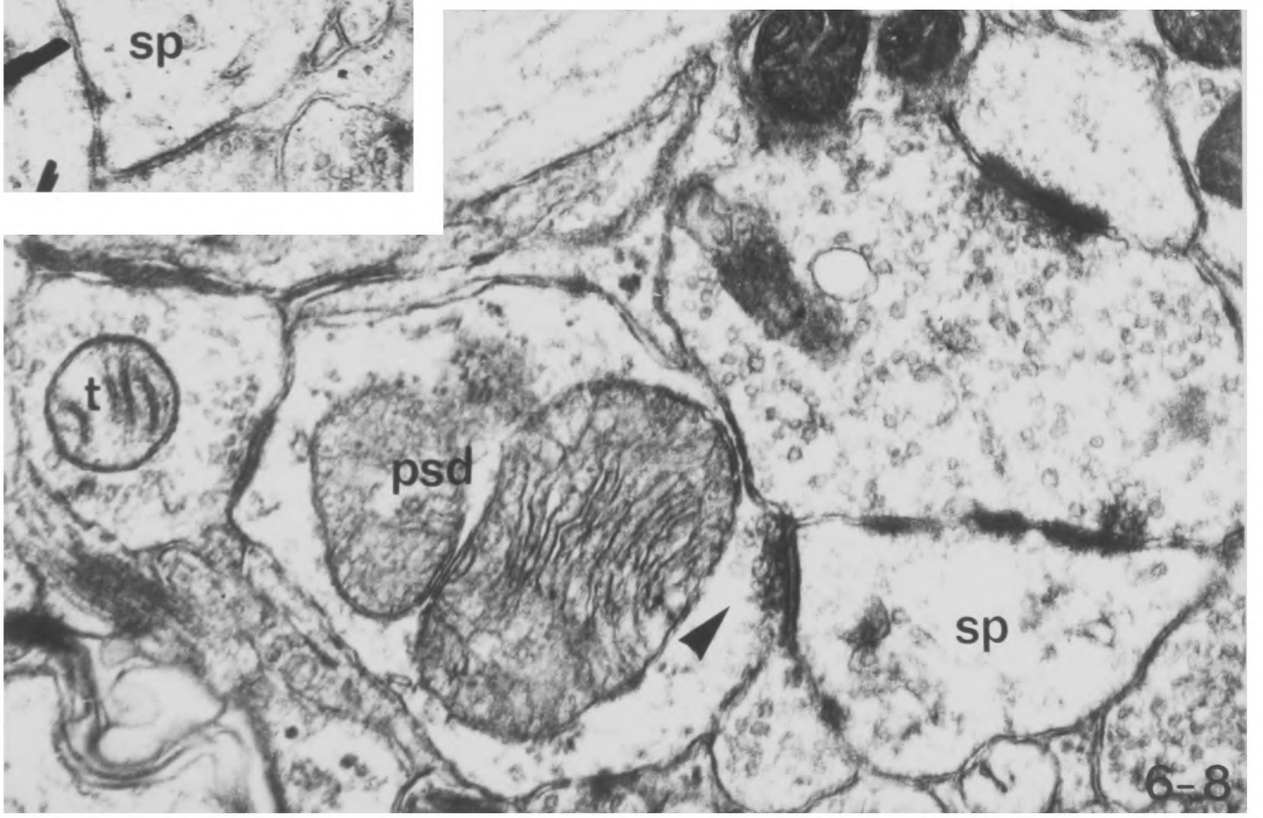
sp
t
psd
sp
6-8

Figs. 6-9 and 6-10 — Presynaptic dendrite. Fig. 6-9 shows a dendrite having the typical appearance of a varicose dendrite from motor cortex. In a serial section however (fig. 6-10) this dendrite itself makes a typical synapse on to a small dendrite (d). Note how the synaptic vesicles occur only close to the synaptic membrane complex, and note the cluster of ribosomes and dense cored vesicle. Sections Nos. 6 and 9. Both X 29,000

Fig. 6-11 — Typical axon terminal from motor cortex making an 'en passage' symmetrical synapse on to a spine. Note how the synaptic vesicles are spread throughout the axon terminal in contrast to those at the dendro-dendritic synapses. X 29,000

Fig. 6-12 — Dendro-dendritic synapse between a pre-synaptic dendrite and a large dendrite. The pre-synaptic dendrite itself received a synapse in a serial section. Note the large size of the pre-synaptic dendrite, its clusters of ribosomes and the way the synaptic vesicles are grouped close to the membrane complex. X 18,000

Fig. 6-13 — Higher magnification of the dendro-dendritic synapse of fig. 6-12. Note that the synaptic membrane complex is of the symmetrical type. X 69,000

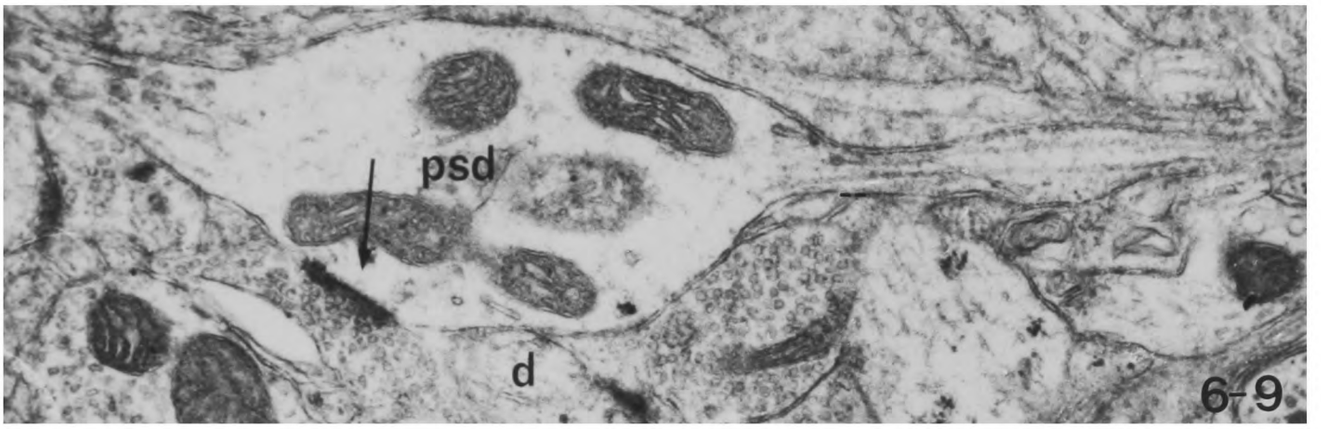

6-9

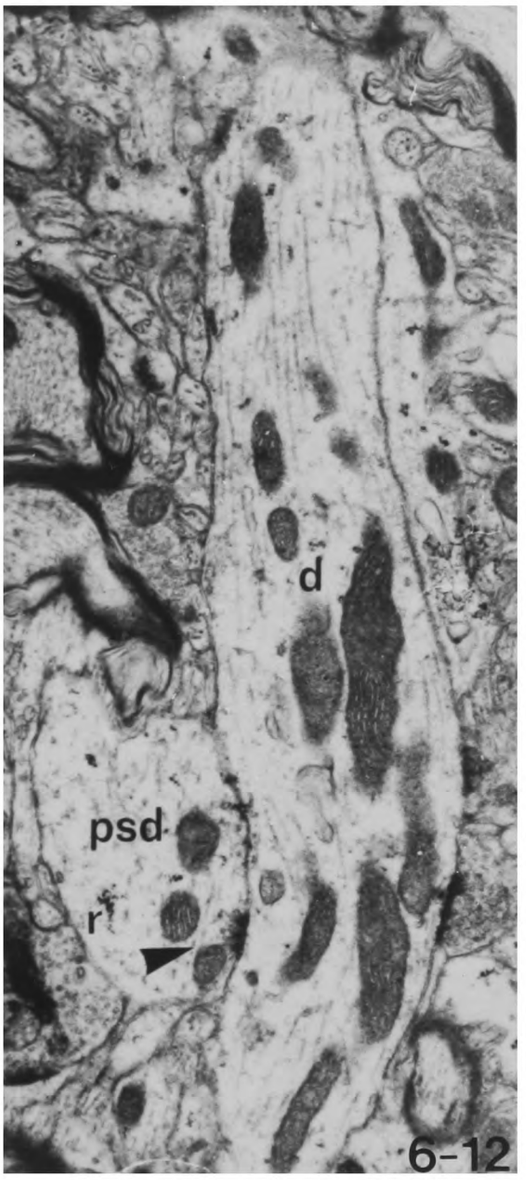

6-12

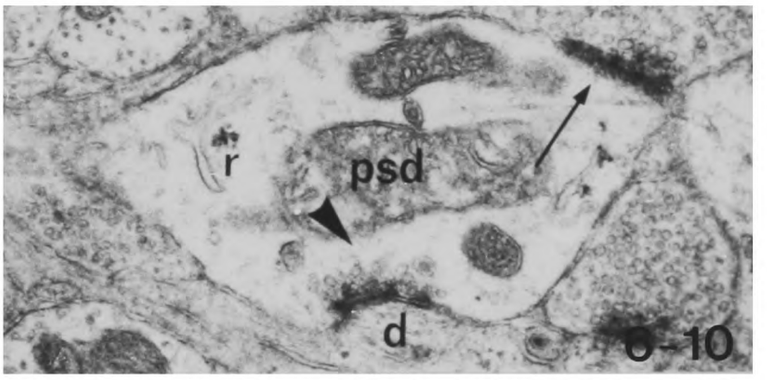

6-10

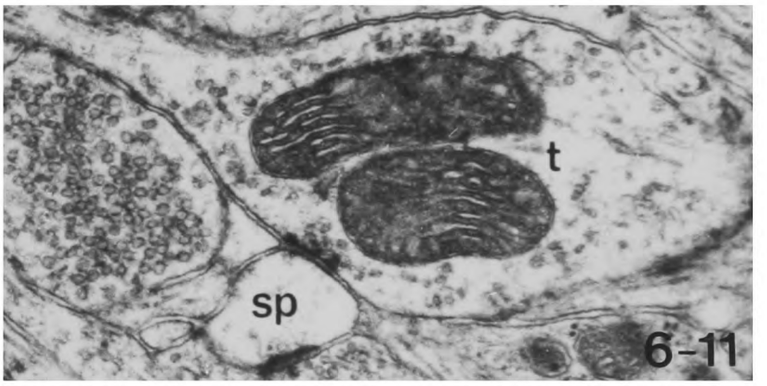

6-11

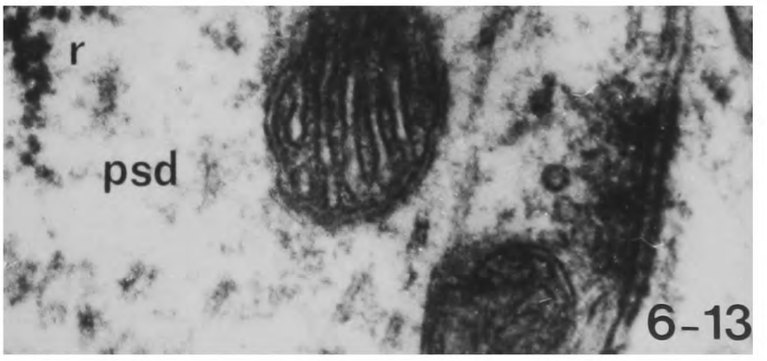

6-13

Figs. 6-14 and 6-15

Serial sections 15 and 18 of a series through a pre-synaptic dendrite. In fig. 6-14 the pre-synaptic dendrite receives a synapse from the "en passage" axon terminal (t1) and makes a dendro-dendritic synapse (arrowhead) on to a spine which also receives a synapse from the axon terminal (t6). In serial sections the spine was found to contain a spine apparatus. In fig. 6-15 the pre-synaptic dendrite receives a second synapse from the axon terminal (t3). Note the large size of the pre-synaptic dendrite and the cluster of ribosomes in it. The synapses shown here formed part of a complex arrangement containing a second dendro-dendritic synapse, the whole arrangement being shown diagrammatically in fig. 6-33 E.

Both X 38,000

Figs.6-16 to 6-22

Serial sections 15-21 through the dendro-dendritic synapse of figs. 6-14 and 6-15 to show details of the synaptic ultrastructure. The majority of synaptic vesicles are round but the occasional one is flattened (arrows) and the synaptic membrane complex itself is consistently of the symmetrical type. Note the presynaptic dense projections and the desmosome adjacent to and continuing beyond the synaptic complex in the later figures.

All X 67,000

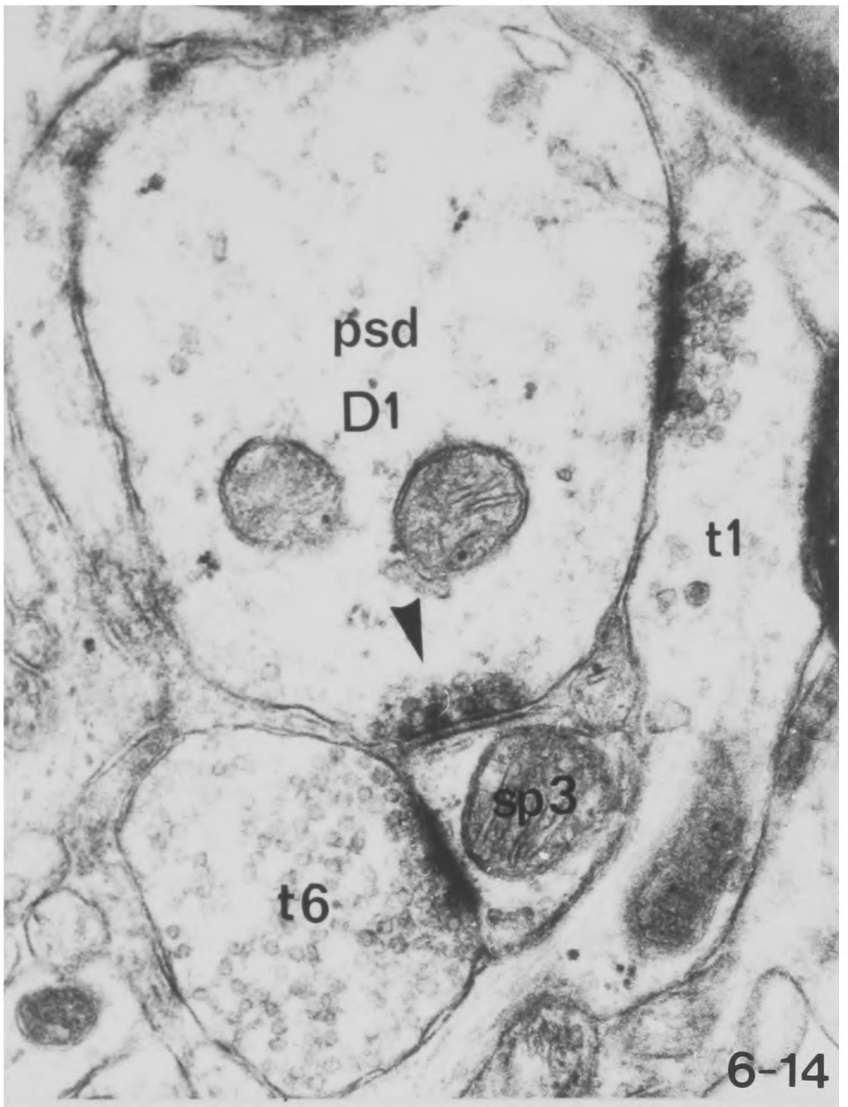

6-14

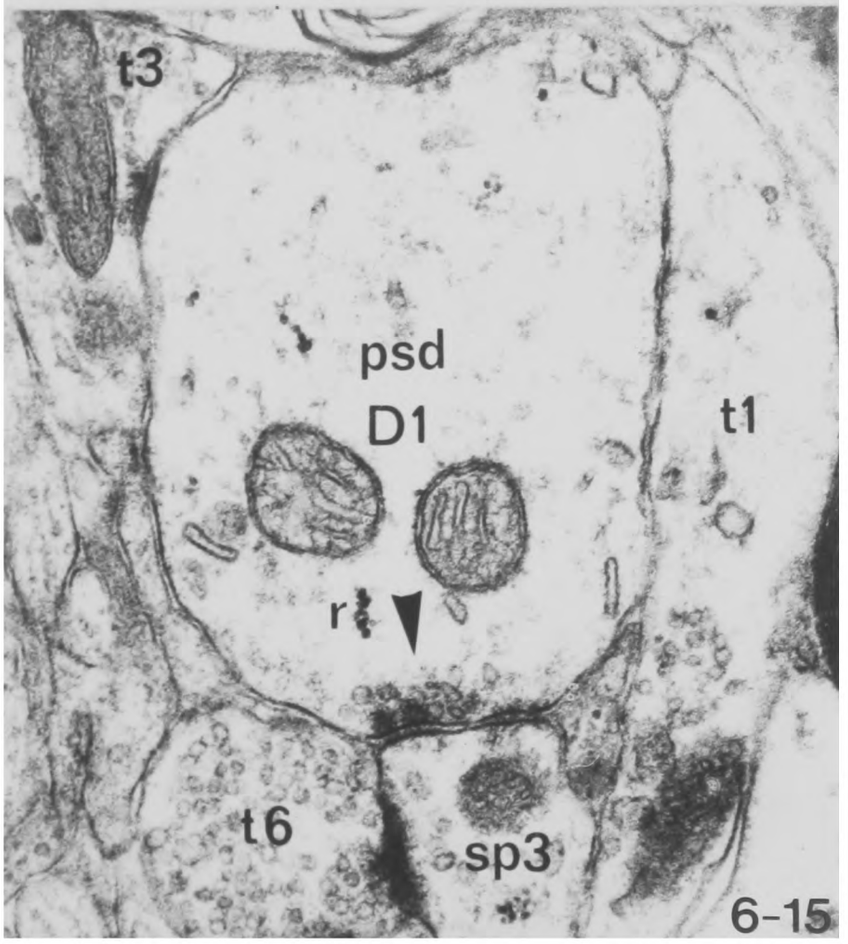

6-15

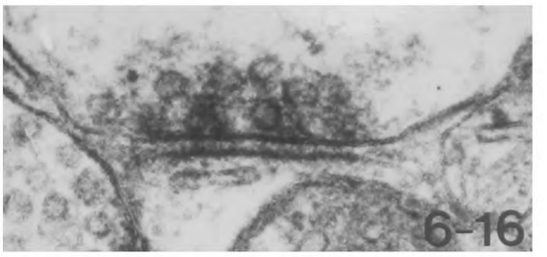

6-16

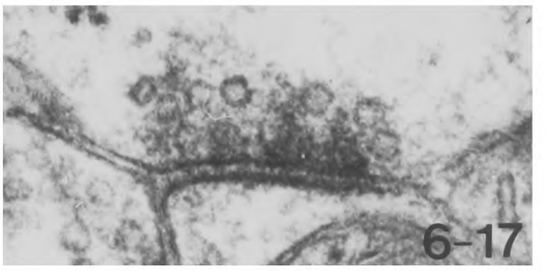

6-17

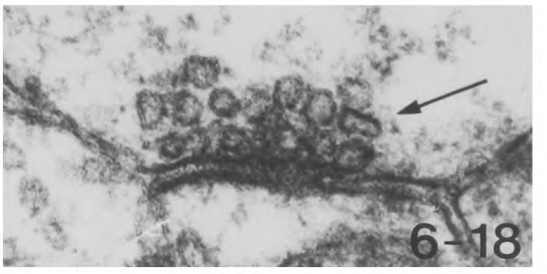

6-18

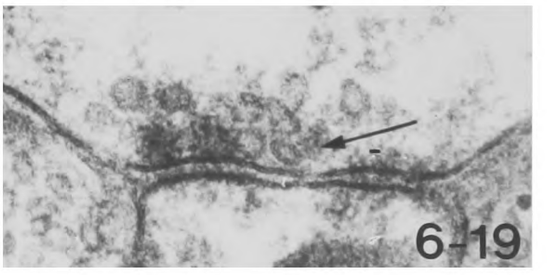

6-19

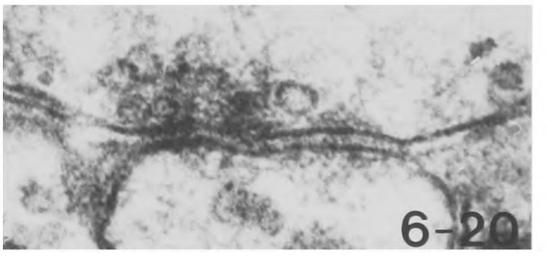

6-20

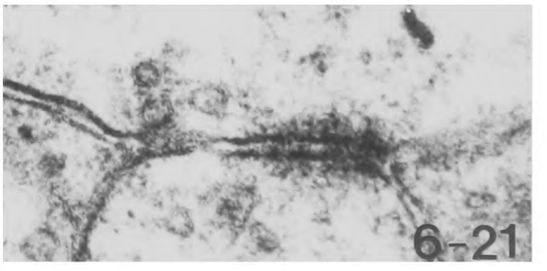

6-21

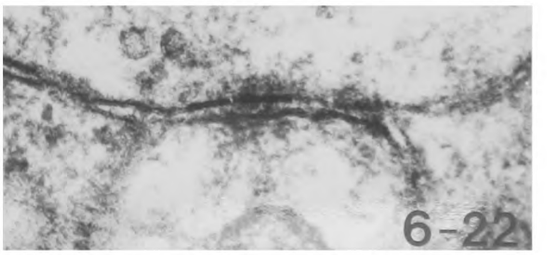

6-22

Figs. 6-23 to 6-32 Tilt series of synaptic vesicles.

Fig. 6-23 Dendro-dendritic synapse and gap junction between a presynaptic dendrite, shown to receive a synapse in a serial section, and another dendrite. X 29,000

Figs. 6-24 to 6-27 The dendro-dendritic synapse of fig. 6-23 tilted at -15^{o}, 0^{o}, $+15^{o}$ and $+30^{o}$ respectively. Note that whereas vesicle 1 remains round vesicle 2 immediately adjacent to the synaptic membrane in fig. 6-24 appears round in that figure but becomes flattened as the section is tilted. X 99,000

Figs. 6-28 to 6-32 The dendro-dendritic synapse of fig. 6-10 in the next serial section tilted at $+30^{o}$, $+15^{o}$, 0^{o}, -15^{o} and -30^{o} respectively. Vesicle 1 changes from flattened to round, and vesicle 2 changes from round to flattened; both vesicles appear to have an electron-dense core. Vesicle 3 is initially flattened and becomes more round although it is incomplete. X 123,000

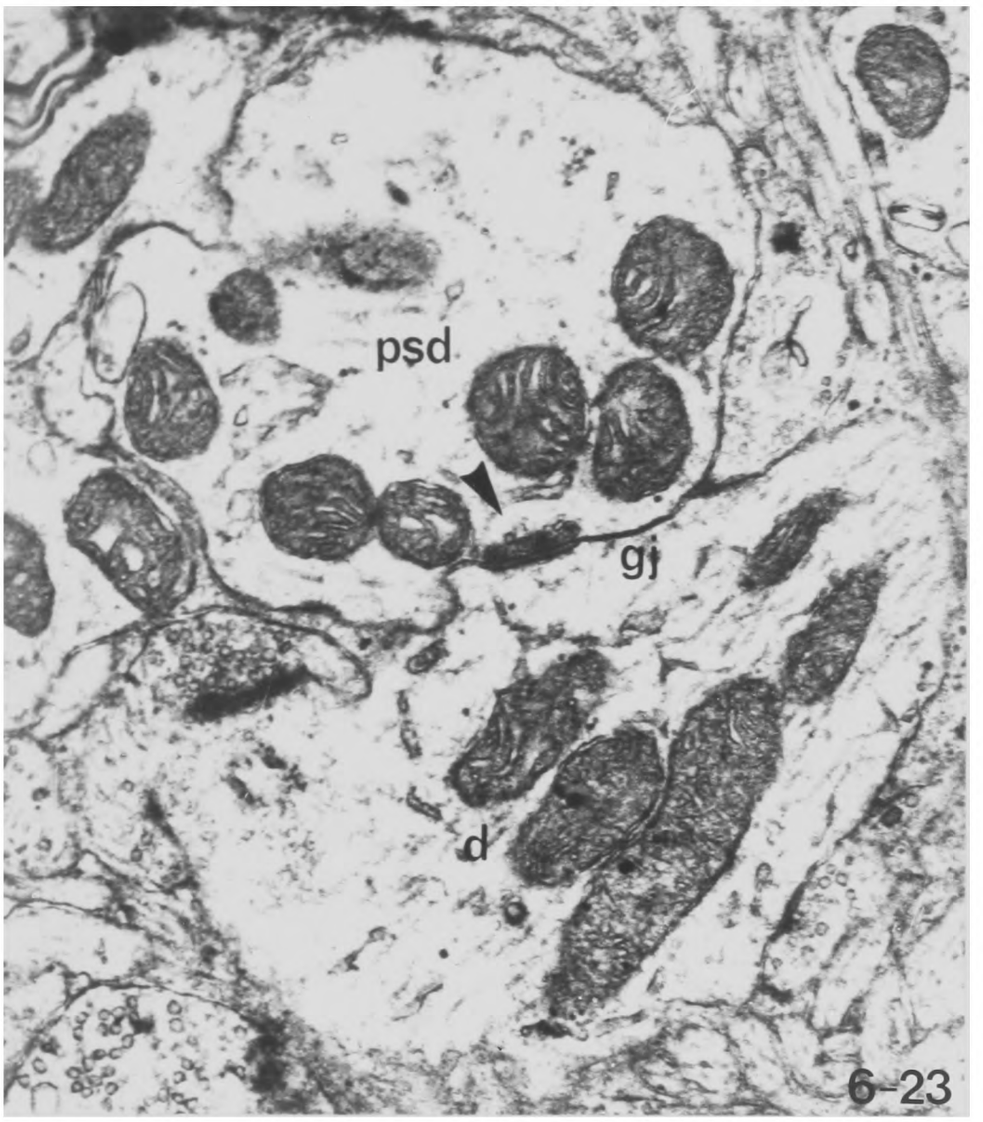
psd
gj
d
6-23

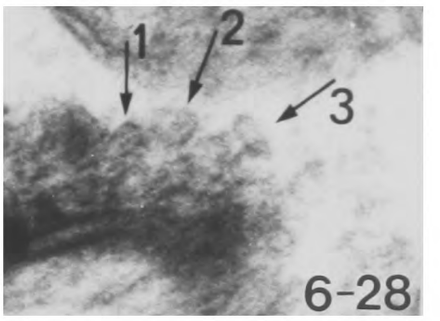
1
2
3
6-28

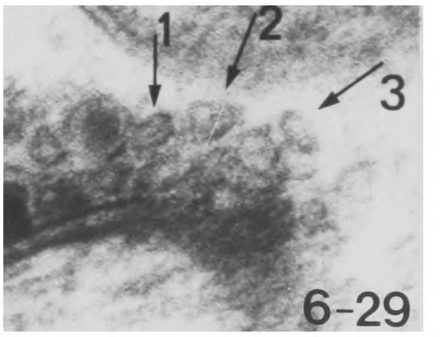
1
2
3
6-29

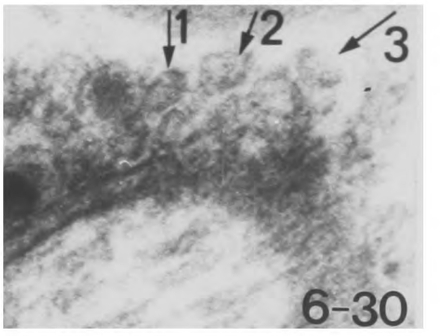
1
2
3
6-30

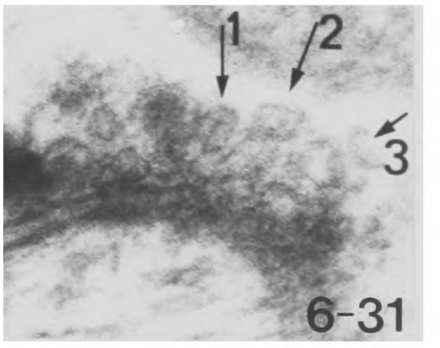
1
2
3
6-31

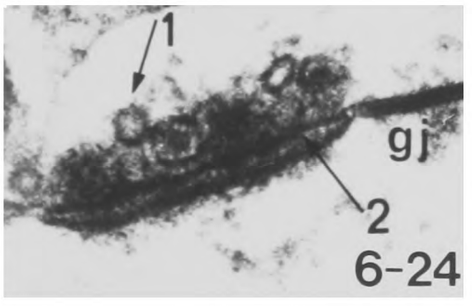
1
gj
2
6-24

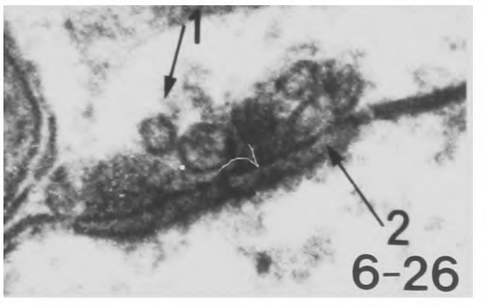
1
2
6-26

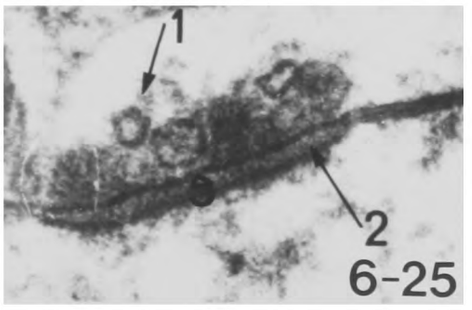
1
2
6-25

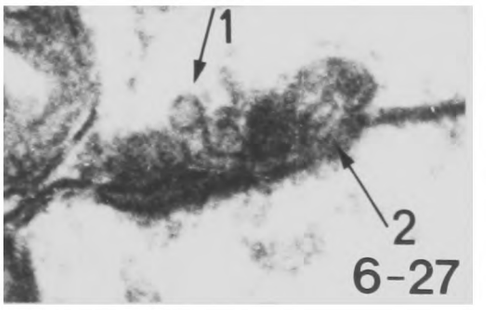
1
2
6-27

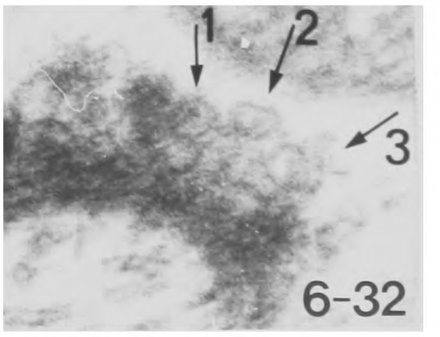
1
2
3
6-32

Fig. 6-33 Diagrams to summarise various arrangements in which dendro-dendritic synapses have been found.

A A simple dendro-dendritic synapse in which the PSD is wrapped round a very thin post-synaptic dendrite (figs. 6-9 and 6-10).

B A PSD making a synapse on to the shaft of a dendrite having two spines which receive asymmetric axo-spinous synapses.

C 1 A dendro-dendritic synapse on to a dendritic spine which also receives both an asymmetric and a symmetrical axo-spinous synapse (figs. 6-6 and 6-7).

D Dendro-dendritic synapse in which an asymmetric axon terminal makes a synapse on to both pre- and post-synaptic dendrites forming a triple arrangement.

E Complex arrangement in which a PSD (D1) makes two dendro-dendritic synapses on to spines (Sp1 and Sp3). One of these spines (Sp1) arises from a dendrite with a second spine (Sp2) which receives an asymmetric synapse from an axon terminal (t 6). This axon terminal also makes a synapse on to the PSD, forming a type of triplet arrangement and also on to the spine receiving the second dendro-dendritic synapse (Sp3), making a second triplet arrangement. A second axon terminal (t5) makes symmetrical synapses on to both the PSD and the shaft of the second dendrite, again forming a type of triplet arrangement (figs. 6-14 to 6-22, and 6-34). (See Fig. 6-34 for details).

F A dendro-dendritic synapse associated with a gap junction and a desmosome (figs. 6-1 to 6-3).

G A reciprocal dendro-dendritic synapse, associated with a gap junction and a desmosome (figs. 6-35 to 6-41).

H A reciprocal dendro-dendritic synapse between two dendrites (psd 1 and psd 2). One of these dendrites receives a dendro-dendritic synapse from a further psd (3) to which it is also linked by a gap junction.

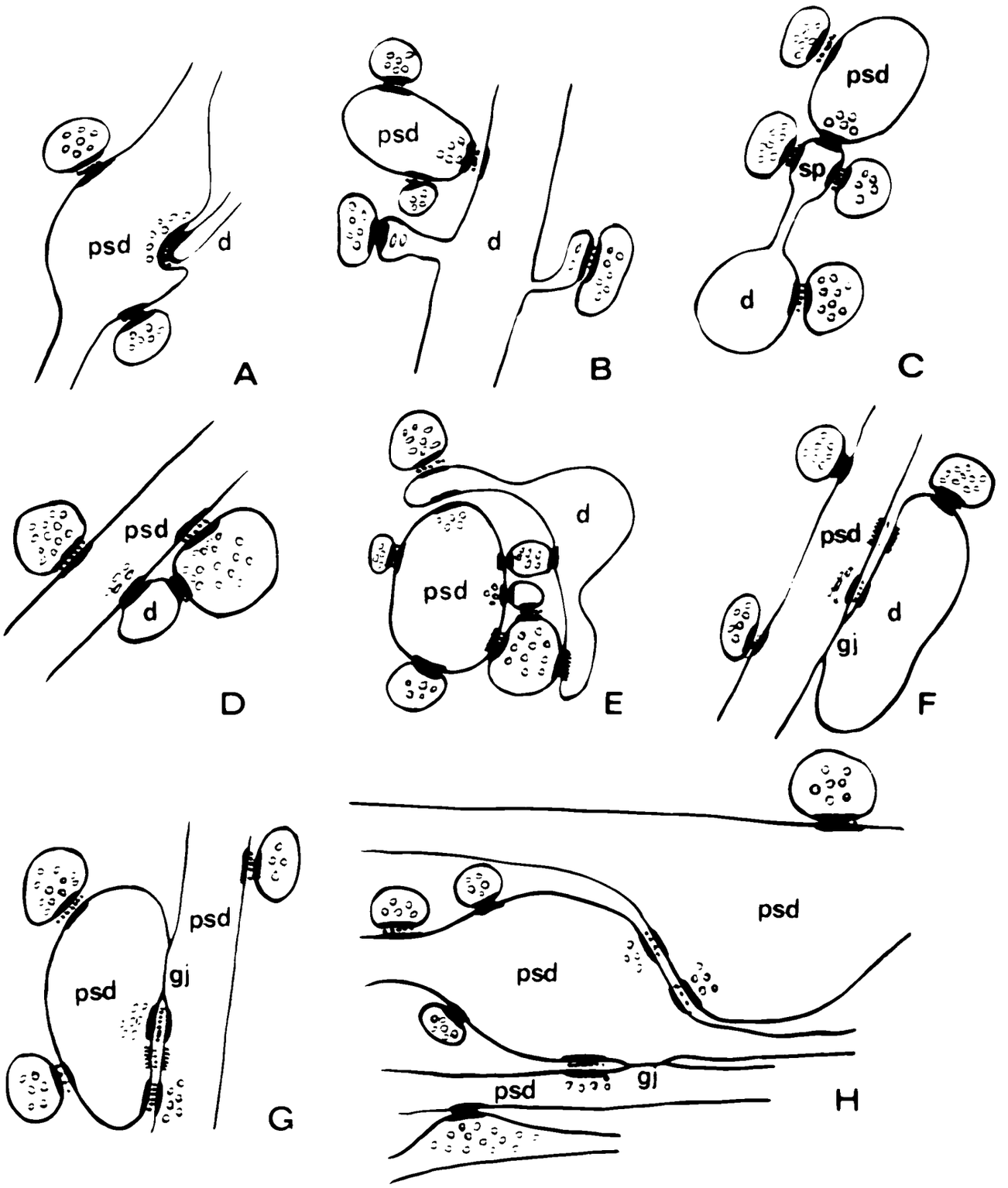
psd
d
A
psd
d
B
psd
sp
d
C
psd
d
D
d
psd
E
psd
d
gj
F
psd
psd
gj
G
psd
psd
psd
gj
H

Fig. 6-34 Diagram showing the reconstructed model of the complex dendro-dendritic synaptic arrangement of figs. 6-14 to 6-22 and 6-33 E. The pre-synaptic dendrite D1 makes dendro-dendritic synapses with two spines Sp1 and Sp3. Sp3 receives an asymmetric synapse from the axon terminal T6 which also makes a synapse on to the shaft of the pre-synaptic dendrite D1 and on to a spine (Sp2). This spine arises from the same parent dendrite as the spine Sp1 which receives one of the dendro-dendritic synapses. Another axon terminal (T5) makes symmetrical synapses on to both the pre-synaptic dendrite and the parent dendrite (D2) of the spines Sp1 and Sp2.

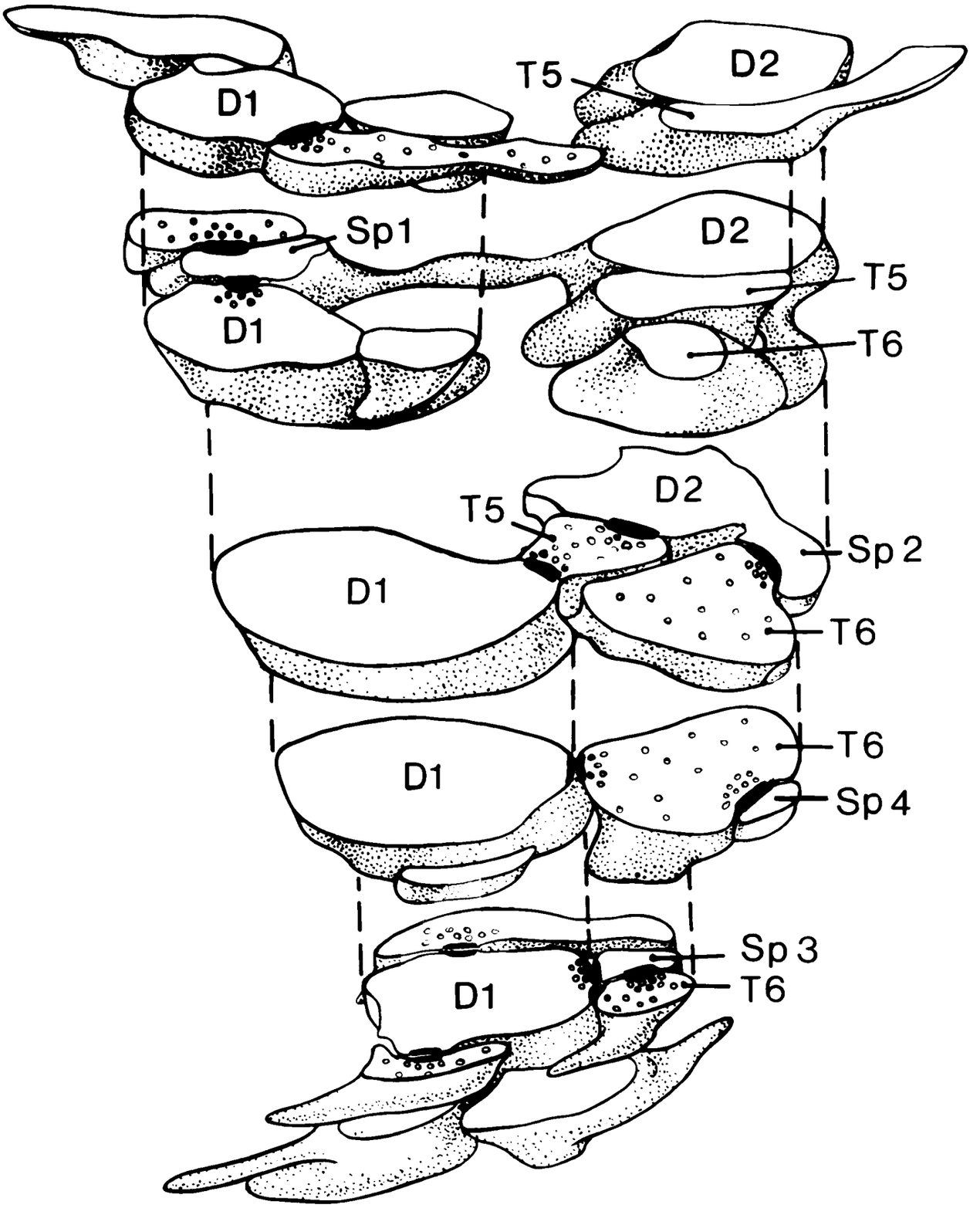
D1
T5
D2
Sp1
D2
T5
D1
T6
T5
D2
Sp 2
D1
T6
T6
D1
Sp 4
Sp 3
D1
T6

Figs. 6-35 to 6-43 Reciprocal dendro-dendritic synapse and gap junction in serial sections.

Fig. 6-35 Dendro-dendritic synapse between dendrite psd2 and dendrite psd1 (arrowhead). Note the other two synapses received by psd1 (arrows).
Section 1 X 29,000

Fig. 6-36 In the next serial section there are vesicles in both dendrites psd1 and psd2 (arrowheads) but the membrane thickening appears to be that of a desmosome. Note the gap junction now present between psd1 and psd2.
Section 2 X 29,000

Fig. 6-37 Section 3 shows a typical dendro-dendritic synapse from psd1 to psd2 and the gap junction is still present. Note that the dendro-dendritic synapse is in the opposite direction to that in fig. 6-35 and there is therefore a reciprocal synaptic arrangement.
Section 3 X 29,000

Figs. 6-38 and 6-39 In the next two serial sections the dendro-dendritic synapse from psd1 to psd2 enlarges. Note the pre-synaptic dense projections and also the axo-dendritic synapse received by psd2 in fig. 6-39 (arrow).
Sections 4 and 5 Both X 29,000

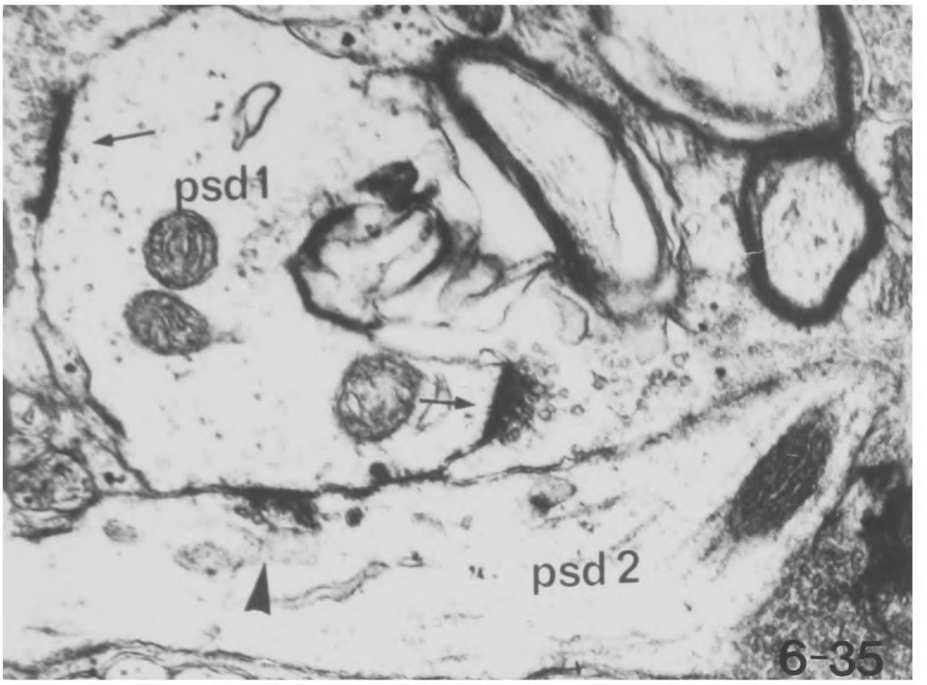
psd1
psd2
6-35

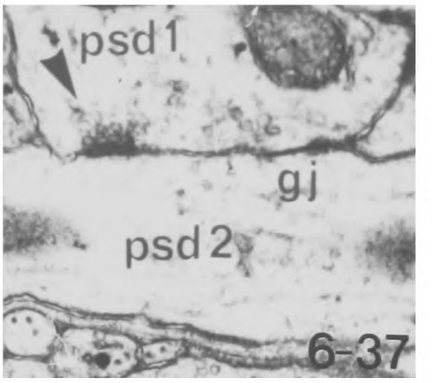
psd1
gj
psd2
6-37

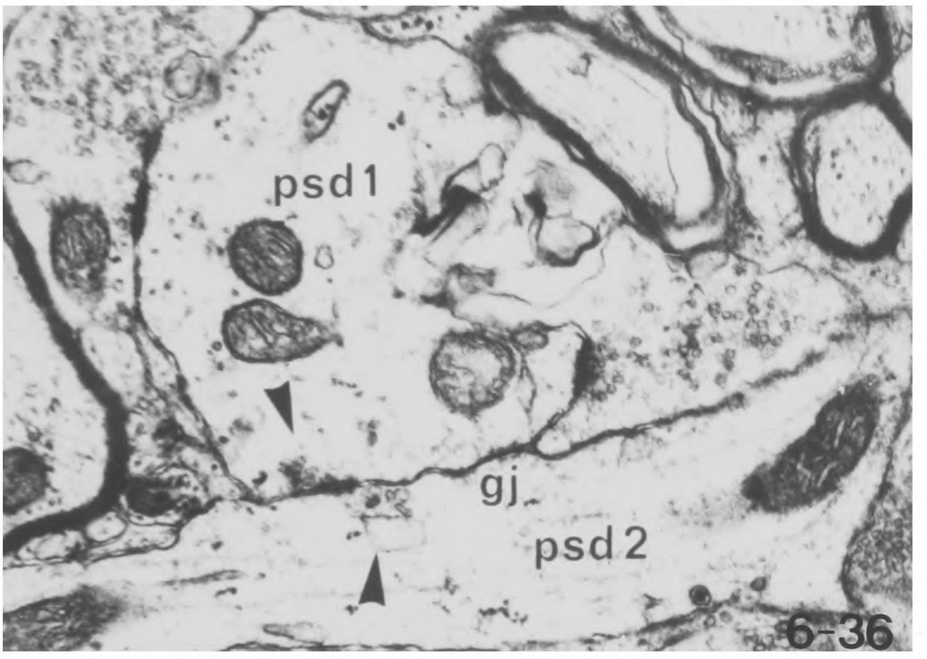
psd1
gj
psd2
6-36

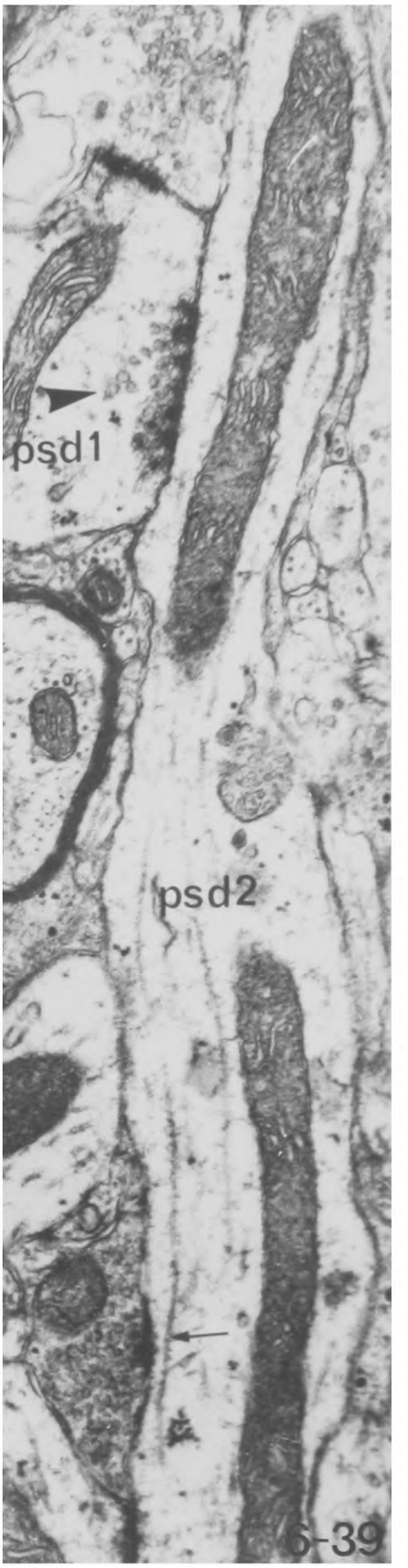
psd1
psd2
6-39

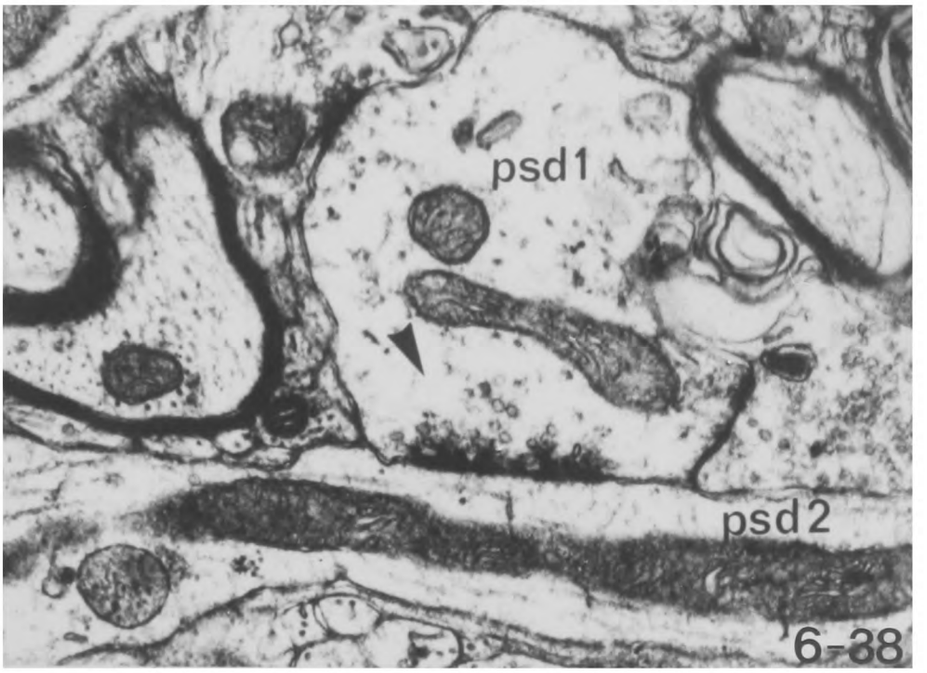
psd1
psd2
6-38

Higher magnifications of the reciprocal dendro-dendritic synapses and gap junction of figs. 6-35 to 6-39.

Fig. 6-40 Section 1. Dendrodendritic synapse from psd2 to psd1 (arrowhead). Note that the membrane complex is of the symmetrical type and that one of the vesicles is clearly flattened. X 67,000

Fig. 6-41 Section 2. Vesicles are present in both dendrites but the membrane specialisation in this section is a desmosome (arrow). Note the gap junction. X 160,000

Fig. 6-42 Section 3. The dendro-dendritic synapse from psd1 to psd2 (arrowhead). Note that its membrane specialisation is also of the symmetrical type, and that the gap junction is still present. X 67,000

Fig. 6-43 Section 4. The dendro-dendritic synapse from psd1 to psd2. Note its unusually large extent and the presence of flattened vesicles and a dense-cored vesicle. X 67,000

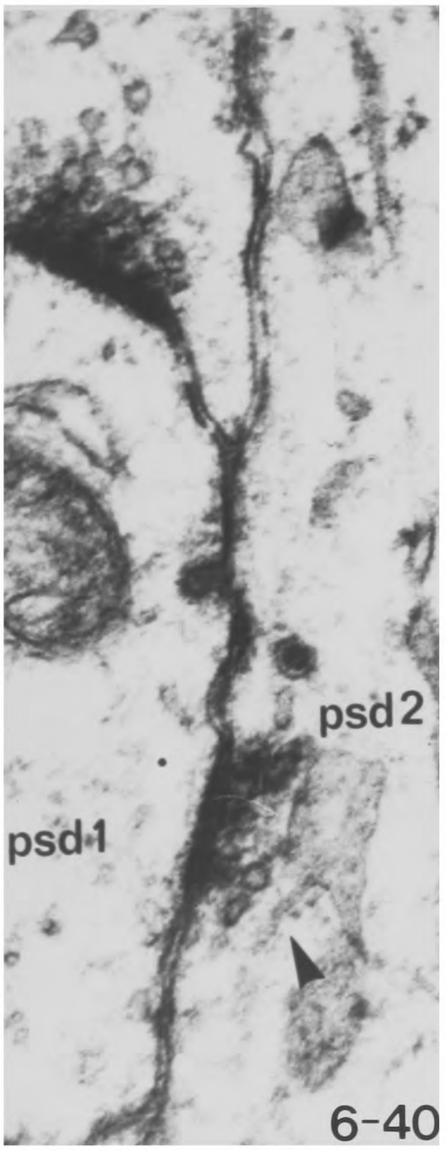
psd2
psd1
6-40

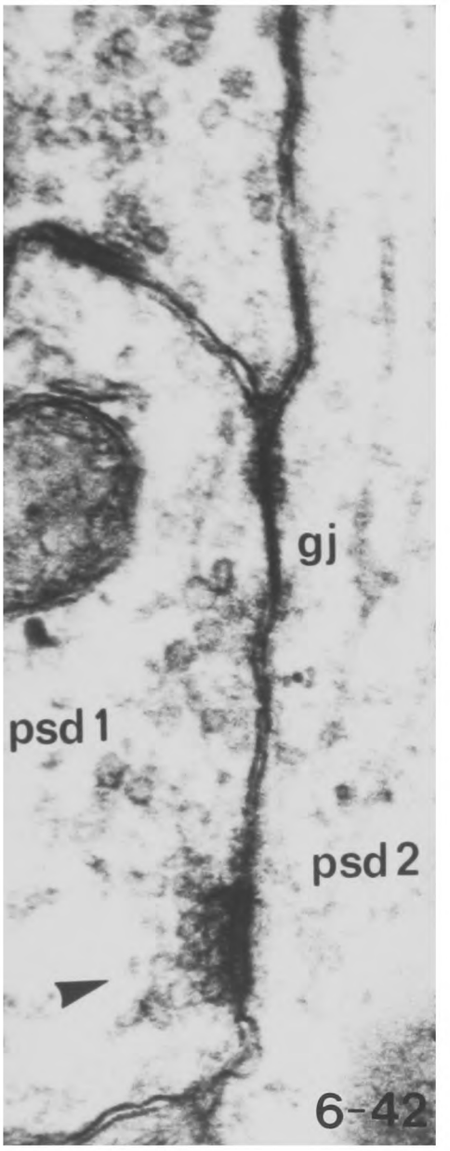
gj
psd1
psd2
6-42

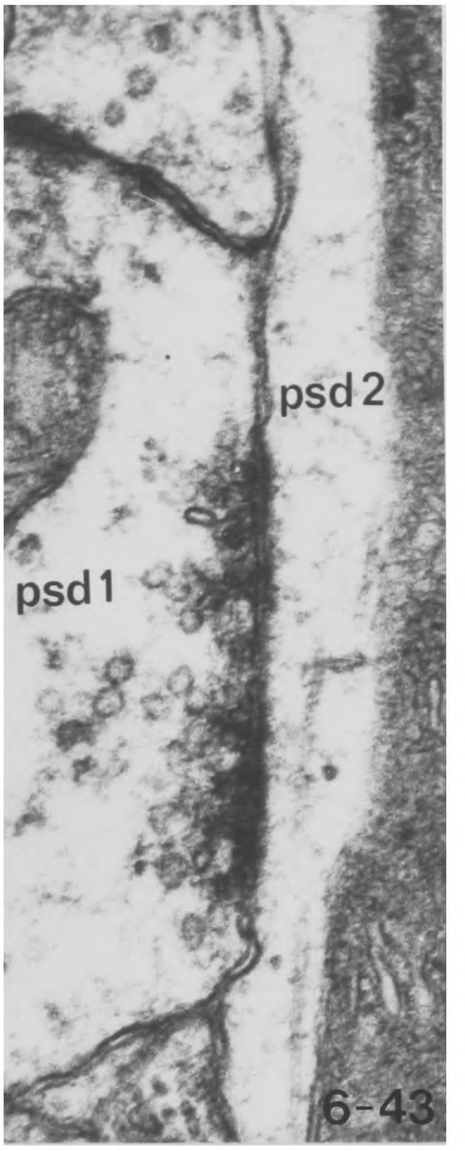
psd2
psd1
6-43

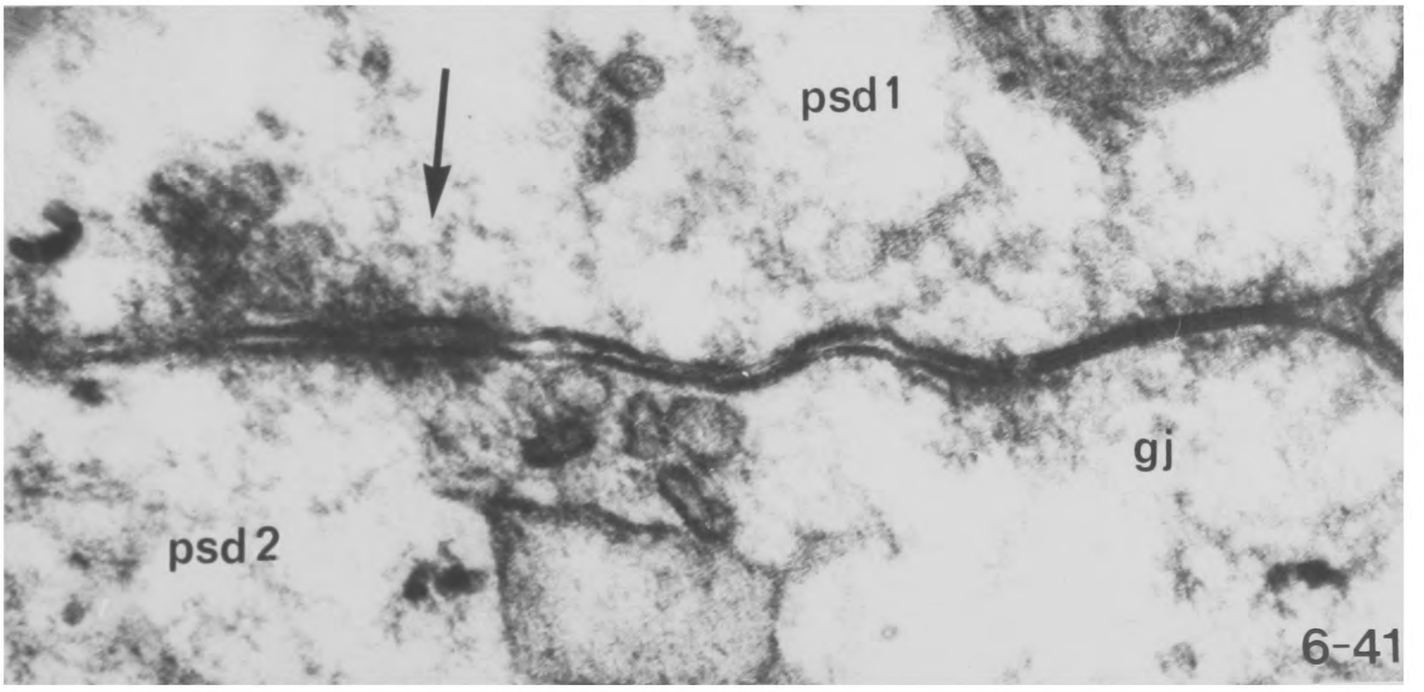
psd1
gj
psd2
6-41

Illustrations to Chapter 7

GAP JUNCTIONS BETWEEN DENDRITES AND SOMATA OF NEURONS IN THE SENSORI-MOTOR CORTEX

Figs. 7-1 to 7-4 Serial sections of a gap junction between two dendrites in layer IV of motor cortex.

Fig. 7-1 A gap junction between two dendrites d1 and d2. Note the synapse from axon terminal t on to dendrite d1.

Section 1 X 29,000

Fig. 7-2 The same gap junction as fig. 7-1 in the next serial section. Note that the axon terminal t now synapses on to dendrite d2 as well as on to dendrite d1.

Section 2 X 29,000

Fig. 7-3 The edge of the same gap junction as figs. 7-1 and 7-2, several sections away. Note the other synapses received by both dendrites.

Section 6 X 29,000

Fig 7-4 Higher magnification of the gap junction in fig. 7-1. Note the 2 nm 'gap' between the attenuated outer leaflets of the two plasma membranes, the periodic cross-bridges in this gap and the dense material in the dendritic cytoplasm adjacent to the gap junction.

Section 1 X 250,000

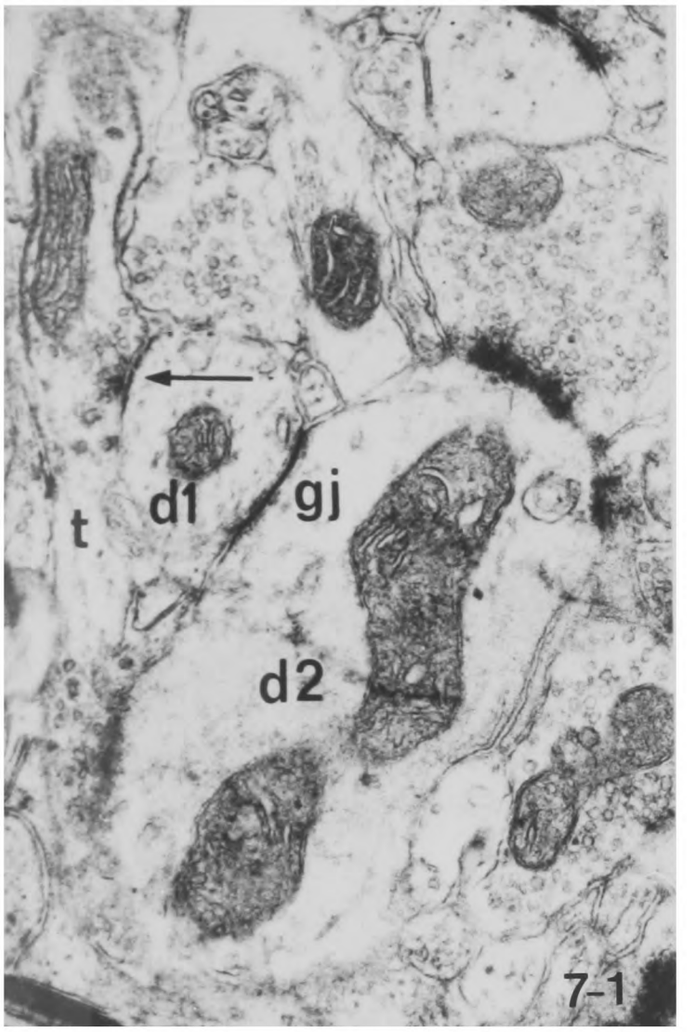
t
d1
gj
d2
7-1

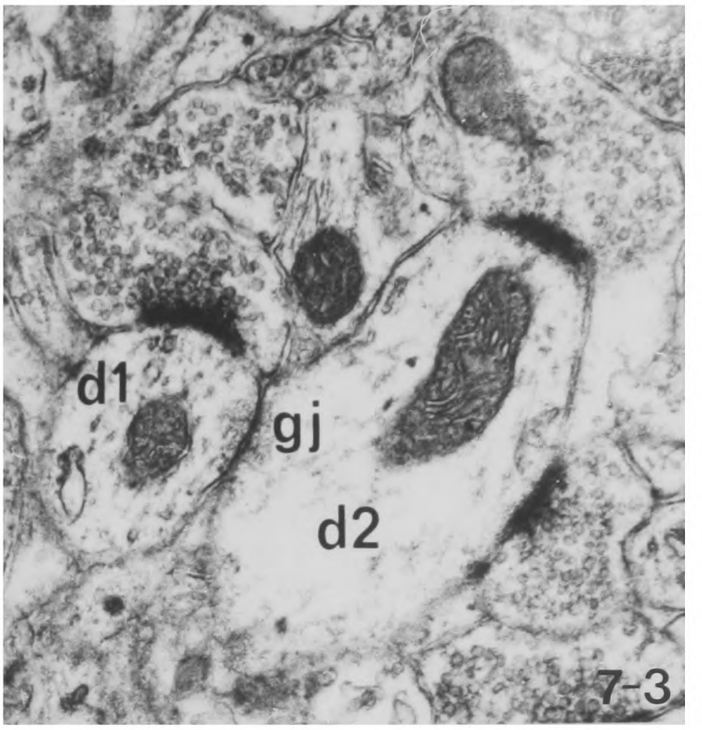
d1
gj
d2
7-3

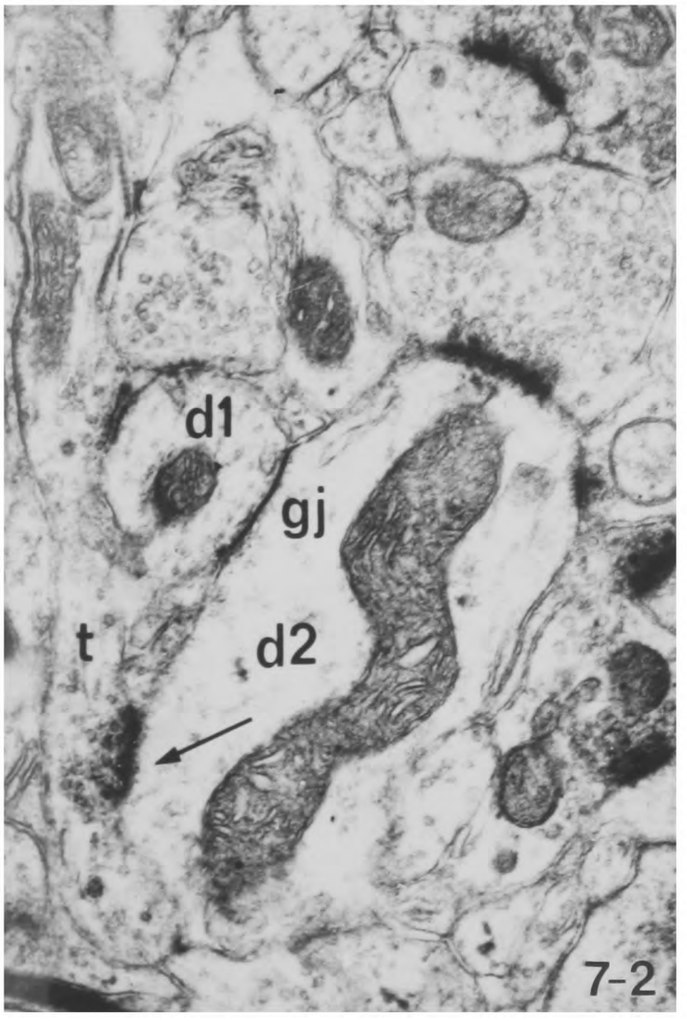
d1
gj
t
d2
7-2

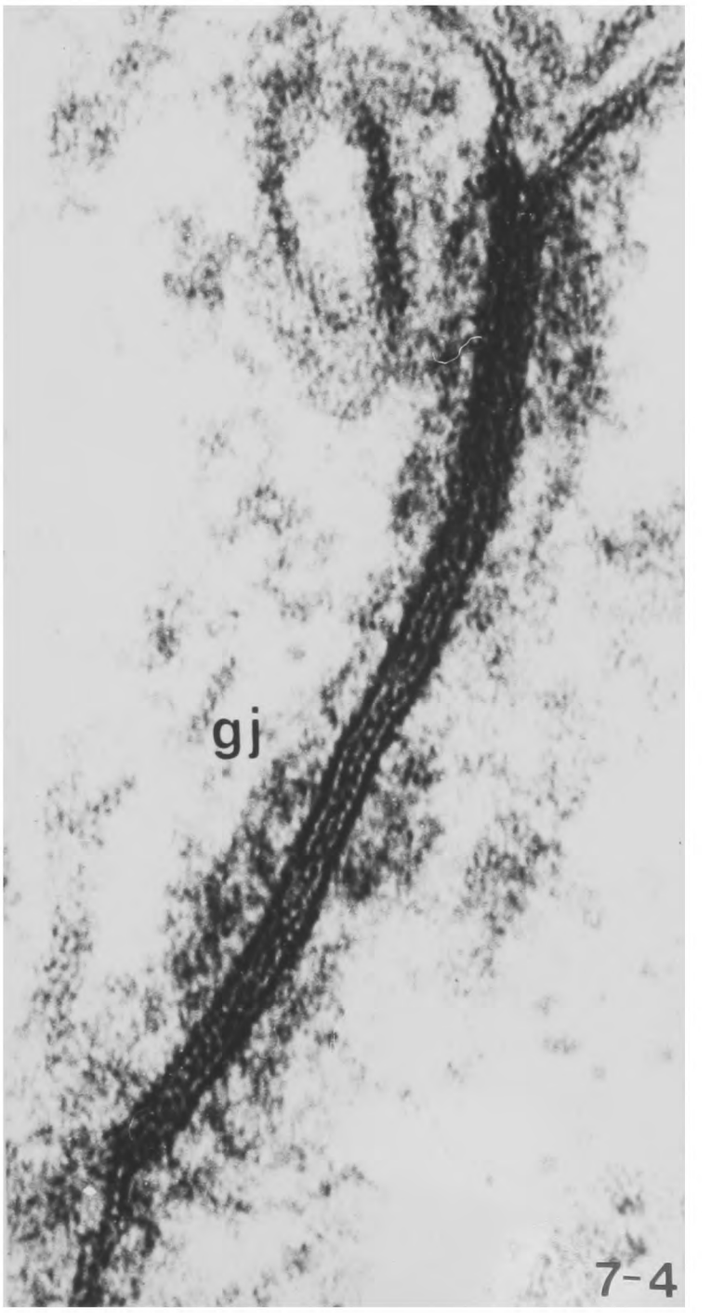
gj
7-4

Fig. 7-5 A gap junction between two large dendrites in layer V of motor cortex. Note the high concentratior of organelles in the smaller dendrite and the other synapses received by both dendrites.

X 29,000

Fig. 7-6 A gap junction between two dendrites in layer IV of motor cortex. Note the organelles in both dendrites and the asymmetric synapses they receive.

X 29,000

Fig. 7-7 Higher magnification of the gap junction of Fig. 7-6 shows its typical structure (arrow) (cf. Fig. 7-4) but to the left it is sectioned tangentially and shows its hexagonal subunits. These are best seen opposite the arrowhead.

X 240,000

7-5

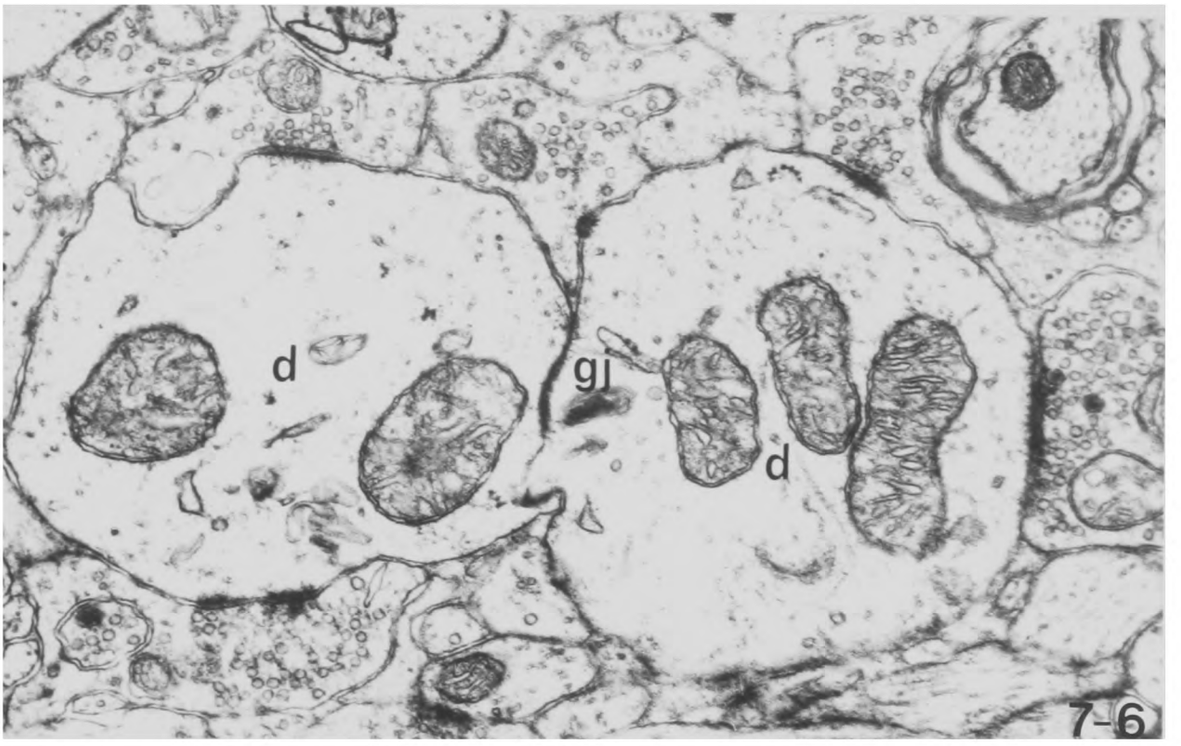

7-6

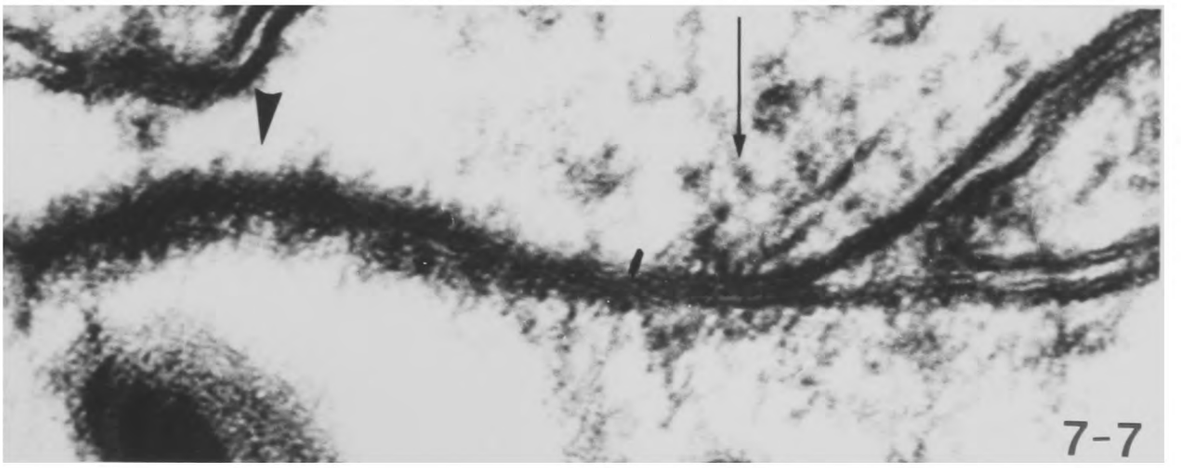

7-7

Fig. 7-8 A gap junction and adjacent desmosome (arrowhead) between two dendrites in layer IV of somatic sensory cortex (area 3b). Note the large number of synapses received by the lower dendrite and the varicose shape of the upper dendrite.
X 14,000

Fig. 7-9 Higher magnification of the gap junction and desmosome (arrowhead) of fig. 7-8. Note the contrasting arrangements of the plasma membranes in the two structures. X 160,000

Fig. 7-10 A gap junction between a dendrite and a dendritic spine. Note the small area of the gap junction. Section 8. X 29,000

Fig. 7-11 The same gap junction as in fig. 7-10 in the next serial section. Note the sac reminiscent of a spine apparatus in the dendritic spine. Section 7. X 29,000

Fig. 7-12 Higher magnification of the gap junction in figs. 7-10 and 7-11.
Section 8 X 67,000

Fig. 7-13 A long gap junction between two dendrites.
X 67,000

Fig. 7-14 Lower magnification of the gap junction of fig. 7-13 showing it to be between a small and a large dendrite. Note the four synapses received by the large dendrite, two of which are of the asymmetric type. X 8,400

7-8

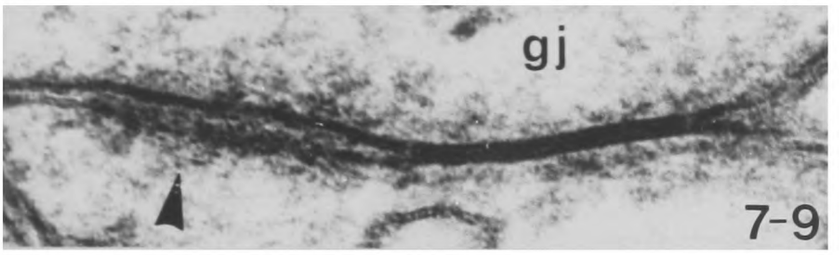

7-9

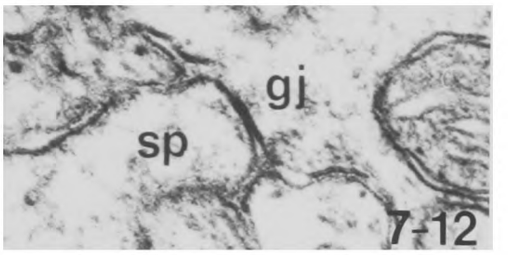

7-12

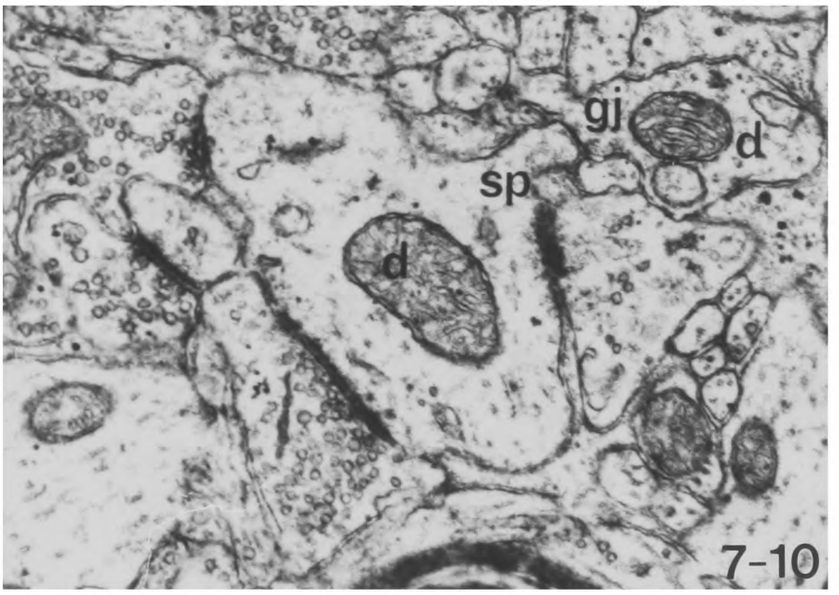

7-10

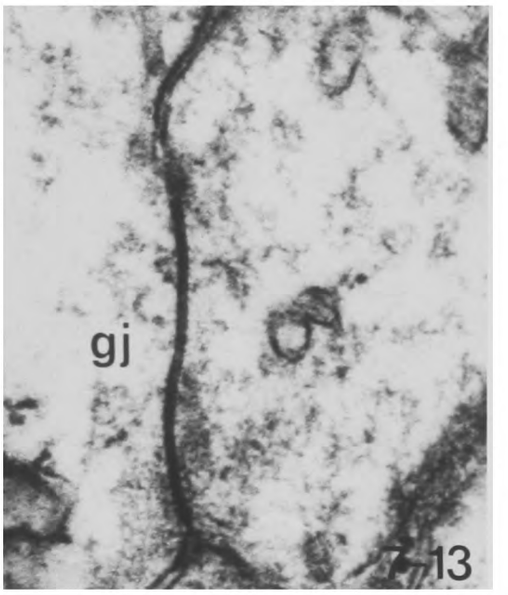

7-13

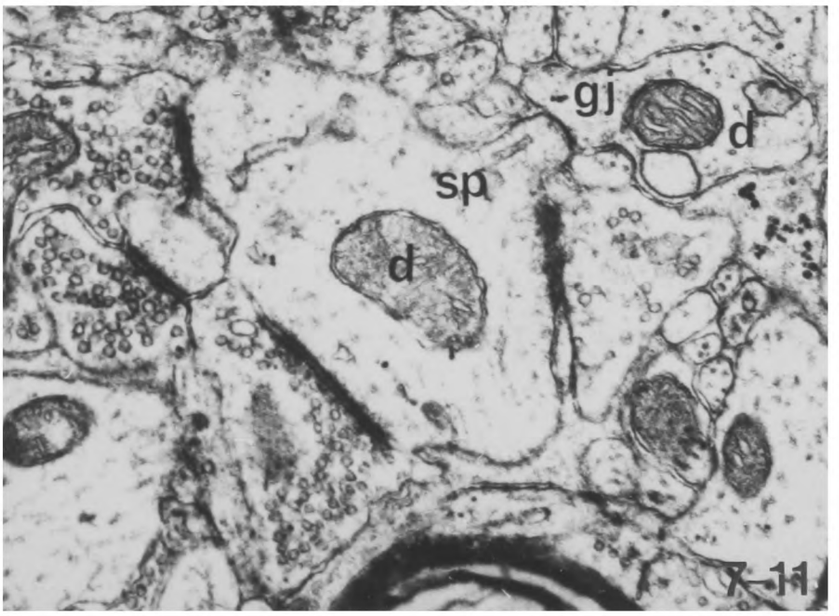

7-11

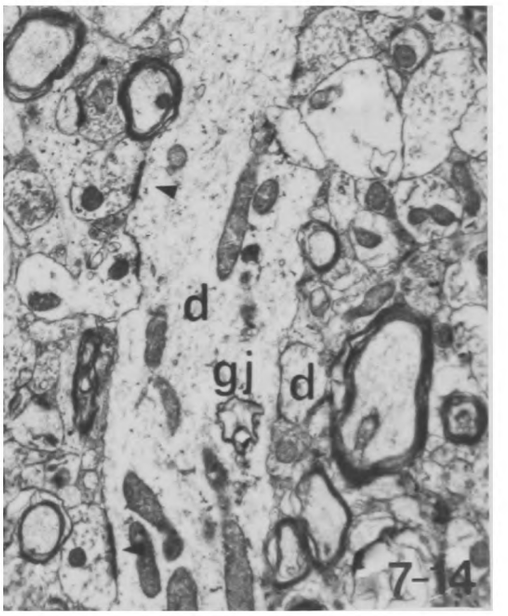

7-14

Fig. 7-15 Diagrams to summarise various positions in which gap junctions have been found.

A A gap junction between the shafts of two dendrites.

B A gap junction between a dendrite and a cell soma.

C A gap junction between a dendritic spine and a dendritic shaft.

D A gap junction between two dendrites, both of which receive asymmetric synapses from the same axon terminal.

E A gap junction associated with a dendro-dendritic synapse and a desmosome.

F A gap junction associated with a reciprocal dendro-dendritic synapse and a desmosome.

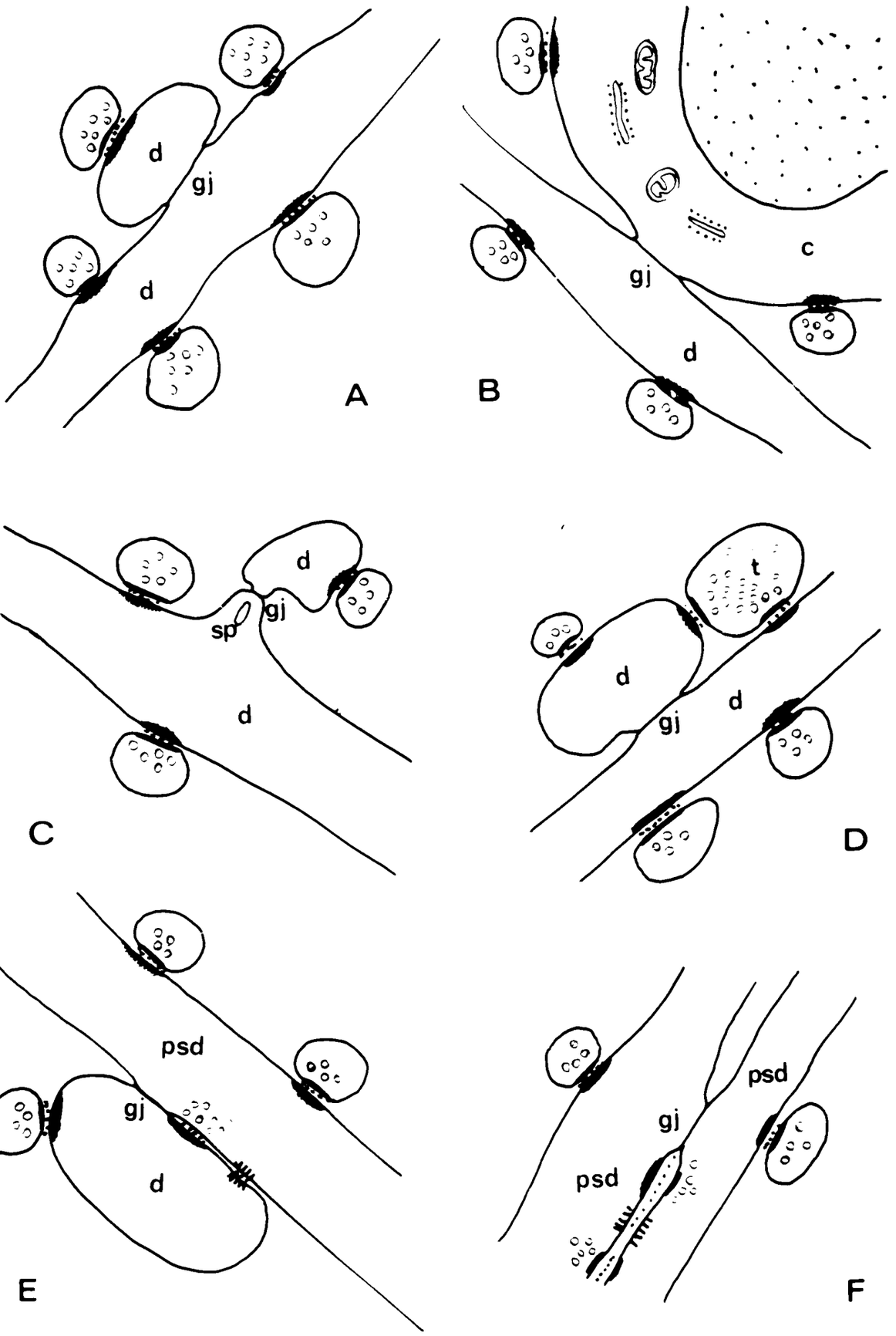
d
gj
d
A
B
c
gj
d
C
sp
gj
d
d
t
d
gj
d
D
psd
gj
d
E
psd
gj
psd
F

Fig. 7-16 A gap junction between a dendrite and a large stellate cell soma in layer IV of somatic sensory cortex. X 8,400

Fig. 7-17 Higher magnification of the somato-dendritic gap junction of fig. 7-16. Note the associated desmosome (arrowhead). X 29,000

Fig. 7-18 Higher magnification of the gap junction and desmosome of figs. 7-16 and 7-17. X 67,000

Fig. 7-19 A gap junction between a dendrite and part of a large stellate cell soma in layer V of motor cortex. Note the desmosome (arrowhead) which is also between the dendrite and cell soma. The cell soma was shown to receive a number of asymmetric synapses in this and other serial sections. X 29,000

Fig. 7-20 Higher magnification of the somato-dendritic gap junction of fig. 7-19. X 160,000

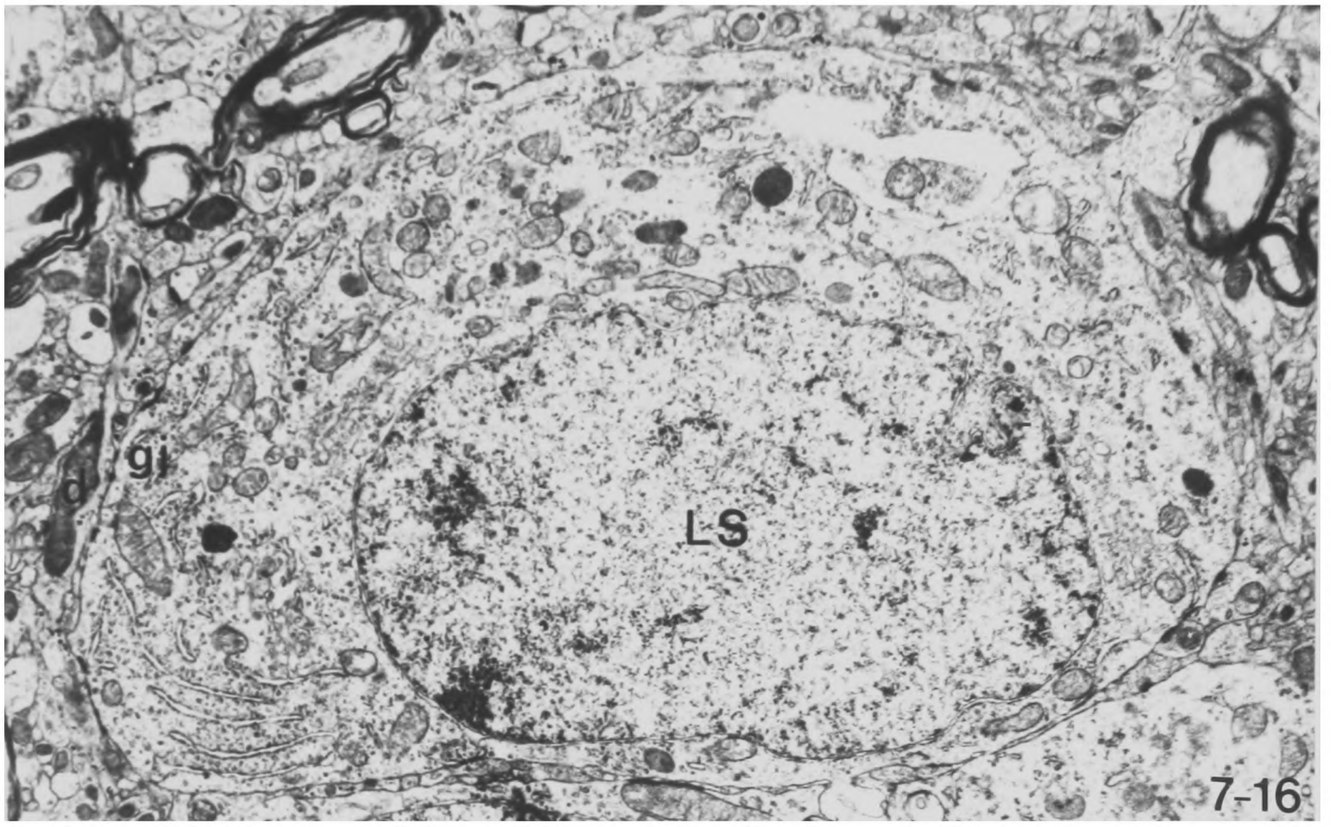
gj
d
LS
7-16


gj
d
7-17

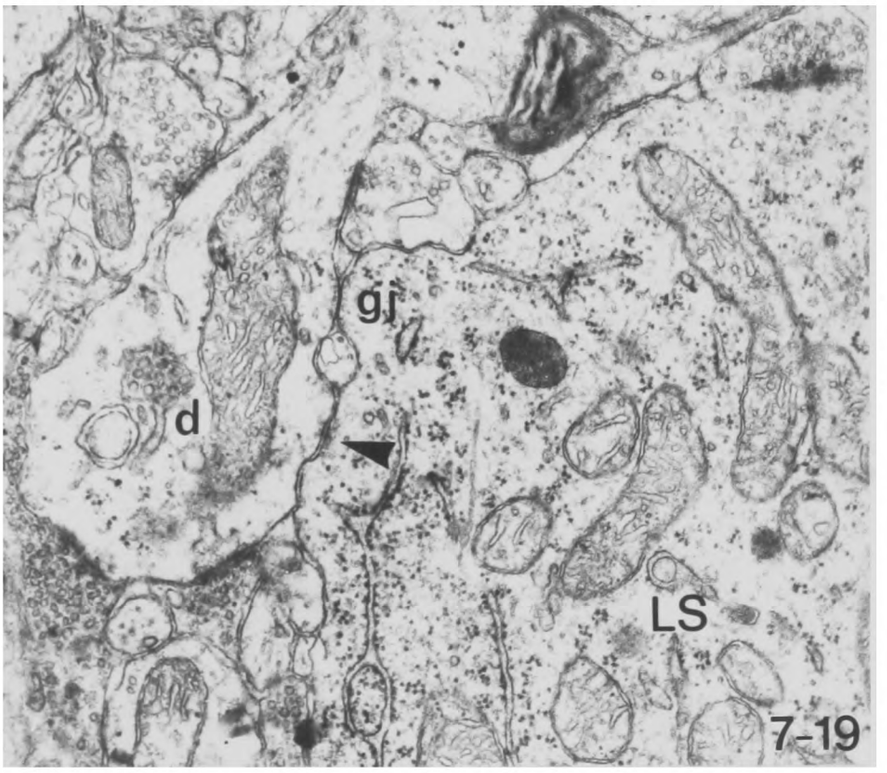
gj
d
LS
7-19

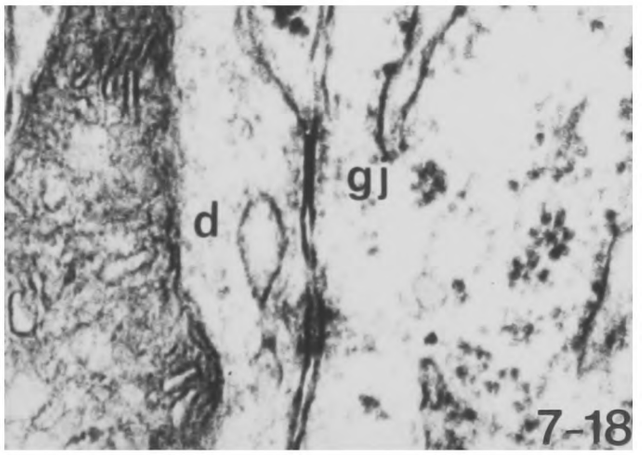
d
gj
7-18

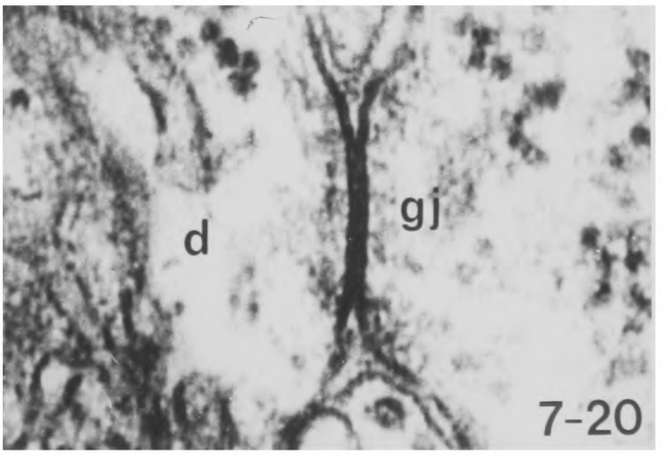
d
gj
7-20

Fig. 7-21 A gap junction between a dendrite and a large stellate cell soma in layer V of motor cortex. Note the proximity of the gap junction to the axon initial segment which is directed toward the cortical surface. X 18,000

Inset - Higher magnification of the gap junction X 67,000

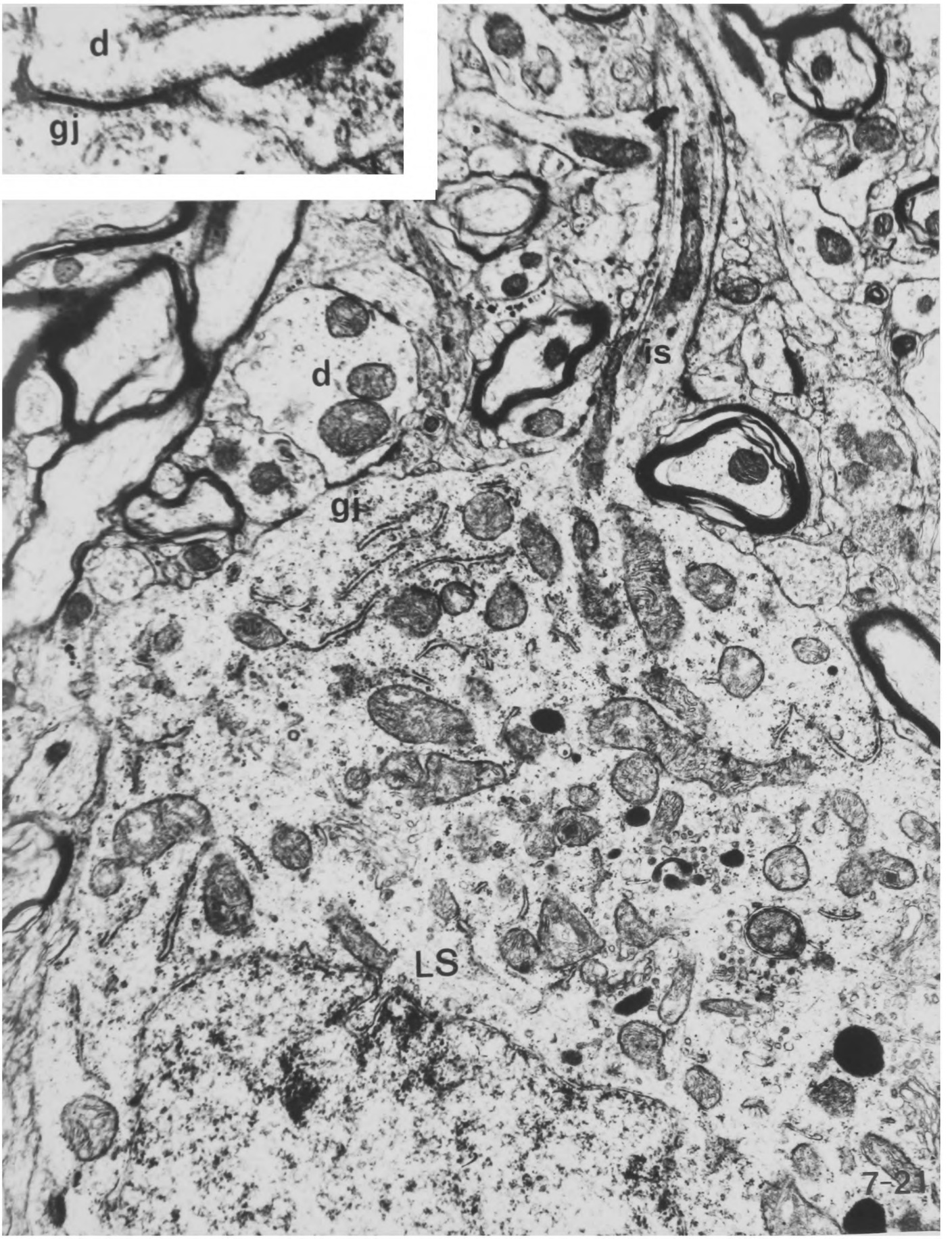
d
gj
d
gj
is
LS
7-21

Fig. 7-22 A large stellate dendrite from layer IV of motor cortex in an animal in which a thalamic lesion had been placed 5 days before death. The dendrite both receives synapses from two degenerating thalamocortical axon terminals and also makes a gap junction with a spine. Serial sections confirmed the identification of this profile as a spine and also the synapses from both degenerating axon terminals. X 11,100

Fig. 7-23 Higher magnification of the upper end of the dendrite of fig. 7-22 showing the two degenerating thalamo-cortical axon terminals X 32,000

Fig. 7-24 Higher magnification of the gap junction between the dendrite and spine of fig. 7-22. X 94,500

7-22

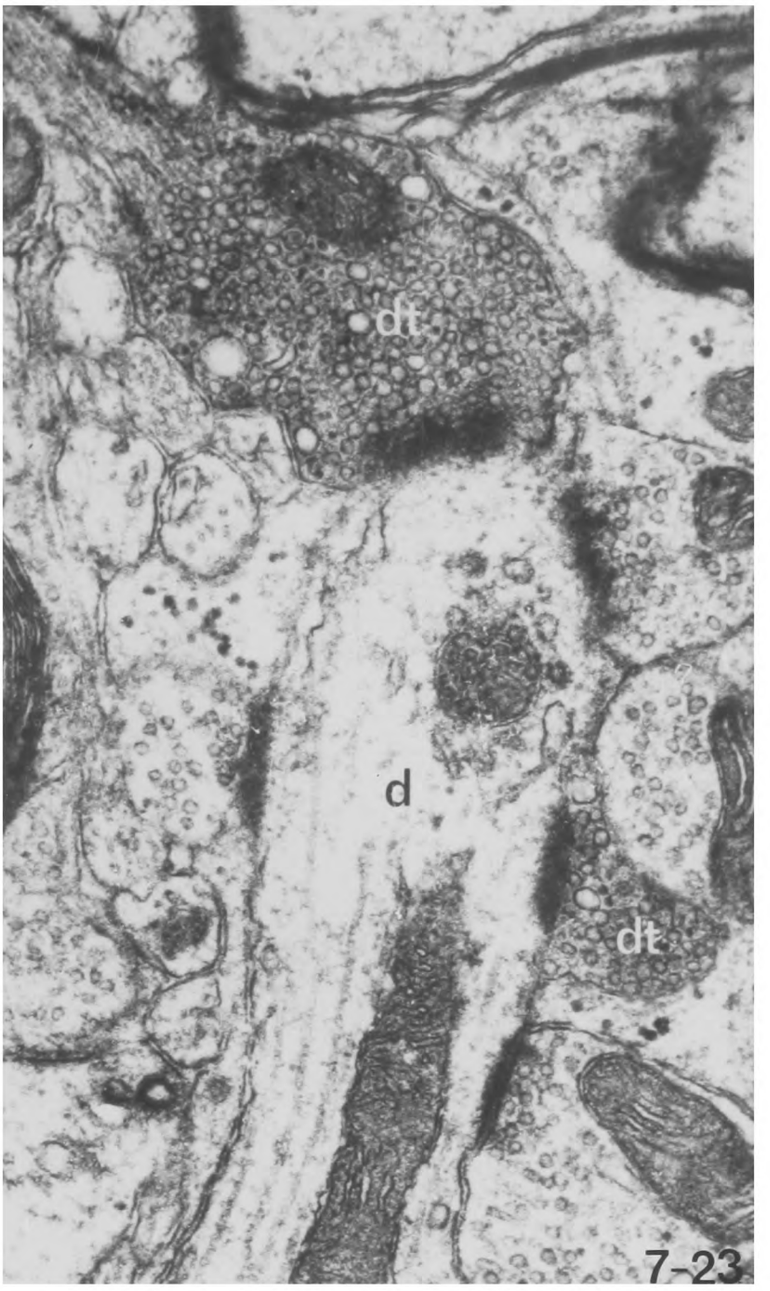

7-23

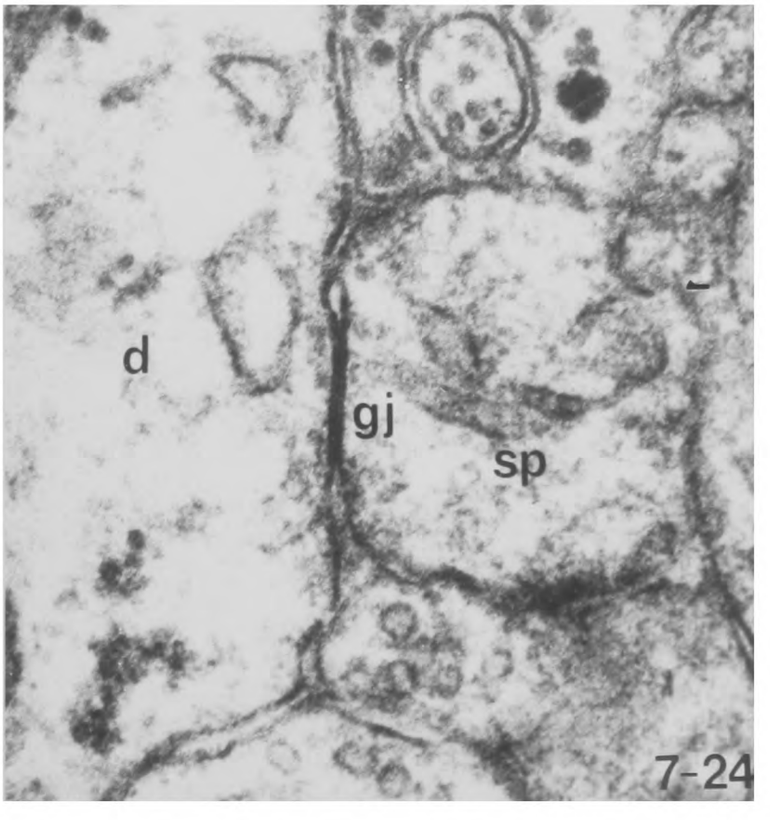

7-24

Illustrations to Chapter 8

OBSERVATIONS ON THE PROCESS OF DEGENERATION IN THE SENSORI-MOTOR CORTEX

Figs. 8-1 to 8-6 A comparison of different stages of degeneration in thalamo-cortical and commissural axon terminals.

Fig. 8-1 An early stage of degeneration in a thalamo-cortical terminal in motor cortex at 4 days' survival. Note the prominent meurofilaments and large size of the terminal. X 29,000

Fig. 8-2 A similar early stage of degeneration in a commissural terminal in the motor cortex at 4 days' survival. Note the slight darkening of the terminal and irregular synaptic vesicles but the lack of neurofilaments and the small size of the axon terminal. X 35,000

Fig. 8-3 An intermediate stage of degeneration in a thalamo-cortical axon terminal from motor cortex at 5 days' survival. Note the large size of the terminal, the prominent glycogen granules and the irregularly swollen "glossy" vesicles. X 52,000

Fig. 8-4 An intermediate stage of degeneration in a commissural axon terminal at 6 days' survival. Note the lack of glycogen granules and the different appearance of the synaptic vesicles compared with fig. 8-3. X 52,000

Fig. 8-5 A late stage of degeneration of a thalamo-cortical axon terminal from motor cortex. Note the large size of the terminal and its engulfment by glia. X 32,000

Fig. 8-6 A late stage of degeneration of a commissural axon terminal from motor cortex. Note its small size and its engulfment by glia. X 37,000

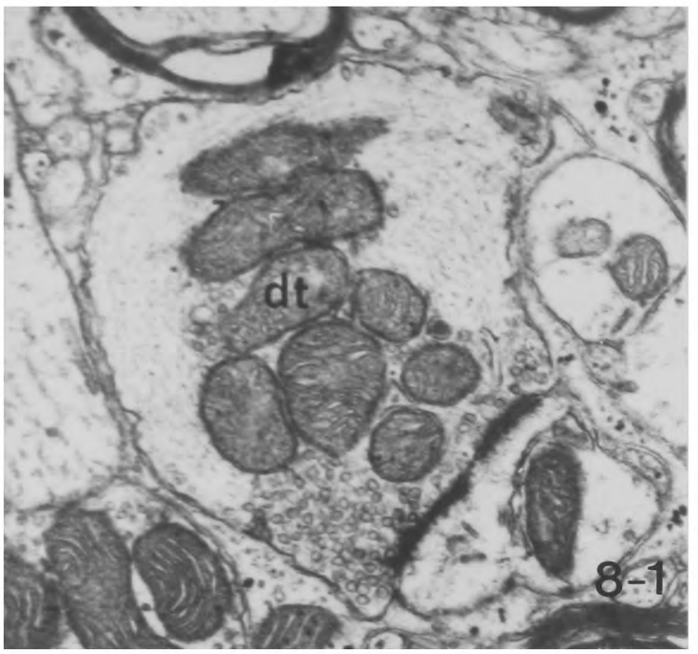

8-1

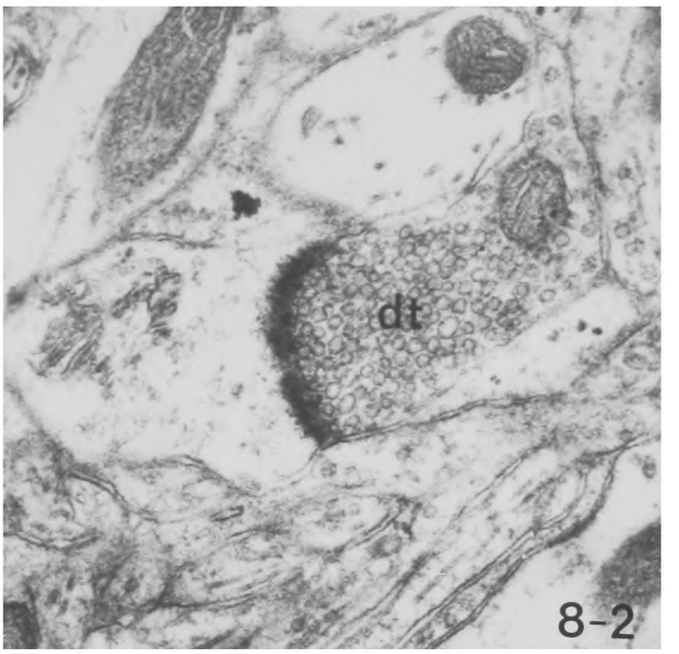

8-2

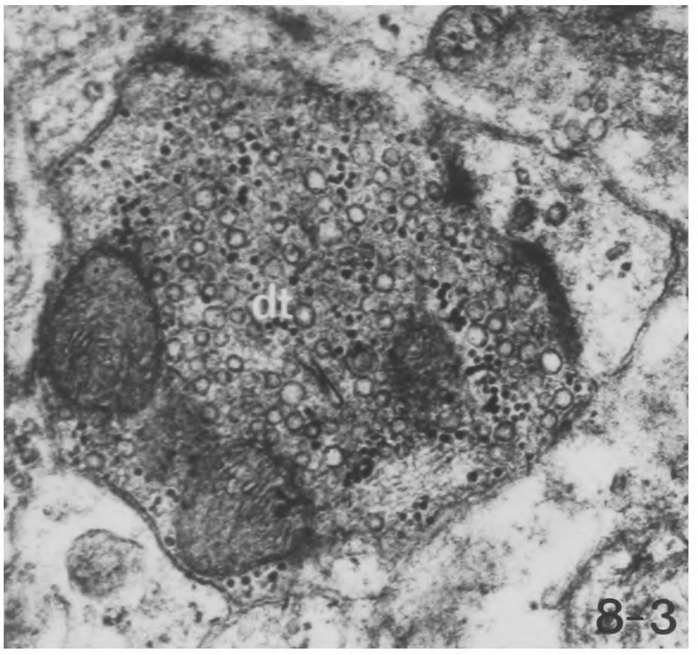

8-3

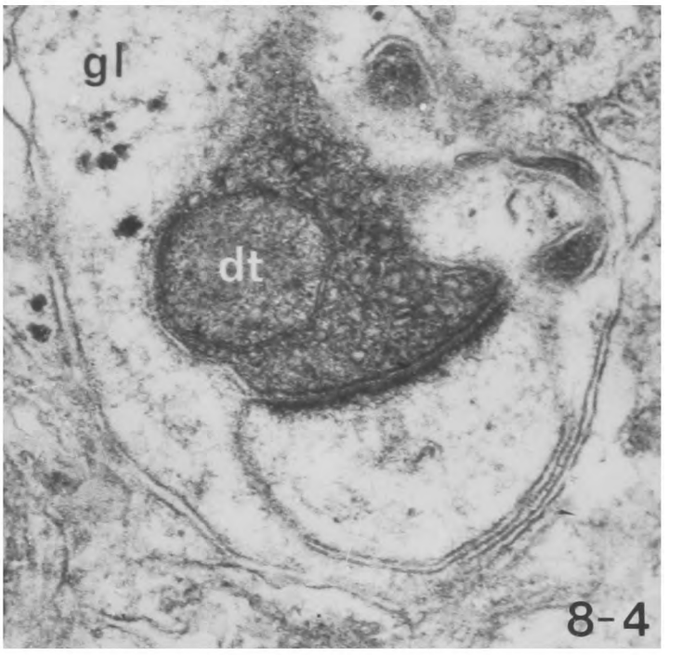

8-4

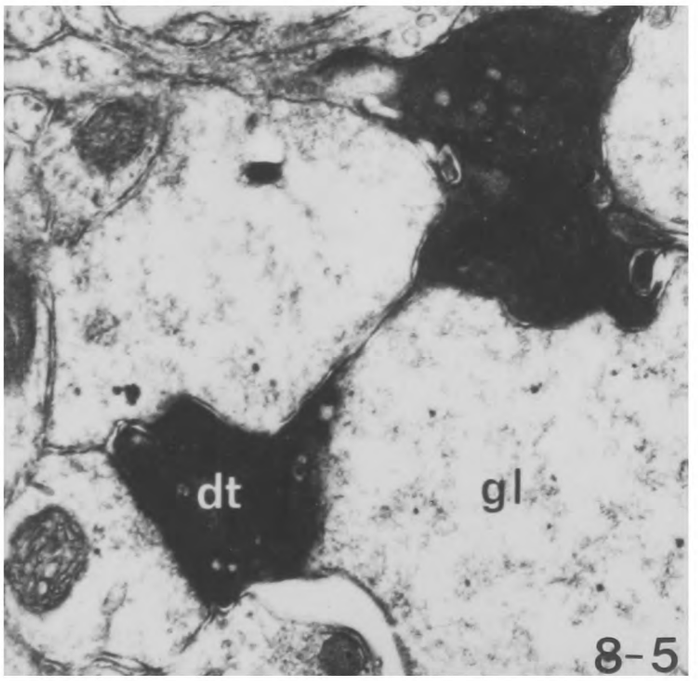

8-5

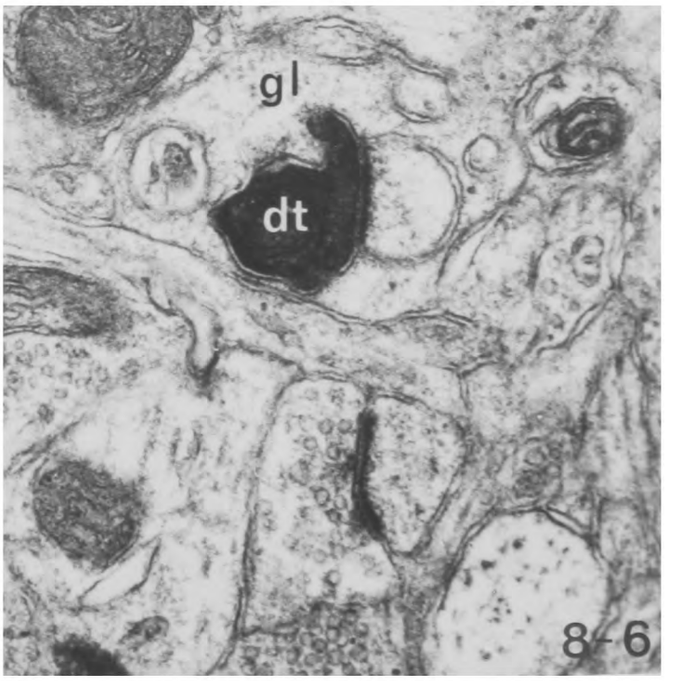

8-6

Fig. 8-7 A rare example of neurofilamentous hypertrophy of an axon preterminal following removal of the contralateral motor cortex. X 25,200

Fig. 8-8 A rare example of neurofilamentous hypertrophy in a degenerating association axon terminal from motor cortex following a lesion of the ipsilateral somatic sensory cortex.

X 28,300

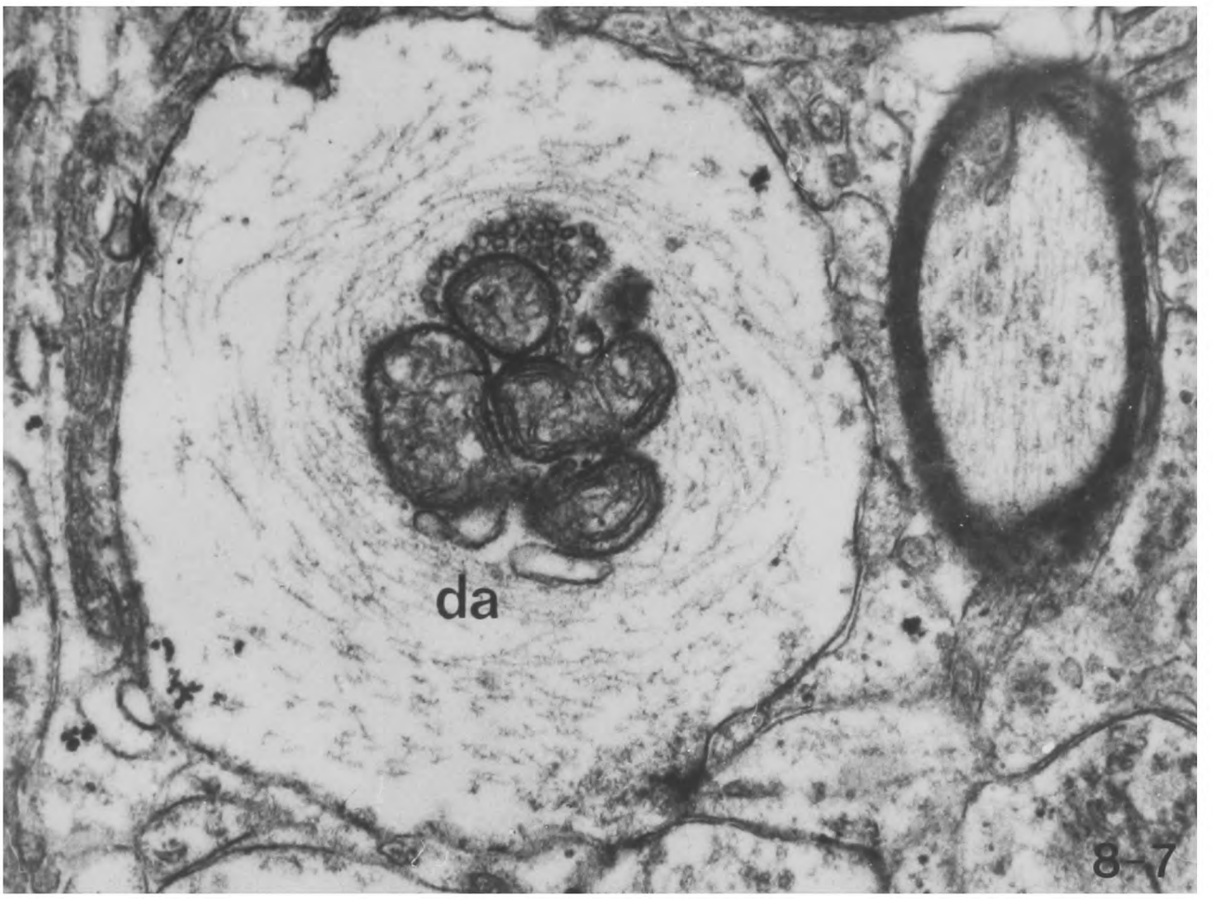

8-7

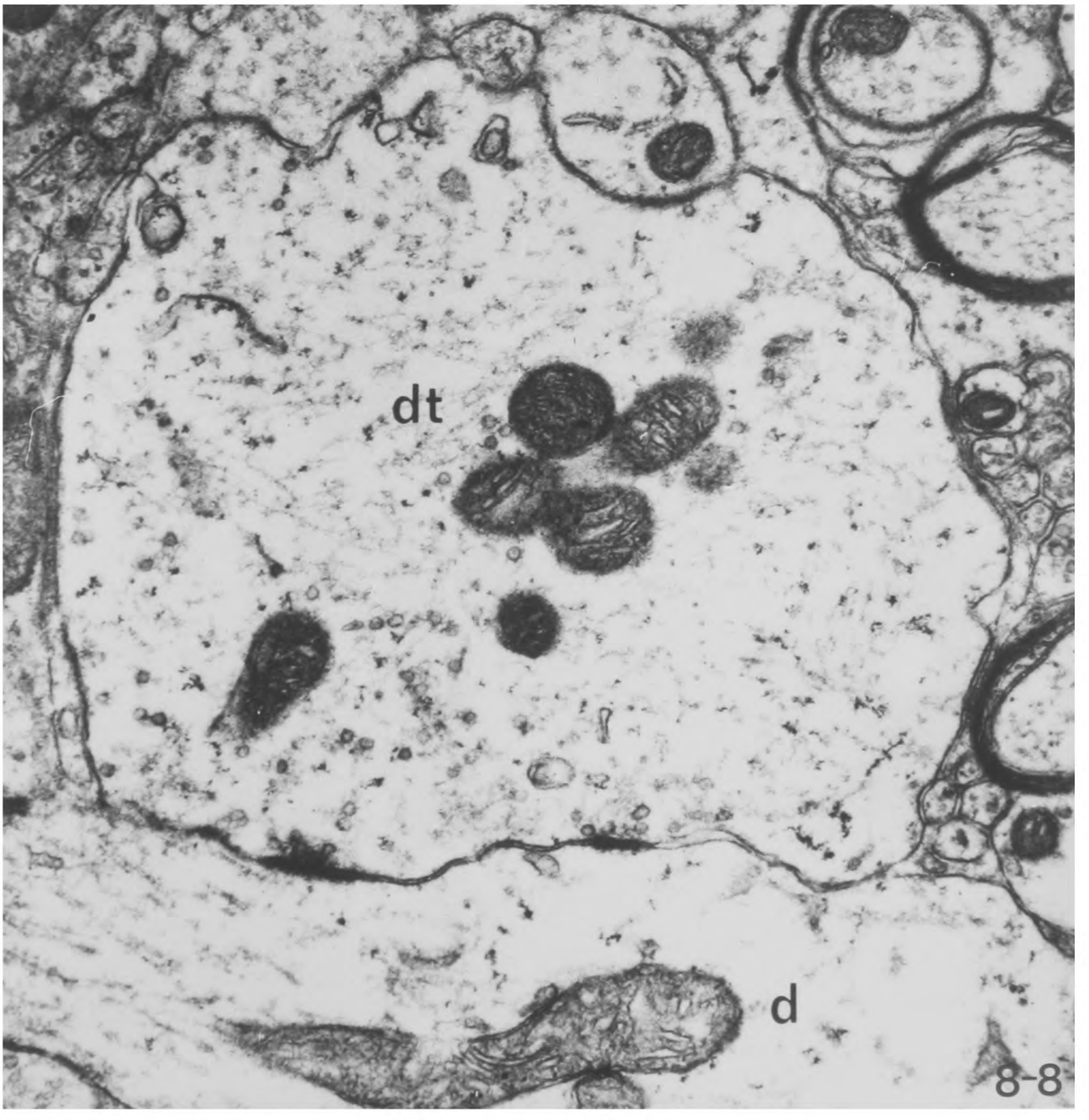

8-8

Figs. 8-9 to 8-14 Phagocytosis of degeneration.

Fig. 8-9 A degenerating axon terminal making a synapse on to a spine in the motor cortex 4 days after removal of ipsilateral areas 1 and 2 of somatic sensory cortex. Note the glial cytoplasm with a coated pit engulfing part of the degenerating axon terminal (arrowhead). X 67,000

Fig. 8-10 Part of a degenerating pre-terminal axon being engulfed in a large coated pit by glial cytoplasm (arrowhead). X 55,000

Fig. 8-11 A degenerating axon terminal from the somatic sensory cortex 4 days after a thalamic lesion. The degenerating terminal makes a synapse on to a spine which also receives a synapse from a normal axon terminal. Note the coated pit in the glia which is engulfing part of the degenerating axon terminal (arrowhead). X 63,000

Fig. 8-12 Part of a degenerating preterminal axon being engulfed by glia. One coated vesicle is almost completely pinched off (arrowhead) while a second is at an early stage of engulfment (arrow). X 67,000

Fig. 8-13 A degenerating commissural axon terminal from the somatic sensory cortex which makes a synapse on to a spine. Note the coated vesicle in the glial cytoplasm which has almost completely pinched off part of the degenerating axon terminal (arrowhead). X 55,000

Fig. 8-14 A degenerating commissural axon terminal from the motor cortex which makes a synapse on to two spines. One of these spines contains a coated vesicle with an electron-dense core (arrow). X 58,000

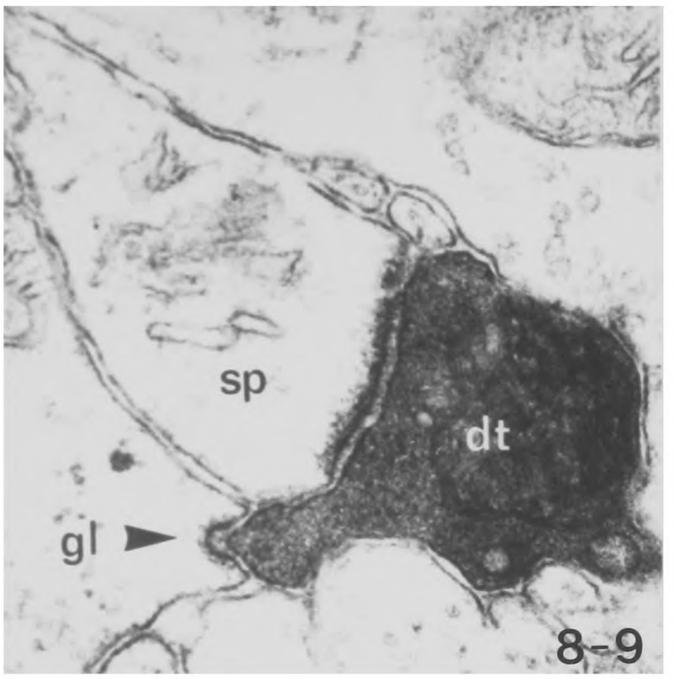

8-9

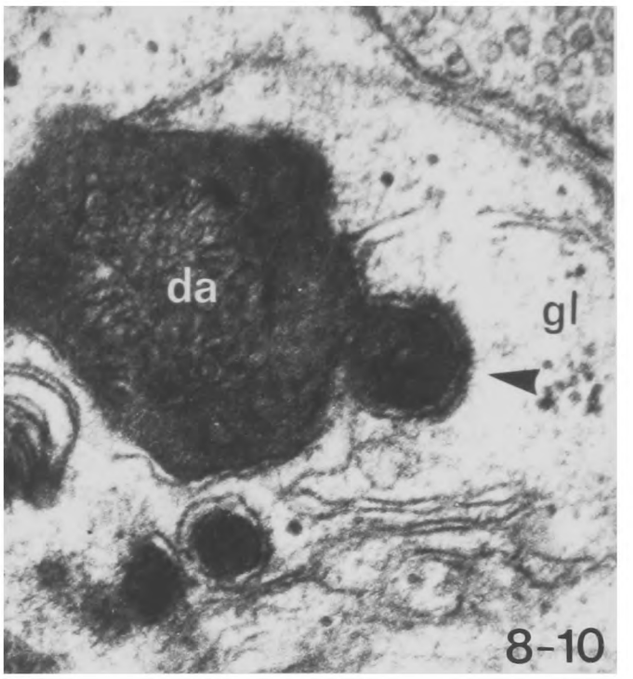

8-10

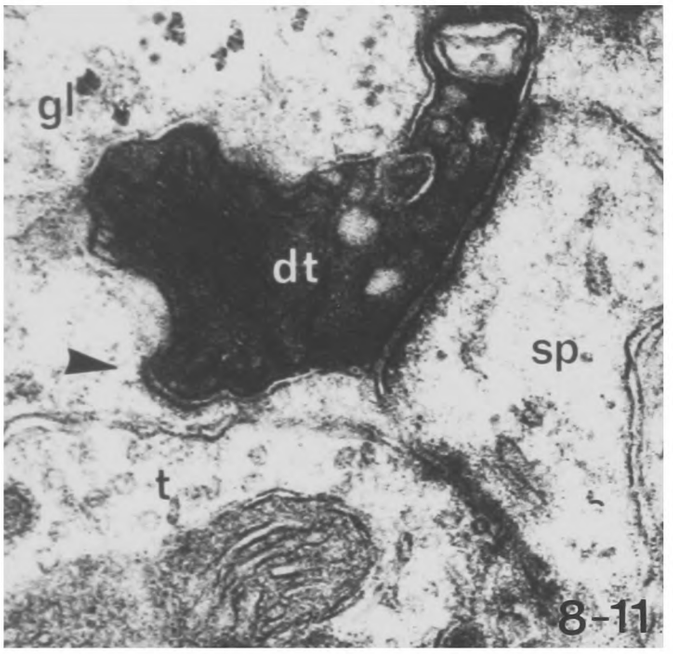

8-11

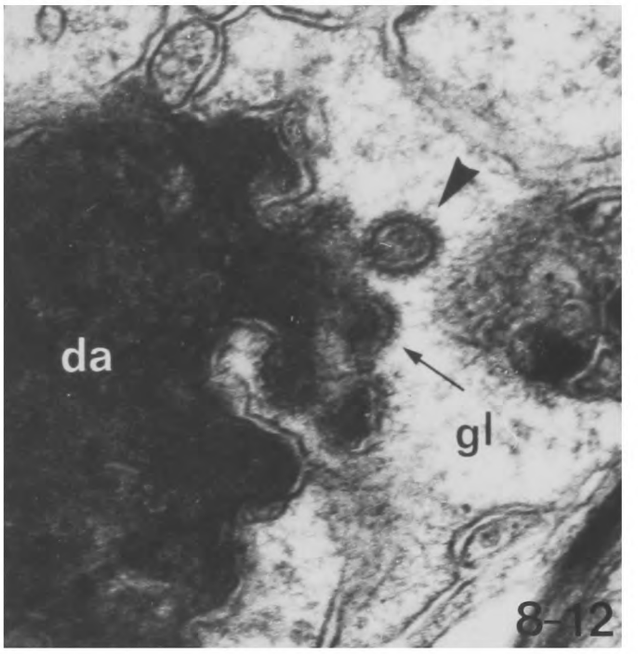

8-12

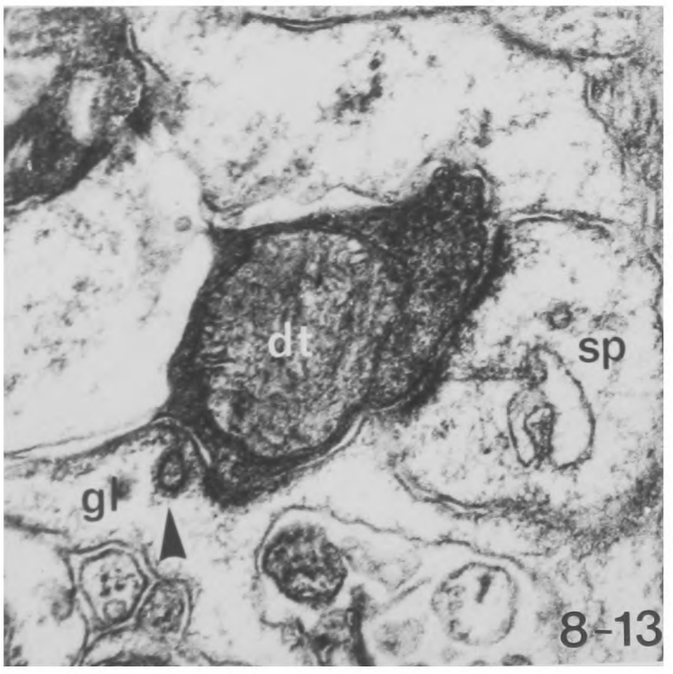

8-13

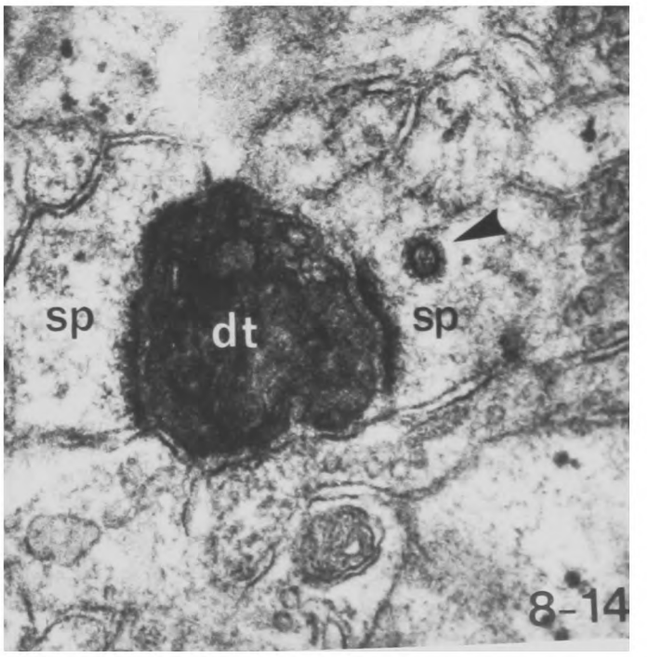

8-14

Figs. 8-15 to 8-20 Phagocytosis of degeneration by neurones.

Fig. 8-15 A pyramidal cell from the motor cortex which has a coated pit engulfing part of a degenerating thalamo-cortical axon terminal (large arrow). Note the synapses received by the pyramid (small arrows). X 8,400

Fig. 8-16 Higher magnification of fig. 8-15 showing the coated pit engulfing part of the degenerating axon terminal (arrowhead). X 67,000

Fig. 8-17 A coated pit (arrowhead) which has almost pinched off part of the cytoplasm of a degenerating pre-terminal axon. X 67,000

Fig. 8-18 Lower magnification of fig. 8-17 showing the coated pit being taken into a neuron. Note the synapse received by the neuron (arrow). X 29,000

Fig. 8-19 An early stage of formation of a coated pit (arrow-head) in a neuron which is engulfing part of a degenerating pre-terminal axon. X 40,000

Fig. 8-20 Higher magnification of the coated pit of fig. 8-19. X 83,000

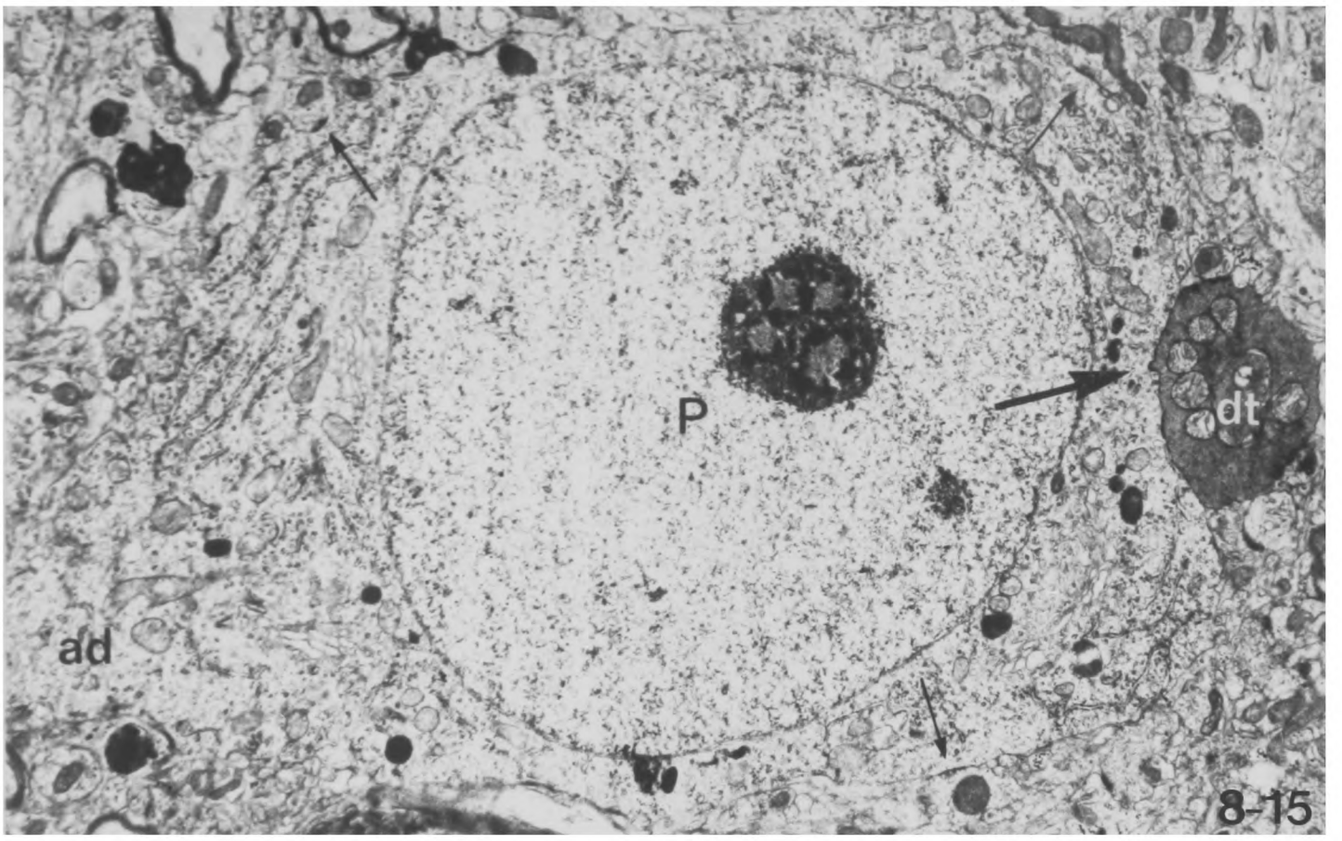
P
dt
ad
8-15

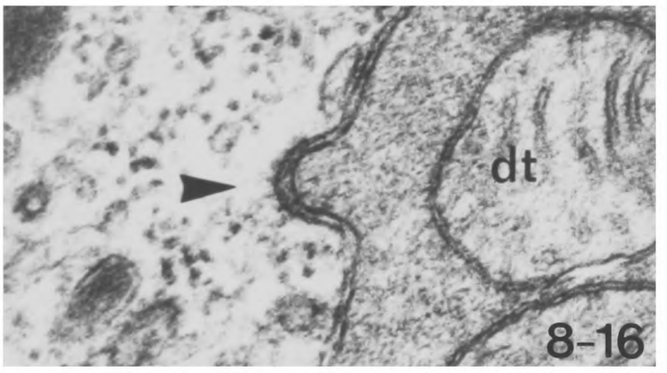
dt
8-16

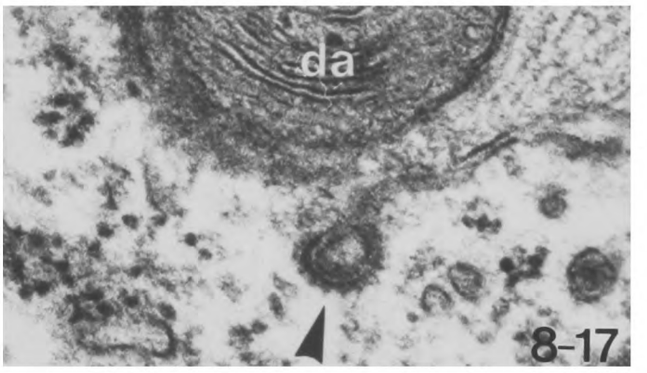
da
8-17

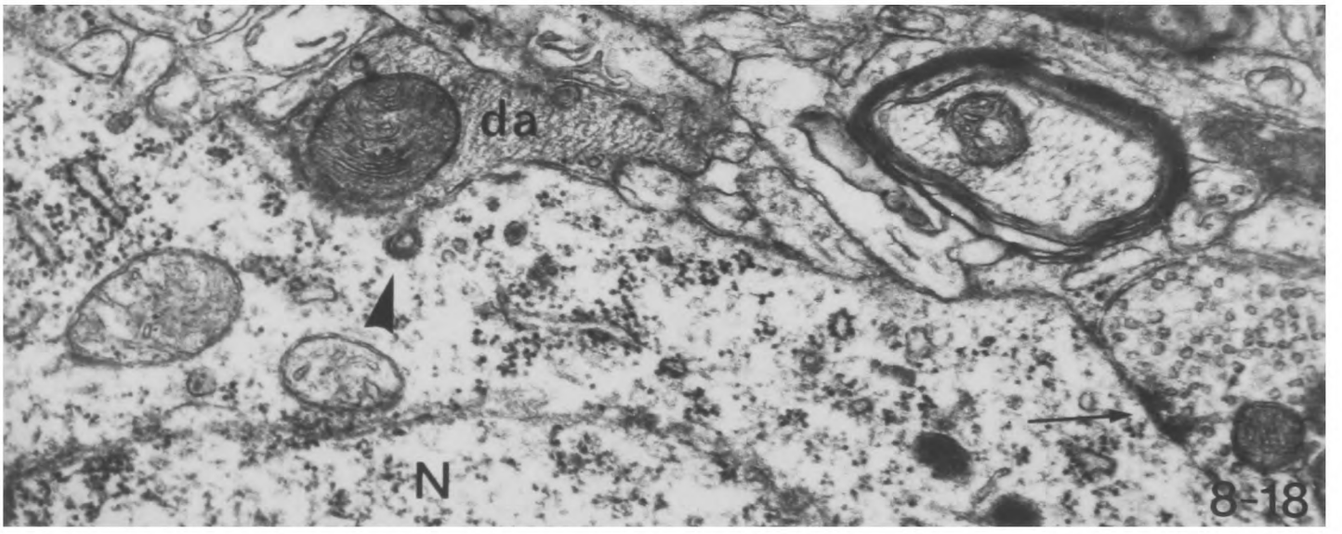
da
N
8-18

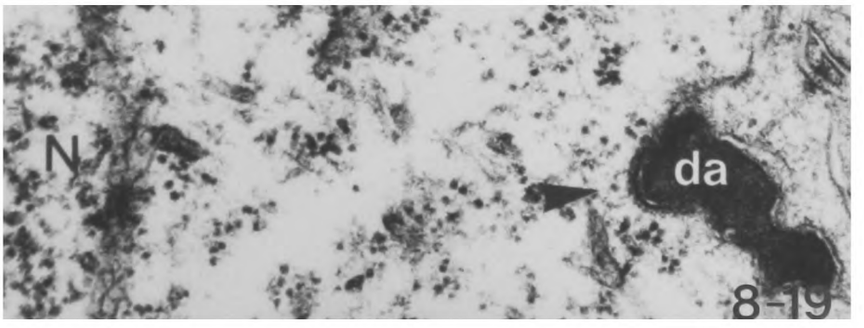
N
da
8-19

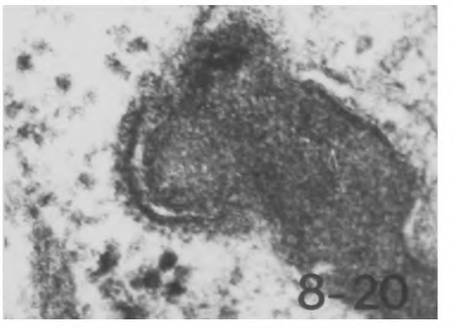
8-20

Fig. 8-21 A degenerating commissural axon terminal from the motor cortex. Note that there is only a thin sliver of degenerating cytoplasm apposed to the postsynaptic membrane specialisation of the lower spine and that both terminal and spines are engulfed by glia. X 52,000

Fig. 8-22 A degenerating commissural axon terminal from the motor cortex. Note that the cytoplasm of the axon terminal has become partially detached from the post-synaptic membrane specialisation of the left hand spine (arrowhead) and there appears to be an intervening tongue of glia cytoplasm. X 35,000

Fig. 8-23 A degenerating commissural axon terminal from the motor cortex synapsing on to a spine, which has an exposed postsynaptic membrane thickening on its other side (arrowhead). X 45,000

Fig. 8-24 A degenerating thalamo-cortical axon terminal from the motor cortex which synapses on to both sides of a spine. Note the thin tail of cytoplasm connecting the two parts of the axon terminal (arrowhead). X 32,000

Fig. 8-25 An exposed postsynaptic membrane thickening on dendrite d1 (arrowhead) has become apposed to another dendrite d2 which contains a subsurface cistern. This material was taken from the motor cortex 4 days after an ipsilateral Area 6 lesion. X 29,000

Fig. 8-26 Higher magnification of the exposed membrane thickening and subsurface cistern of fig. 8-25. Note the exposed postsynaptic thickening (arrowhead), the extracellular cleft material immediately adjacent to it and the dense material between the cistern and the plasma membrane of its dendrite. X 67,000

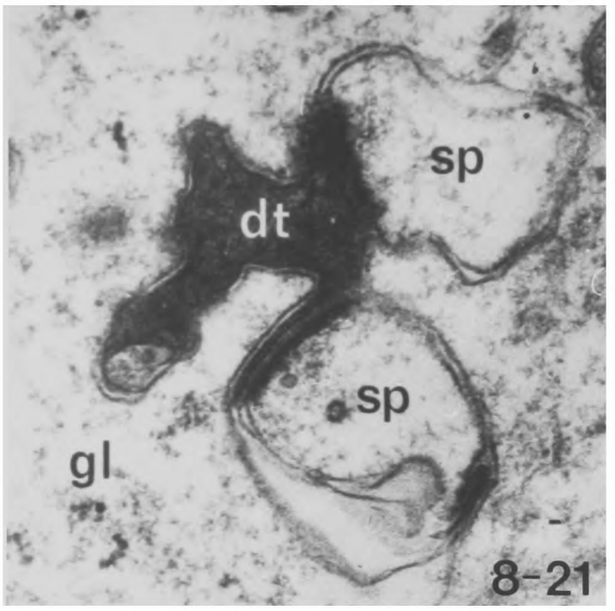

8-21

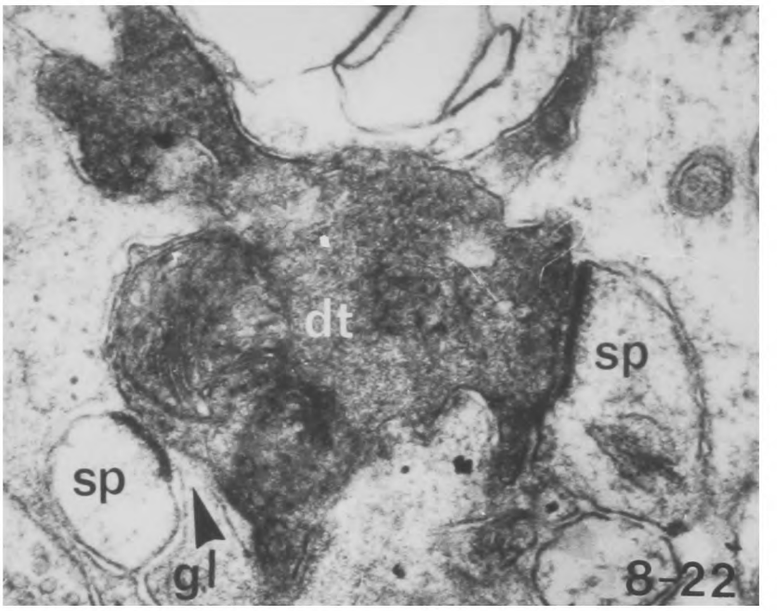

8-22

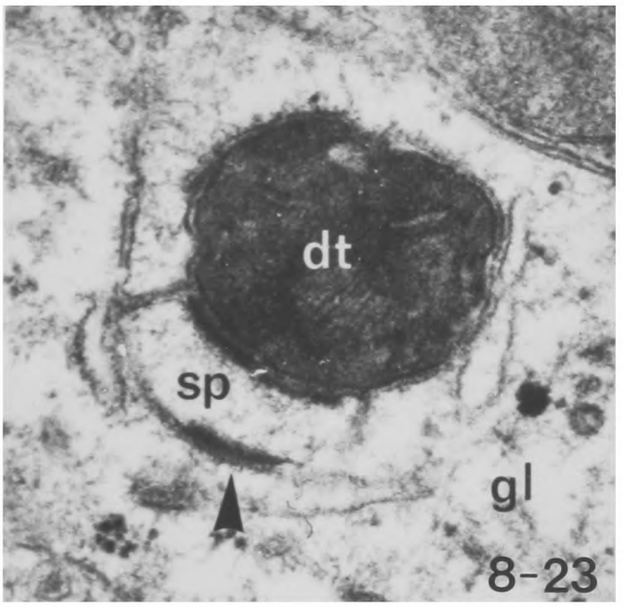

8-23

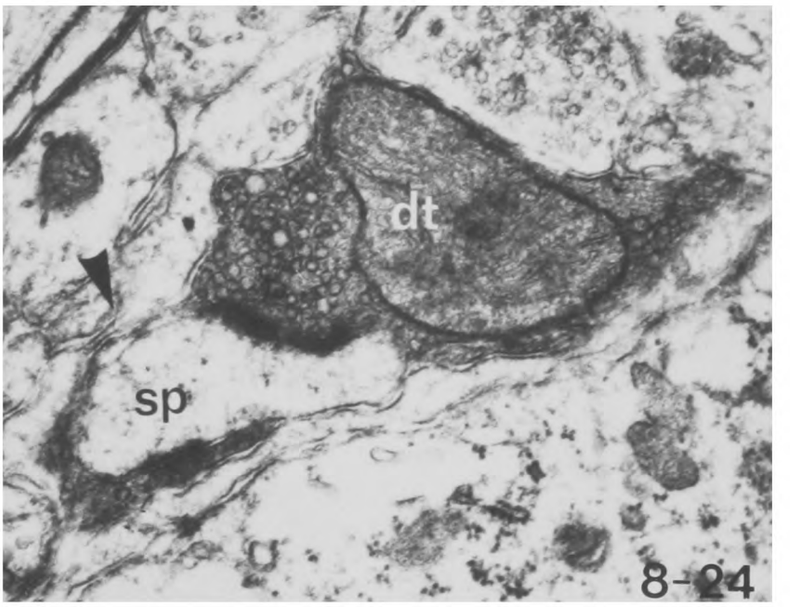

8-24

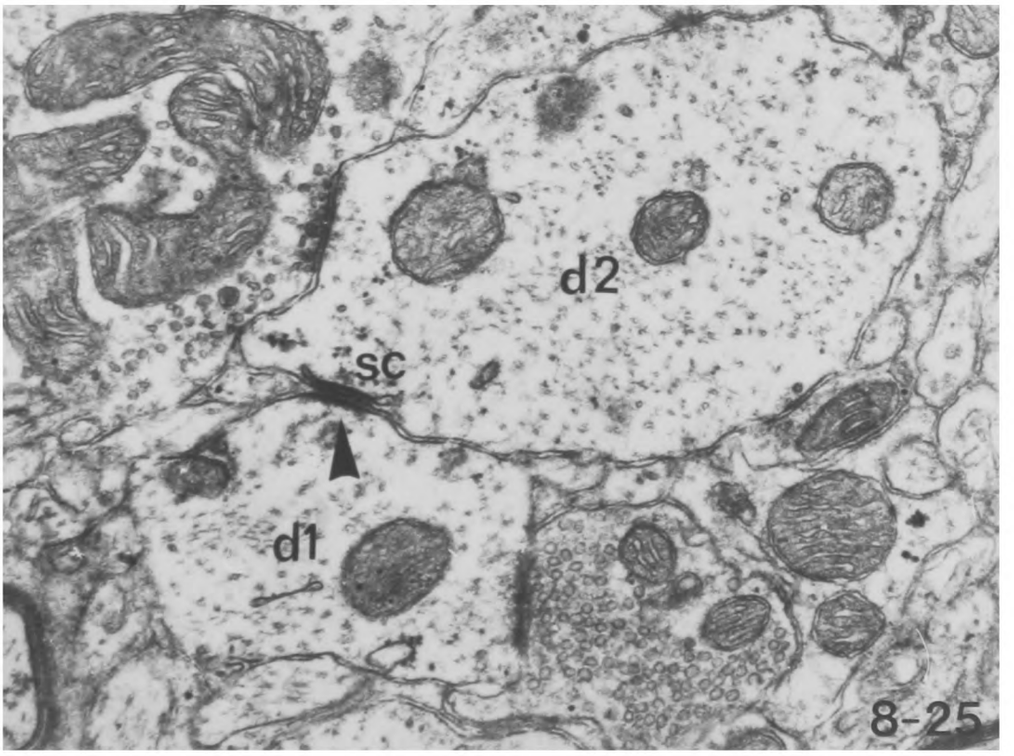

8-25

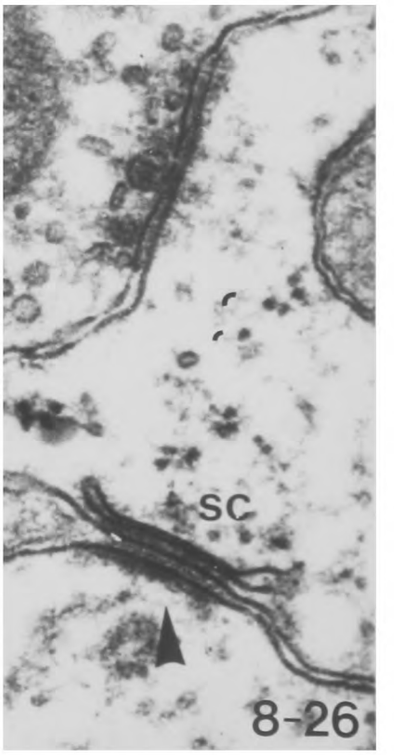

8-26

Fig. 8-27 An exposed asymmetric postsynaptic membrane thickening (arrow) on a spine containing a spine apparatus. The exposed thickening is apposed to a large dendrite which contains an immediately adjacent subsurface cistern. X 56,000

Fig. 8-28 An exposed symmetrical postsynaptic membrane thickening (arrow) on a dendrite. This has become apposed to the soma of a neuron and has a subsurface cistern immediately opposite itself. X 67,000

Fig. 8-29 An exposed asymmetric postsynaptic membrane thickening on a small profile, which is probably a spine (arrow). There is an apposed subsurface cistern in the adjacent dendrite. X 42,000

Fig. 8-30 An exposed asymmetric postsynaptic thickening on a dendrite (arrow) which has an immediately apposed subsurface cistern in the adjacent neuronal cell soma. X 42,000

Fig. 8-31 An exposed membrane thickening (arrow) on a dendrite is apposed to an unmyelinated axon in which there is a small subsurface cistern. This unmyelinated axon was the immediate continuation of an axon initial segment. X 30,000

Fig. 8-32 An exposed membrane thickening on a small dendrite (arrow) is adjacent to a large dendrite which contains an apposed subsurface cistern and an associated mitochondrion. X 39,000

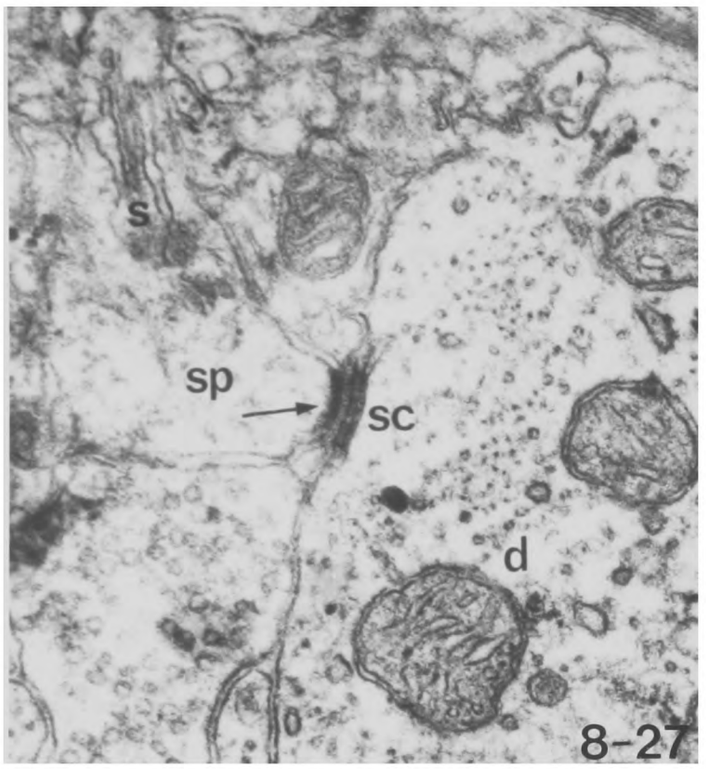
s
sp
sc
d
8-27

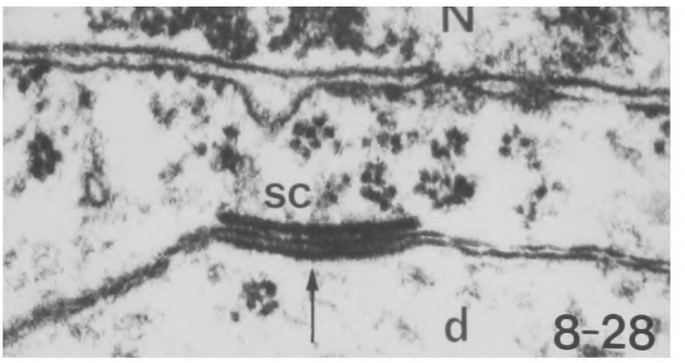
N
sc
d
8-28

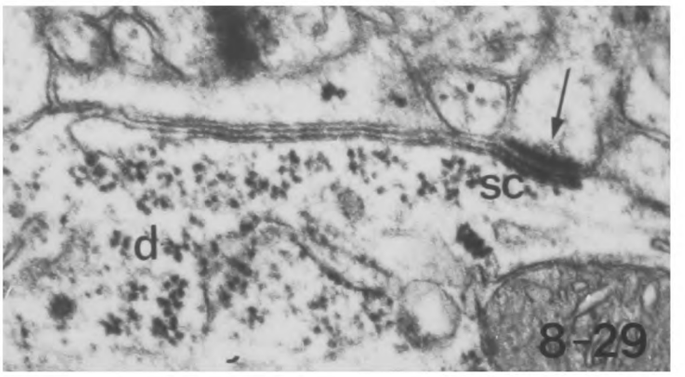
sc
d
8-29

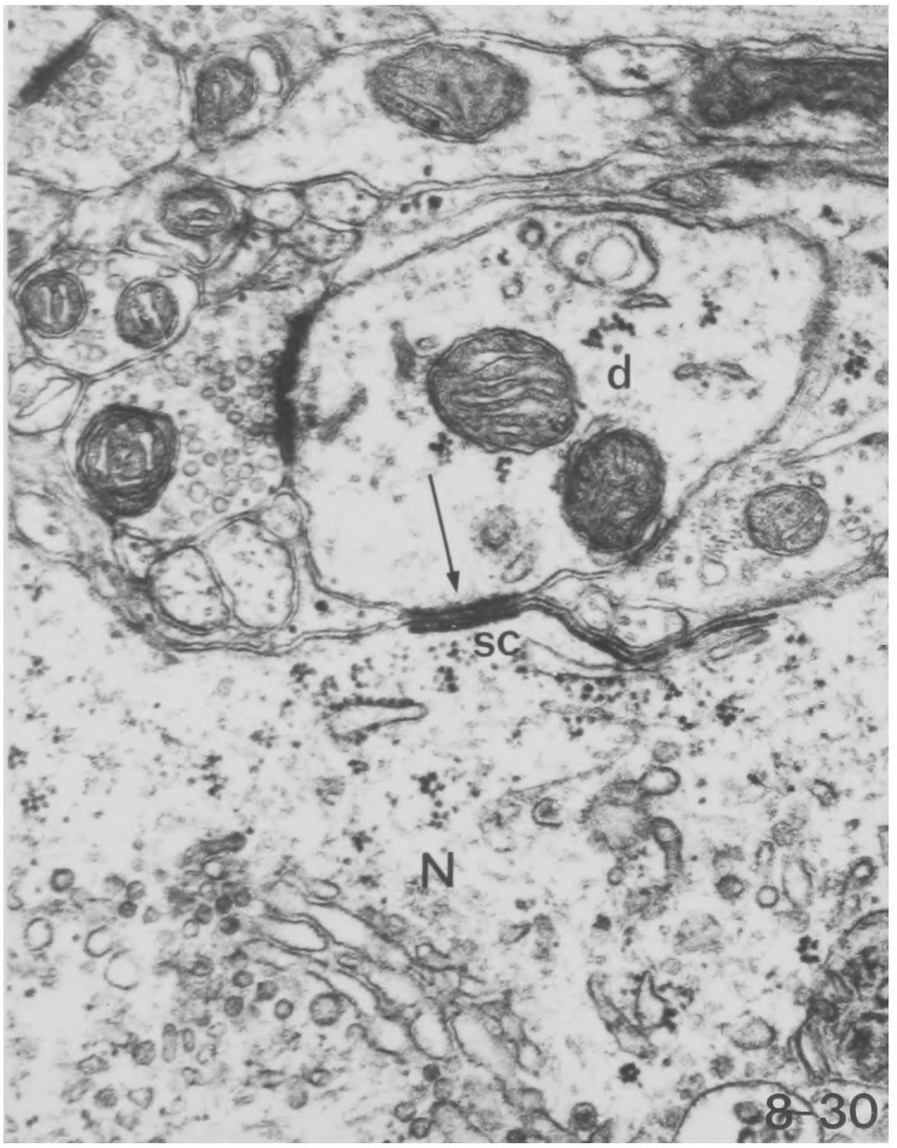
d
sc
N
8-30

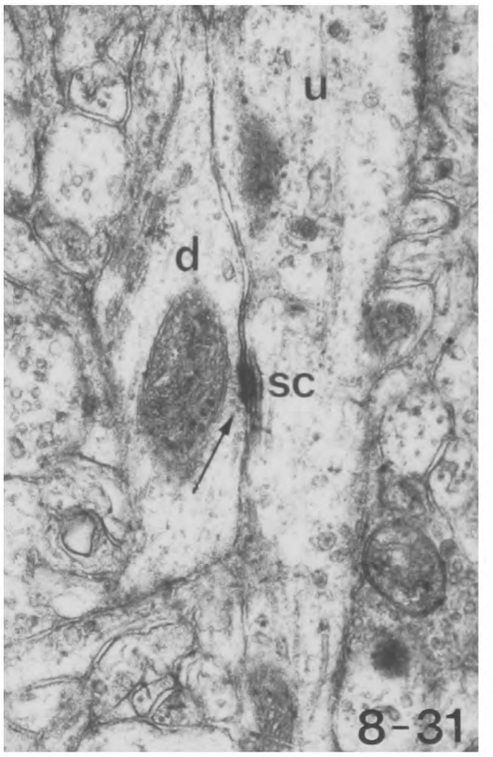
u
d
sc
8-31

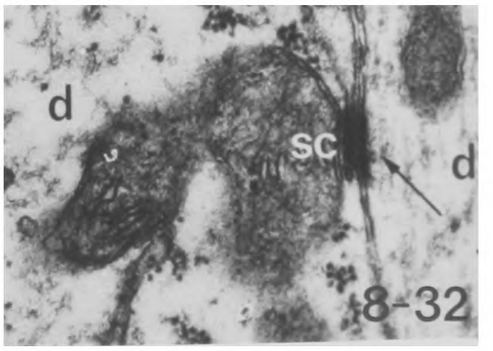
d
sc
d
8-32

Fig. 8-33 A large degenerating myelinated axon (da). Glial cell cytoplasm has invaded the myelin sheath and surrounds the degenerating axon. Note the gaps in the myelin through which the glial cytoplasm passes (arrows). X 11,300

Fig. 8-34 A degenerating commissural axon terminal in material block-stained with E-PTA. Note that the post-synaptic membrane specialisation (arrowhead), the cleft material and the cytoplasm of the degenerating terminal are stained but the plasma membranes are not. X 60,000

Fig. 8-35 A degenerating thalamo-cortical axon terminal which makes a synapse on to a spine in material block-stained with E-PTA. Note the spine apparatus. X 52,000

Fig. 8-36 A degenerating thalamo-cortical axon terminal with two separate specialisations (arrowheads) in material block-stained with E-PTA. X 52,000

Fig. 8-37 A late degenerating commissural axon terminal in material block-stained with E-PTA. Note the faint pale outline of the mitochondrion within the degenerating terminal. X 48,000

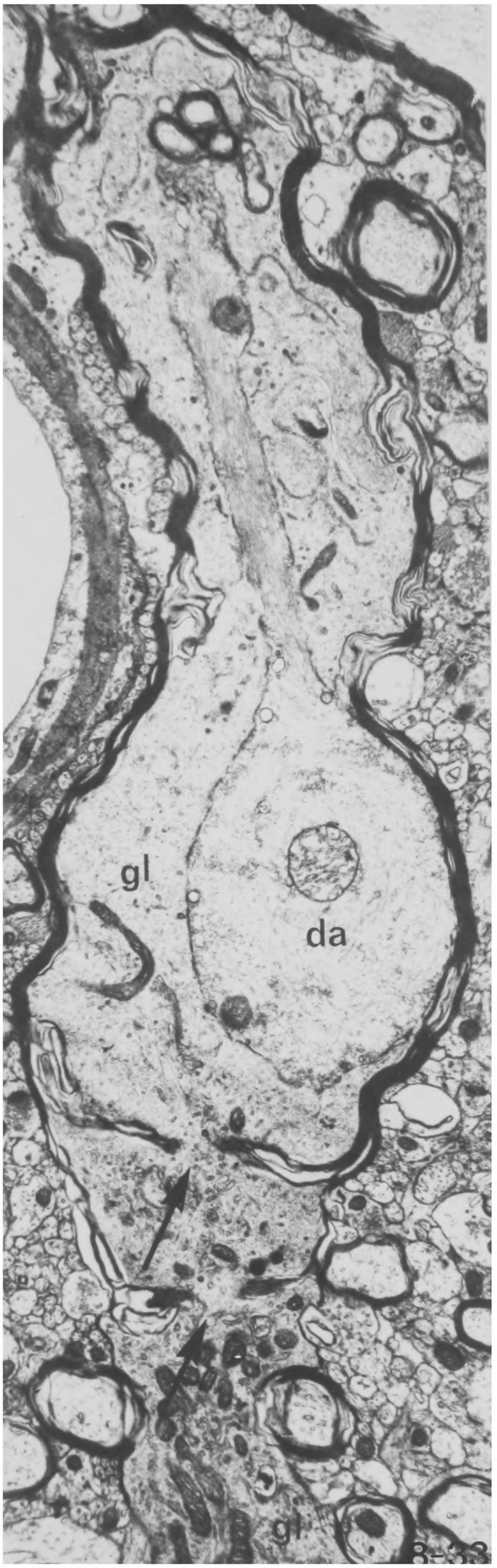
gl
da
gl

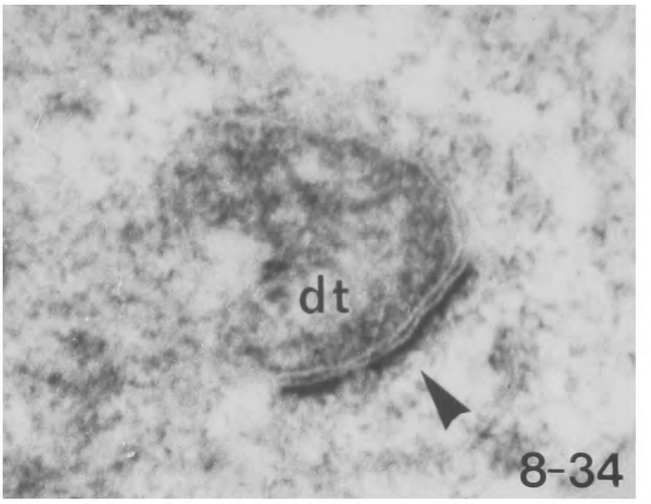
dt
8-34

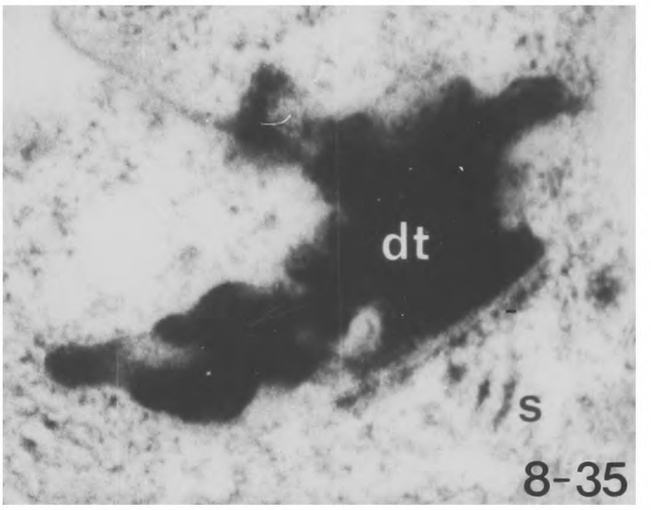
dt
s
8-35

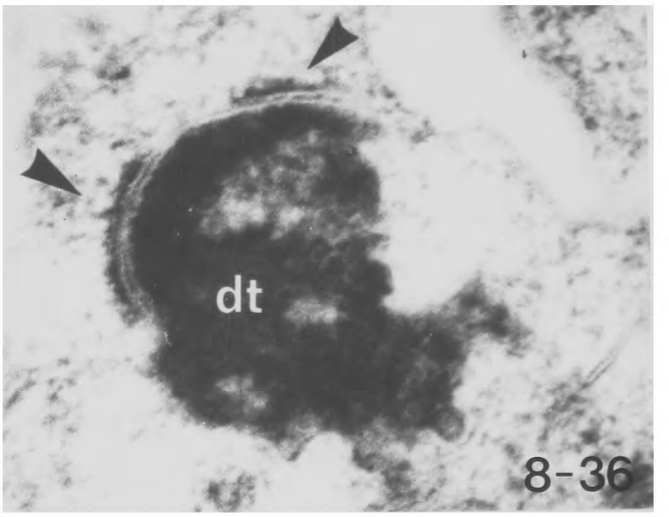
dt
8-36

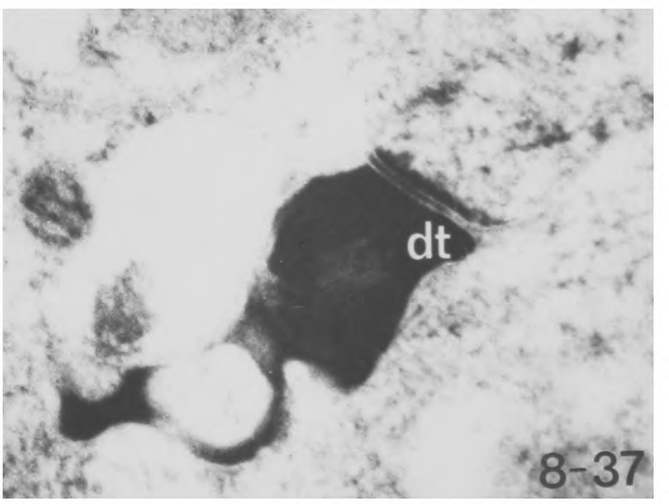
dt
8-37

Fig. 8-38 A degenerating commissural axon terminal in the motor cortex makes a synapse on to a spine.

X 40,400

Fig. 8-39 In an adjacent serial section to fig. 8-38 the spine receiving the synapse from the degenerating axon terminal can be seen to arise from the small dendrite d.

X 40,400

Fig. 8-40 A spine which appears to receive two synapses from degenerating thalamo-cortical axon terminals.

X 32,000

Fig. 8-41 The spine of fig. 8-40 in a serial section. The spine can now be seen to arise from a small dendrite. Other serial sections showed that both degenerating terminals of fig. 8-40 appear to be part of a single terminal which wrapped round the spine.

X 32,000

Fig. 8-42 A degenerating thalamo-cortical axon terminal which makes a synapse on to a spine and the shafts of two dendrites. A normal axon terminal t makes symmetrical synapses on to one of these dendrites and also on to an axon initial segment cut in transverse section.

X 29,000

8-38

8-39

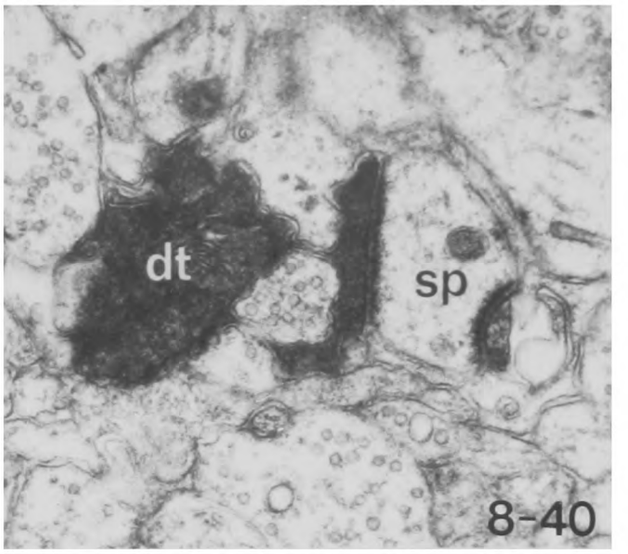

8-40

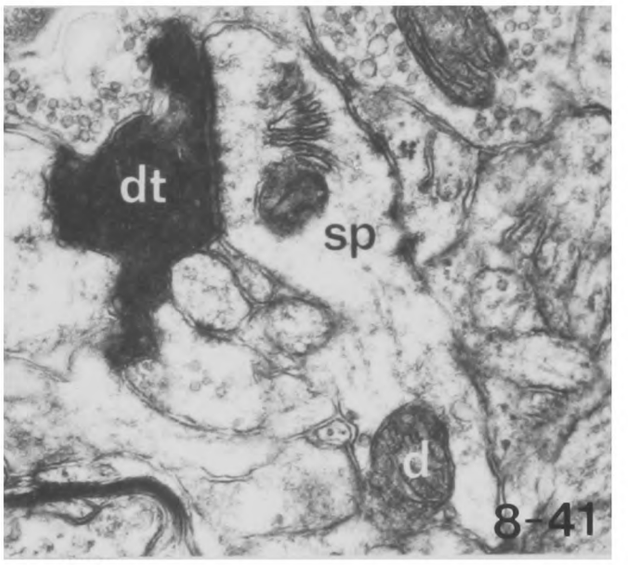

8-41

8-42

Fig. 8-43 A dark neuron from the same brain as the degenerating symmetrical-type axon terminal of figs. 8-47 to 8-50. From the number of synapses it receives and its abundant cytoplasm it can be identified as a large stellate cell.

X 6,700

Fig. 8-44 A dark dendrite. This can be identified as being of the large stellate type because of the large number of synapses it receives, of which a considerable proportion are of the asymmetric type.

X 21,000

Fig. 8-45 An intramitochondrial inclusion in a dark dendrite.

X 33,000

Fig. 8-46 A dark neuron at a late stage of degeneration showing extreme darkening, vacuolation, fragmentation and extensive glial reaction.

X 6,700

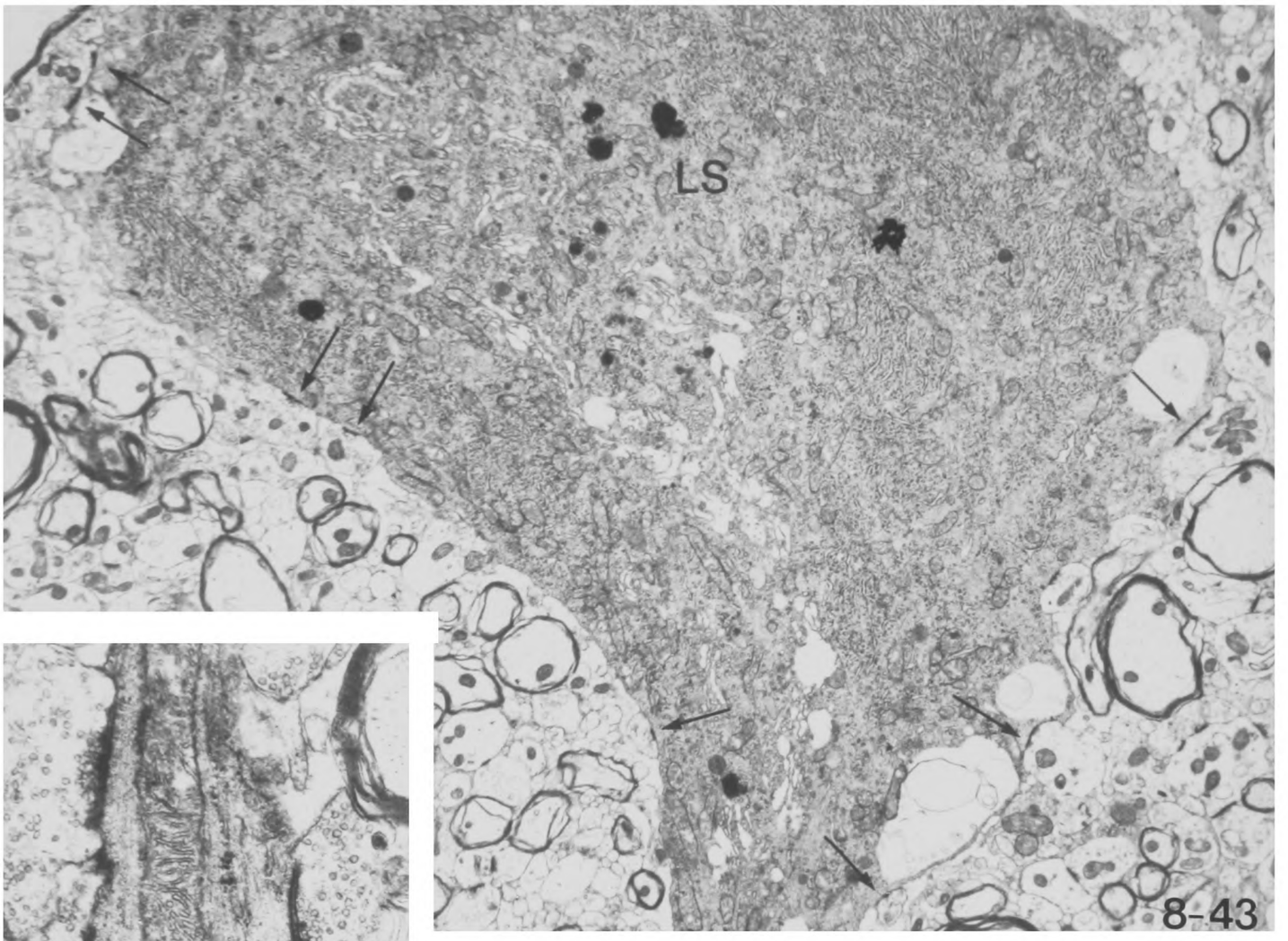

8-43

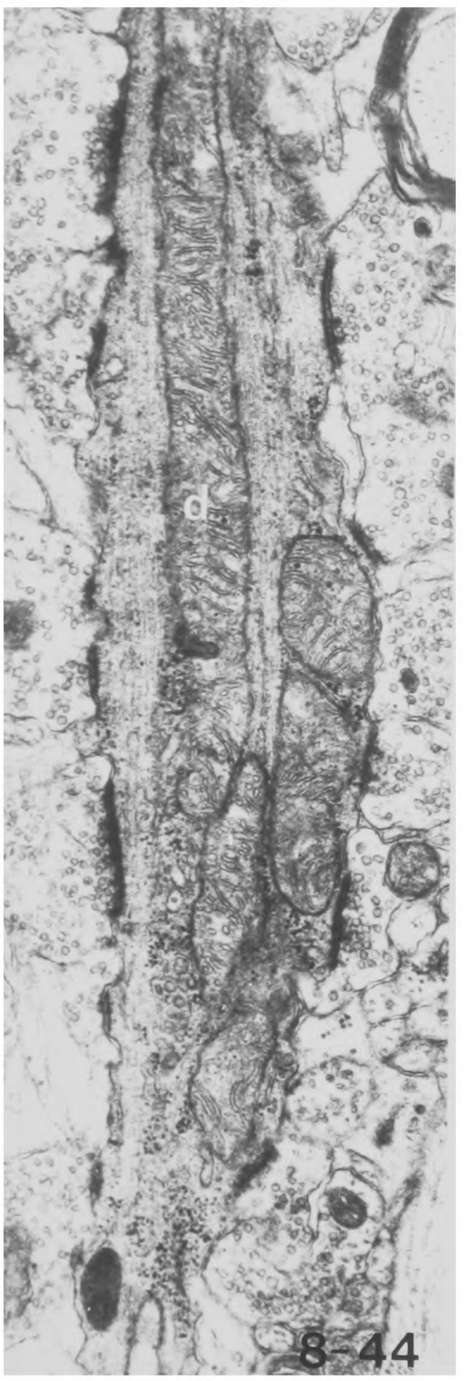

8-44

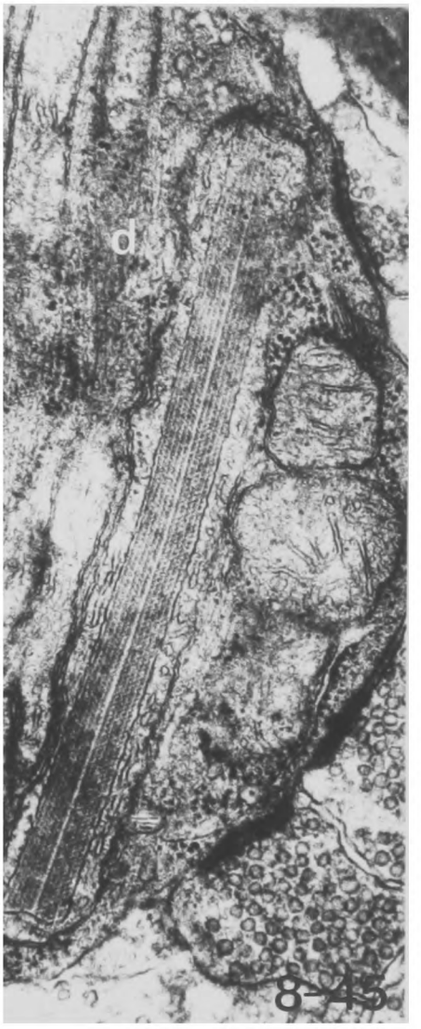

8-45

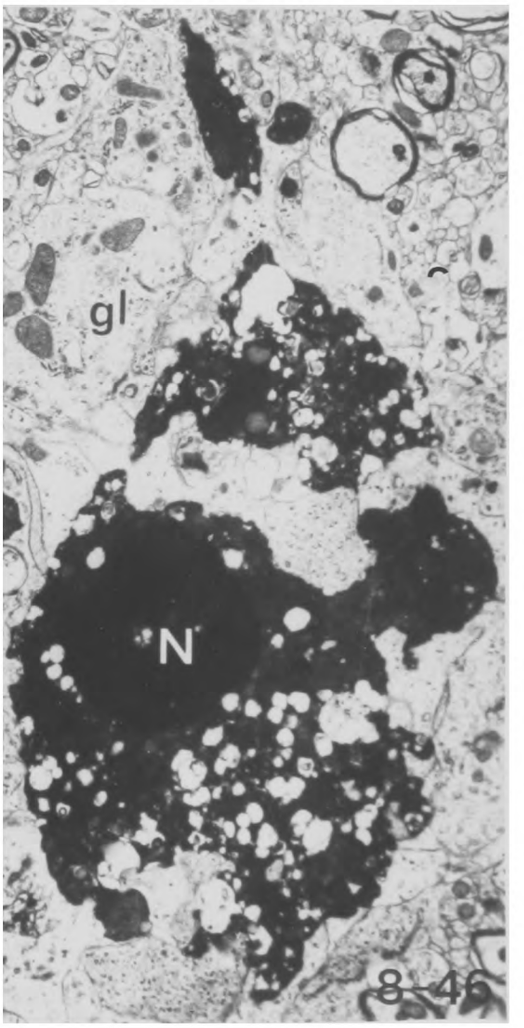

8-46

Fig. 8-47 A pyramidal cell soma in layer V of the motor cortex which receives a symmetrical synapse from a degenerating axon terminal (arrow).

X 7500

Fig. 8-48 Higher magnification of the degenerating axon terminal of fig. 8-47 showing it making a symmetrical synapse on to the cell soma. Serial sections confirmed that the postsynaptic membrane specialisation was consistently of the symmetrical type.

X 38,400

Fig. 8-49 A degenerating axon terminal making symmetrical synapses on to two spines, both of which also receive asymmetric synapses from normal axon terminals. The symmetrical nature of the synapses from the degenerating axon terminal was confirmed in serial sections.

X 29,000

Fig. 8-50 A degenerating axon terminal makes a symmetrical synapse on to a large dendrite. Serial sections again confirmed the symmetrical nature of the synapse.

X 18,000

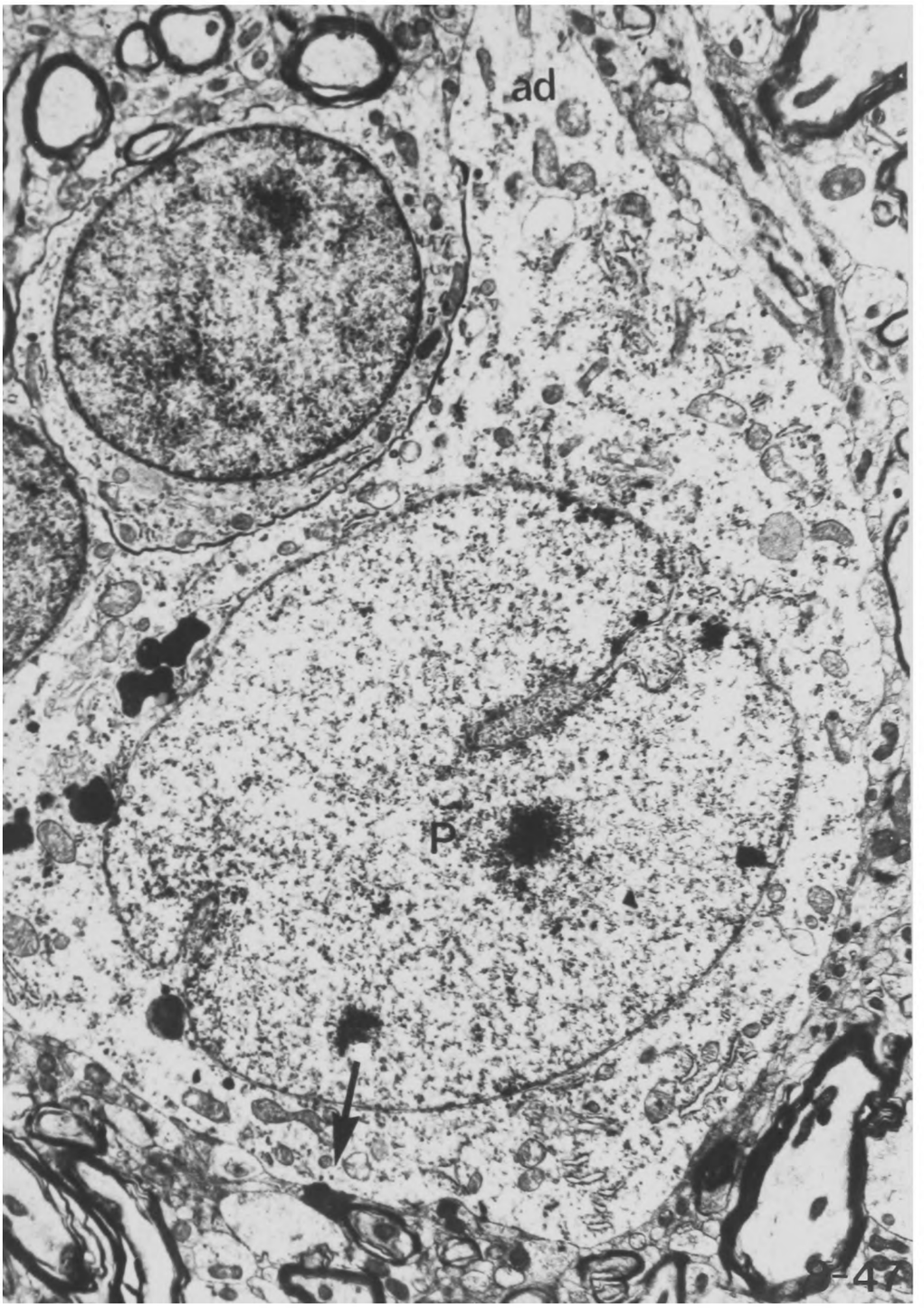

8-47

8-48

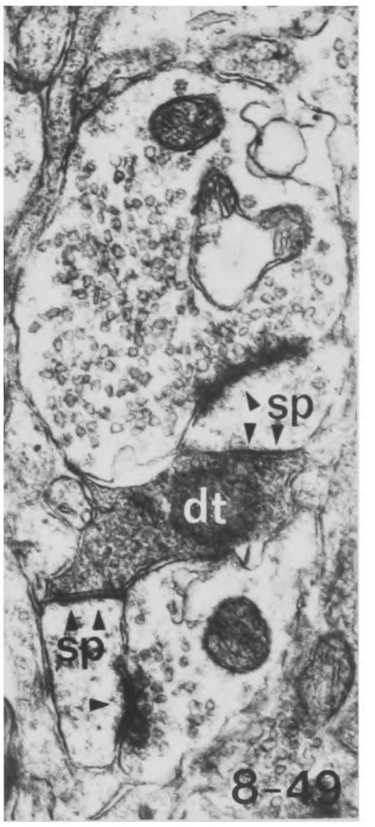

8-49

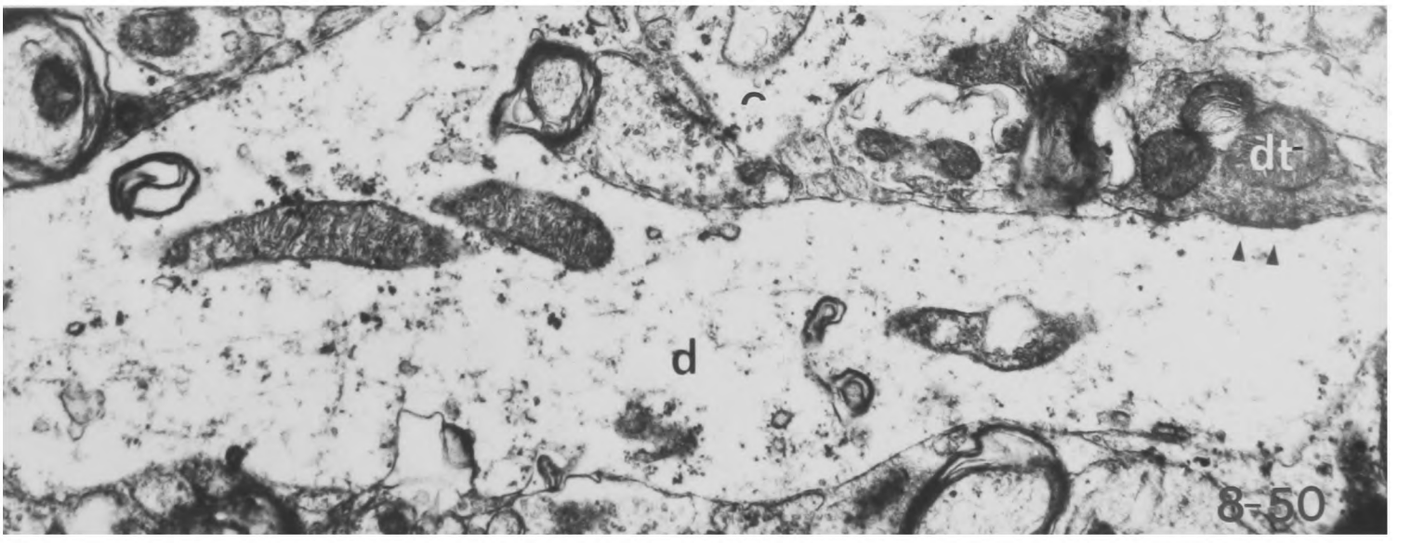

8-50

Illustrations to Chapter 9

AN EXPERIMENTAL ELECTRON MICROSCOPIC STUDY OF AFFERENT CONNECTIONS TO THE MOTOR AND SOMATIC SENSORY CORTICES

Figs. 9-1 to 9-7 Degenerating motor thalamo-cortical terminals making synapses on to spines.

Fig. 9-1 An early degenerating thalamo-cortical terminal in motor cortex making an en passage synapse on to a spine containing a spine apparatus.

X 29,000

Fig. 9-2 An early degenerating thalamo-cortical terminal in motor cortex making a synapse on to a spine. Note the glycogen and prominent neurofilaments in the terminal.

X 19,500

Fig. 9-3 A large early degenerating motor thalamo-cortical terminal making a synapse on to a spine. Note the irregularly swollen synaptic vesicles.

X 29,000

Fig. 9-4 A late degenerating thalamo-cortical terminal making a synapse on to a spine containing a spine apparatus in motor cortex. Note the glial engulfment.

X 48,000

Fig. 9-5 A late degenerating motor thalamo-cortical axon terminal making a synapse on to a spine and engulfed by glia. X 29,000

Fig. 9-6 An early degenerating motor thalamo-cortical terminal making en passage synapses on to two spines.

X 29,000

Fig. 9-7 A late degenerating motor thalamo-cortical terminal making synapses on to two spines and engulfed by glia. X 29,000

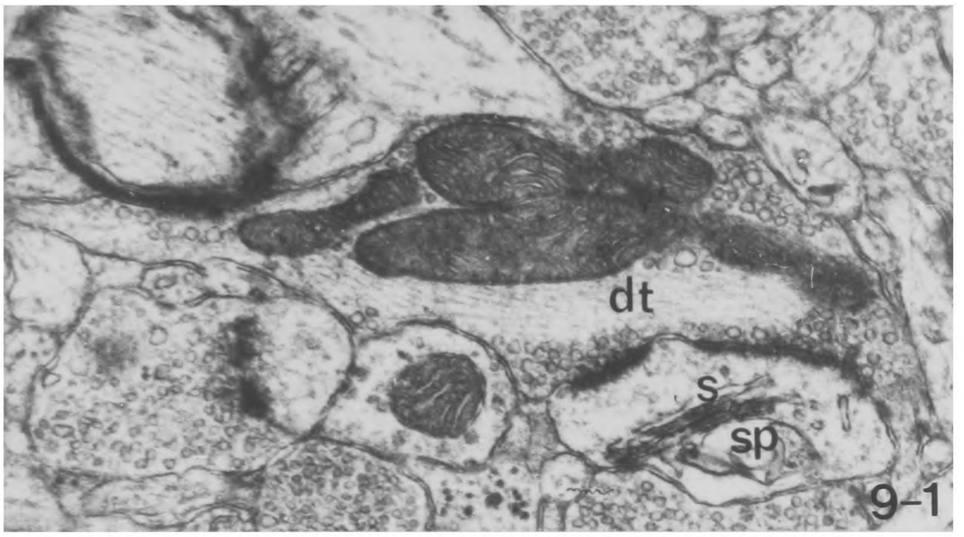

9-1

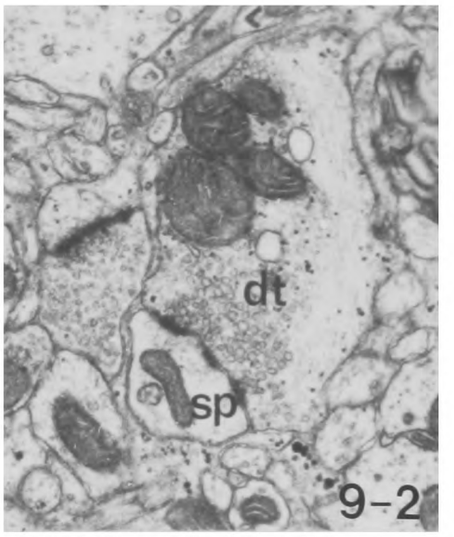

9-2

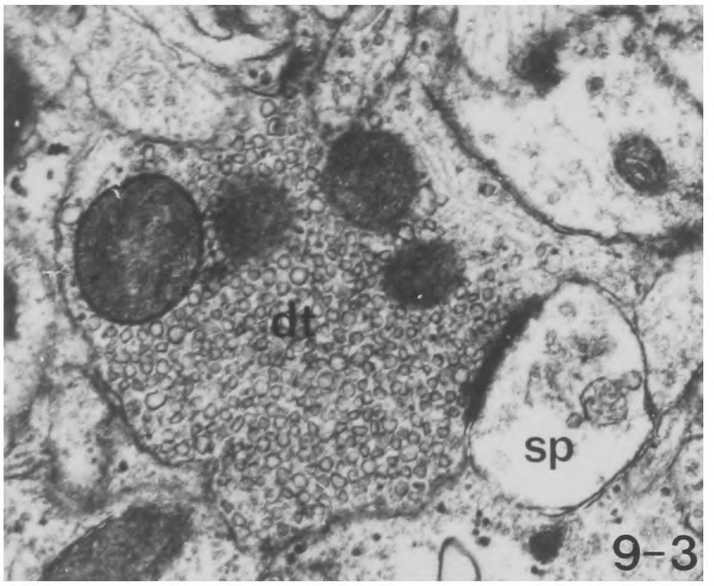

9-3

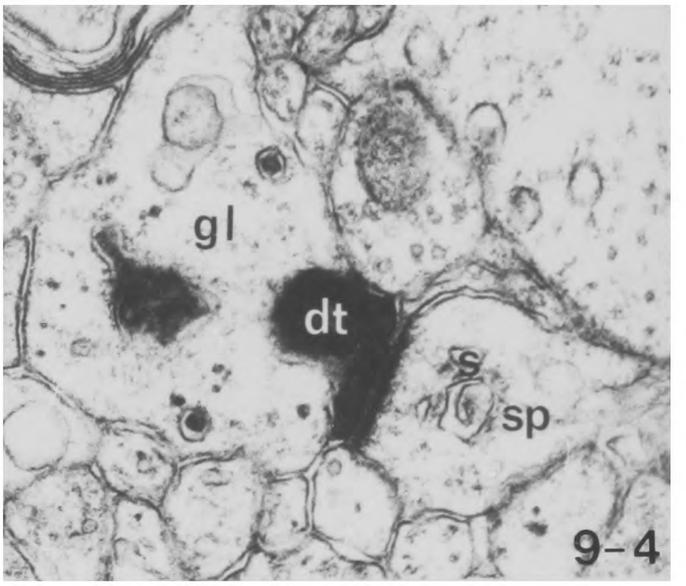

9-4

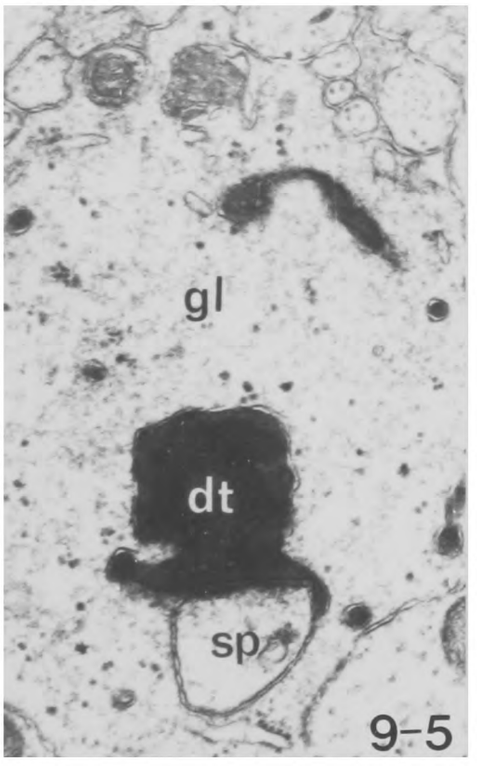

9-5

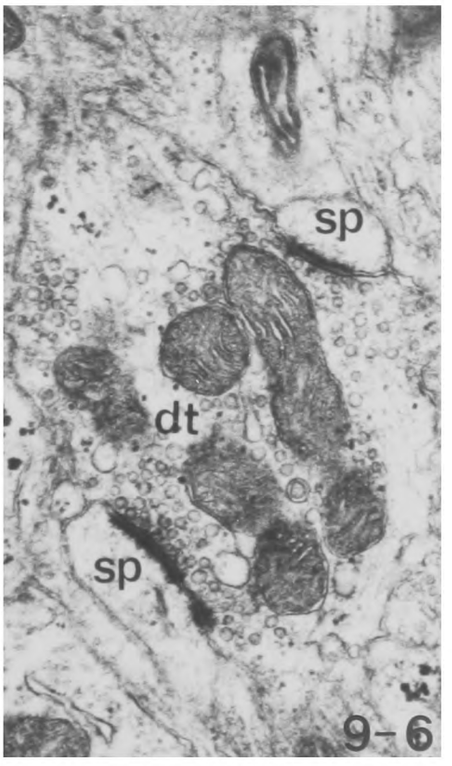

9-6

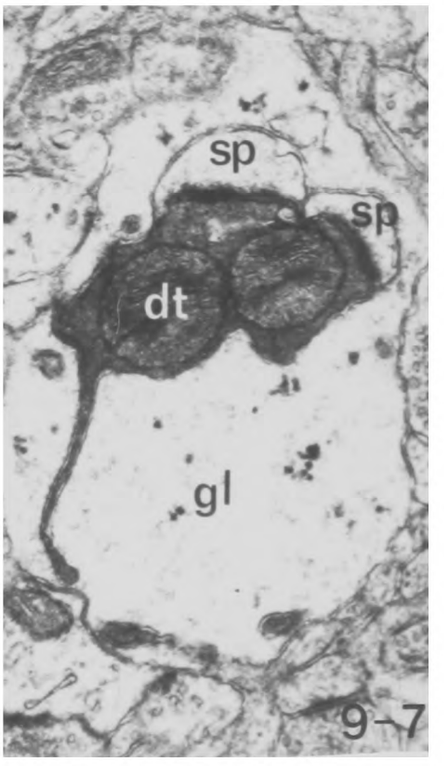

9-7

Fig. 9-8 A degenerating thalamo-cortical terminal in the motor cortex making a synapse on to a spine which also receives a synapse from a normal axon terminal t and which is cut in continuity with its parent dendrite. Note the large diameter of the parent dendrite and the lack of other synapses on to it. X 29,000

Fig. 9-9 A degenerating thalamo-cortical terminal in motor cortex making a synapse on to a spine which also receives an asymmetric synapse from a normal axon terminal. X 46,000

Fig. 9-10 A degenerating thalamo-cortical terminal in motor cortex making a synapse on to a spine which also receives a symmetrical synapse. X 46,000

Fig. 9-11 A degenerating thalamo-cortical terminal in the motor cortex making a synapse on to a spine which contains a spine apparatus and which is cut in continuity with the parent dendrite. Note the small diameter of the parent dendrite and the lack of synapses on its shaft. X 29,000

Fig. 9-12 A degenerating thalamo-cortical terminal from the motor cortex which makes a synapse both with a spine and the shaft of a dendrite. X 29,000

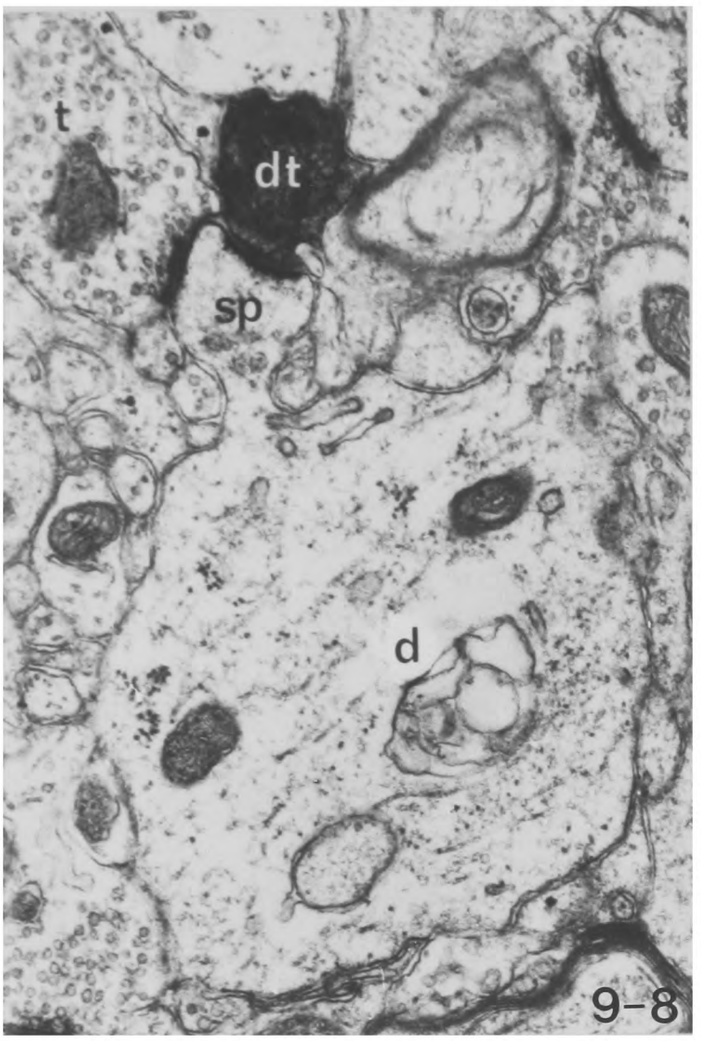

9-8

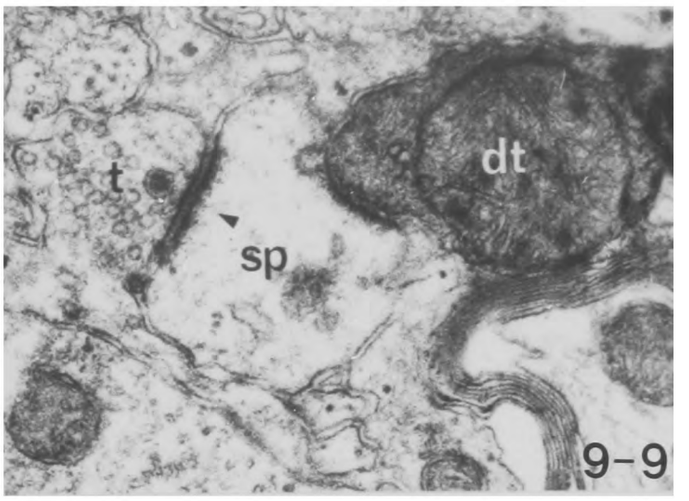

9-9

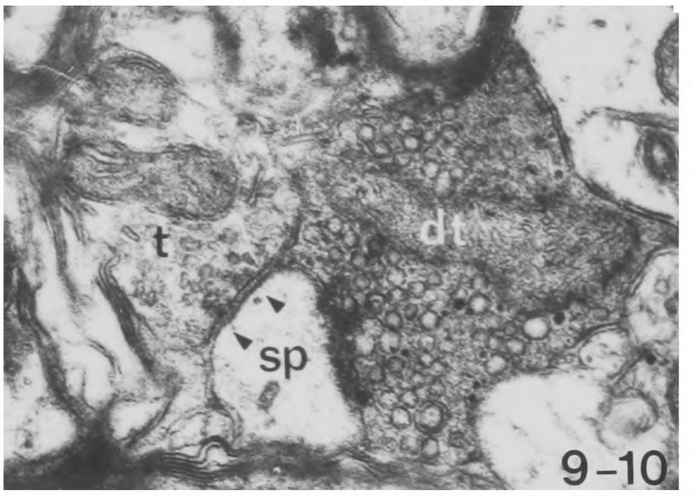

9-10

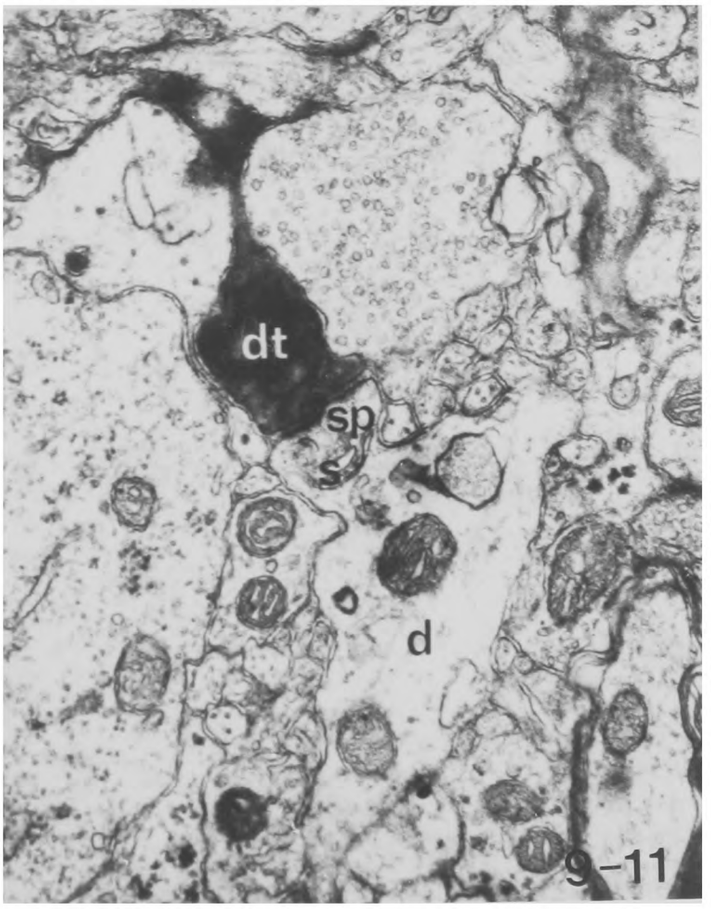

9-11

9-12

Figs. 9-13 to 9-16 Thalamo-cortical to somatic sensory cortex.

Fig. 9-13 An early degenerating thalamo-cortical axon terminal making a synapse on to a spine in area 3b of the somatic sensory cortex. Note the irregularly swollen vesicles and the glycogen in the axon terminal. X 29,000

Fig. 9-14 A late degenerating thalamo-cortical terminal making a synapse on to a spine in area 3b of the somatic sensory cortex. Note its engulfment by glia and the coated pit being formed (arrowhead). X 29,000

Fig. 9-15 A degenerating thalamo-cortical axon terminal which makes a synapse on to a spine cut in continuity with its parent dendrite in the somatic sensory cortex. X 48,000

Fig. 9-16 A degenerating thalamo-cortical terminal which makes a synapse on to two spines in the somatic sensory cortex. One of these spines also receives a symmetrical synapse from normal axon terminal containing flattened vesicles. X 32,000

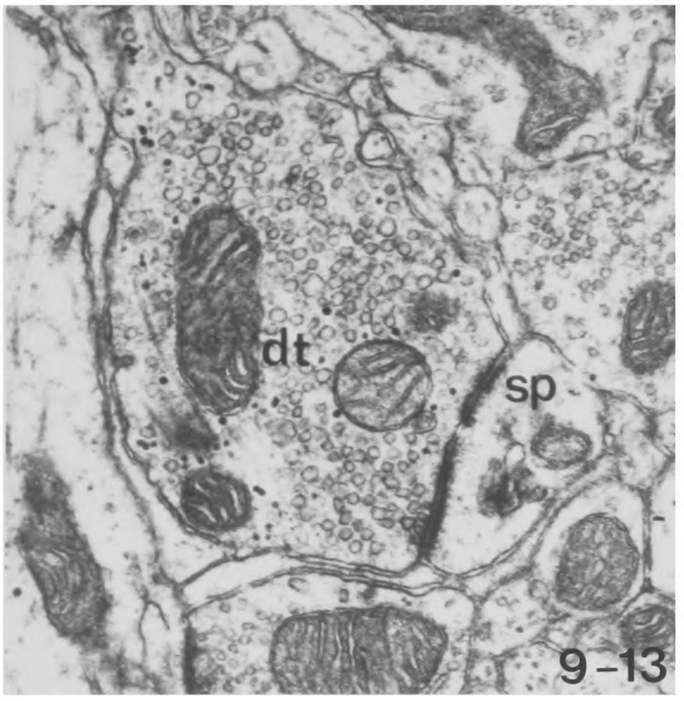
dt
sp
9-13

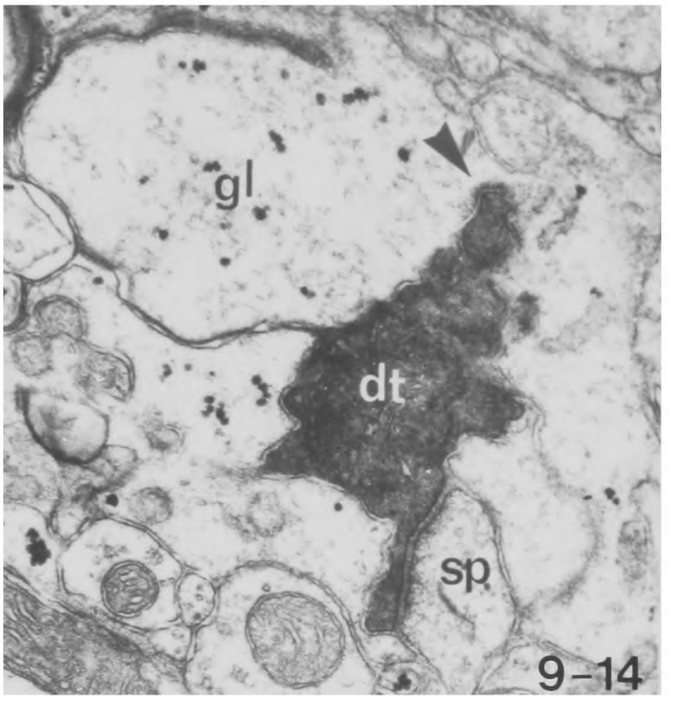
gl
dt
sp
9-14

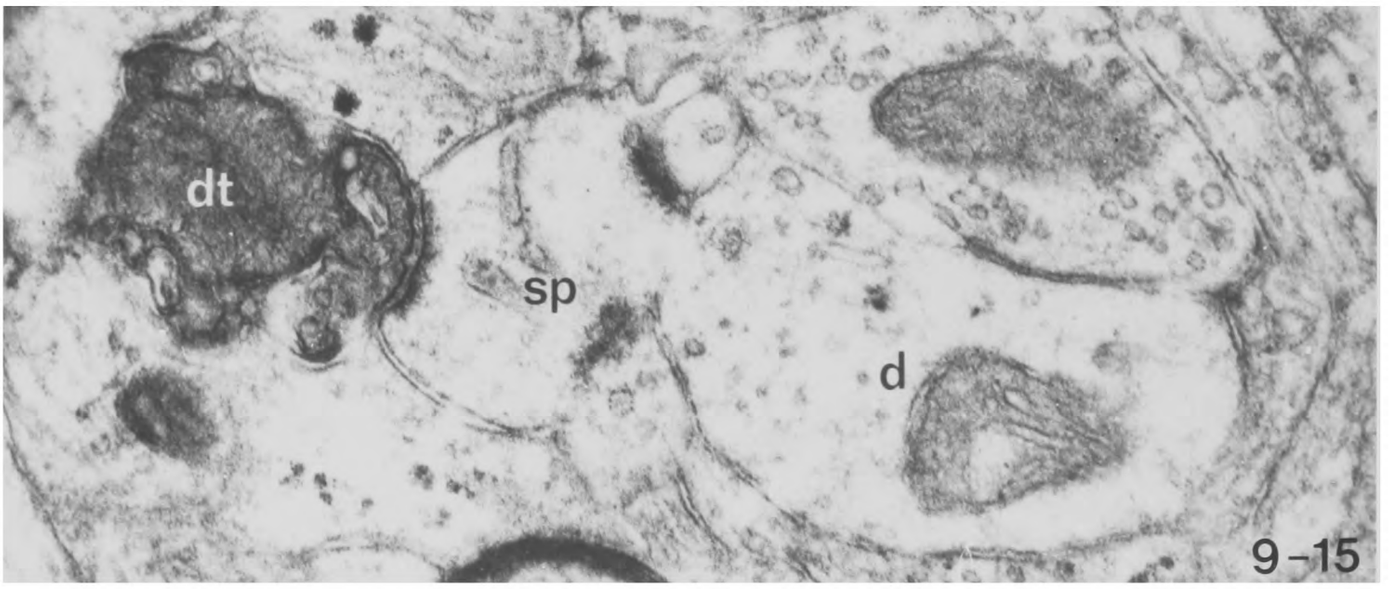
dt
sp
d
9-15


dt
t
sp
sp
d
9-16

Fig. 9-17 A large dendrite in layer IV of the motor cortex which receives synapses from two degenerating thalamo-cortical terminals. Note the large number of other synapses received by the dendrite and the high concentration of organelles within it. The dendrite was traced into continuity with a typical large stellate cell soma which itself received a synapse from a degenerating thalamo-cortical terminal.

X 8,400

Fig. 9-18 Higher magnification of the lower degenerating thalamo-cortical terminal of fig. 9-17.

X 29,000

Fig. 9-19 A degenerating thalamo-cortical axon terminal which makes a synapse on to the shaft of a dendrite. Note the large number of other synapses received by the dendrite, one of which is clearly asymmetric, and the high concentration of organelles in its cytoplasm.

X 29,000

Fig. 9-20 A late degenerating thalamo-cortical axon terminal which makes a synapse on to the shaft of a dendrite. Note the other asymmetric synapse received by the dendrite.

X 29,000

9-17

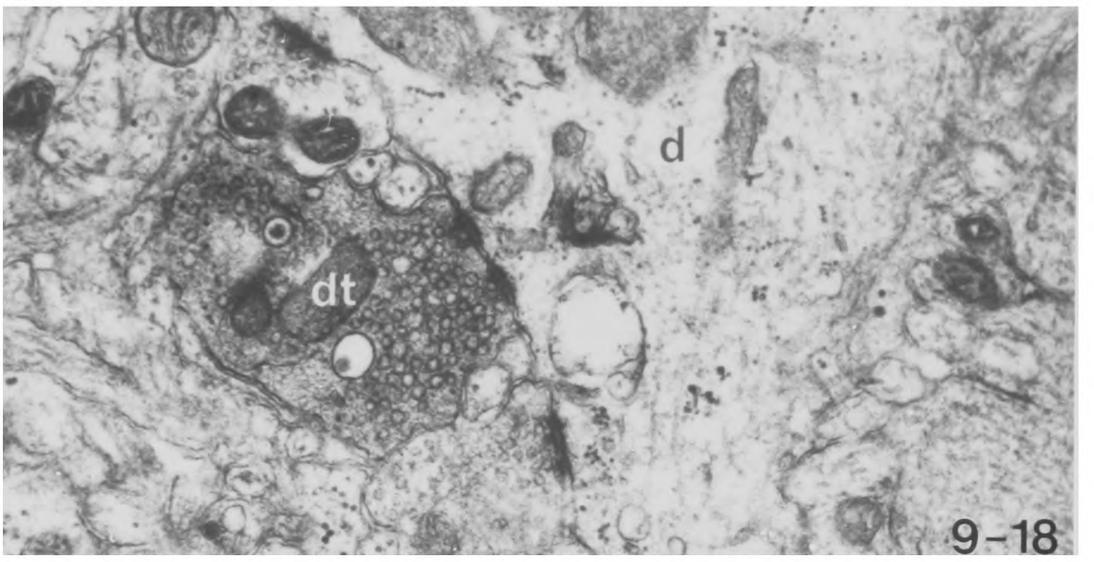

9-18

9-19

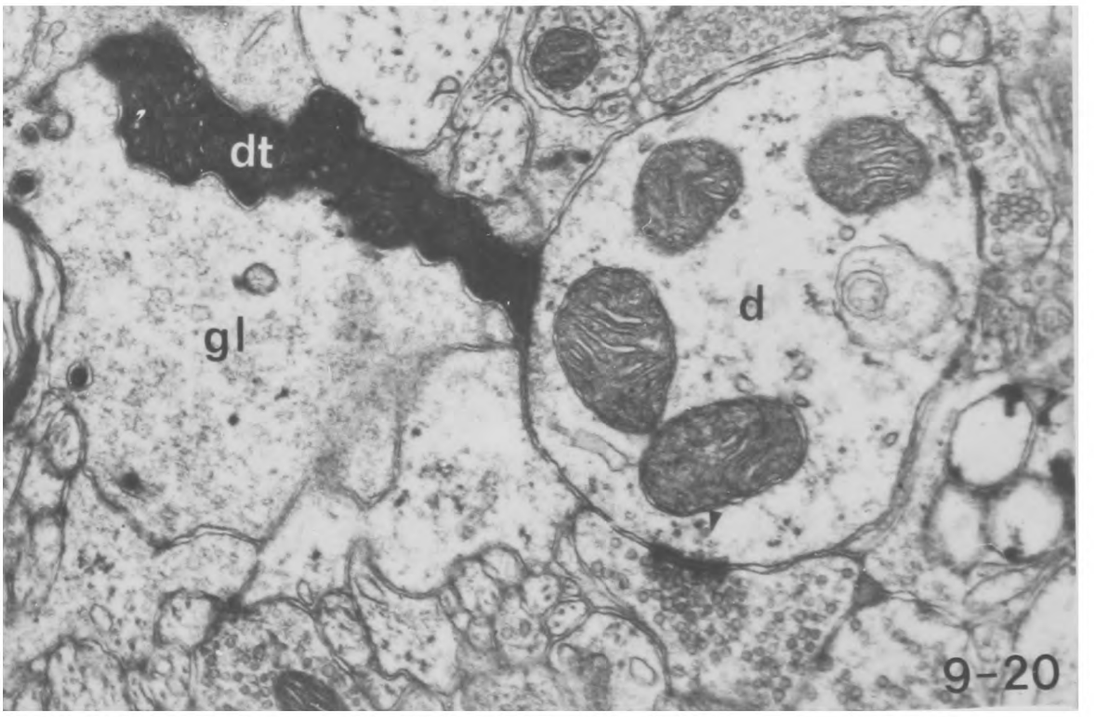

9-20

Fig. 9-21 A degenerating thalamo-cortical axon terminal which makes an en passage synapse on to a dendrite in the somatic sensory cortex. Note the large size of the dendrite and the other synapses it receives, one of which is clearly of the asymmetric type.

X 29,000

Fig. 9-22 A degenerating thalamo-cortical terminal which makes a synapse on to a very large vertically running dendrite at the base of a side branch in layer IV of somatic sensory cortex. This dendrite is probably the apical dendrite of a pyramidal cell in layer V.

X 8,400

Fig. 9-23 Higher magnification of the degenerating thalamo-cortical terminal of fig. 9-22.

X 29,000

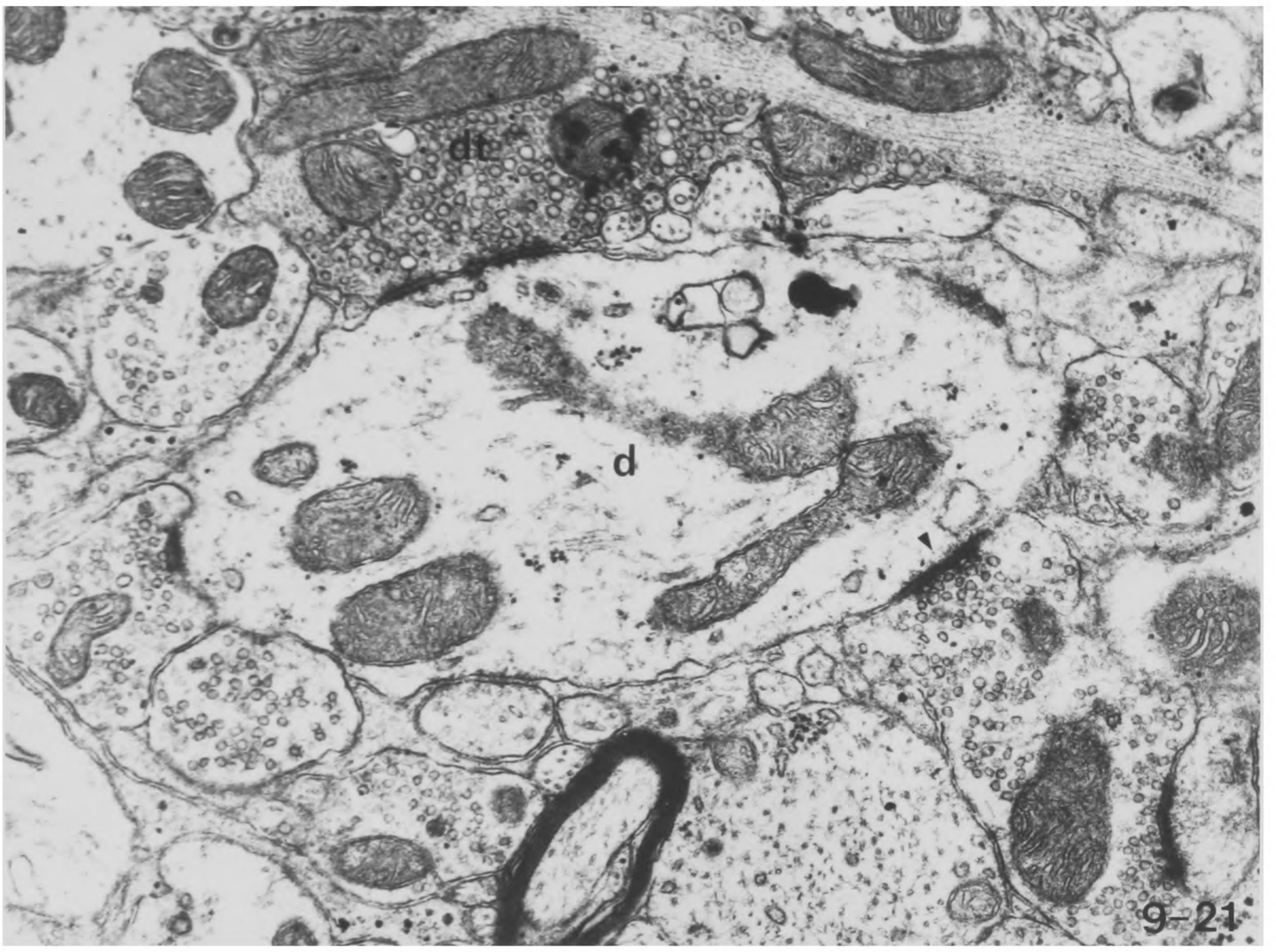
dt
d
9-21

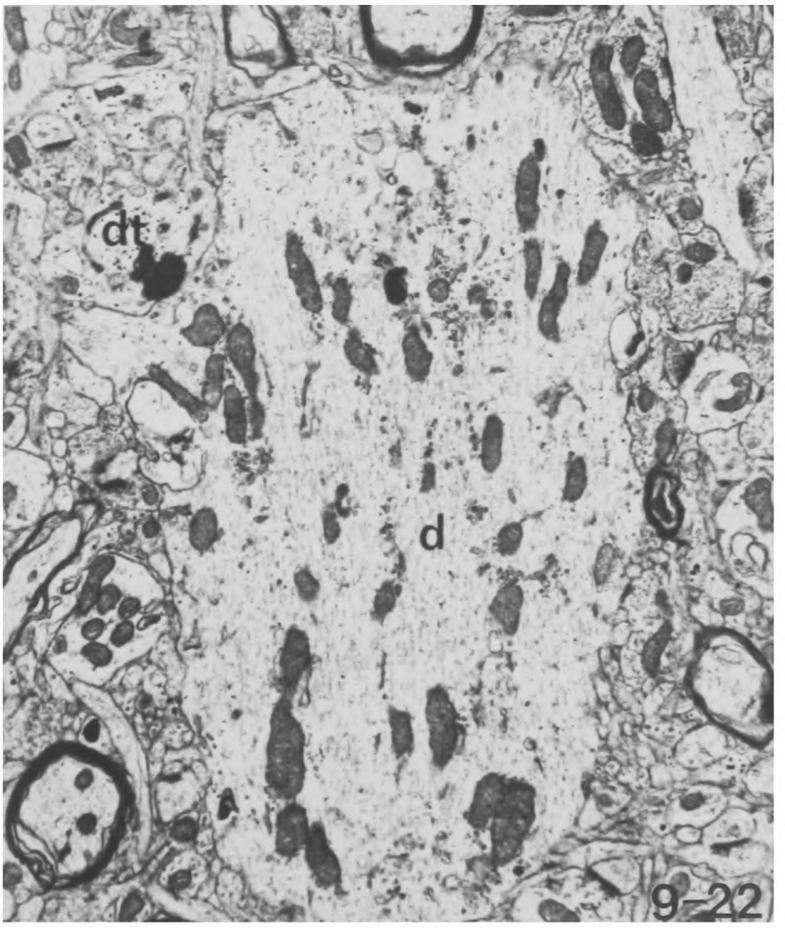
dt
d
9-22


gl
dt
9-23

Fig. 9-24 A degenerating thalamo-cortical axon terminal which makes an axo-somatic synapse on to a large stellate cell in layer IV of the motor cortex. Note the large number of other synapses received by the cell soma and its abundant cytoplasm full of organelles.

X 8,400

Fig. 9-25 Higher magnification of the degenerating thalamo-cortical terminal of fig. 9-24.

X 29,000

Fig. 9-26 A degenerating thalamo-cortical axon terminal making an axo-somatic synapse on to part of a large stellate cell soma. This large stellate cell received 8 normal axo-somatic synapses in the same section.

X 29,000

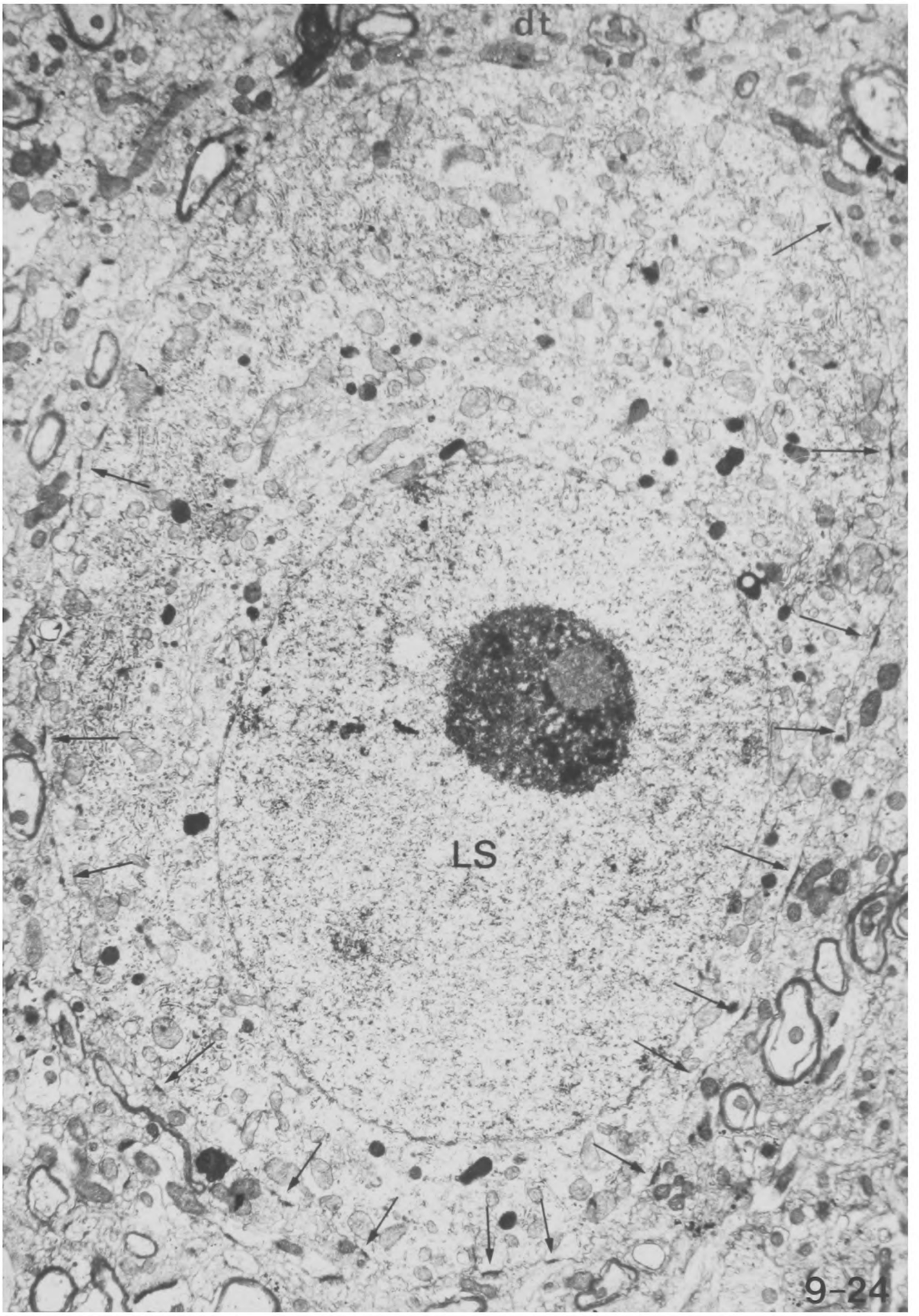

9-24

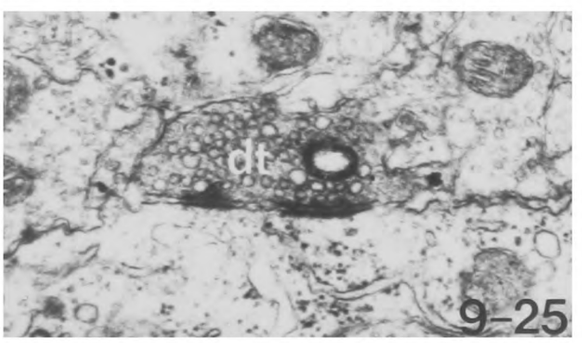

9-25

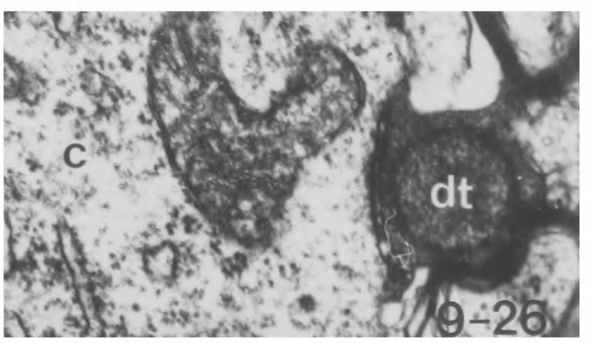

9-26

Fig. 9-27 Histograms showing the distributions of the mean cell diameters and numbers of synapses received per cell profile for all those cell somata found to receive axosomatic synapses from degenerating thalamo-cortical axon terminals in the motor cortex. These distributions correspond to those of the large stellate cell population (Figs. 4-36 and 4-43).

MEAN DIAMETERS AND NUMBERS OF SYNAPSES RECEIVED BY CELL SOMATA RECEIVING DEGENERATING THALAMO-CORTICAL TERMINALS. IN THE MOTOR CORTEX

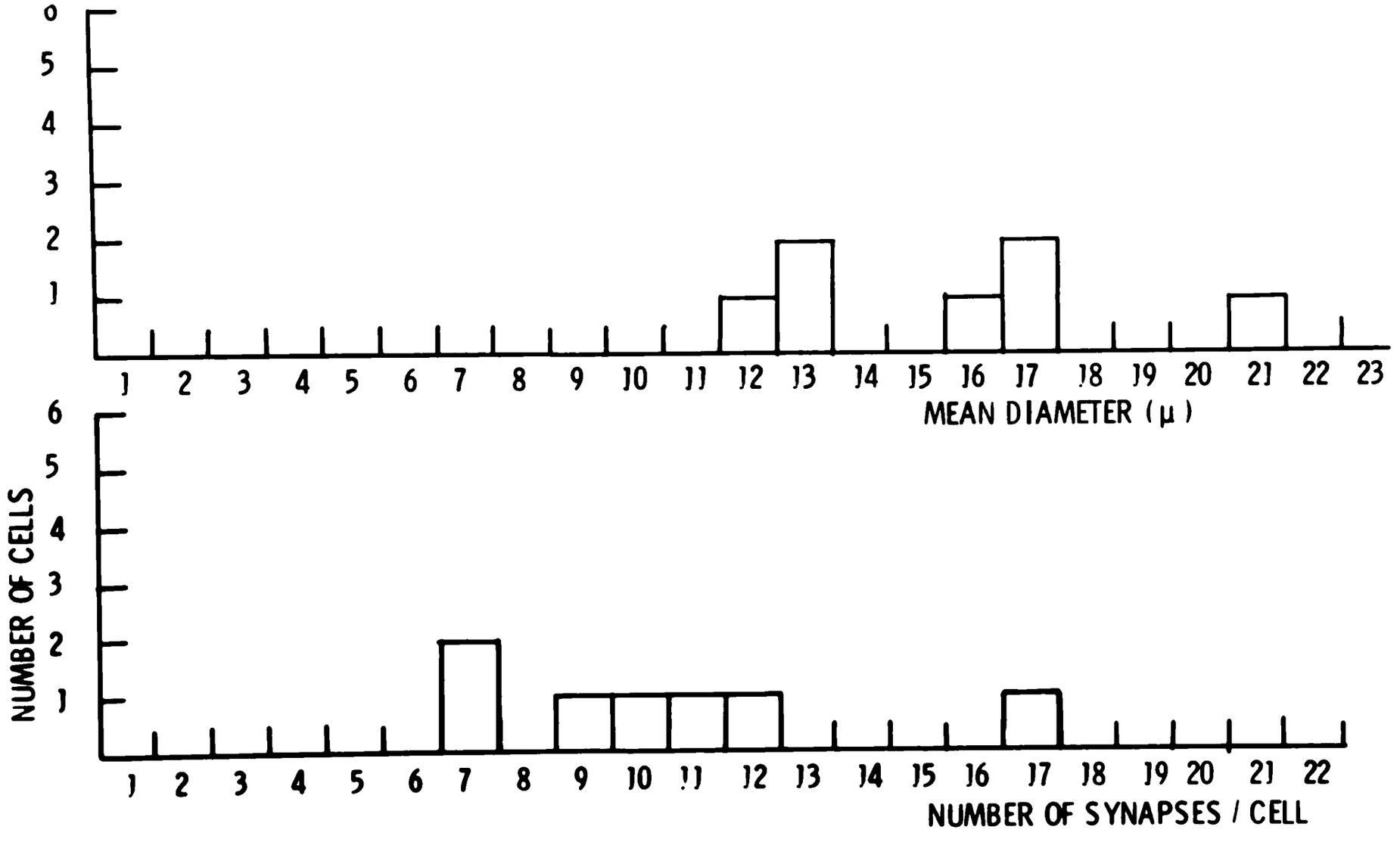

Fig. 9-28 A map and histogram showing the depth distribution of degenerating thalamo-cortical axon terminals in the motor cortex, a single section having been mapped at each of the three levels. Note that the dense band of degeneration is in the upper two-thirds of layer IV and the lower half of layer III and that there is a second smaller concentration of degeneration in the deep part of layer V. The histograms were prepared from a constant width strip running through the whole depth of the cortex for all maps.

THALAMO-CORTICAL TERMINALS IN THE MOTOR CORTEX

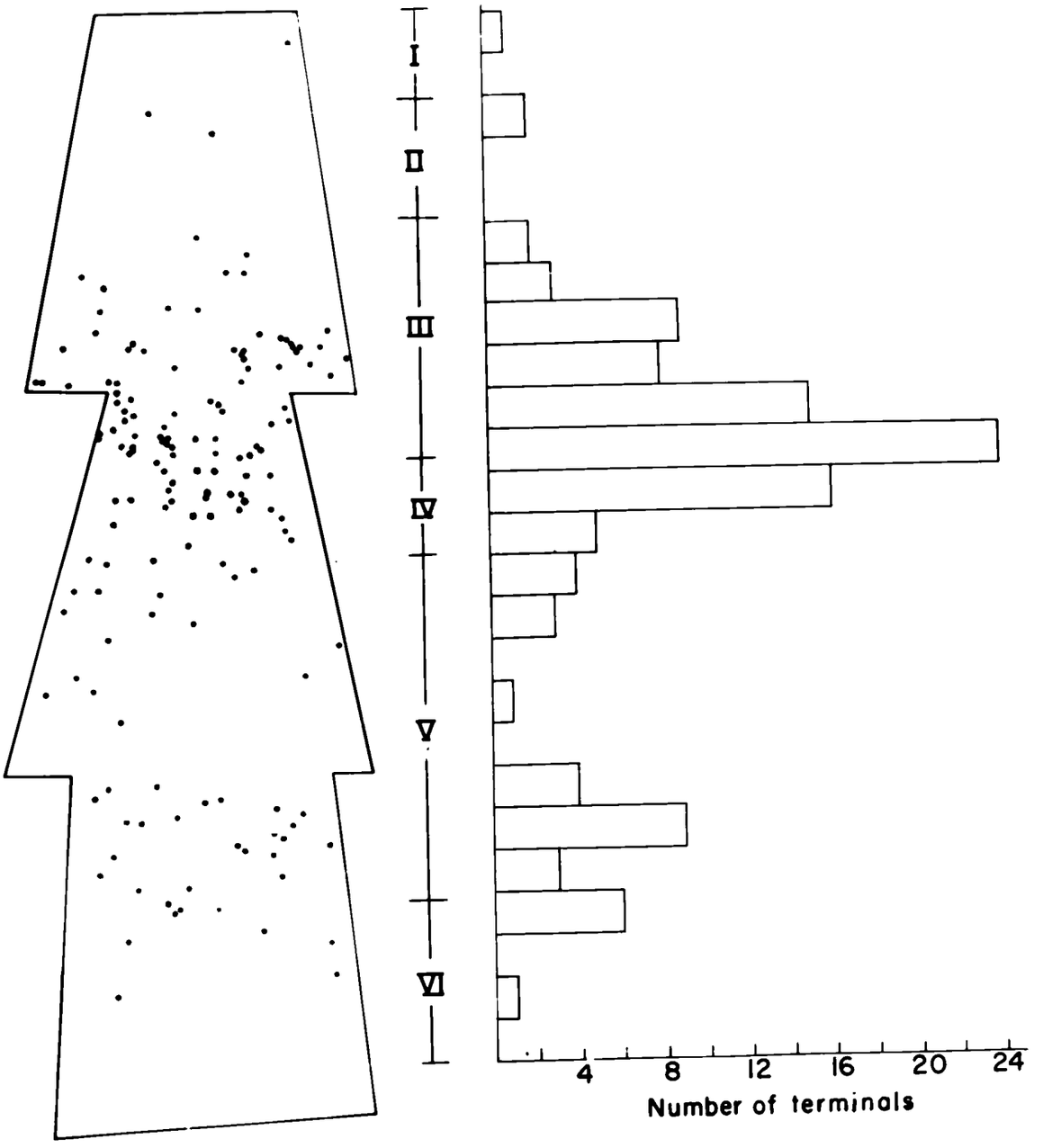

Fig. 9-29 A map and histogram showing the depth distribution of degenerating thalamo-cortical axon terminals in area 3b of the somatic sensory cortex, a single section having been mapped at each of two levels. Note that, as in the motor cortex, the dense band of degeneration is in the upper two-thirds of layer IV and the lower half of layer III but although degeneration is present in layer V it does not appear to form a separate band as in the motor cortex.

THALAMO-CORTICAL TERMINALS IN AREA 3b OF THE SOMATIC SENSORY CORTEX

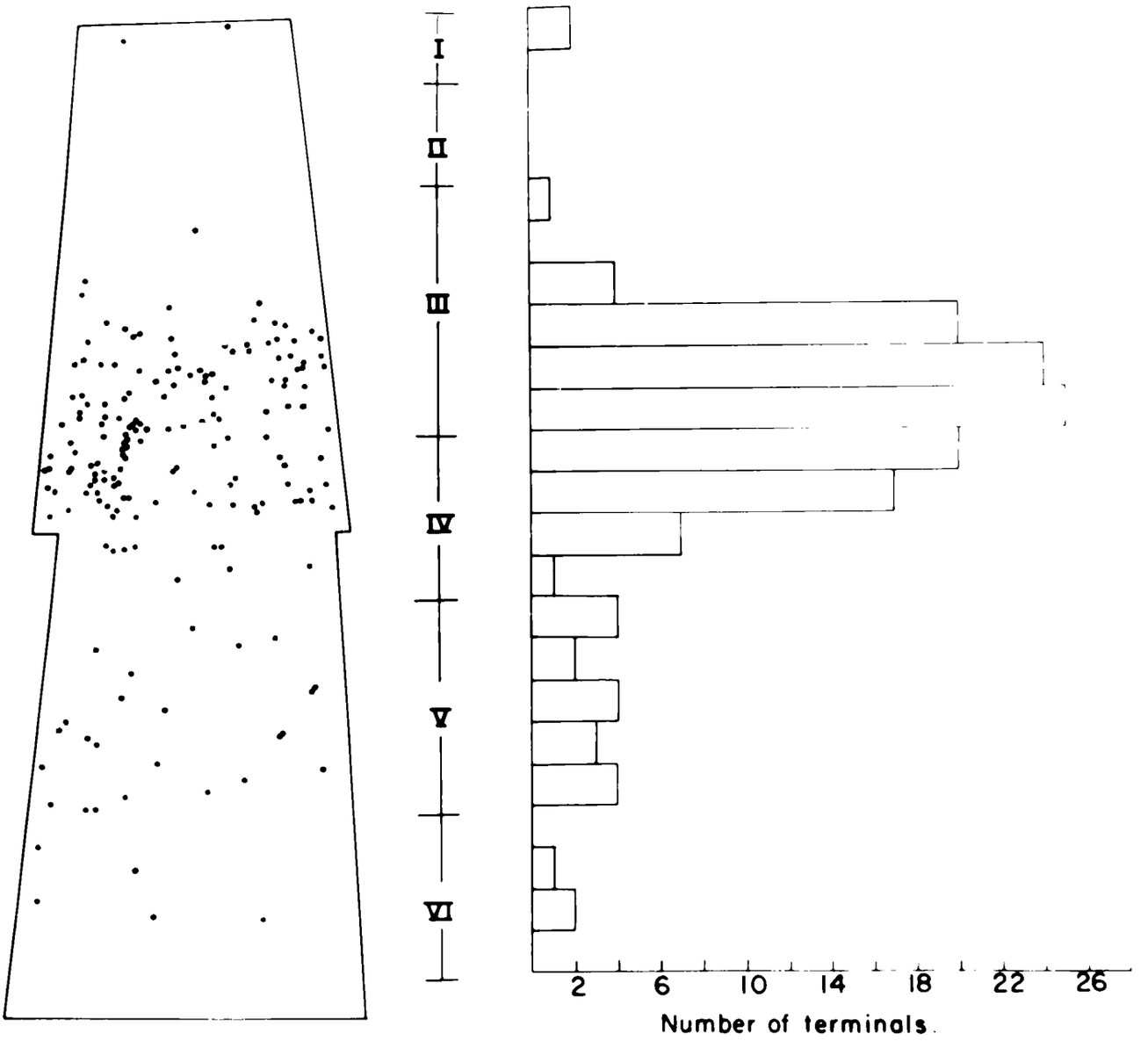

Fig. 9-30 A map and histogram of the same sections of the motor cortex as Fig. 9-28 but showing the depth distributions of the different types of post-synaptic profile contacted by degenerating thalamo-cortical axon terminals. Note that whereas most of those contacting spines are in the dense band of degeneration in layers III and IV, those contacting dendrites and cell somata are spread through the deeper layers of the cortex.

THALAMO-CORTICAL TERMINALS IN THE MOTOR CORTEX

LAMINAR DISTRIBUTION OF POST-SYNAPTIC PROFILES.

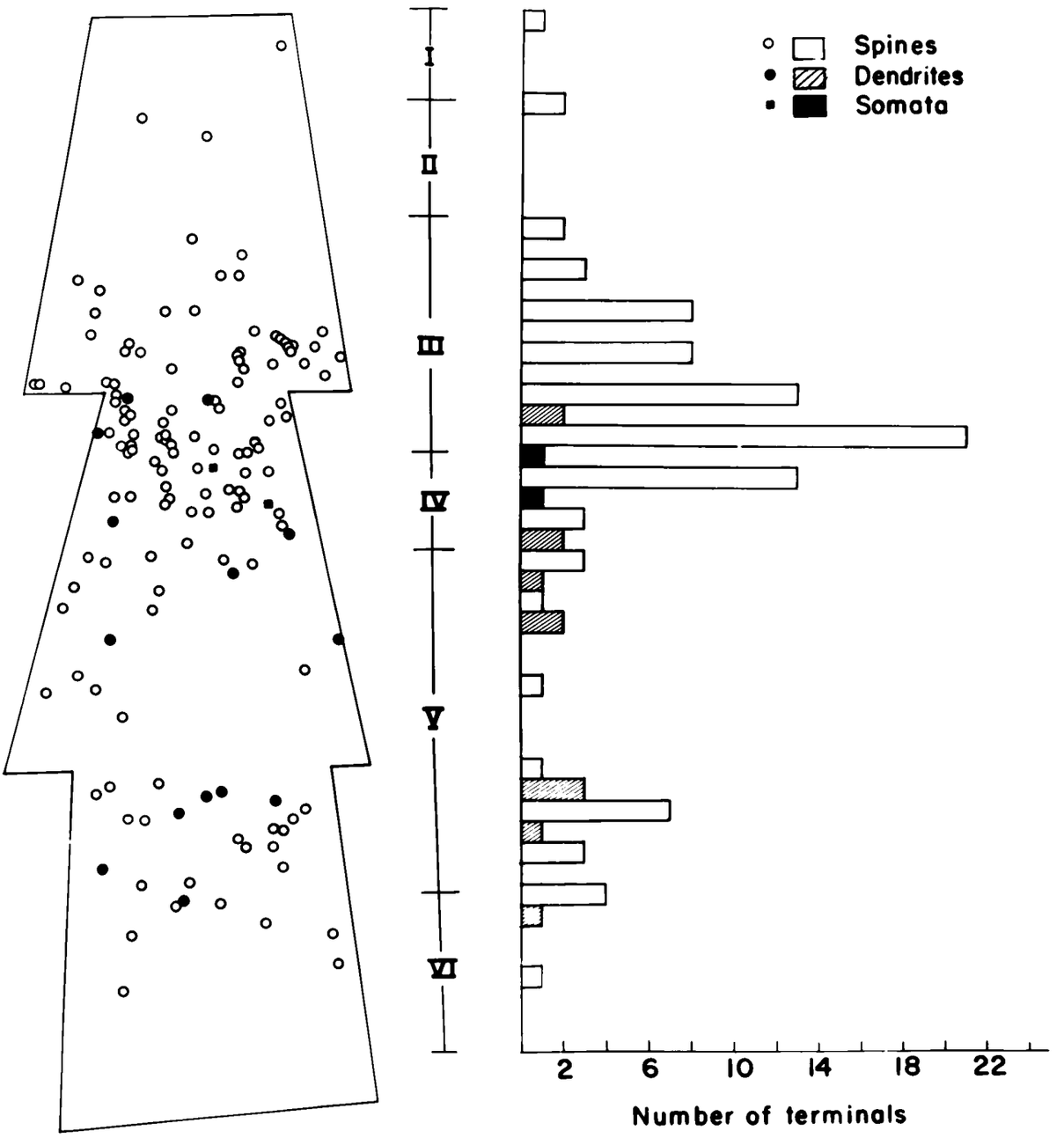

Fig. 9-31 Map and histogram of the same sections of the somatic sensory cortex as Fig. 9-29 but showing the depth distributions of the different types of postsynaptic profile contacted by degenerating thalamo-cortical axon terminals. Although not as obvious as in the motor cortex there appears to be some tendency for those terminals contacting dendrites to be deeper in the cortex than those contacting spines.

THALAMO-CORTICAL TERMINALS IN AREA 3b OF THE SOMATIC SENSORY CORTEX.

LAMINAR DISTRIBUTION OF THE POST-SYNAPTIC PROFILES.

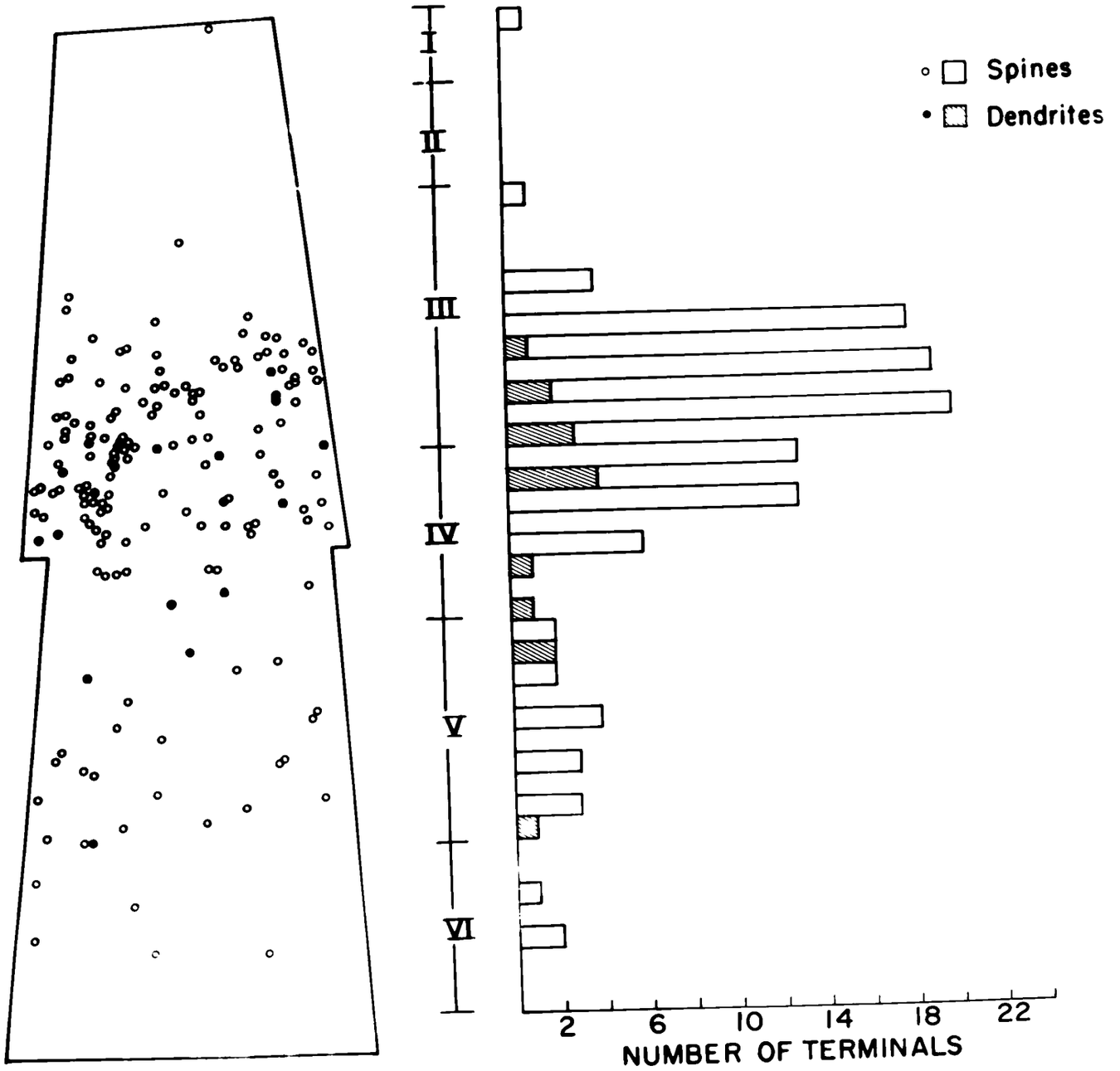

Fig. 9-32 A section of layer IV of the motor cortex taken parallel to the pial surface showing a bundle of apical dendrites cut in transverse section, together with a degenerating thalamo-cortical axon terminal which makes a synapse on to a spine, a degenerating myelinated axon running vertically with the bundle of apical dendrites and a degenerating preterminal axon.

X 29,000

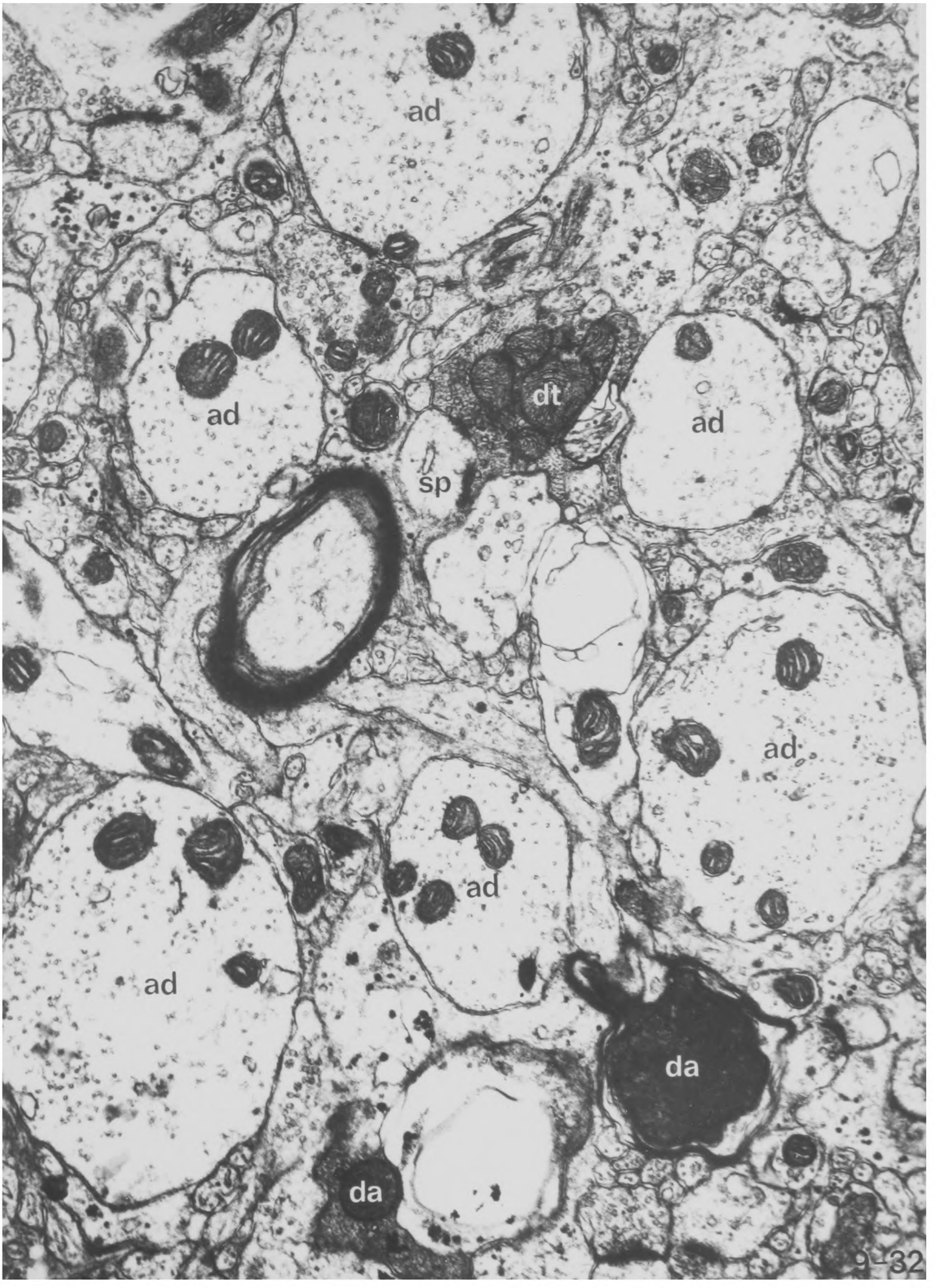
ad
ad
dt
ad
sp
ad
ad
ad
ad
da
da

Fig. 9-33 A map of layer IV of the motor cortex cut parallel to the pia, showing the positions of apical dendrites (cut transversely) and degenerating thalamo-cortical axon terminals. Note that the apical dendrites tend to occur in groups and that the degenerating thalamo-cortical axon terminals frequently occur in association with the apical dendrites.

MAP OF LAYER IV OF THE MOTOR CORTEX CUT PARALLEL TO THE PIA SHOWING APICAL DENDRITES AND DEGENERATING THALAMO-CORTICAL AXON TERMINALS

- ○ Apical dendrites
- ● Degenerating Thalamo-cortical terminals

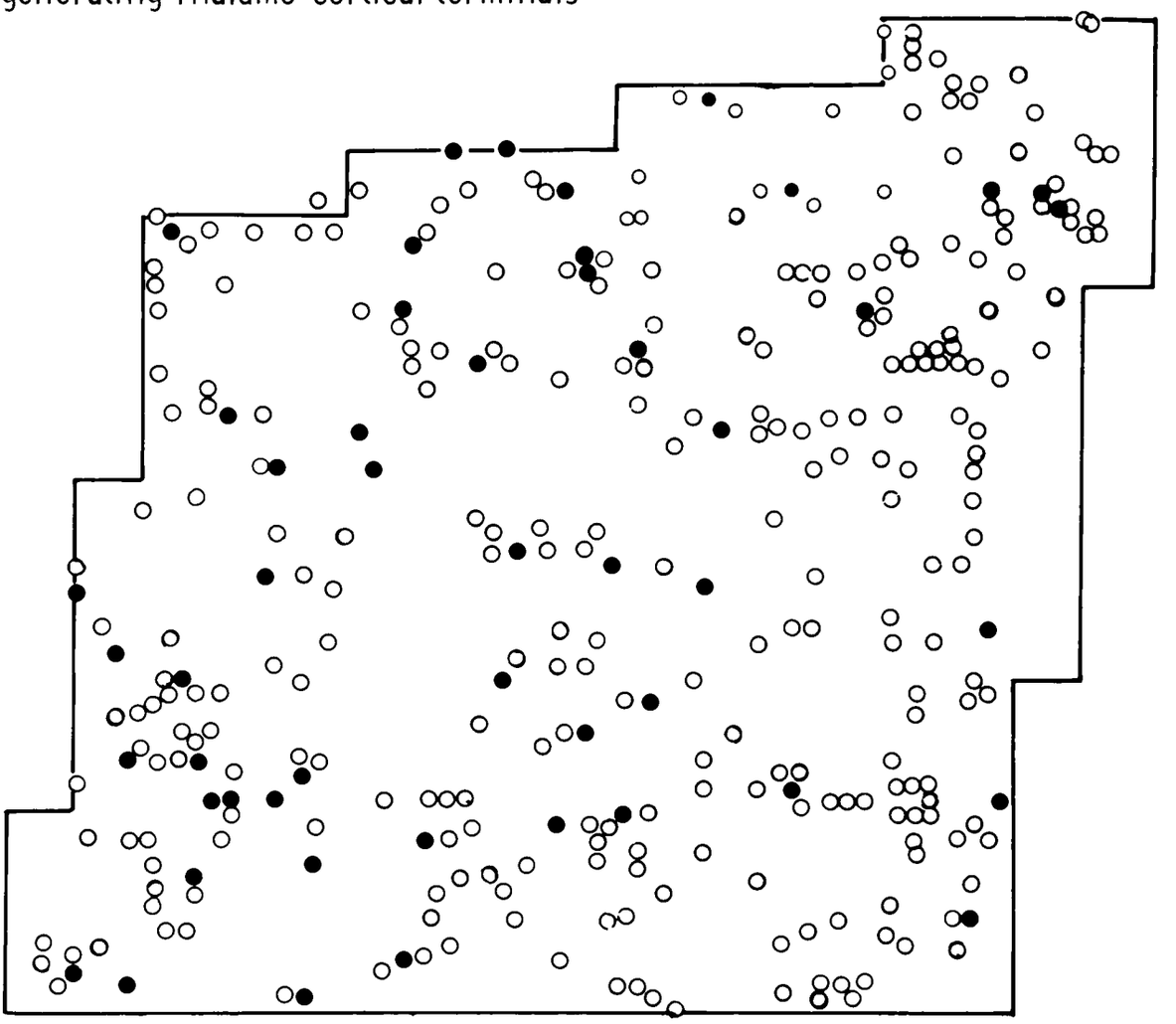

Fig. 9-34 A degenerating commissural axon terminal making a synapse on to a spine containing a spine apparatus in motor cortex.

X 53,000

Fig. 9-35 A degenerating commissural axon terminal making a synapse on to two spines in the motor cortex, one of which contains a spine apparatus.

X 67,000

Fig. 9-36 A degenerating commissural axon terminal which makes a synapse on to a sessile spine cut in continuity with its parent dendrite in the motor cortex. Note the flocculent cytoplasm in the spine which contained a small spine apparatus and the lack of synapses on the shaft of the parent dendrite.

X 36,000

Fig. 9-37 A degenerating commissural axon terminal which makes two synapses on to a spine in the motor cortex. Continuity between the two parts of the degenerating axon terminal was demonstrated in serial sections.

X 36,000

Fig. 9-38 A degenerating commissural axon terminal making a synapse on to a spine in layer V of the motor cortex, which receives a symmetrical synapse from a normal axon terminal. This normal terminal also makes a synapse on to a second spine which itself receives an asymmetric synapse from a further normal axon terminal.

X 36,000

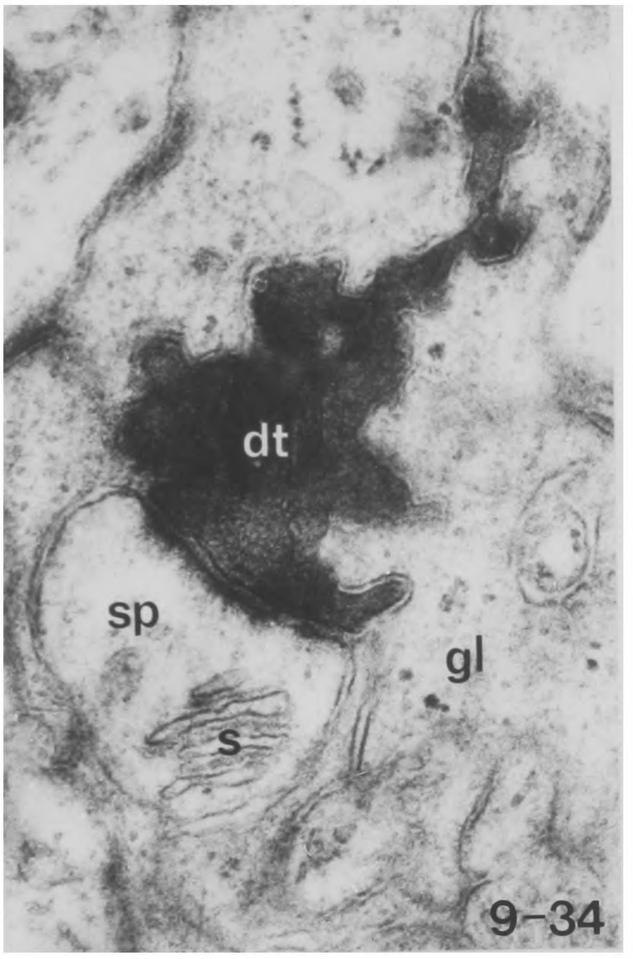
dt
sp
gl
s
9-34

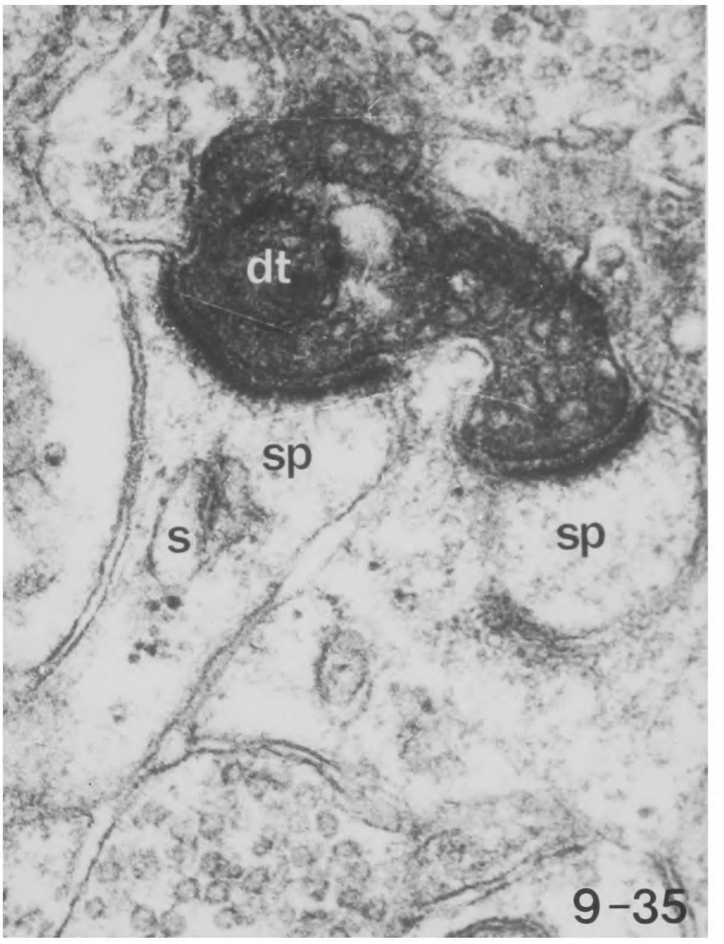
dt
sp
s
sp
9-35

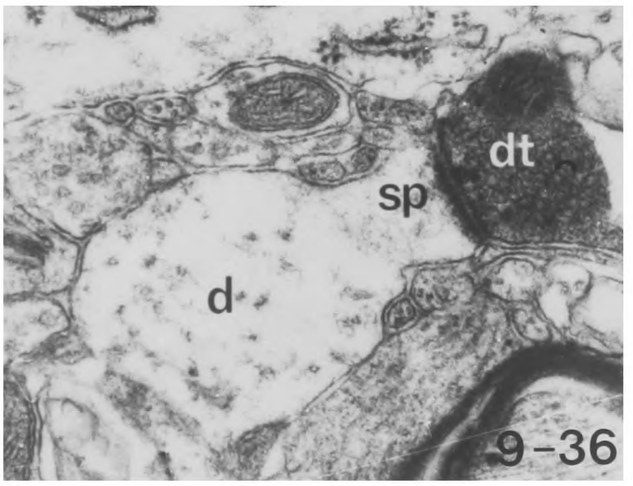
dt
sp
d
9-36

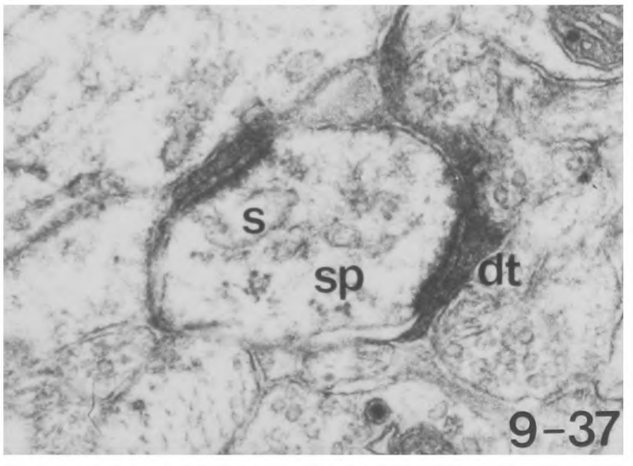
s
sp
dt
9-37

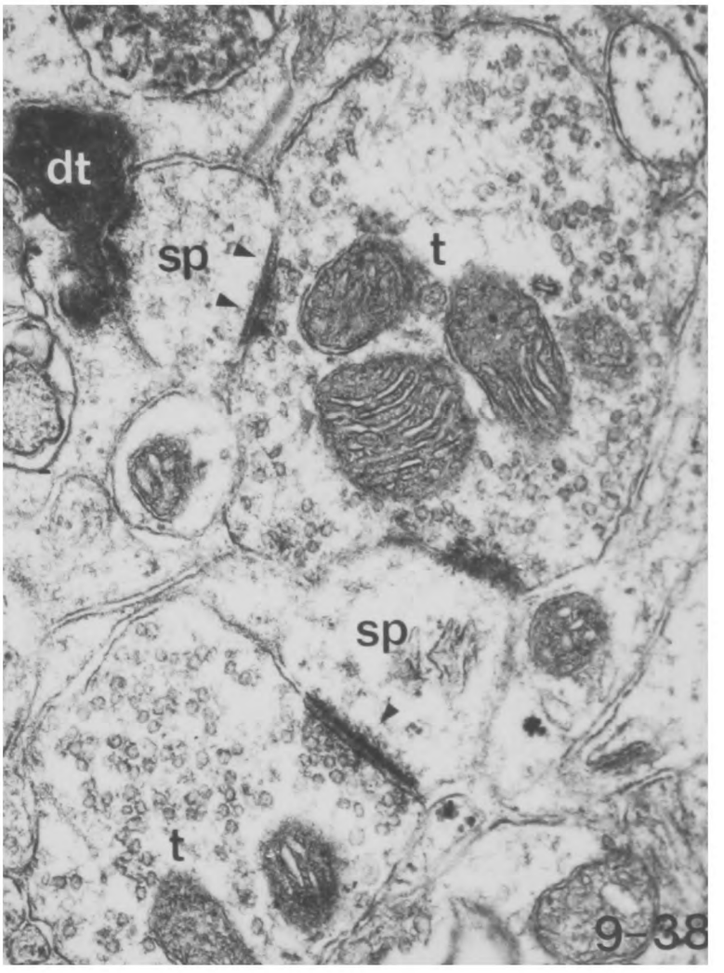
dt
sp
t
sp
t
9-38

Fig. 9-39 Two adjacent degenerating commissural axon terminals in area 3b of the somatic sensory cortex, both of which make synapses on to spines, one of which contains a spine apparatus.

X 32,000

Fig. 9-40 An early degenerating commissural axon terminal which makes synapses on to two spines in area 3b of the somatic sensory cortex, both of which contain a spine apparatus. Note the very irregular synaptic vesicles and the darkening of the axon terminal.

X 29,000

Fig. 9-41 A late degenerating commissural axon terminal making a synapse on to a spine in area 3b of the somatic sensory cortex.

X 32,000

Fig. 9-42 A degenerating commissural terminal in area 3b of somatic sensory cortex which makes synapses on to three spines, one of which is cut in continuity with its parent dendrite. Note the small size of the parent dendrite, the lack of synapses on it and the contrasting appearance of the flocculent cytoplasm on the spine and the clear cytoplasm with neurotubules in the dendritic shaft. Note also the spine apparatus in the spine.

X 53,000

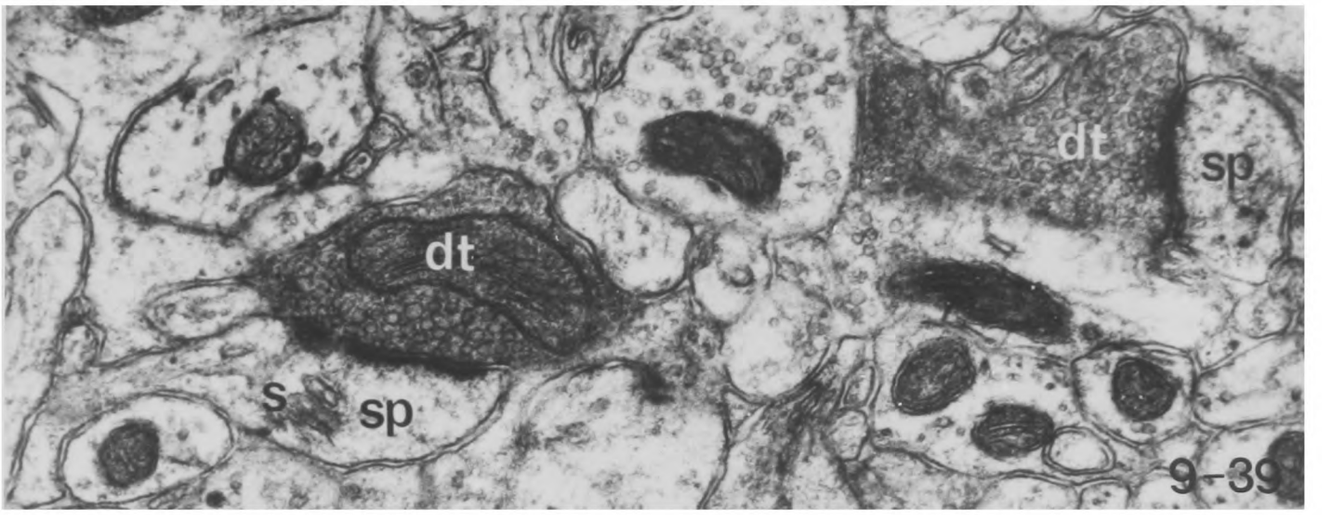
dt
sp
dt
s
sp
9-39

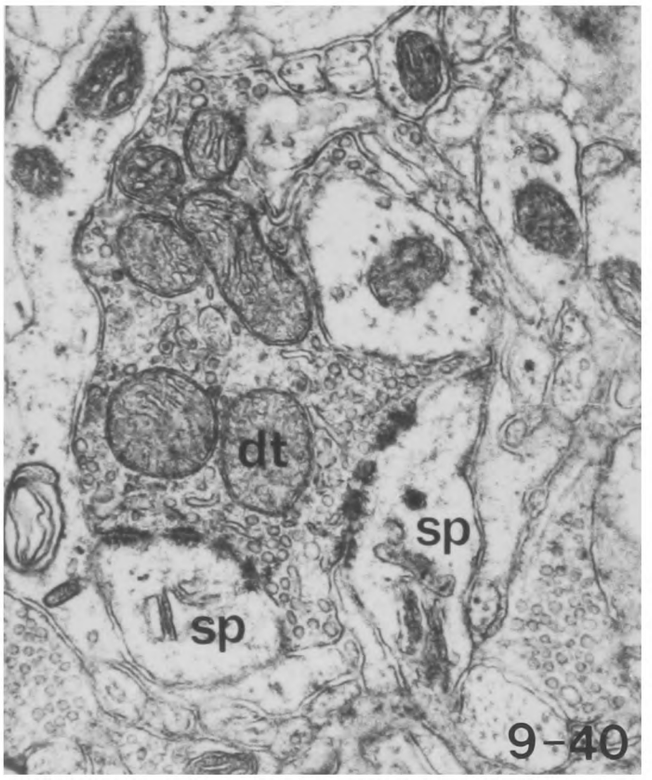
dt
sp
sp
9-40

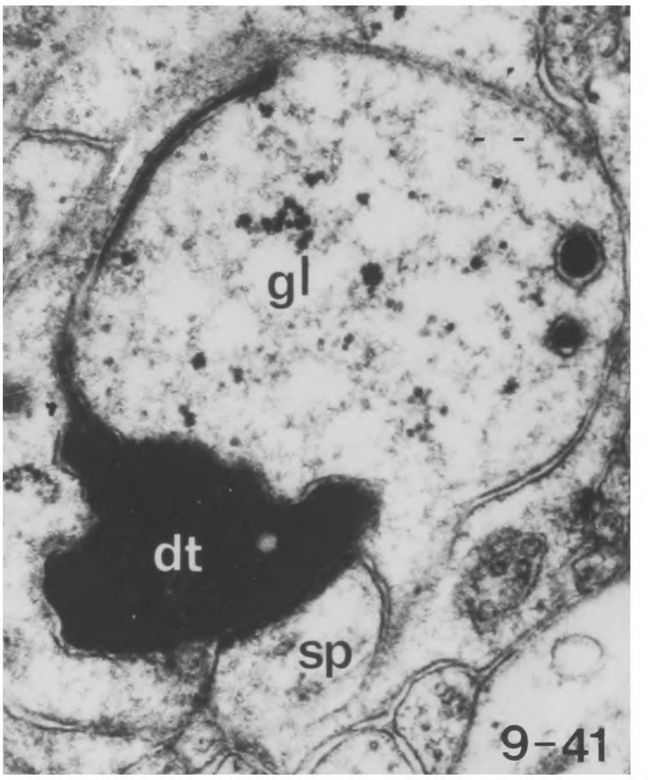
gl
dt
sp
9-41

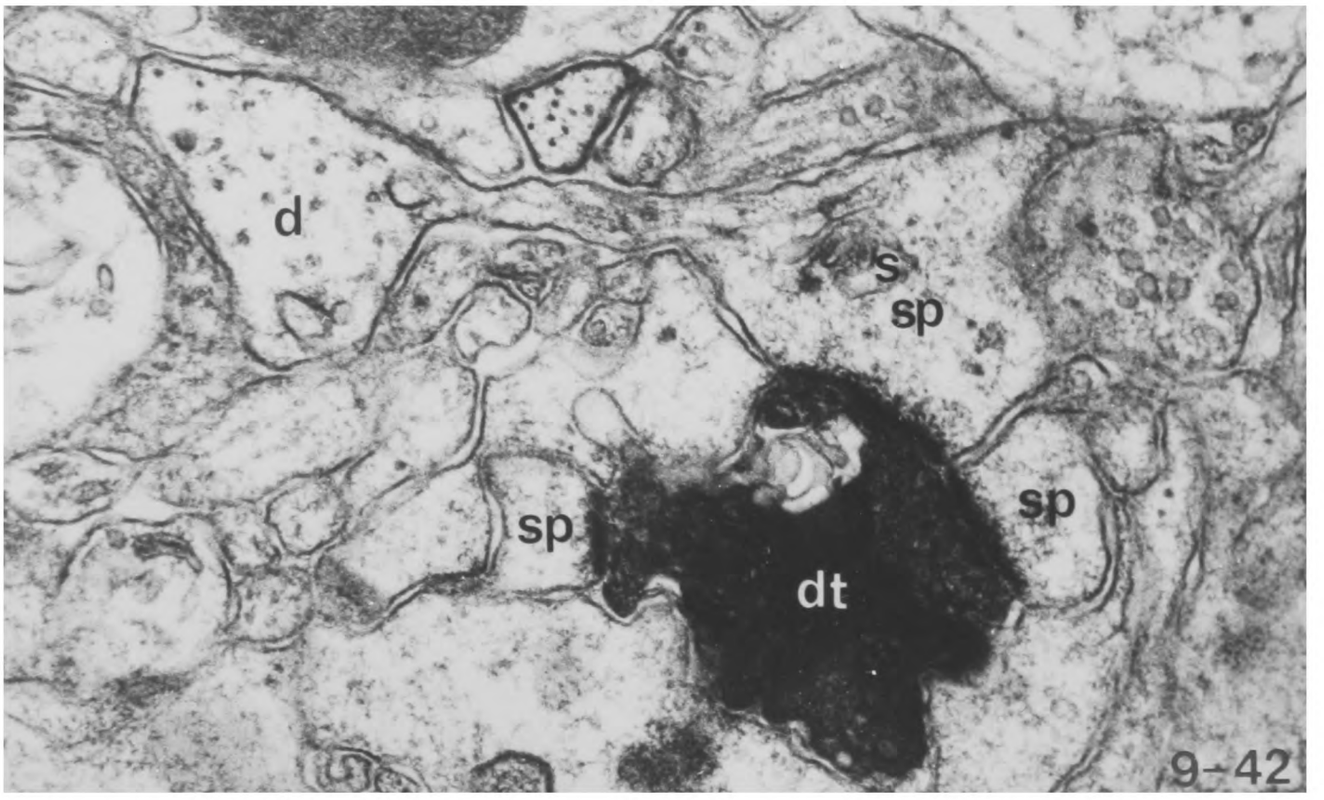
d
s
sp
sp
sp
dt
9-42

Fig. 9-43 A degenerating commissural axon terminal making a synapse on to the shaft of a dendrite in the motor cortex. Note the moderately varicose shape of the dendrite, the large number of other synapses upon it and the high concentration of organelles within it. X 18,000

Fig. 9-44 A degenerating commissural axon terminal which makes a synapse on to the shaft of a dendrite in the motor cortex. Note the other synapse received by the dendrite and the high concentration of organelles it contains. X 39,000

Fig. 9-45 A degenerating commissural terminal in the motor cortex making a synapse on to the shaft of a dendrite which receives another asymmetric synapse from a normal axon terminal. X 29,000

Fig. 9-46 A degenerating commissural axon terminal which makes a synapse on to a large stellate cell soma in layer IV of the motor cortex. Note the other synapses received by the cell soma (arrows), and its abundant cytoplasm full of organelles. X 8,400

Fig. 9-47 Higher magnification of the degenerating commissural terminal of fig. 9-46. X 29,000

9-43

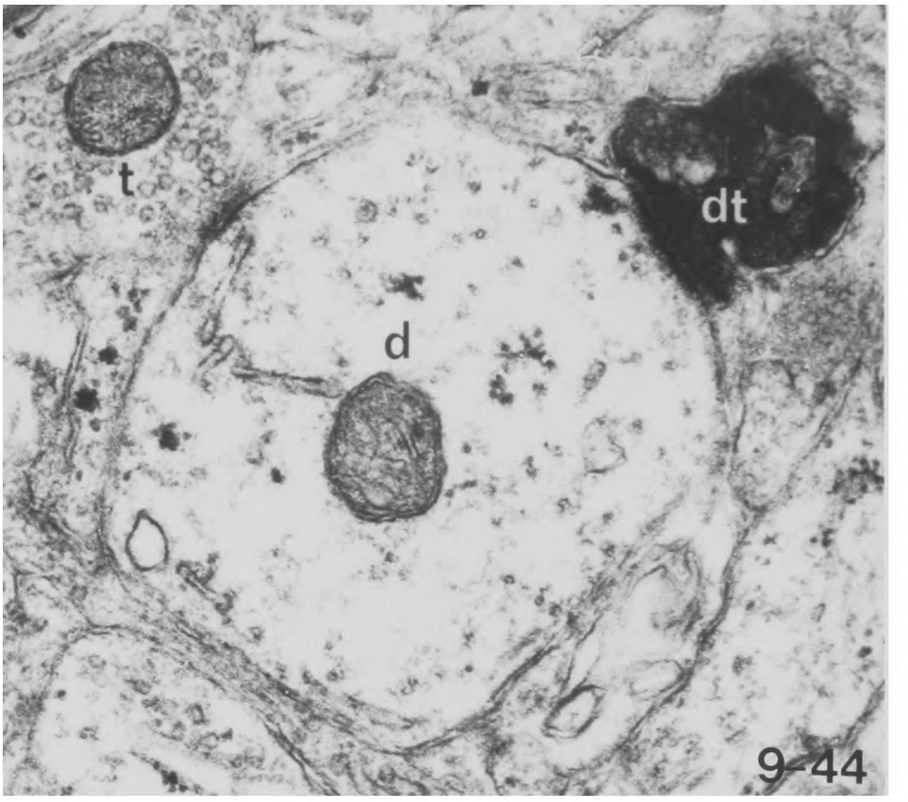

9-44

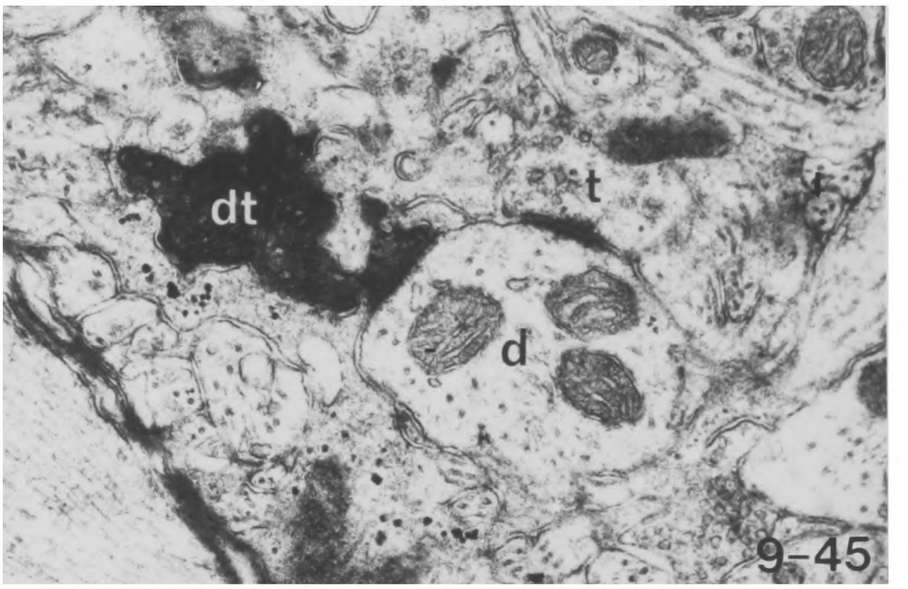

9-45

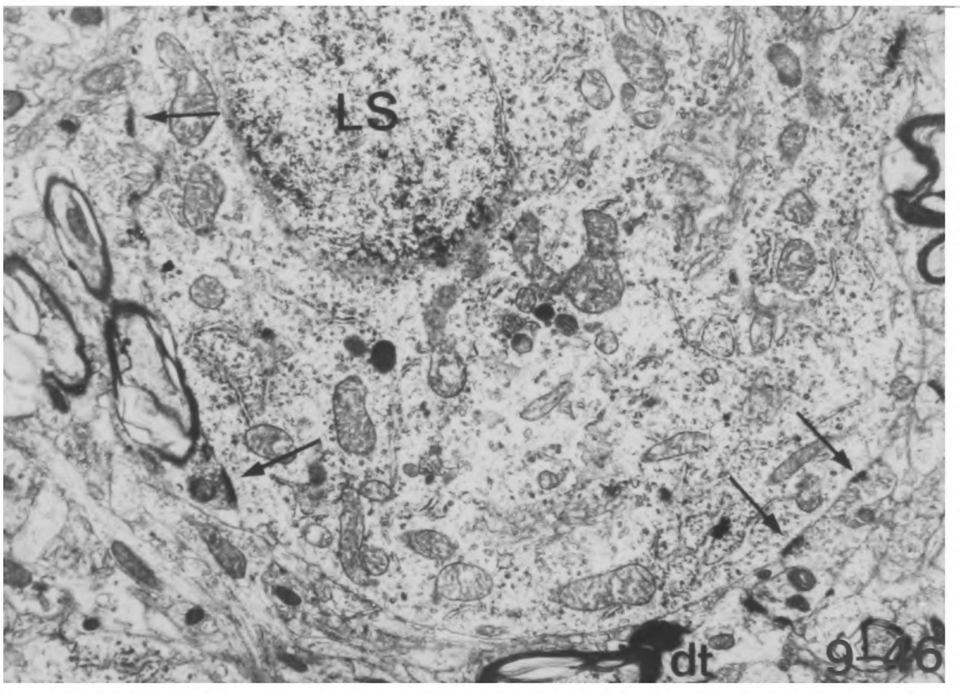

9-46

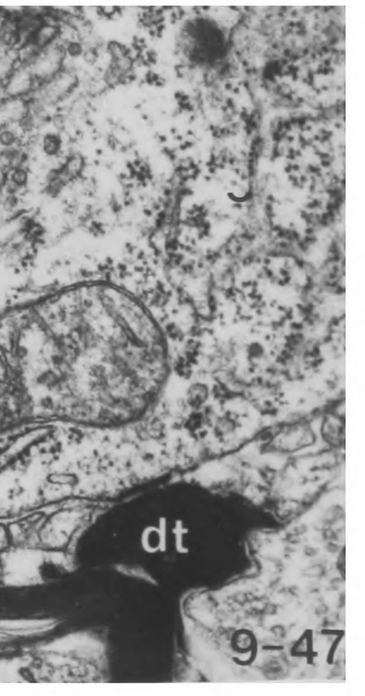

9-47

Fig. 9-48 A map and histogram showing the depth distribution of degenerating commissural axon terminals in the motor cortex. The map at the top left is of a single section to show the density of degeneration present. The composite map shows three sections from the same block superimposed at each of three levels, making a total of nine sections. The histograms for all maps are derived from a constant width strip through the full depth of the cortex. Note the relative concentrations of degenerating terminals in layer I, the upper part of layer III, the upper part of layer V and in the lower part of layer V and upper part of layer VI, with relatively clear bands in layer IV and the middle of layer V.

COMMISSURAL TERMINALS IN THE MOTOR CORTEX

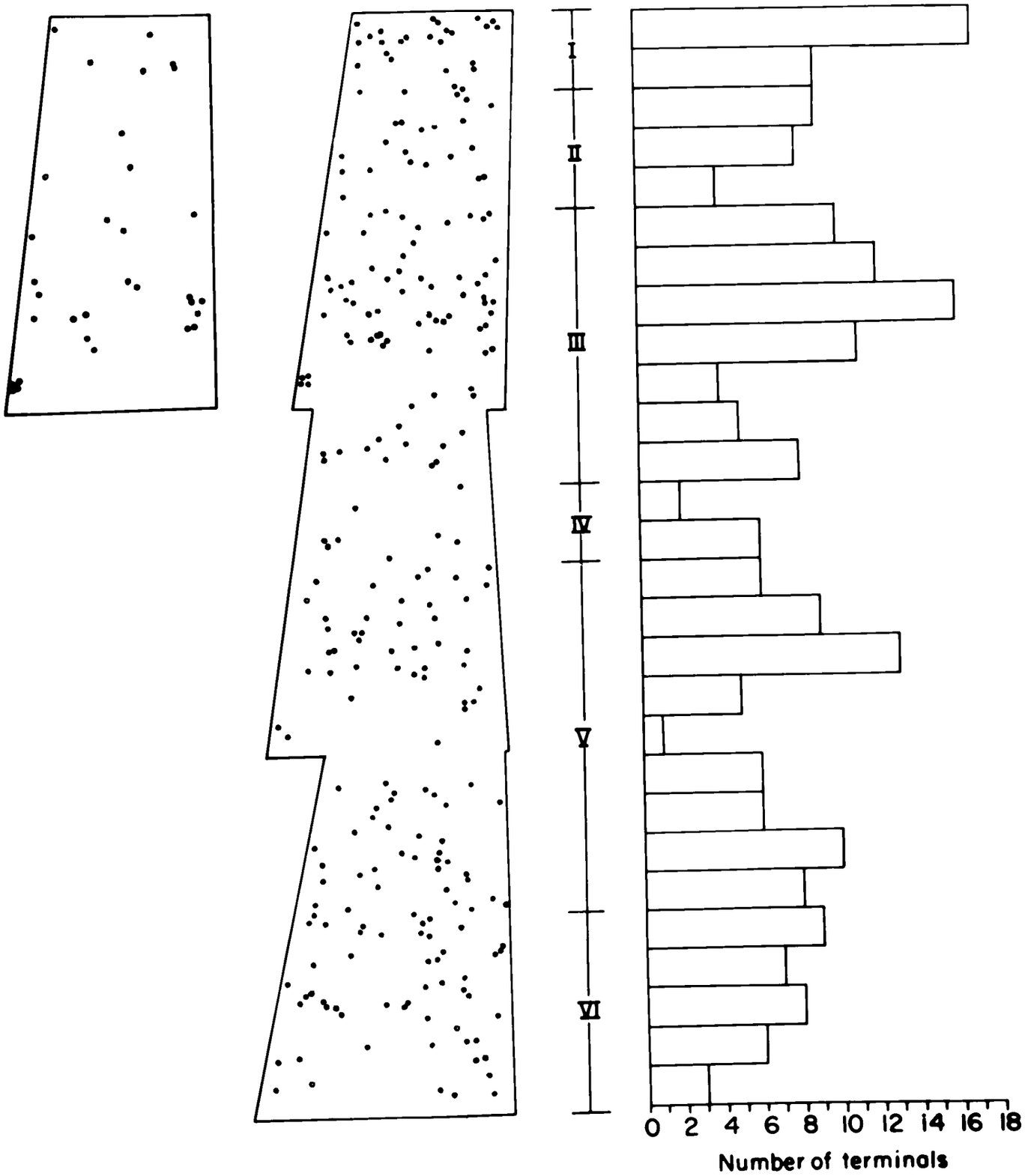

Fig. 9-49 A map and histogram showing the depth distribution of degenerating commissural axon terminals in area 3b of the somatic sensory cortex. The map at the top left is of a single section to show the density of degeneration; the composite map consists of three superimposed sections of each of the superficial and deep parts of the cortex.

COMMISSURAL TERMINALS IN AREA 3b OF THE SOMATIC SENSORY CORTEX.

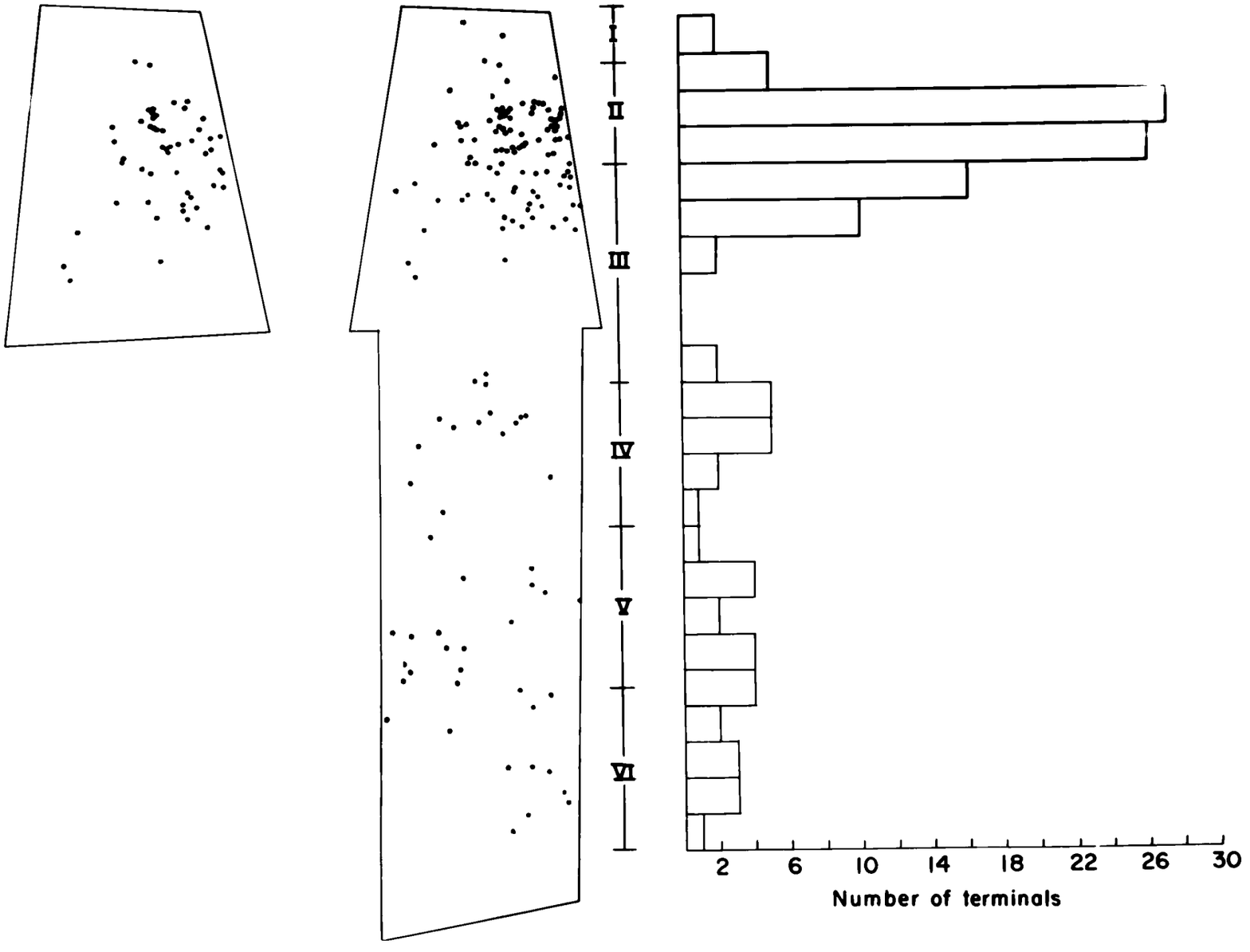

Fig. 9-50 A map and histogram of the same sections of the motor cortex as Fig. 9-48 showing the depth distribution of the different types of postsynaptic profile receiving synapses from degenerating commissural axon terminals. The five dendrites postsynaptic to commissural terminals are scattered through the depth of the cortex although those in the deep layers happen to come outside the constant width strip from which the histogram was compiled.

COMMISSURAL TERMINALS IN THE MOTOR CORTEX

Laminar distribution of post synaptic profiles

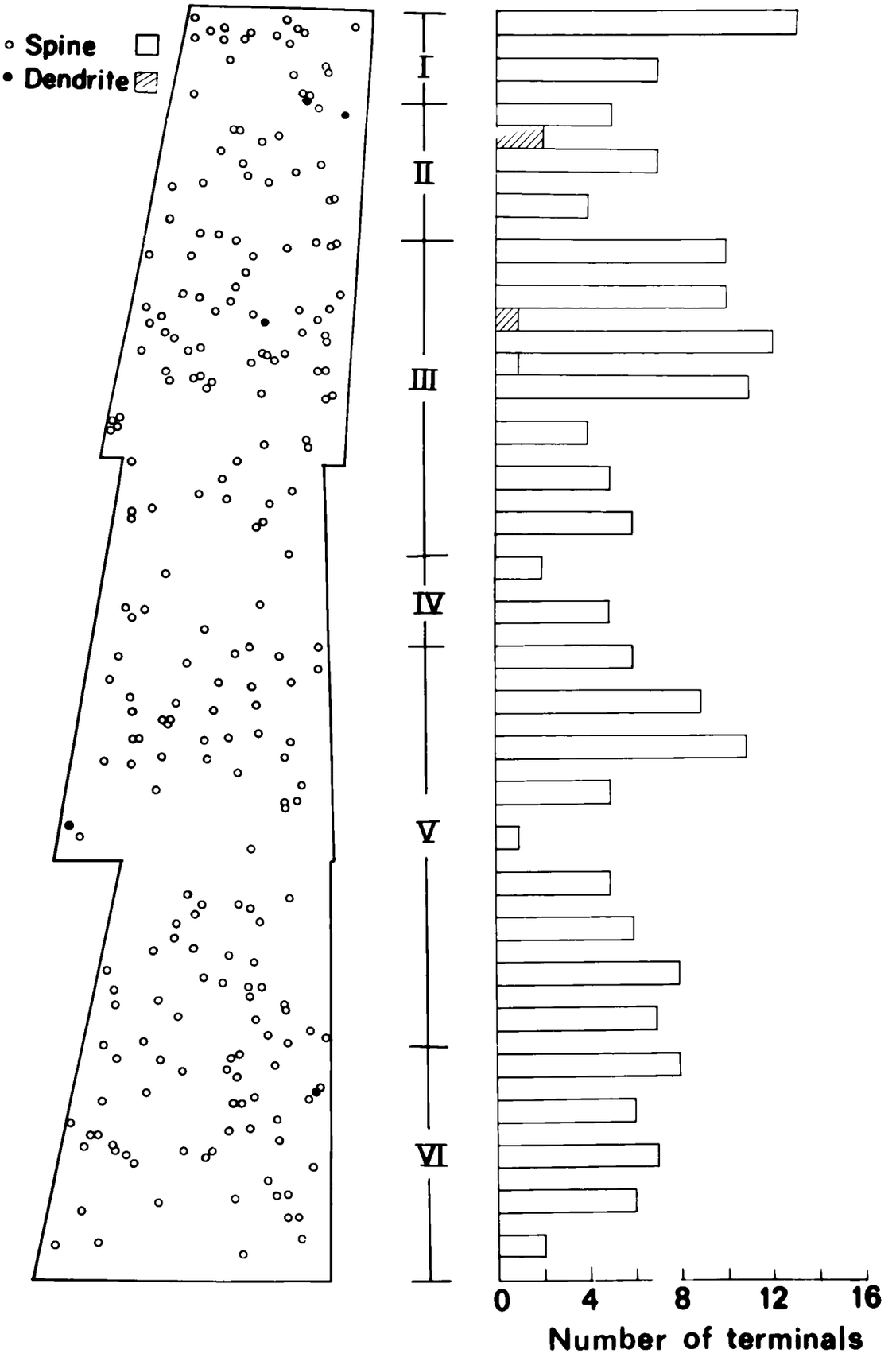

Fig. 9-51 A map and histogram of the same section of the somatic sensory cortex as Fig. 9-49 showing the laminar distribution of the different kinds of postsynaptic profile receiving synapses from degenerating commissural axon terminals. The few dendrites postsynaptic to commissural terminals are scattered through the depth of the cortex.

COMMISSURAL TERMINALS IN AREA 3b OF THE SOMATIC SENSORY CORTEX

Laminar distribution of post-synaptic profiles

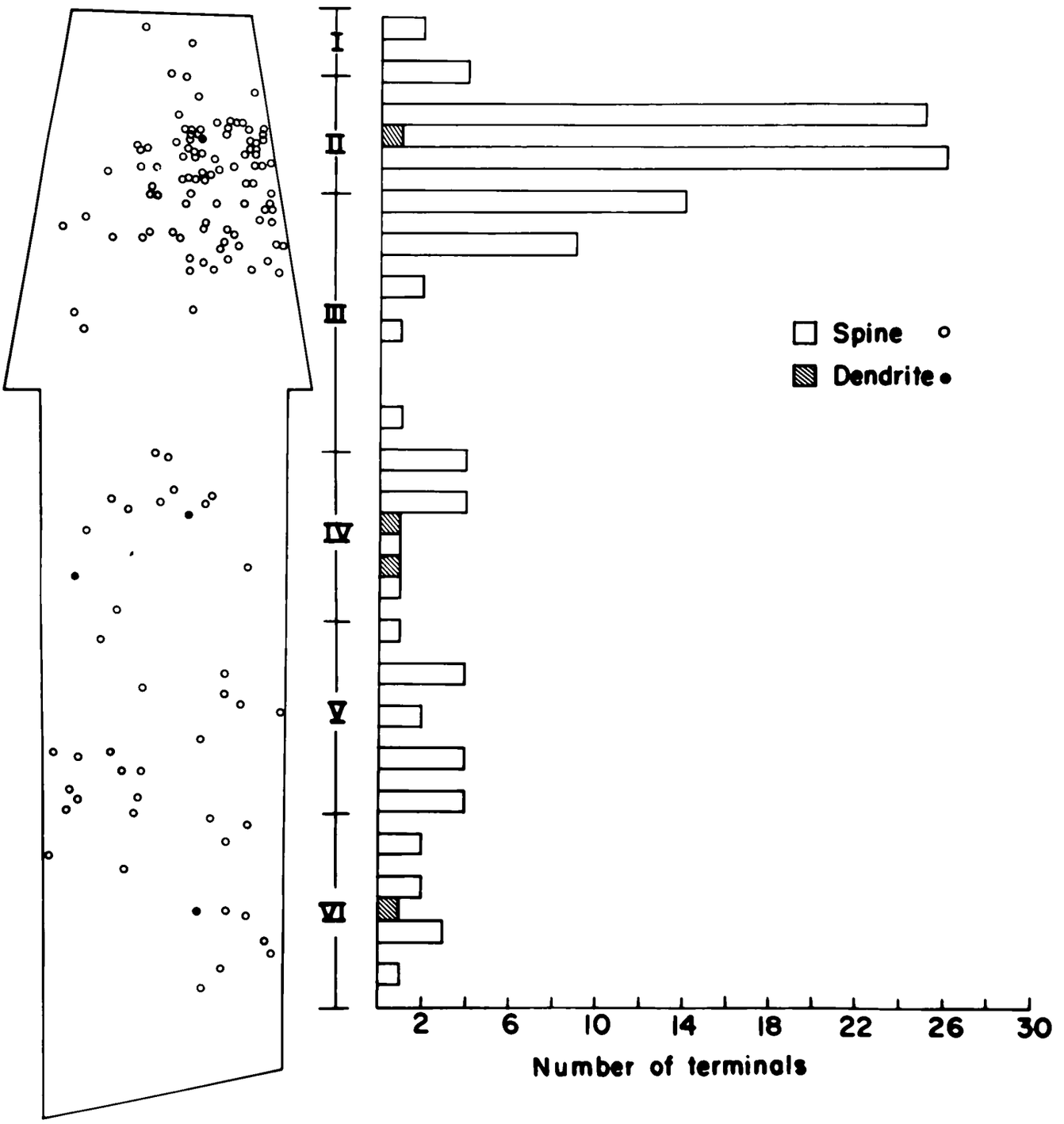

Fig. 9-52 An early degenerating association axon terminal making a synapse on to a spine in the motor cortex following an SI lesion. X 38,000

Fig. 9-53 An early degenerating SI association axon terminal making a synapse on to a spine in the motor cortex. X 41,000

Fig. 9-54 A late degenerating SI association terminal making a synapse on to a spine containing a spine apparatus in the motor cortex. X 38,000

Fig. 9-55 A late degenerating SI association terminal in the motor cortex making synapses on to three spines. X 35,000

Fig. 9-56 A late degenerating SI association axon terminal making a synapse on to a spine in the motor cortex. X 39,000

Fig. 9-57 A late degenerating SI association axon terminal making a synapse on to the shaft of a dendrite in the motor cortex. Note the normal asymmetric synapse received by the dendrite. X 29,000

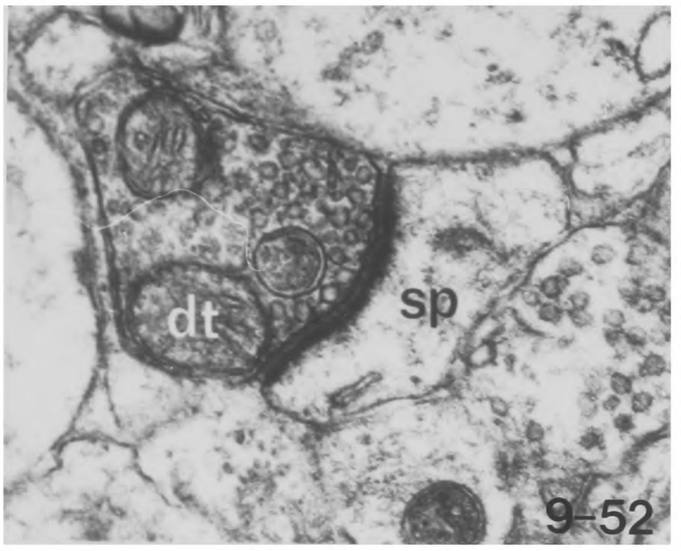
dt
sp
9-52

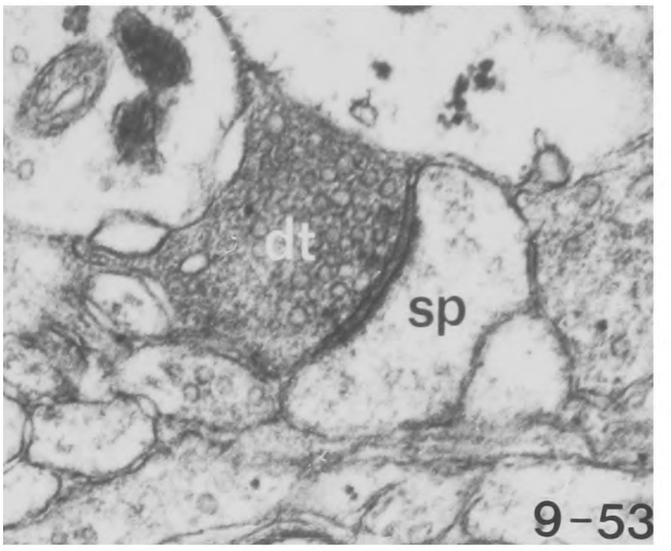
dt
sp
9-53

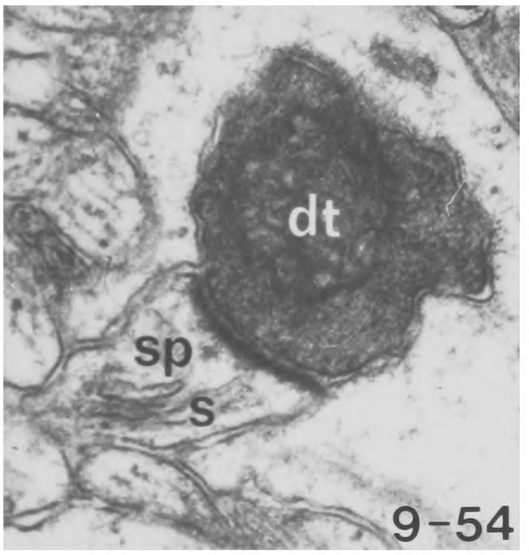
dt
sp
s
9-54

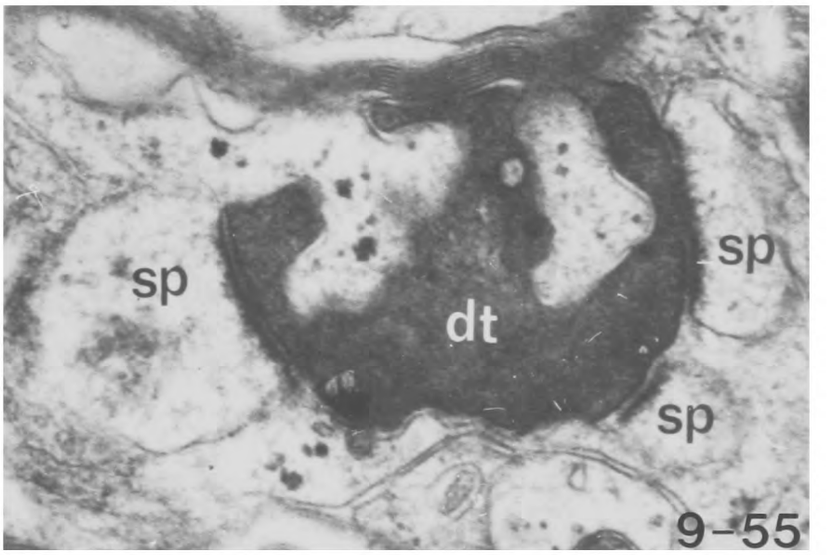
sp
sp
dt
sp
9-55

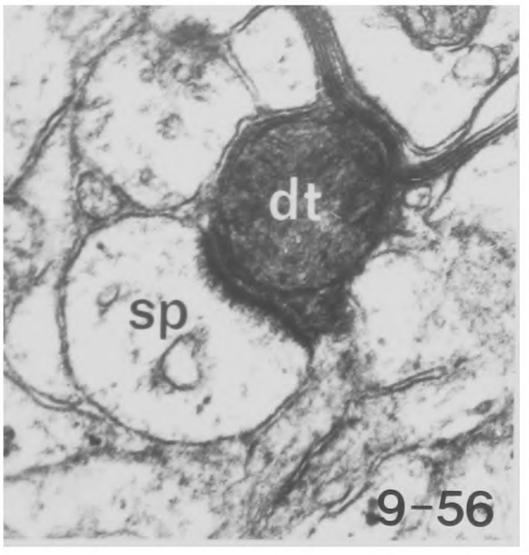
dt
sp
9-56

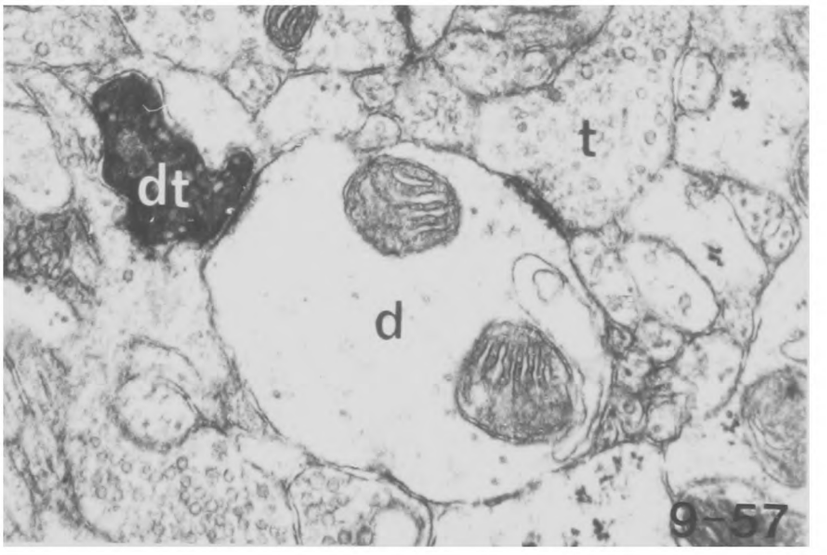
dt
t
d
9-57

Fig. 9-58 A degenerating association axon terminal which makes a synapse on to the shaft of a large dendrite in the motor cortex following a lesion of SI. Note the large size of the dendrite, the large number of synapses it receives and the high concentration of organelles in its cytoplasm. X 18,000

Fig. 9-59 A higher magnification of the degenerating SI association terminal of fig. 9-58. X 53,000

Fig. 9-60 A degenerating association axon terminal making a synapse on to a spine in the motor cortex following a lesion of area 6. X 29,000

Fig. 9-61 A degenerating association axon terminal from area 6 making a synapse on to a spine in the motor cortex. X 29,000

Fig. 9-62 A rare example of an axon terminal making a synapse on to a dendritic shaft and showing neurofilamentous hypertrophy in the motor cortex. Note the small cluster of vesicles still adjacent to the synaptic membrane complex. Area 6 lesion. X 18,000


d
dt
9-58

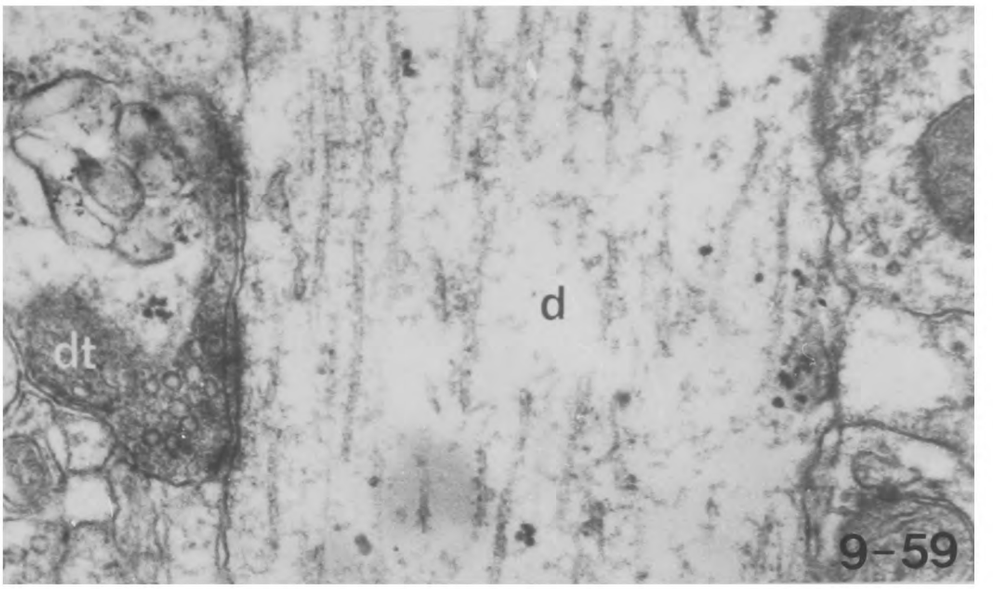
dt
d
9-59

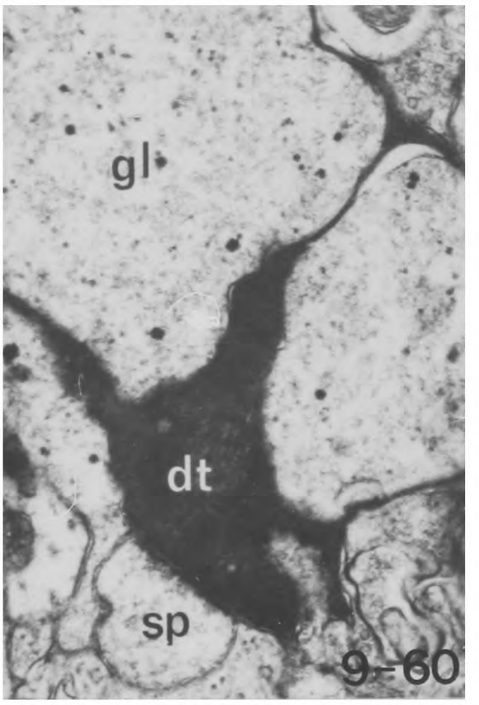
gl
dt
sp
9-60

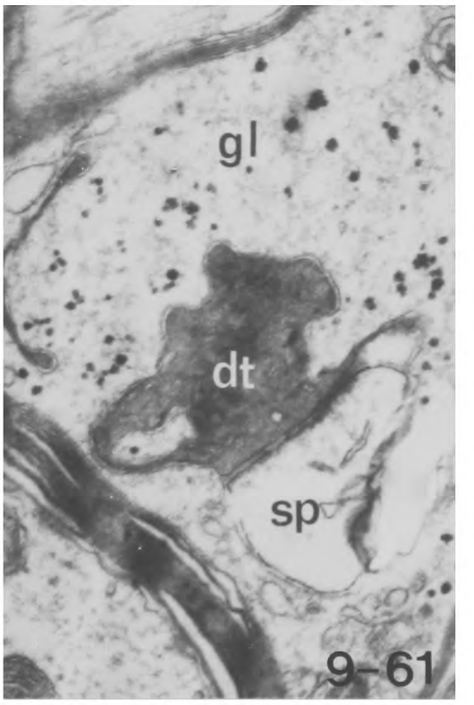
gl
dt
sp
9-61

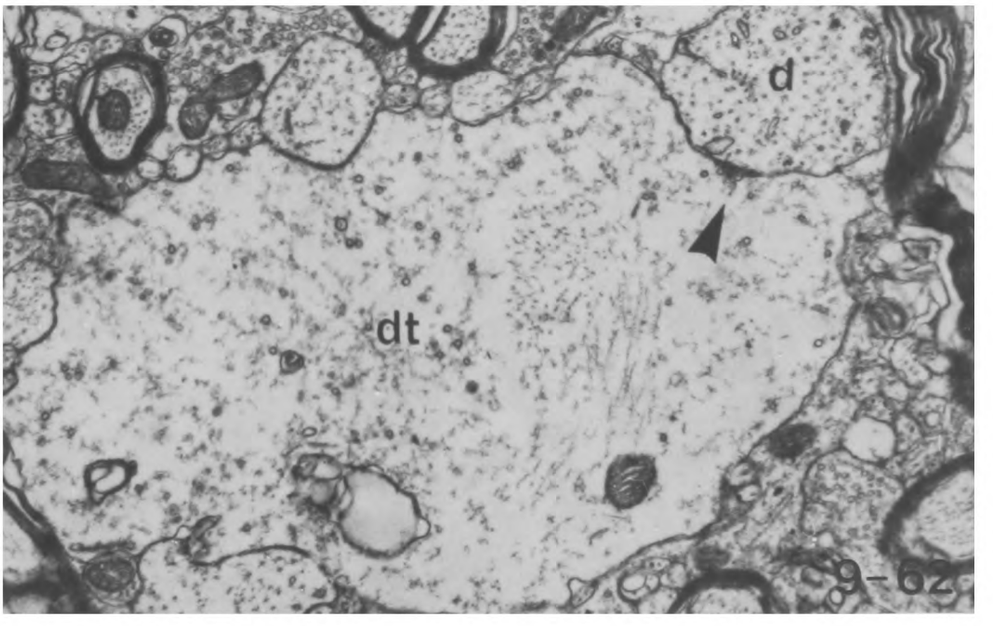
d
dt
9-62

Fig. 9-63 A map and histogram showing the depth distribution of degenerating association axon terminals in the motor cortex following a lesion of the somatic sensory cortex. The map to the left is of a single section of the middle third of the cortex to show the density of degeneration and the composite map consists of two superimposed maps at each of the three levels. Degeneration occurs in all cortical layers but appears to be a little more dense in the superficial half of the cortex.

TERMINALS FROM SOMATIC SENSORY CORTEX IN THE MOTOR CORTEX.

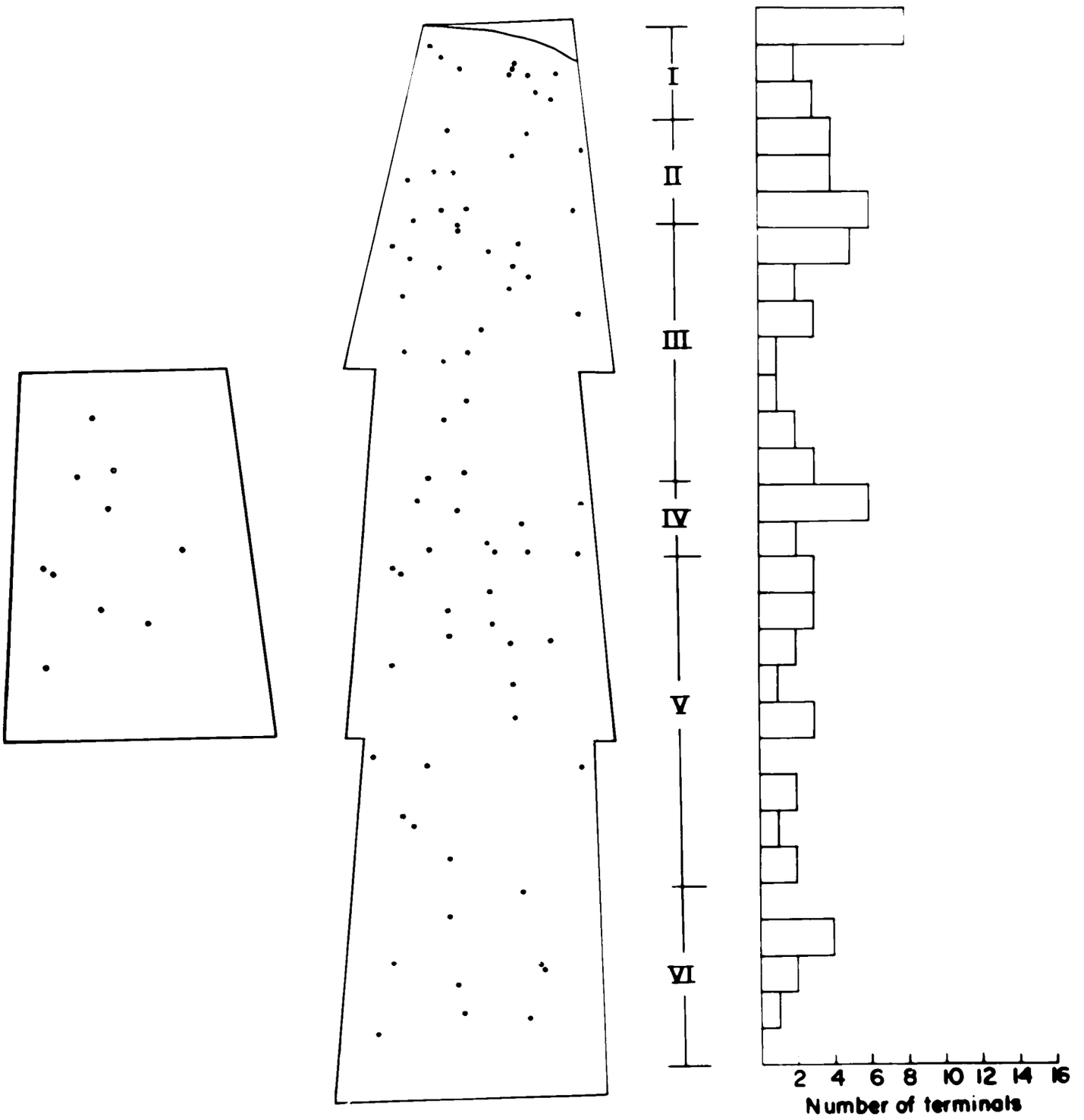

Fig. 9-64 Map and histogram of the same sections of the motor cortex as Fig. 9-63 showing the depth distribution of the different types of post-synaptic profiles which receive synapses from SI association axon terminals. Dendrites postsynaptic to these terminals occur throughout the depth of the cortex.

TERMINALS FROM SOMATIC SENSORY CORTEX IN THE MOTOR CORTEX.

LAMINAR DISTRIBUTION OF POST SYNAPTIC PROFILES

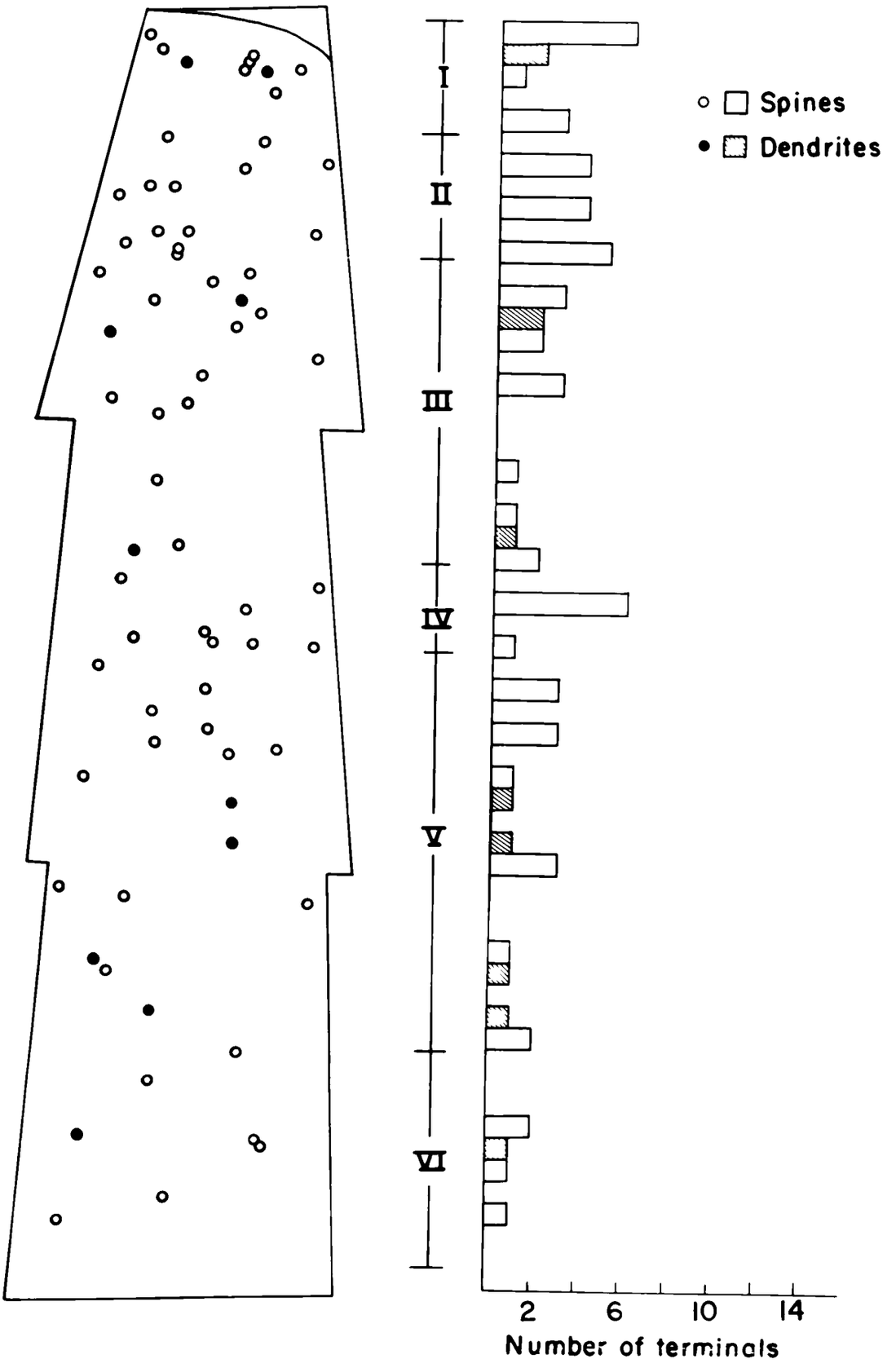

Illustrations to Chapter 10

GENERAL DISCUSSION

Fig. 10-1 Diagram summarising the connections on which the model of the neocortex is based. The cells with triangular somata represent pyramidal cells and those with round somata represent an inhibitory interneuron, thought to be the large stellate cell. Cell A represents all those neurons receiving monosynaptic activation from the input under consideration and similarly cell B represents all those neurons receiving monosynaptic connections from the neurons of set A.

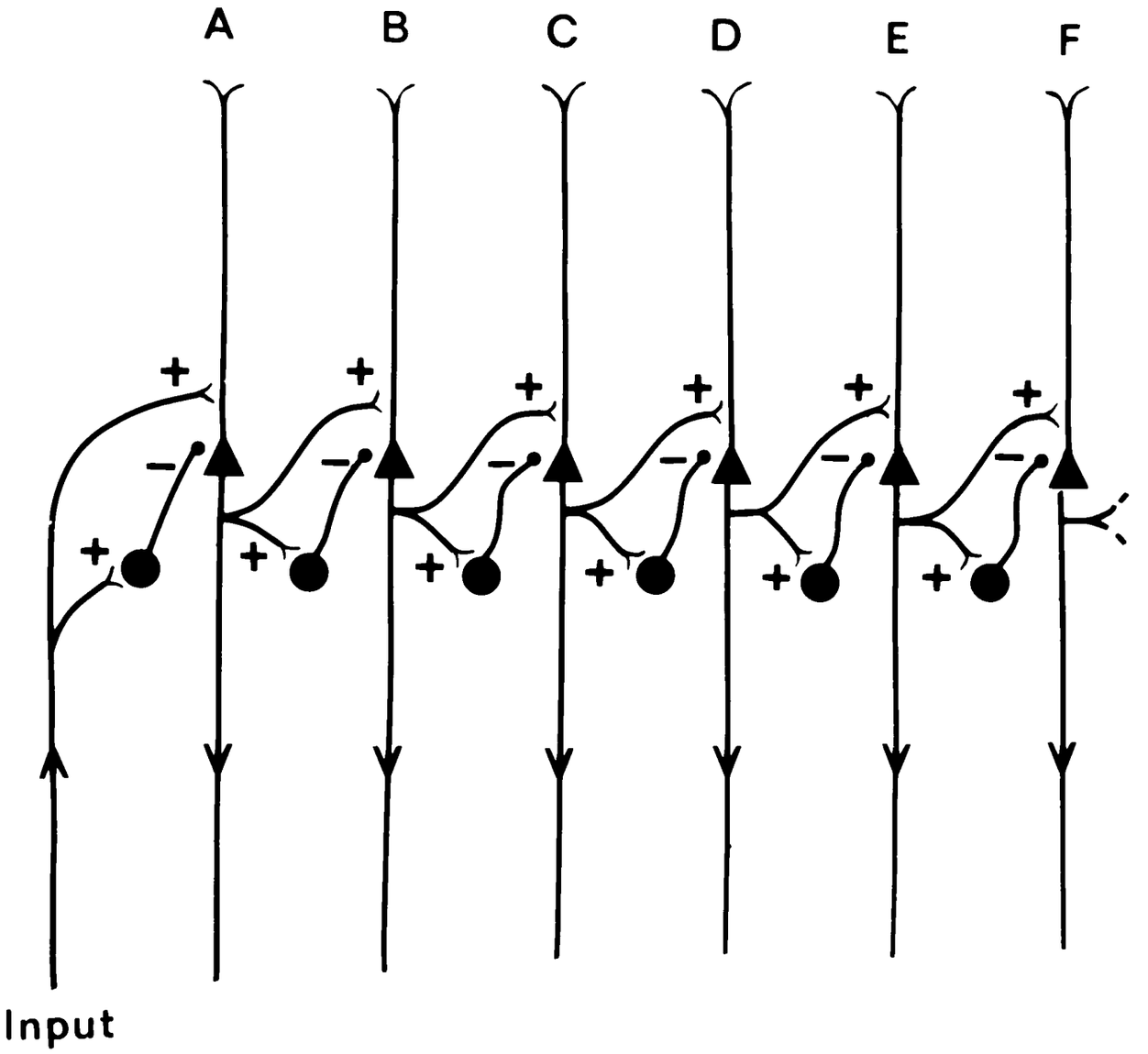
A
B
C
D
E
F
Input

Fig. 10-2 Graphs showing the behaviour of the model of cortex for a constant single input and different values of the difference between the excitatory and inhibitory coefficients $(\Theta - \phi)$. When $(\Theta - \phi)$ is less than one activity dies away but when it exceeds one the resulting activity increases indefinitely.

BEHAVIOUR OF MODEL - SINGLE INPUT WITH NO MAXIMA

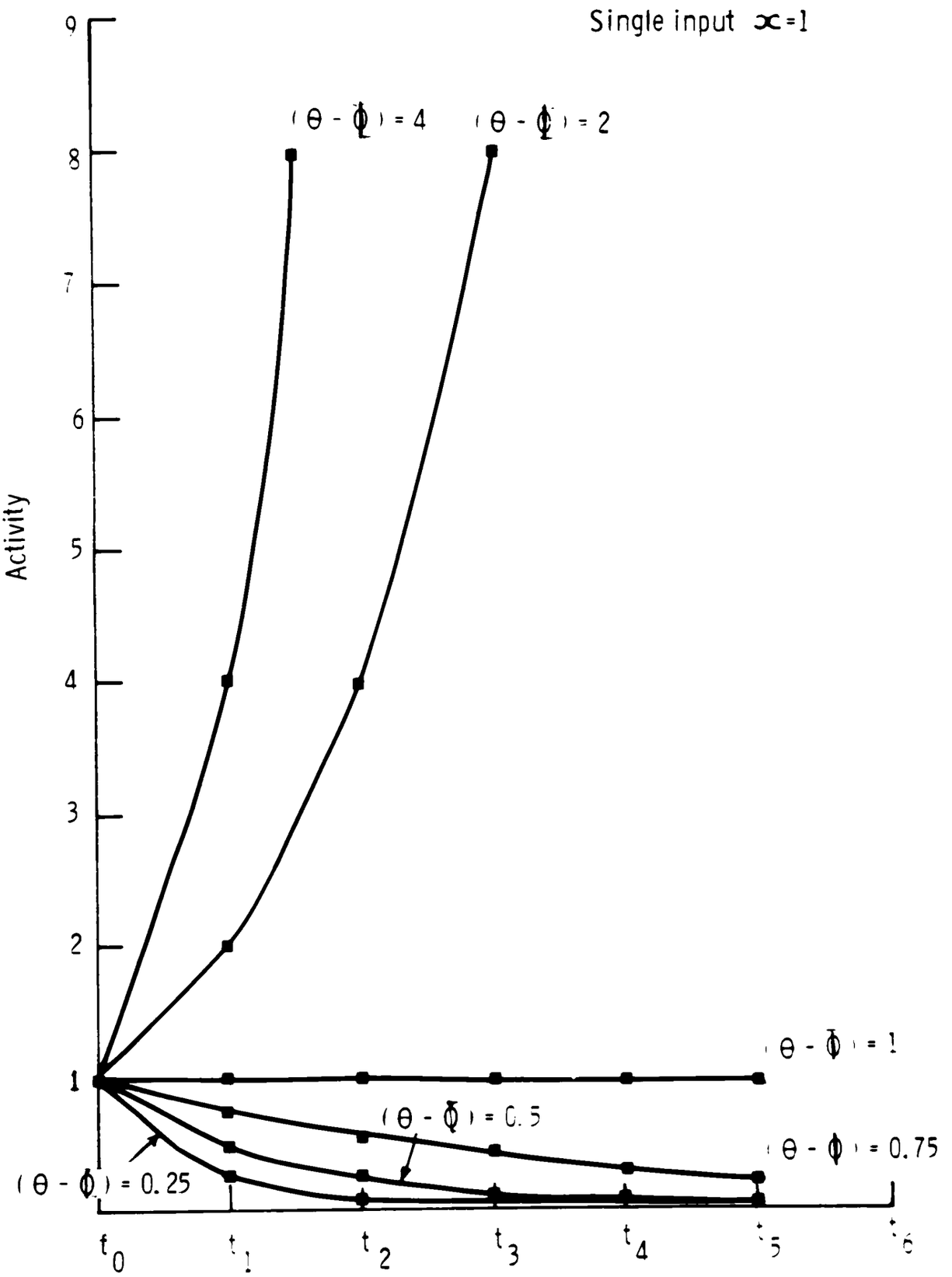

Fig. 10-3 Graphs showing the behaviour of the model of the cortex for different values of a single afferent input of 5 to 20 with maxima imposed on the total levels of excitatory and inhibitory activity (Emax = 40, Imax = 10) and with an excitatory coefficient of 2 and an inhibitory coefficient of 1.5. At low levels of inputs ($x < 10$) activity dies away but at higher levels of input ($x > 10$) the resulting activity increases to Emax.

BEHAVIOUR OF MODEL - SINGLE INPUT WITH MAXIMA

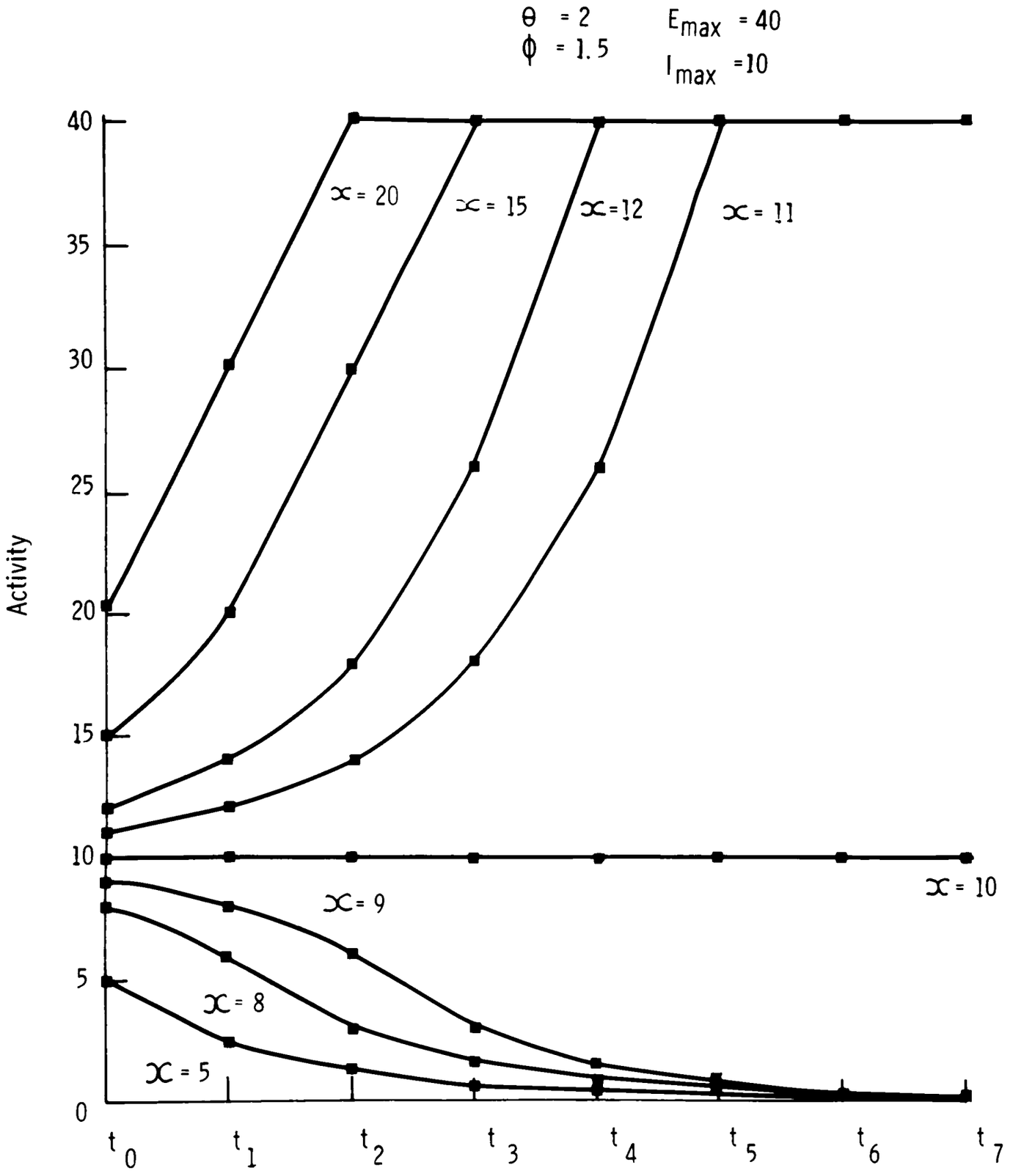

Fig. 10-4 Graphs showing the behaviour of the model of the cortex to a sustained input of ($x = 1$) with different values of the excitatory and inhibitory coefficients ($\Theta - \phi$ from 0.25 to 4) and no maxima. With values of ($\Theta - \phi$) of less than one activity increases to a stable maximum but when ($\Theta - \phi$) exceeds one activity increases indefinitely. The input was removed at the vertical arrows. For ($\Theta - \phi$) of less than one activity then dies away but when ($\Theta - \phi$) exceeds one activity continues autonomously and increases indefinitely (lower curve of ($\Theta - \phi$) = 2).

BEHAVIOUR OF MODEL -SUSTAINED INPUT WITH NO MAXIMA

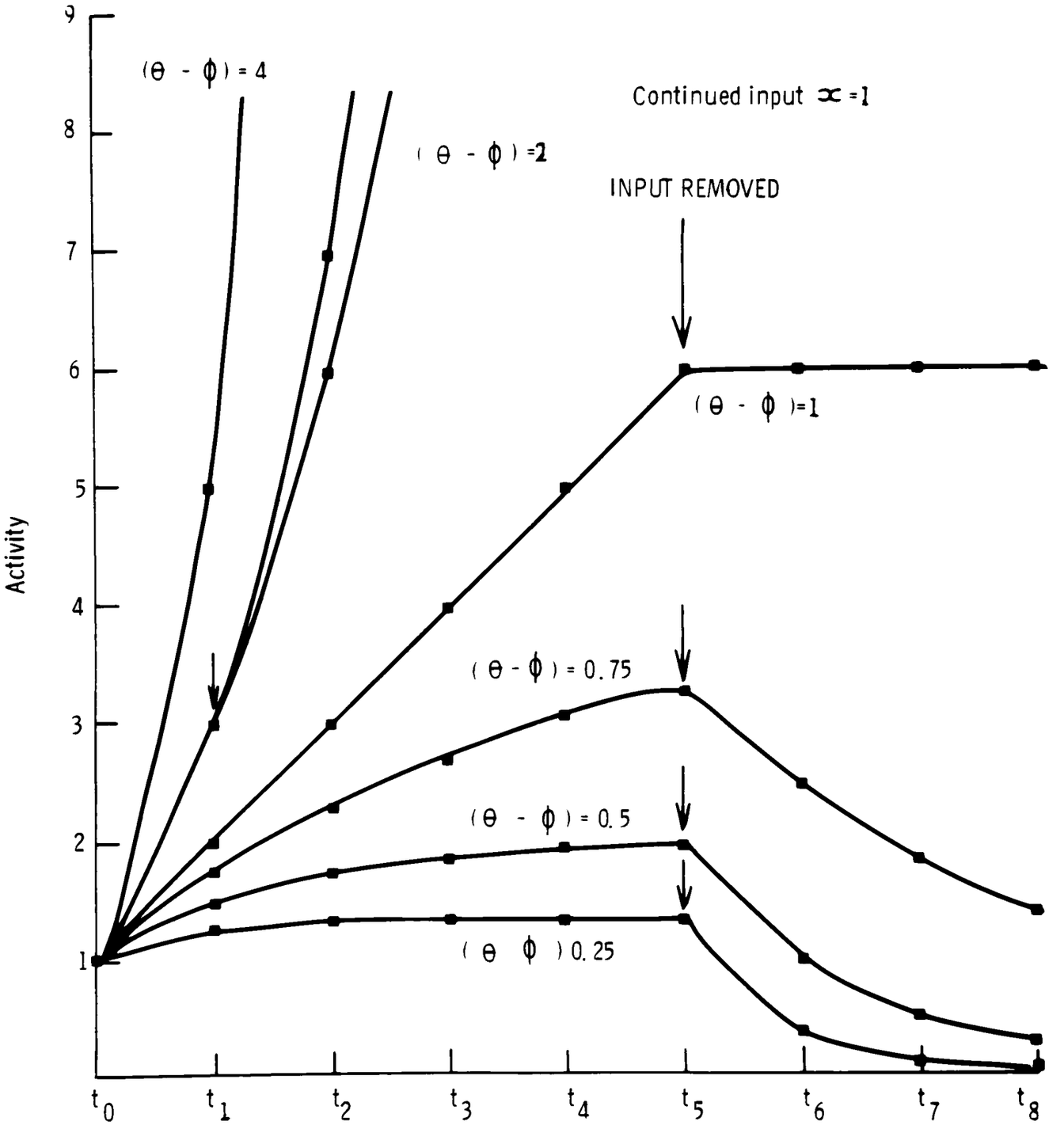

Fig. 10-5 Graph showing the behaviour of the model of the cortex for different levels of a sustained input ($x = 2$ to $x = 10$) with Maxima ($E_{max} = 40$ and $I_{max} = 10$) and an excitatory coefficient of 2 and an inhibitory coefficient of 1.5. For a low level of input ($x = 2$ and $x = 3$) activity increases to a stable maximum but at higher levels ($x = 4$, 5 and 10) activity increases to Emax. The effect of stopping the input at different times is shown for $x = 4$ (input removed at vertical arrows). If the input is removed at t_3 activity dies away but if it is allowed to continue to t_5 then the activity becomes autonomous and continues to increase even if the input is removed.

BEHAVIOUR OF MODEL - SUSTAINED INPUT WITH MAXIMA

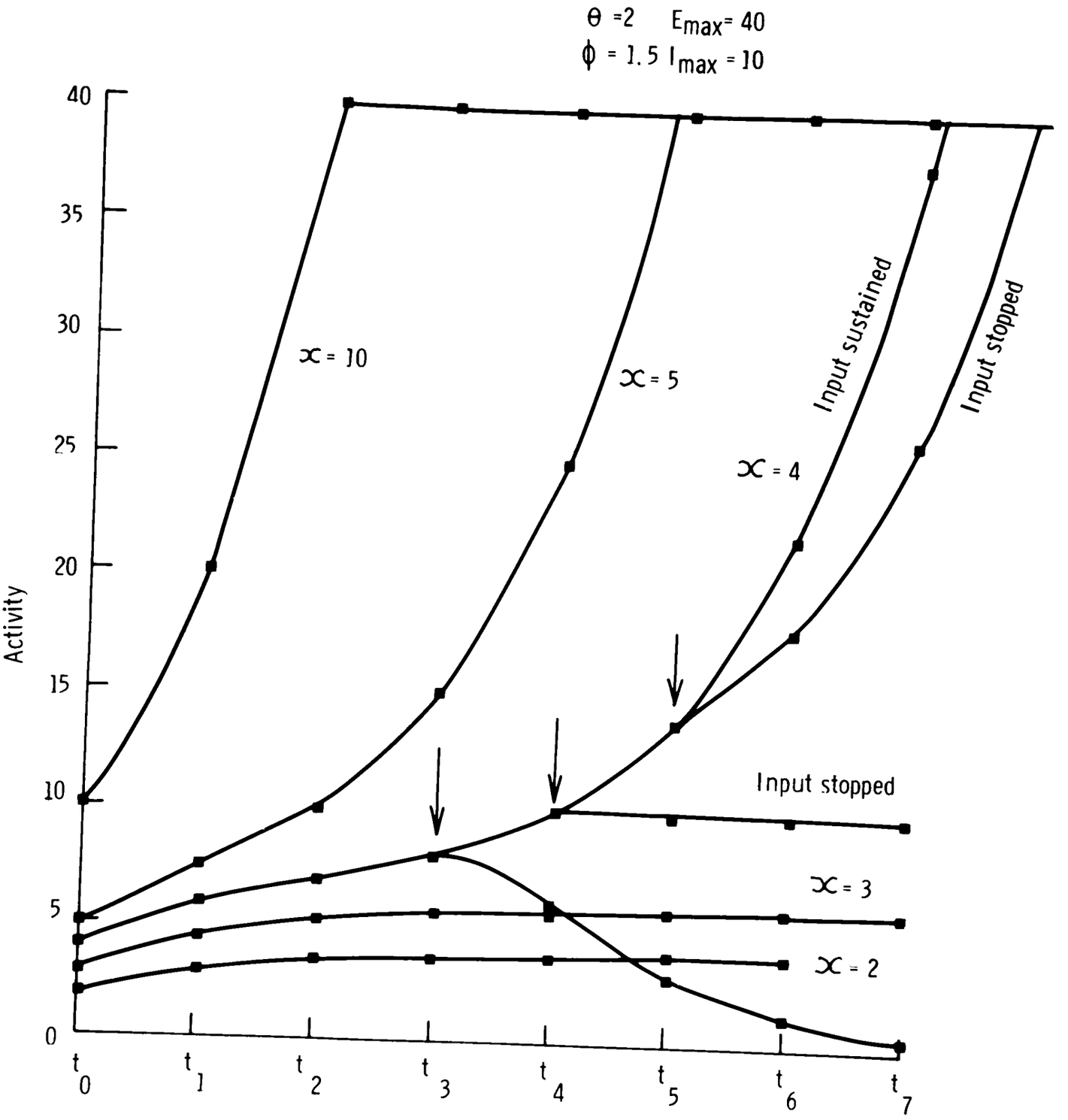

Illustrations to Appendix 2

Fig. A-1 Theoretical transverse section of an axon initial segment to show that synapses lying between the positions VX and XZ or vx and xz and therefore having centres between W and Y or w and y will be detected by the section AA' and therefore the proportion of the total number of synapses detected by the section AA' will be the distances WY plus wy, equal to two synaptic diameters, divided by the circumference of the initial segment IId (see text).

Fig. A-2 Three-dimensional expansion of the theoretical diagram of an initial segment of Fig. A-1 showing that the proportion of synapses detected by the section AA' is the area WYY'W' plus the equal area on the opposite side of the cylinder which is the projection of wy, divided by the total area of the curved surface of the cylinder (see text).

Fig. A-3 Theoretical transverse section of an axon initial segment to show that an off-centre section BB' parallel to the long axis of the initial segment will detect the same proportion of synapses as the section AA' through the centre of the initial segment (Fig. A-1) (see text).

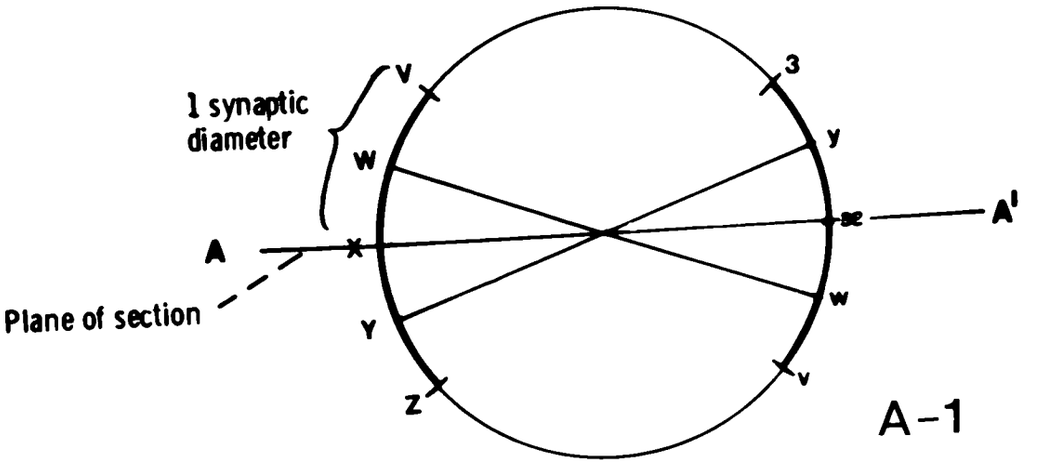
1 synaptic diameter
V
3
y
W
A'
A
x
Plane of section
w
Y
v
Z

A-1

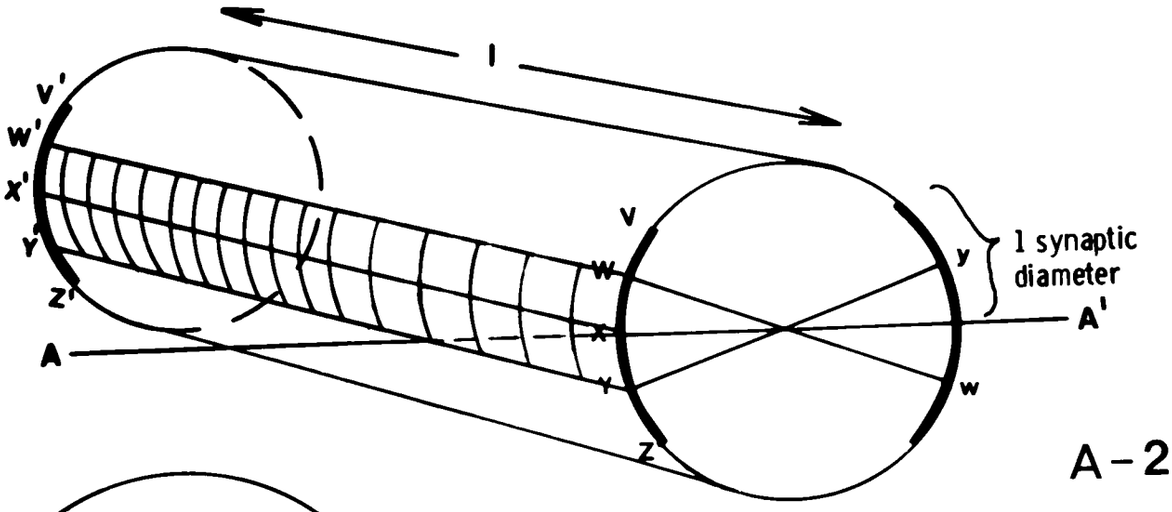
l
V'
W'
X'
Y'
Z'
A
V
W
x
Y
Z
y
1 synaptic diameter
A'
w

A-2

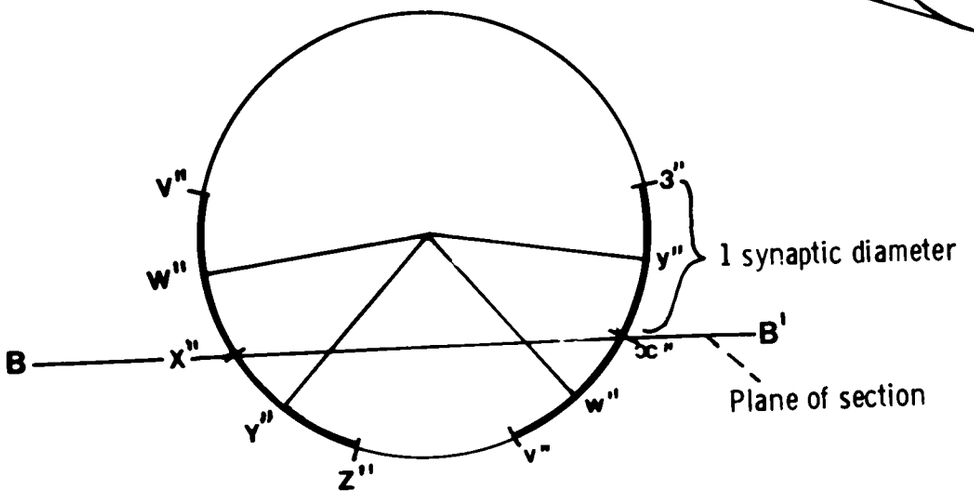
V"
3"
W"
y"
1 synaptic diameter
B
X"
B'
Plane of section
Y"
w"
Z"
v"

A-3

Fig. A-4 Graph to show the proportion of the total number of synapses on to an initial segment which will be found by a single longitudinal section through the initial segment. This curve is calculated on the basis of the model described in the appendix using a synaptic diameter of 0.35 μ.

PROPORTION OF TOTAL SYNAPSES ONTO AN INITIAL SEGMENT FOUND IN A SINGLE LONGITUDINAL SECTION OF INITIAL SEGMENTS OF DIFFERING DIAMETERS.